AN ANALYSIS FOR BRACED EXCAVATIONS IN CLAY

HUANLIANG XIA,


CENTRE FOR NFLD. STUDIES
MEMORIAL UNIVERSITY
OF NEWFOUNDLAND

AN ANALYSIS FOR

BRACED EXCAVATIONS IN CLAY

by

Huanliang Xia, B. Sc., M. Sc.

A thesis submitted to the School of Graduate Studies

in partial fulfilment of the requirements for

the degree of Doctor of Philosophy

Faculty of Engineering and Applied Science

Memorial University of Newfoundland

March 1999

St. John's Newfoundland Canada

Abstract

This thesis studies braced excavations in clay with centrifuge tests and finite element analyses.

Centrifuge experiments of 72 g are carried out to investigate earth pressures on the back of sheet piles, forces in the struts, the surface settlement and bottom heaving. The simulated depth of excavation is 11.5 m and the width is 17.3 m. The struts are applied before excavation for the convenience of the tests. Heavy liquid of sodium polytungstate ($3Na_2WO_4.9WO_3.H_2O$) is used to simulate the soil which would be excavated. The excavations are simulated by draining the liquid during the tests.

The details of designing the model, preparing the soil, assembling the equipment and experimental procedures are described. Compression and triaxial tests are also carried out to obtain the mechanical parameters for the numerical analysis.

A finite element analysis is carried out for the model and the results are compared with experimental data and established methods. The Cam-clay model is used for the soil. Eight node rectangular elements with pore pressures on the corners are used for the soil and block elements are used for the sheet piles. The results show that the finite element may predict most behaviour of the excavation.

The finite element model is used to perform parametric studies where each layer of struts is applied after the soil of the corresponding layer is excavated. The effects of variation of the properties of soil, the stiffness of sheet piles and struts and the vertical distances between the struts are investigated.

In memory of my parents

Acknowledgements

I am deeply indebted to my supervisor, Dr. G. C. W. Sabin, for his patient guidance, insistent encouragement and extensive kindness during this research. I would also like to express my sincere thanks to him for his financial support, especially for his generosity to allow me to freely select my research topic and his coverage for the expense. I would also like to thank the other members of my supervisor committee, Dr. J. I. Clark and Dr. P. Morin, for the time they spent on reading my proposal and thesis and the suggestions they made for the revision.

I am grateful to Dr. Ryan Phillips, the Director of the centrifuge facility, for his insistent concerns, deep insights, creative advice, and many invaluable comments and suggestions. Especially for his help in designing the connection between the outlet of the heavy liquid bag and the drainage tube. Great thanks go to Mr. Michael Paulin for his instructions in excavating the soil and installing the PPTs. Many thanks go to Mr. Don Cameron, the technician of the Centrifuge for his great help during the experiments, Mr. Karl Tuff and Mr. Steve Smyth for their help in coping with the electrical system for the tests and Mr. Shawn Hurley for his advice on the experiments.

Thanks also are due to Mr. Humphrey Dye, the Director of the Machine Shop of the Division of Technical Service, and Mr. Chris Conners, Mr. Leo Spurrell, Mr. Jerry Smith and Mr. Robert Walsh, the technicians of the Division, for their help in manufacturing the parts of the test equipment, especially Mr. Chris Conners who did most of the work. Thanks are due to Mr. Austin Bursey for his sincere and fast work in applying the strain gauges and calibrating the design. Thanks also to Mr. Steve Foster and Mrs. Diane Learning for their effort in making the

woodblock and the rubber bags. I would also like to thank Mr. Jim Andrews, Mr. Mac Butter and other members of the welding shop for their welding work.

I would like to thank those who helped me in different ways during my study for this thesis, among them I would like to mention Mr. Fanyu Zhu, Mr. Paul Lach, Mr. M. S. Prasad, the Ph. D. candidates during the time, and Dr. Y. Prasad.

I would like to thank the Center of Cold Ocean Resources Engineering (C-CORE) of Memorial University of Newfoundland for providing me with the facility to carry out the experiments. I would also like to thank Memorial University of Newfoundland, especially the Faculty of Engineering and Applied Science and the School of Graduate Studies for admitting me to study in this school and the financial and facility support. The staff in the Center of Computer-Aided Design should be specially mentioned, their help was highly appreciated.

Finally, I would like to express my thanks to my dear wife, Ms. Xuejun Li for her sincere love and support during the time of my study. Thanks also go to my brother, my sisters and other relatives and friends for their love and concern from the other side of the world.

Contents

List of Tables

List of Figures

List of Symbols

a	coefficient of compression
a_c	Coriolis acceleration
a_h	horizontal component of acceleration
a_i	centripetal acceleration
a_v	vertical component of acceleration
A	coefficient of pore pressure
b	width of centrifgue model
B	width of foundation
c	cohesion
c_{cu}	cohesion in undrained shear test
c_v	coefficient of consolidation
c_{vm}	coefficient of consolidation in model
c_{vp}	coefficient of consolidation in prototype
C_c	compression index
C_s	swelling index
D_f	depth of footing
e	void ratio
e_0	initial void ratio

E	Young's modulus
F_s	safety factor
g	gravity
G'	shear modulus for soil
h	thickness of beam
h_e	effective depth in centrifuge model
h_m	depth of model
h_p	depth of prototype
H	depth of excavation
H_0	initial height of sample
H_d	distance of drainage path
H_m	distance of drainage path in model
H_p	distance of drainage path in prototype
H_s	height of solids of soil sample
H_t	height of soil sample
i	hydraulic gradient
i_m	hydraulic gradient in model
i_p	hydraulic gradient in prototype
I	moment of inertia
k	permeability
k_m	permeability in model
k_p	permeability in prototype
K	intrinsic permeability of soil
K_0	earth pressure coefficient at rest

K_A	Peck's earth pressure factor
K'	bulk modulus
L	span of beam
m	coefficient
m_v	coefficient of volume compressibility
M	moment
N	centrifuge simulation scale
N_b	stability number defined by Terzaghi and Peck
N_c	bearing capacity coefficient related to c
N_q	bearing capacity coefficient related to surcharge
N_s	stability number defined by Clough and Schmidt
N_γ	bearing capacity coefficient related to γ
p	pressure
p_0'	initial vertical effective stress
p_c	bearing capacity
P	axial force
P'	mean effective stress
q	deviator stress
r	radius of rotation
R_e	effective radius for rotation
R_t	radius of rotation at the surface of the model
S_u	undrained shear strength
S_{ub}	undrained shear strength of base soil
t	time

t_{90}	time required for 90% of consolidation
t_m	consolidation time in model
t_p	consolidation time in prototype
T_v	time factor in consolidation
u_f	excess pore pressure at failure
u_m	excess pore pressure in model
u_p	excess pore pressure in prototype
v	flow velocity
w	water content
w_0	initial water content
w_f	water content at failure
w_L	liquid limit

α	angle
γ	unit weight of soil
γ_{sat}	unit weight of saturated soil
γ_w	unit weight of water
γ_{wm}	unit weight of water in model
γ_{wp}	unit weight of water in prototype
$\gamma_\prime$	buoyant unit weight of soil
ϵ	strain
ϵ_f	axial strain at failure
ϵ_p	volume strain
ϵ_q	shear strain

ϵ_v	volume strain
ϵ_{vm}	volume strain in model
ϵ_{vp}	volume strain in prototype
κ	slope of unloading-reloading line
λ	slope of normal consolidation line
ν	dynamic viscosity
ρ	density
ρ_0	initial density
ρ_d	dry density
σ	stress
σ_1	major stress
σ_3	minor stress
σ_1'	major effective stress
σ_3'	minor effective stress
σ_{max}	maximum stress
σ_{v0}	initial vertical stress
σ_{vm}	vertical stress in model
σ_{vp}	vertical stress in prototype
σ_z'	vertical effective stress
ϕ	internal friction angle
ω	angular velocity of rotation in centrifuge

Chapter 1

INTRODUCTION

1.1 Nature of the problem

Braced excavations have been widely applied in foundation engineering projects. The stability of the braced system itself and the resulting settlement of the neighbouring structures are of most concern. Much research has been devoted to this subject. Both empirical and numerical methods have been applied in the previous studies. However the effectiveness of these analyses depends on the correct parameters obtained from the sites. It is particularly important in the numerical models that the correct soil parameters for strength and deformation properties be used. Because the complexity of the soil deposit, the procedures of construction and many other uncontrollable factors, the problem of analyzing real construction projects is not feasible.

For a better understanding of the stresses and strains in the soil and the structures, a controllable experiment is an ideal way to conduct research on this problem.

However because of dimensional considerations, a prototype experiment is out of reach and a small model cannot cover the total range of the stresses and strains encountered during the actual excavation.

Fortunately, centrifuge tests provide a solution to the study of this problem. A small controllable model may simulate a problem of very large scale. This study uses a series centrifuge tests to study the problem of excavation.

1.2 Objective of the study

The objective of this study is to investigate the developing earth pressures on the back of sheet piles, forces in struts, bottom heaving and the surface settlement during excavations. To accomplish this goal, a finite element model is created to analyze the problem. This model is then used to carry out parametric studies for normal excavations. To support this approach, a physical model is developed and tested in a centrifuge. Results from the centrifuge tests provide insight into the complicated nature of this problem and support the numerical model.

To conduct the centrifuge experiments, the following steps were followed:

1. Design a centrifuge test package to simulate the braced excavation, including selecting the equipment, the material and organizing the manufacturing work;
2. Compact and consolidate the clay in the strong box for the tests;
3. Carry out a series of centrifuge tests to investigate the loads on the sheet piles

and the struts, bottom heaving and the settlement of the soil surface;

4. Test properties of the soil.

5. Process and interpret the data obtained from the tests.

1.3 Organization of the thesis

Since the experimental model test results provide input to the numerical model, the discussion of these models is presented in that order.

Chapter 2 describes the problem of braced excavations and reviews previous studies.

Chapter 3 introduces the theoretical and practical considerations which relate to centrifuge tests. The design of experimental model and the procedures followed in carrying out the tests are described in Chapter 4.

Chapter 5 outlines the method of obtaining the strength, deformation and seepage parameters of the soil with the results summarized.

Chapter 6 details the results of the centrifuge tests and Chapter 7 provides the finite element simulation of the prototypes of the same models. In Chapter 8, parametric studies are carried out and the results are summarized.

Finally Chapter 9 concludes the study and proposes the future areas of research.

Chapter 2

BRACED EXCAVATIONS

2.1 Introduction

Excavation work is frequently carried out in foundation engineering. The purpose of excavation is mostly for constructing the subsurface structures. The size of the projects may be dozens of meters in plan and in depth. An example of braced excavation is shown in Fig. 2.1.

The procedure for an excavation is that, after the sheet piles on both sides are driven into the ground, the first layer of soil is excavated and then the first layer of struts or other supports is applied. This procedure is repeated till the required depth is reached, and the excavation is completed.

Alternatively the surrounding soil may be supported with retaining diaphragm walls or lagged H piles. However sheet piles are frequently used because of their strength and the convenience of handling. This research will only focus on the

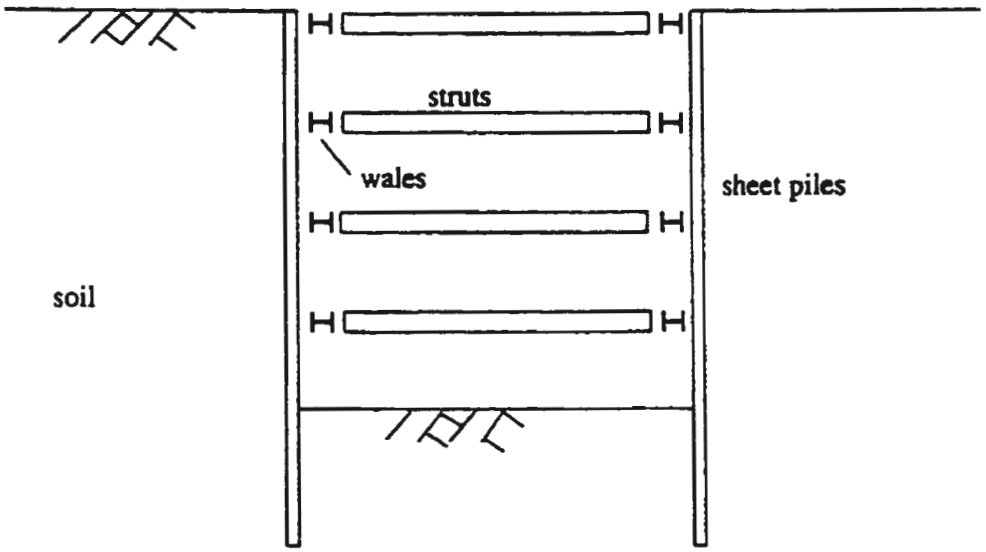

Figure 2.1: Braced excavations

application of sheet piles. The braced excavation is the excavation where the struts are used to support the sheet piles on both ends. A project may expect more struts for the stability of the bracing system and less struts for the convenience of construction work.

The stability of these sheet pile structures is very important to the completeness of the corresponding project. A failure of the system may result in much more expense to the project or even result in the damage to the buildings nearby; some times it is disastrous. Therefore to find an economical and reliable method to support the soil is very important for construction.

Failure of the supporting system can come from large lateral displacement of the sheet piles, the buckling of the struts, excessive bottom heaving and large ground settlement. As for clay, failure may also result from seepage failure around the bottom of the sheet piles.

Stability is determined by many factors, such as the strength of the soil, the water table in the soil, the stiffness of the sheet piles and the struts, and the vertical and horizontal distances between the struts. The settlement of the ground around excavation sites is of concern because of increased costs. More fill is needed to keep the ground at the required level. More importantly, if there is a building around the site, this ground settlement implies an uneven settlement of the foundation of the building. If this uneven settlement is too large, large extra stresses will be produced in the structures in the building, and sometimes may result in damage of the building and failure of the foundation. This could result in a lawsuit and

therefore it is also a factor for the engineers to consider in designing the excavation system. Points to consider are the method of support (bracing or anchoring), the strength of the sheet piles, the dimension of the struts and the distances between the struts. In some cases there are few choices, for example, in soft clay, anchoring cannot be used, only braced excavation is available. There are often compromises required in selecting the distance between the struts; from the view point of the stiffness of supporting the soil, a smaller distance is better, however, in the view point of carrying out the excavation and construction, a larger distance would be more convenient because there would be less blocking.

For a strong design, large section struts are required. The large sections are very hard to handle and the expense is much higher. Some sites may be very difficult for the excavation because of such things as the water lines and waste drainage lines. These lines are obstacles for carrying out the excavation.

It is the common opinion among researchers that this problem is very complex. The strength and deformation properties of soil are very hard to simulate in analyses, and these properties are subject to change with a lot of factors such as the weather, the stress and strain history, etc. The deposit of the soil is quite different from site to site. The soil can be layered with soils of very different properties. Some soils may be almost of no strength and some soil may have very low strength and be highly compressible.

Clough and Schmidt (1981) summarized the factors which affect the stability and deformation of the bracing system and the soil as the following:

- type of support system;
- stiffness of support system;
- degree of wall embedment;
- degree of preloading;
- method of support system construction;
- time period for construction;
- method of construction of structures within excavation;
- size of surcharge loads;
- weather;
- subsoil condition and properties;
- surrounding structures; and
- excavation shape and depth.

Only part of these factors can be controlled by designers, and this research will only deal with some of those controllable factors.

2.2 Major Problems in Excavations

A braced excavation is a temporary structure. The design is to keep the structure stable during the time of its use, and to prevent the neighbouring buildings or structures and the bottom of the excavation from being damaged. The rest of this section discusses the problems related to an excavation.

2.2.1 Pressures on sheet piles and the forces in struts

The pressures on sheet piles are the main concern, because these pressures determine the lateral stability of the structure in terms of the stress in the sheet piles and the loads in the struts. At first, the soil is in a state of equilibrium. The vertical stress comes from the self weight and the lateral stress may be evaluated with K_0, which is the coefficient of static earth pressure. After sheet piles are driven into the ground, the soil is disturbed. As a result, this disturbance affects the strength of the soil, especially for those sensitive soils. However, normally this effect is ignored.

Proceeding with the excavation, the soil between the sheet piles is removed, and so is the lateral pressure of this soil on the sheet piles. The soil behind the sheet pile is subject to some deformation, and mostly displaces toward the excavated space, leading to some degree of mobilization of the active strength. Meanwhile, the soil at the bottom of the excavation area develops toward the mobilization of passive earth pressure. However this pressure is not reliable either because the deformation is not large enough or the soil is not strong enough. With the application of the

struts, the development of the deformation is retarded by the struts, and the lateral pressure of the soil is supported by the struts when the excavation proceeds.

The variation of the pressure on the sheet piles (because of excavation) causes a variation of the stress in the sheet piles. This variation may pass the stress to the neighbouring spans, because sheet piles are continuous beams. This causes the redistribution of stress and moment in the sheet piles, as a result, the displacement also keeps changing. This in turn, causes the earth pressure on the back of the sheet piles to change. However, for selecting sheet piles, designers are concerned about the maximum moment in the sheet piles. For selecting struts, designers are interested in the maximum forces in the struts. Both of these selections are determined by the earth pressures (plus pore pressure if applicable) on the back of the sheet piles. For an actual structure, the maximum moment in the sheet piles and the maximum forces in the struts do not occur at the same time, and are not concordant with the maximum earth pressure.

The theory of the distribution of earth pressures originated in the 19th century. Initially, the pressures on the sheet piles are calculated using the Rankine theory. However, Terzaghi and Peck (1967, page 261) said "the active earth pressure against the bracing in the cut cannot be computed by means of Coulomb's or Rankine's theory. A method must be developed that takes into consideration the influence of the deformation conditions in the type of failure." They also said "the real curve of sliding can be closely approximated by a logarithmic spiral equation", and "since the upper part of the sliding wedge cannot move laterally, the surface of sliding intersects the ground surface at a right angle (page 262)."

They calculated the results of their assumption and presented the so-called "Apparent pressure diagram" for the effective earth pressure on the back of sheet piles, which is shown in Fig. 2.2. Their conclusion was that "the value of K_A can be approximated with reasonable accuracy by the Rankine value:

$$K_A = 1 - \frac{4c}{\gamma H}." \tag{2.1}$$

They used this value for soft to medium clay when $N_s < 4$, where N_s is the dimensionless number for accounting the stability of the bottom heaving and $N_s = \gamma H/c$. "It has been found that movement of the sheeting and settlements of the ground surface adjacent to an open cut in clay become significant for values of N_s on the order of 3 to 4. At about this value, a plastic zone begins to form in the clay near the lower corners of the excavation and as N_s increases the plastic zone enlarges (page 408)." They also stated that as a rough approximation, the previous equation can be modified empirically to incorporate a reduction factor m to be applied to the shear strength c. Thus

$$K_A = 1 - m\frac{4c}{\gamma H} \tag{2.2}$$

and for N_s greater than 4, m is 0.4.

Although the envelopes are presented with the form of the pressures acting on the sheet pile, the purpose is not to show the actual possible pressures on the sheet piles, but are used to estimate the maximum moments in the sheet piles and

the maximum forces in the struts that might be expected in a braced excavation. Although sheet piles are continuous beams, they are considered as several simple beams. The struts are regarded as the supports of the beams, and the load is the pressure given by the envelope. In such a way, the loads on the struts may be calculated.

For soft to medium clay, the maximum pressure is $K_A \gamma H$, and $K_A = 1 - m\frac{4s_u}{\gamma H}$, where γ is the unit weight of soil, H is the maximum depth of the excavation, s_u is the undrained strength of the soil and m is a coefficient.

Peck (1969) stated that the apparent pressure diagram for estimating strut loads in sand agreed well with the data, but in soft to medium clay, was far less satisfactory. Peck revised the theory by recommending a stability number N_s, where $N_s = \gamma H / s_u$. When N_s equals 6 to 8, m takes the value of 0.4 to modify the strength s_u. Peck (1969) noted that this method cannot cope with the effect of stratification, the variation of the strength with the depth and the effect of the length of sheet piles.

Another distribution was proposed by Tschebotarioff (1951). The distribution is triangular and is suitable for clay (Fig. 2.3). However this distribution underestimates the value of the earth pressure on the sheet piles according to the finite element analysis (Xia, 1996).

It is realized that the displacement of the soil also plays an important role in the stability of surrounding structures. Furthermore, the displacement of soil is determined by the constitutive relations of the soil. Therefore it is impossible to

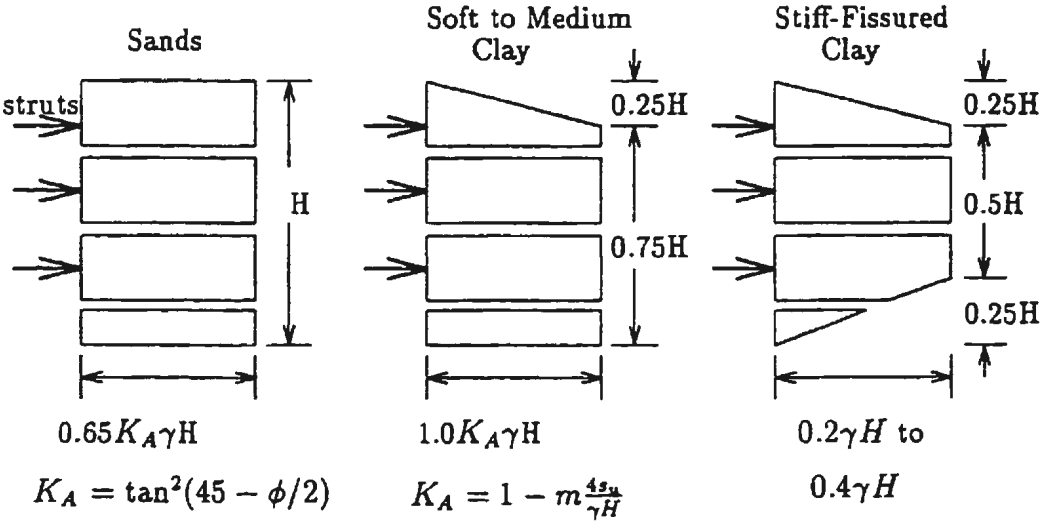

Figure 2.2: Apparent pressure diagrams, after Peck, 1969

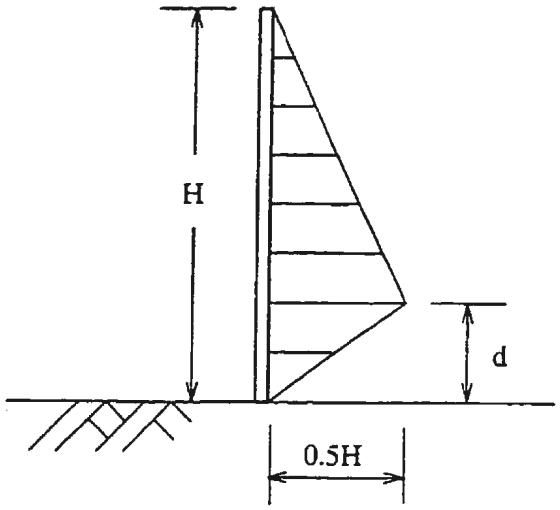

Stiff Clay: d=0.4H
Medium Clay: d=0.25H
Soft Clay: d=0

(after Tschebotarioff, 1951)

Figure 2.3: Lateral earth pressure diagrams, after Tschebotarioff, 1951

predict the earth pressures on the sheet piles only using Peck's apparent diagram and the soil parameter, s_u. There are many researchers using numerical methods to analyze this problem.

2.2.2 Lateral movement of sheet piles

Lateral displacement (deflection) is an important datum to assess the stability of the bracing structure. Lateral displacement is mostly determined by the property of the surrounding soil, the stiffness of the bracing system, and the workmanship.

Several approaches (Peck, 1969) reveal that different patterns of lateral displacement exist according to the different stages of the excavation. At the beginning of the excavation, the largest displacement happens at the top of the sheet piles. If earlier bracing is applied at the top, lateral displacement of the sheet piles could be effectively reduced. Peck (1943) and Ward (1955) recommended that the top strut should be inserted before the excavation exceeds a depth equal to $2s_u/\gamma$, where s_u is the undrained strength of the surrounding soil and γ is its unit weight. With deepening of the excavation, the pattern of lateral displacement changes into the shape of a reverse S, that means the largest displacement happens just below the bottom of the excavation.

Peck (1969) pointed out that experience indicates that ordinary sheet piles do not have much affect in reducing the lateral displacement. The more effective way to reduce the lateral displacement is to increase the stiffness of the lateral supports such as stronger struts and smaller vertical distance between struts. The most

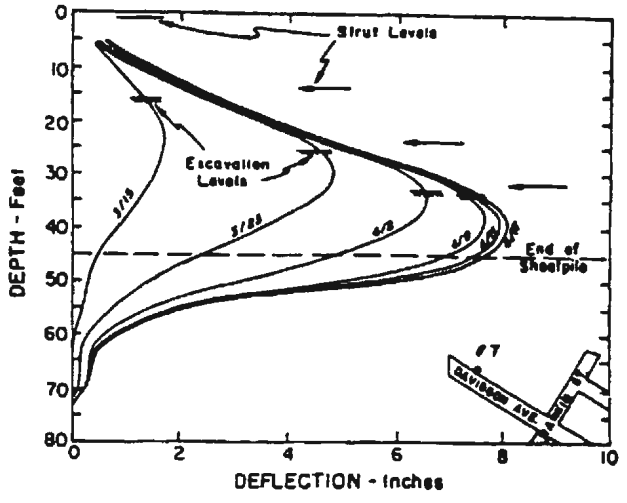

Figure 2.4: Typical measured lateral movements for deepening excavation on Davidson Avenue, after Clough and Reed, 1984

effective factor is the surrounding soil.

Construction procedures also greatly affect the lateral displacement. Construction procedure also includes the term "workmanship" given by Peck. The construction procedures are in terms of the time spent excavating each layer of soil and applying the struts. The more time spent means more lateral displacement of soil. Applying the struts later allows displacement to develop without resistance. Thus the major portion of the displacement has taken place prior to the application of the struts. Applying struts earlier may reduce the displacement.

Clough and Reed (1984) reported an excavation failure in the Islais Creek Basin near San Francisco Bay for sewer culverts 8 m wide and 9 m deep (Fig. 2.5). The soil was soft clay with a shear strength of 300 psf to 700 psf increasing with depth. The water content ranged from 80% to 100%. Three layers of struts were used, and there was a couple of temporary supports between the second and bottom layers of struts for excavating the soil at that section. It was believed that the wales and struts were strong enough. The failure began with a local slope slide of the soil between second and third layers of struts along the direction of the length of the excavation. The failure exposed the corresponding sheet pile wall with no third level support. The next day, the wales immediately above the slope failure rotated upwards about its back edge. This occurred probably as a result of wracking of the system, and was apparently accentuated as a result of the small slope failure. Consequently, the corresponding struts reacting against the wale moved upwards and slid over the top of the wale. Finally, the lateral movement increased rapidly. It was concluded that the only temporary solution was to dump fill into the excavation until it stabilized.

A week later, the excavation was restarted, using the extended support system, and some channels to prevent the wales from rotating. Large lateral deflection of sheet piles may result in large lateral and vertical displacements in the surrounding soil. Both of the displacements may result in damages in nearby buildings and structures.

Finno et al (1991) analyzed the performance of pile groups adjacent to deep tie-back excavations. Poulos and Chen (1997) studied the pile response due to excavation-induced lateral soil movement with numerical methods (Fig. 2.6). They used the finite element method to analyze the soil movement during braced excavations, and used the results of this analysis as input into a boundary element program for pile response analysis. They investigated the influences of various parameters on pile response and presented design charts for estimating pile bending moments and deflections.

2.2.3 Settlement of the ground

The settlement of the surface of the soil around the excavation is also called ground loss. This settlement does not only cause the loss of the soil but more importantly it will cause extra stresses in the structures of the buildings near the excavation. These stresses may result in damage to the buildings such as cracking. The most disastrous problem is the failure of the foundation. Therefore the possible damage caused by the excavation to nearby buildings should be assessed carefully, and sometimes underpinning should be applied. However underpinning is expensive and if possible should be avoided. This decision should be made upon careful

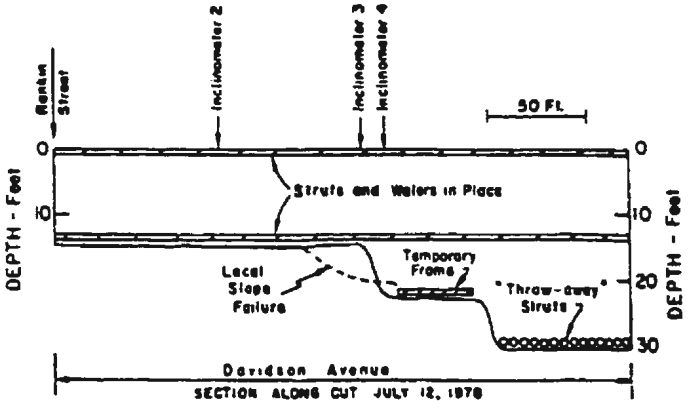

Figure 2.5: Levels of excavation just prior to rotation of waler section, after Clough and Reed, 1984

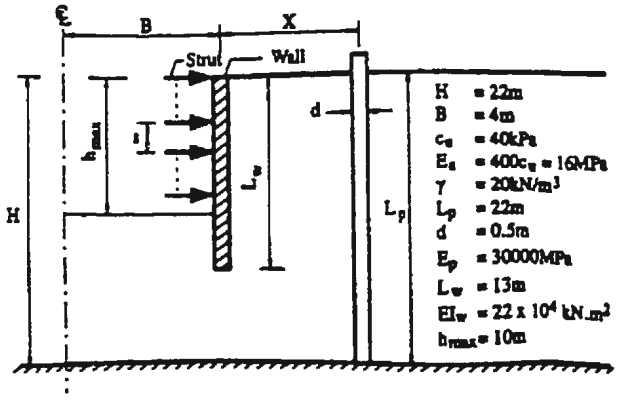

Figure 2.6: Pile close to an excavation, after Poulos and Chen, 1997

study.

The movement of the surrounding soil may also cause damage on underground structures such as various pipelines. The following information is helpful in assessing the possible damages:

1. The magnitude of the settlements, settlement difference and their patterns of distribution along the line from the sheet piles to the soil beneath the footings.

2. The magnitude of the tolerable settlements and settlement differences which will not result in the damage to the buildings.

O'Rourke et al (1976) recommended the allowable settlement of ground surface which would not cause the damage to the buildings nearby. However, Boone (1996) pointed out that using single criteria, such as angular distortion, for assessing damages on buildings excluded many important factors. He presented a new concept for the evaluation of building damage resulting from differential ground movement. This method may consider factors such as flexural and shear stiffness of building sections, nature of the ground movement profile, location of the building within the settlement profile, degree of slip between the foundation and ground and building configuration. Therefore a more accurate prediction of possible damages to the nearby buildings relies on a comprehensive study considering the mechanical properties of the building, the soil and the bracing system, and especially the details of the performance of the excavations, in other words, workmanship or construction techniques.

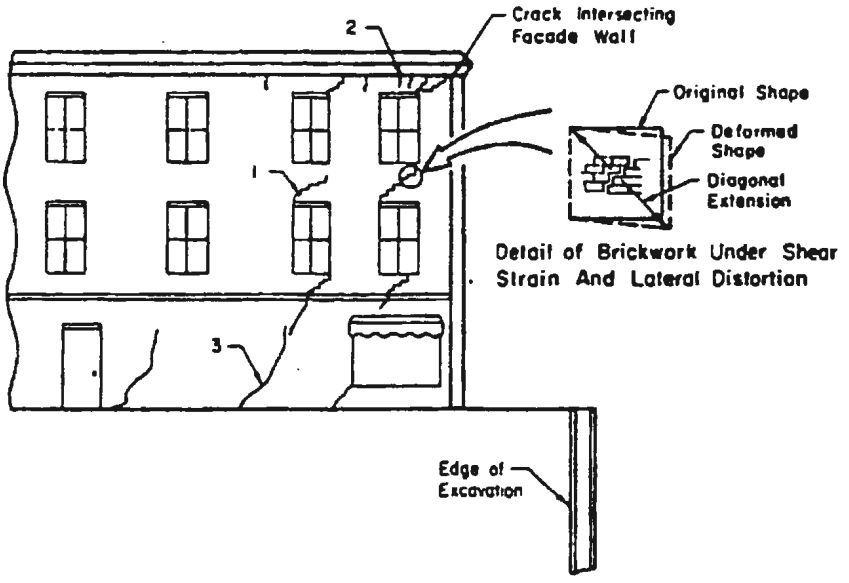

Figure 2.7: Typical fracture patterns observed in brick-bearing wall structures adjacent to excavations, after O'Rourke et al, 1976

Upon the data obtained from the excavation sites of Oslo and Chicago both in sand and clay sites, Peck presented the well-known figure plotted on Fig. 2.8, in which both the magnitude of the settlement and their distribution as a function of distance from the cut are presented. Because this figure covers data from several sites, it cannot be as accurate as one expects from a special site with specified soil. Clough and Schmidt (1981) pointed out that the shape of the distribution of the settlements depends on their amplitude. When the settlements are small, the maximum value appears at some distance from the sheet piles, and when the settlements are large, the maximum settlement appears close to the sheet piles (Fig. 2.9).

Actually ground loss is affected by many factors such as the properties of soil, the dimension of the excavation, the stiffness of the sheet piles and struts, the procedures of excavation and bracing, and greatly on workmanship.

Peck (1969) pointed out that the volume of settlement surrounding the structure is approximately equal to the volume of lost ground associated with the inward movement of the vertical walls. He concluded that settlement near an open cut could be reduced only if the inward movement of the sheeting and the heave could be substantially reduced. However, in unsaturated soil, the volumes may not be equal to each other, but the reduction of the lateral displacement of the sheet piles can still effectively reduce the settlement. The distinguishing characteristic of the settlement of saturated clay is that appreciable delayed settlement may develop on account of consolidation.

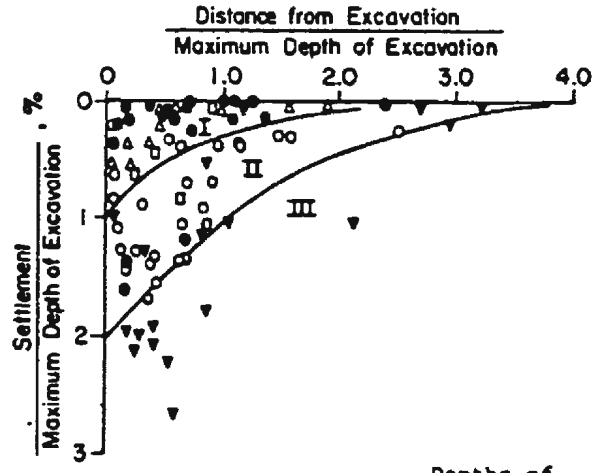

Soft to Medium Clay	Depths of Excavation, ft.
● Chicago, Illinois	30 - 63
○ Oslo, Norway, Excluding Vaterland 1,2,3	20 - 38
▼ Oslo, Norway, Vaterland 1,2,3	32 - 35
▲ Stiff Clay and Cohesive Sand	34 - 74
□ Cohesionless Sand	39 - 47

Zone I
. Sand and Soft to Hard Clay
Average Workmanship

Zone II
a) Very Soft to Soft Clay
1) Limited depth of clay below bottom of excavation
2) Significant depth of clay below bottom of excavation but $N_b < N_{cb}$ (See Chapter 8)
b) Settlements affected by construction difficulties

Zone III
Very Soft to Soft Clay to a significant depth below bottom of excavation and with $N_b \leq N_{cb}$

Note:
All data shown are for excavations using standard soldier piles or sheet piles braced with cross-bracing or tiebacks.

Figure 2.8: Summary of settlement adjacent to open cuts in various soils, as function of distance from edge of excavation, after Peck, 1969

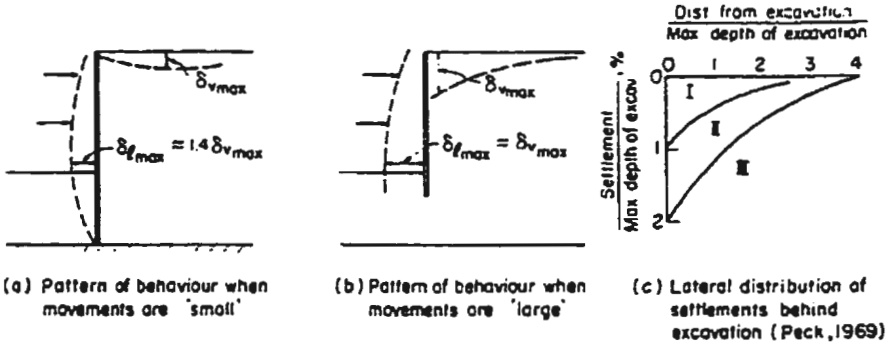

(a) Pattern of behaviour when movements are 'small'

(b) Pattern of behaviour when movements are 'large'

(c) Lateral distribution of settlements behind excavation (Peck, 1969)

Figure 2.9: Ground movements in the vicinity of an excavation, after Clough and Schmidt, 1981

2.2.4 Bottom heaving

Bottom heaving causes the upward movement of the vertical supports to the struts inside an excavation, which may result in the failure of the supporting system. It may be a symptom of the failure of the foundation. Therefore bottom heaving is taken very seriously. Unfortunately there has not been a systematical and reliable method to predict the possible failure of the foundation in terms of large bottom heaving. Bottom heaving is especially a serious concern for soft clay. This is because of its low strength and possible large deformations. There is a critical depth for deep excavation in soft clay, such that beyond this depth, excavation cannot be carried out.

A simple model for limit analysis was proposed by Terzaghi and Peck (1967). The analysis was carried out using the bearing capacity theory for shallow foundations. For an idealized situation, as in Fig. 2.10 the soil above the dredge line is regarded as the load and the soil below the dredge line as the foundation. The soil in the "foundation" is assumed to be weightless, frictionless and undrained, in other words, it is a $\phi = 0$ analysis. According to the theory, the bearing capacity, p_c, of the "foundation" is given as

$$p_c = cN_c + \gamma D_f N_q + \frac{1}{2}\gamma B N_\gamma, \tag{2.3}$$

where γ is unit weight, ϕ is internal friction angle and c is internal cohesion,

$$N_q = e^{\pi \tan\phi} \tan^2(\frac{\pi}{4} + \frac{\phi}{2}), \tag{2.4}$$

$$N_c = (N_q - 1)\cot\phi. \tag{2.5}$$

Assuming $\gamma = 0$, for ϕ=0 analysis, $N_c = \pi + 2$, or 5.14. Therefore

$$p_c = cN_c. \tag{2.6}$$

The load is γH. Therefore the safety factor is

$$F_s = \frac{p_c}{\gamma H} = \frac{cN_c}{\gamma H}. \tag{2.7}$$

Normally for $\phi = 0$ analysis, c is written as s_u.

A dimensionless number N_b is recommended to judge the stability of the "foundation", where

$$N_b = \gamma H / s_{ub}, \tag{2.8}$$

and s_{ub} is the undrained shear strength of the soil of the base. If N_b is less than 3.14, the soil would be in an elastic state, and the bottom is stable. When the number N_b is increased from 3.14, a plastic area appears. If N_b is increased until it reaches 5.14, or $F_s = 1$, then the bottom fails. Bjerrum and Eide (1956) proposed

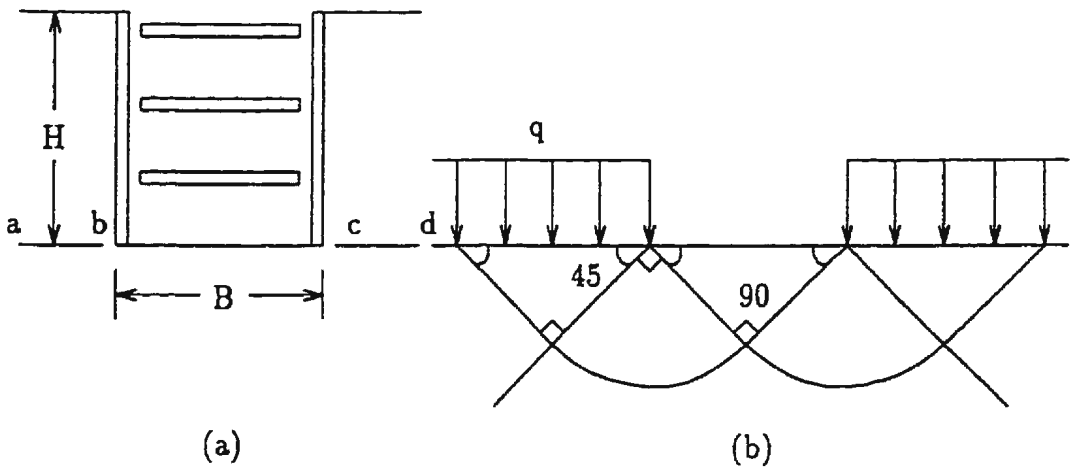

Figure 2.10: Stability of bottom heaving

a more realistic method to evaluate the possibility of the bottom failure, in which N_b ordinarily ranges from 6.5 to 7.5.

Tanaka (1994a) reported a braced excavation in soft ground in the Tokyo International Airport. The outstanding point of the project was that the total thickness of the soft clay layer of the site was over 50 m. However, the excavation was 35 m wide and 11 m deep. After considering different design methods, sheet piles were driven to the depth of 24.25 m. This implies that the sheet piles still "floated" in the soft clay although the length of the sheet piles doubled the depth of the excavation. As a result, large lateral displacements of the sheet piles and large heaving of the vertical support occurred. Consequently, the excavation work was stopped.

With the help of dewatering, the work was continued and finished successfully.

The author blamed the problem which arose in this project to the overuse of the soil strength in design. He pointed out that, earth pressures mobilized on the excavated side were considerably smaller than those based on Rankine's passive earth pressure theory. In his calculation, the strength parameters from the extension triaxial test instead of from compression were used. Yet the lateral displacement of the sheet piles was great enough to mobilize the passive earth pressure. That means that the mobilized shear strength in the excavated ground should be given by the undrained shear strength obtained from the triaxial extension test. The author also examined the effects of adhesion acting between the sheet pile and the ground, strength reduction due to swelling, strain rate and progressive failure, and differences in the confining conditions.

Tanaka (1994b) also reported another problem in the excavation in Tokyo International Airport. The dimension of the excavation was 19.5 m deep and 30.5 wide. The deposit of the soft clay was the same as in the previous problem. In order to improve the strength of the soil, a DM (Deep Mixing) method was applied to the soil at the bottom to increase its strength. In this method, a "stabilizer" (usually a mixture of Portland cement and water) is put into the ground and mixed with the soil in situ. However, when the excavation proceeded to the depth of 15.1 m, bottom heaving reached the value of 300 mm. This bottom heaving was measured on the vertical supports for the struts. This vertical movement of the supports could enable the struts to buckle. Although the bottom heaving was large, the displacement of the retaining wall was so small that the bending stress did not exceed

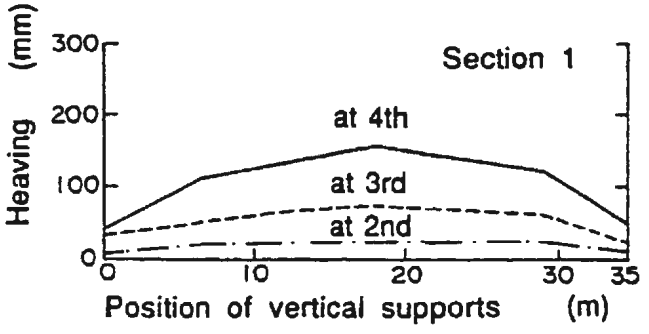

Figure 2.11: Bottom heaving, after Tanaka, 1994a

the allowable stress of the retaining wall, and the struts were also within the range of their allowable stress. The author concluded that the treated soil gave a high resistance against the horizontal force caused by the active earth pressure, but a low resistance against the vertical force caused by the reduction of the burden pressure from the soil in the back of the sheet piles. Finally the work was accomplished by lowering the ground level at the back sides of the excavation. Although the author recommended a new stability number, because of the difficulties of determining the strength of the soil at the bottom which had been treated with the DM method and several other uncertainty factors, application of this formula is not feasible.

Wong (1985) reported on using embankment piles driven into the bottom of an tie-back excavation to increase the stability of a 7.0 m deep excavation. The piles were long timber piles of 6 m in length and 100 mm in diameter. The spacing between the piles were 0.4 to 0.6 m. The author explained that the stability was increased by increasing the passive earth pressures, which was the result of an increment of the unit weight and shear strength of the mixed materials in front of the lower part of the sheet piles.

Clough and Schmidt (1981) presented the relation between the strength of the soil, the depth of excavation and the stability of the bracing system as shown in Fig. 2.12 and Fig. 2.13, where N is the stability number defined as

$$N = \frac{\sigma_{v0}}{s_u}. \tag{2.9}$$

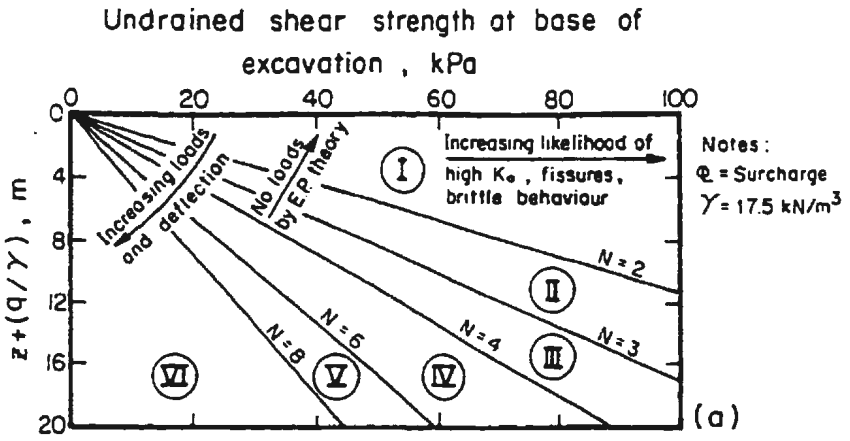

Figure 2.12: Classification chart for excavation, after Clough and Schmidt, 1981

σ_{v0} is the total overburden pressure at the bottom of excavation before excavation and s_u is the undrained shear strength of the soil. In the figures, q represents possible surcharge on the surface of the ground. The common surcharge is the load of mechanical equipment during excavation. γ is the unit weight of the soil.

In the figures, the stability lines divided the area into several zones and in each zone, a certain type of behaviour may be expected based on the nature of the stability criteria and past experience. For example, in zone I (Fig. 2.12), "it is uncommon for any type of excavation in clay to cause problems, since the factor of safety against shear failure of even an unsupported vertical slope is greater than 1.5. Increasing zone numbers indicates an increasing need for excavation support and probably more severe stability and deformation problems.

Fig. 2.13 shows the effect of the degree of overconsolidation. For normally

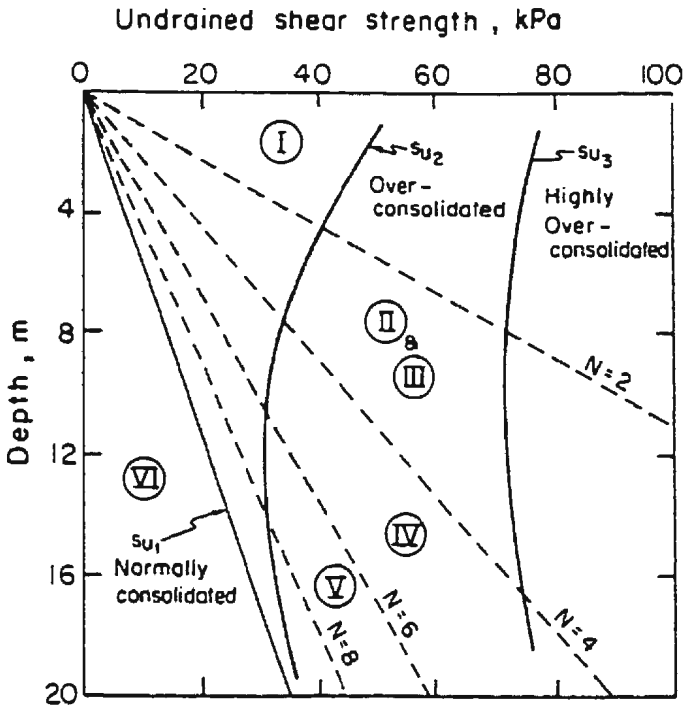

Figure 2.13: Relation between shear strength profiles and zones of excavation behaviour, after Clough and Schmidt, 1981

consolidated soil, there are always some possible problems and for highly overconsolidated soil, there are few problems.

Clough and Reed (1984) presented the relation between the factor of safety against basal heave and the maximum sheet pile deflection (Fig. 2.14), where the factor of safety is defined as,

$$F_s = \frac{cN_c}{\gamma H}. \tag{2.10}$$

The non-dimensional movements increase rapidly below factors of safety of 1.5 since yielding of the subsoil begins to dominate the response.

Peck (1969) pointed out that although the interdependence of settlement, lateral movement of walls, and upward movement of soil beneath excavation level is realized, no consistent theory has been developed to describe the transition from elastic to plastic states of a homogeneous material that extends from the ground surface to depths well below the zone of influence of the cut. He said, "promising starts have been made with the aid of finite element analyses." However, a finite element method needs a good constitutive model for the soil to be analyzed, and the parameters of the soil should be accurate enough. Unfortunately, although hundreds of model have been presented, there is none that can perfectly describe the behaviour of soil. The difficulties increase when the effects of the stress history and the initial stress state are taken into account. Furthermore, the parameters of soil are hard to accurately measure because it is impossible to obtain an undisturbed sample. Finally, it is difficult to check the results of the numerical analysis with the

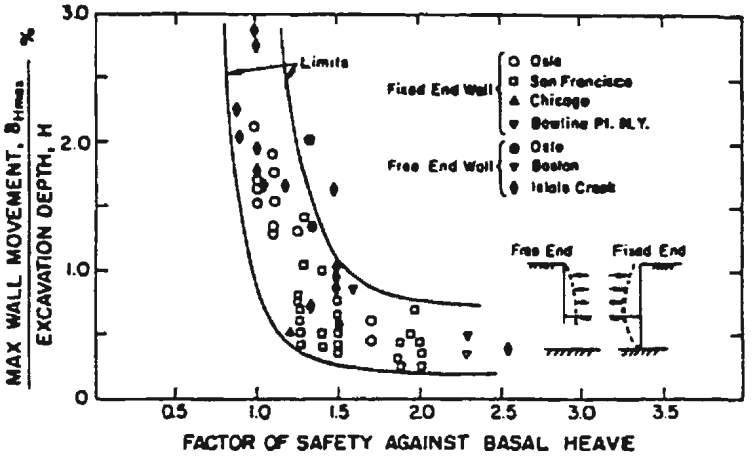

Figure 2.14: Non-dimensionalized lateral movements plotted against factor of safety against basal heave for Davidson Avenue and Rankine Street, after Clough and Reed, 1984

actual results of the excavation. This is because in a real excavation many factors affect the results, some of which are not controllable. One way to overcome this problem is to perform parametric studies. These allow the researcher to use the finite element model to examine a range of parameter values when the exact ones are unknown. Nevertheless, to obtain better data, one should perform controlled experiments such as centrifuge model tests.

2.3 Previous Studies

The analysis of a braced excavation is a complicated problem, since many factors affect the stability of the excavation. Three basic approaches have been taken in trying to understand this problem: site investigations, numerical analyses and experimental studies.

2.3.1 Site investigations

Almost all the attempts to predict the loads on the bracing system are related to full size field projects, because only in those actual projects, can researchers collect the required data and present a model for prediction. According to Flaate and Peck (1973), the earliest attempt may go to Baker. He analyzed the failure of several retaining walls for the excavation of the London Subway in 1881. The following researchers also wrote on similar topics: Meem, for the New York subways in 1908, Miller, for the Brooklyn subway in 1916. Later researchers are Mason and Hanger, who measured strut loads during the construction of the George Washington Bridge in the 1930's; Spilker, on the Berlin subway in 1937 and Prentice, on the New York subway in 1940.

Ohde's observations in 1938 were devoted to the use of wedge theory (Coulomb's method) in determine the earth pressures on sheet piles. Klenner (1941) assumed an equal distribution for the earth pressure in his work on the Berlin subway. Following Klenner, Terzaghi (1941) revised this diagram. A different design in

the form of a trapezoidal distribution was presented by Lehmann (1942) and a triangular distribution by Tschebotarioff (1951). Upon his experience in Chicago in 1939, Peck (1943) presented the early shape of "apparent earth pressure" diagrams. Another attempt was made by Skempton and Ward (1952) in measuring the strut loads in the cuts in soft and sensitive clay at Shelhaven, England.

A special contribution was made by the Norwegian Geotechnical Institute in constructing the Oslo Subway from 1957 through 1962. They conducted a series of comprehensive studies on the problems of excavation and produced several technical reports on strut loads, sheet pile deflections, earth pressures and the displacement of the ground. Upon these results, Kane and Kjaernsli (1963) presented their diagrams for design. These data were also summarized by Peck in his state-of-art report in 1969.

In this report, Peck presented the apparent earth pressure diagrams for design, in which, only the undrained shear strength of the soil was taken as a parameter for calculation. He also analyzed the sheet pile deflections and bottom heavings. He presented the data of surface settlement collected from the sites of Oslo and Chicago.

Bjerrum et al (1972) made a state-of-the-art report on earth pressures on flexible structures in the Fifth European Conference on Soil Mechanics and Foundation Engineering. They reported that: the general validity of Peck's trapezoidal rule has been confirmed by numerous observations carried out in cuts in sand, in sandy clay and even in stiff clay. They stressed that the procedure proved, however, to

be far less satisfactory when applied to soft or medium clay.

Wilson (1992) conducted a comprehensive study on the earth pressures in soft clay in his Ph.D. thesis entitled "The behavior of a deep retained excavation in soft San Francisco Bay Mud". He pointed out that "Site congestion, access and protection of public utilities present design problems which are unique to this type of bracing system." In the thesis, he collected a lot of data from the construction site, and presented a distribution called the Tributary Area Method. He concluded, "With respect to the five earth pressure models selected for comparison, those with a triangular shape performed very slightly better in the prediction of struts loads than did the trapezoidal diagrams."

These envelopes provide a base for engineers to design a braced excavation. However as pointed out by Fernandes et al (1994) these design recommendations are less detailed and vague. For example they cannot provide a clear picture of the actual earth pressure on the sheet piles. Even for the maximum strut loads, they are not clear in determining the value for layered soil. For a deposit composed of sand and clay, two problems arise: (1) should the loads be calculated according to the diagram for sand or for clay; (2) how to decide the undrained shear strength (c_u) in the calculation. It seems that the maximum loads have nothing to do with the deformation property of the soil and also nothing to do with the stiffness of the sheet piles, the stiffness and distribution of the struts.

Bottom heaving was first considered by Terzaghi, and the data collected from Oslo and Chicago were summarized by Peck (1969). Although a theoretical analysis

was presented, the assumptions were too far from the actual situation. The results were not satisfactory. Heaving is more likely to be a problem of deformation instead of strength. Sometimes it is hard to tell how much of the deformation is elastic and how much plastic.

Tanaka (1994a) reported several problems of bottom heaving in the braced excavation in soft ground at Tokyo International Airport. He explained that the strength of soil at the bottom of the excavation plays an important role in the stability of the bottom. He also reported using the "deep mixing" method in improving the strength of the soil at the bottom to prevent the bottom heaving (Tanaka, 1994b). The methods were also adopted by Wong et al (1987) and Woo (1994).

Surface settlement has been a concern for its importance in the possibility of damage to nearby structures including buildings. Interest in this problem grew at the beginning of 1960s. Many observations have been carried out and data collected from Oslo and Chicago. These were summarized by Peck (1969). O'Rourke (1976) conducted a comprehensive study of this problem for the U.S. Department of Transportation. Schlosser et al (1985) made a comprehensive summary on this problem in the Eleventh International Conference of Soil Mechanics and Foundation Engineering. However because of the complexity of the problem, it seems that only numerical analysis may provide a feasible approach to the problem.

In fact, this problem does not only depend on a simple factor such as the undrained shear strength. Bjerrum et al (1972) pointed out that the load in a strut

depends not only on the soil properties but also on the construction procedure. "Even with a uniform construction procedure the details involved in the installation of the individual struts can vary so much that there can be an appreciable difference in load between the various struts at the same level." Temperature changes resulting from weather can greatly affect the properties of the soil and the struts. As a result, the load on the struts and the sheet piles can be very different. In the empirical method, the undrained shear strength is taken as the only factor to determine the pressure distribution. The actual strength is different from the value obtained with vane tests.

In addressing the shear strength of soft clay, Bjerrum et al said, "it cannot always be taken for granted that the undrained shear strength determined by vane tests is equal to the shear strength which can be mobilized in the field". On the contrary , "the vane strength in general is greater than the field strength, and the difference was found to increase with the plasticity of the clay." Laboratory tests on soft clays have demonstrated that the more rapidly the load is applied, the greater is the shear strength measure. Another factor of great importance for a correct evaluation of the undrained shear strength of soft clay is anisotropy. Tests indicate that clay does not show the brittle behaviour in extension which it exhibits in compression. The undrained shear strength of normally consolidated clays is thus not a constant, but varies with the direction in which the stresses are applied. The ability of the structure to resist shear stresses is therefore greater if the shear stresses are acting in the same direction as the in-situ shear stresses and is smaller if the stresses are applied in such a way that the shear stresses are reversed relative

to the in-situ stresses. Therefore two correction factors are recommended to modify the results of a vane test in order to obtain the undrained strength for the analysis of earth pressures on sheet piles in Peck's method.

Moreover surface settlement and the bottom heaving depends very much on the deformation properties of the soil. Therefore, a comprehensive understanding of the problem is necessary in terms of the stress-strain history of the soil and the bracing system. As a theoretical solution cannot be found, numerical analysis becomes a good method in approaching the problem.

2.3.2 Numerical approaches

Many of researchers have contributed to the finite element analyses of the problem of braced excavations. In the 1970s this research became more popular as a result of engineering requirements and more convenient computational techniques. Palmer and Kenney (1972) conducted a parametric study of braced excavations where the soil was simulated by an elastic model. Murphy and Clough (1975) used an undrained, nonlinear pseudo-elastic model to simulate the excavation in varved clay where the surface loading on both sides of the sheet piles were accounted for. The results of sheet pile deflections and strut loads were compared with the measured data from the site. The discrepancy seems reasonably satisfactory. Mana (1978) used an elasto-perfectly plastic model in simulating the behaviour of the undrained clay. His comparison focuses on the deflection of the sheet piles and surface settlement. It seems that the results do not match each other very well. Borja (1990) compared the deflection of sheet piles and pore pressures. He used

the Modified Cam-clay model, and the results seemed in good agreement.

Finno et al (1989) reported a detailed observation of the performance of a deep excavation in clay in Chicago. Then, Finno and Nerby (1989) evaluated the effects of a given set of construction procedures on the soil response by monitoring the strain fields that developed within a soil mass adjacent to an excavation at various stages of construction. They warned that the ability to make a priori predictions of the behavior of braced excavations in clay was limited by an ability to predict a contractor's behaviour that affected the loads applied to the soil (e.g., excavation scheme, amount of preload, workmanship, etc.), as well as an ability to faithfully represent the in situ response of the soil. Later, Finno and Harahap (1991) presented a simulation of construction of a braced excavation in saturated clay by using a coupled finite element formulation. Also, Finno et al (1991) presented a parametric study of a braced excavation based on a coupled finite element formulation. Effects of the constitutive model, boundary conditions, and details of the construction process including sheet pile installation and amount of over excavation are considered in the analyses. In the approach for sheet pile installation, Harahap (1990) assumed that the sheet piles were in position in the soil before excavation and moved backward by an amount equal to one-half the equivalent sheet pile thickness. This approach was to simulate the disturbance of the soil resulting from the dynamic driving.

Instead of using the term of "workmanship", Smith and Ho (1992) used the phrase "construction technique" to describe the factors which affected the stability and deformation of an excavation, such as the stiffness of struts, the depth of each

excavation step and the order of placement of the struts. They used the finite element method to do the numerical analysis. Sheet piles were represented with a column of thin elements of 0.125 m thick. The interfaces between the sheet piles and the soil were also modelled with columns of thin elements on either side of the sheet piles. All the elements were eight-node isoparametric elements formed using reduced 2×2 Gaussian integration. Struts were simulated by adding springs. The soil was simulated with an elastic-perfectly-plastic Mohr-Coulomb model with $\phi_u = 0$. The dimension of the excavation was 30 m wide and 9 m deep. Sheet piles were driven to the depth of 24 m. Four struts were applied.

Several different methods were selected to carry out the excavations including those ideal methods which cannot be realized. In such a way, they compared the results of the numerical analysis. These methods were:

> "Method A: the first and the fourth struts are inserted against the sheet pile wall before the main excavation takes place.
>
> Method B: struts are inserted ahead of the excavation but one at a time. This models the "trench method" suggested by Peck.
>
> Method C: similar to Method B but more struts are placed, hence reducing the vertical spacing between them.
>
> Method D: excavation takes place before struts are inserted, stage by stage."

Two strut stiffnesses were chosen in each case, namely "high" of the order 20,000 kN/m and "low" of the order 2000 kN/m.

Their conclusions were:

> "Whatever soil model is chosen, the technique of construction is at least as important as the characterization of the ground. In principle, collapse

depths and bracing deformations and loads at working depths have been shown to be functions of the efficiency of bracing. Specific computations of deformations and bracing loads at working depths have been compared with field measurements in a class C1 'prediction'.

In the field example, agreement between computation and measurement has been found on the assumption that a relatively 'flexible' form of construction (late insertion of struts of low stiffness) was that adopted on site. By extrapolation, this conclusion is unaltered by the possibility that the bending stiffness of the piling was even lower than that assumed in the computations. Indeed, for some techniques of construction the influence of the wall stiffness is very small.

Deformations in the case history were large, and ultimately would have led to some plastic yielding in the piling. These effects have also been included in the computations. At full excavation depth, pile deflections could have increased by one-third due to pile yield. In addition, major redistributions of bending moments could have led to three positions of potential hinge formation."

Ng (1992) studied the problem of a multi-propped excavation in his Ph.D. thesis. He monitored the performance of the 10 m excavation in Gault soil in the Cambridge area and compared with the results of a finite element analysis where the brick model for soil presented by Simpson (1992) was used.

Hashash and Whittle (1996) carried out a series of finite element analyses for excavations in clay. Hashash (1992) performed his Ph.D. research in this area. Their analysis was based on their "comprehensive effective stress soil model (MIT-E3)". They claimed that this model may "describe important aspects of clay behavior, including small-strain nonlinearity and anisotropic stress-strain-strength". The soil was in a constant overconsolidation ratio and the shear strength and stiffness of the soil were proportional to depth.

A three dimensional analysis was first carried out by Tsui and Clough (1974) to

investigate the three dimensional effects on the struts. Their conclusion was that the discrepancy between two dimensional and three dimensional analyses increased with the horizontal distances between the struts, the stiffness of the sheet piles and the strength of the soil. Recently three dimensional analyses have been carried out for sandy and clayey soil deposits (Ou and Lai, 1994) and for column type improvement for bottom soil for minimizing the ground settlement (Ou, Chiou and Wu, 1996; Ou, Wu and Hsieh, 1996).

There are different theories as to the mechanism of the forces and stresses acting on and within the sheet pile structures as well as their deformation. Bjerrum et al (1972) suggested that "the total pressures on excavation bracing systems generally is controlled by the shear strength of the soil, while the distribution of the earth pressures is determined by arching."

Although various factors affect the stability of the bracing excavation, two important factors are worthy of discussion, the first is the workmanship and the second is the adoption of the strength of the soil. As we know from the previous work of some researchers that the stability of the excavation structures not only relies on the strength but more importantly on the deformation properties of the soil. Therefore model tests are urgently needed to examine the details of the excavation work, and to check the validity of the use of numerical methods to predict the behaviour of the structures.

2.3.3 Experimental approaches

The experimental approach to this problem becomes the weakest point in the research of the problem. This is because of the complexity of the problem, especially procedures in realizing a braced excavation. Yet the physical experiment is an efficient method in obtaining practical data for forming a theory for design and proving the efficiency of the results of numerical methods.

The common approach in the experimental method is to observe and monitor the actual sites of excavation. However the collected data is hard to interpret because the deposit and properties of the soil cannot be determined with sufficient accuracy, especially the stress-strain history of the soil which cannot, in general, be known. Under this situation, the data cannot be reasonably interpreted.

The experimental approach for braced excavations was reported in the 1994 International Centrifuge Conference. Zhang and Zhang (1994) reported a centrifuge simulation for braced excavations in muddy clay using diaphragm walls. A piece of perpex of 8 mm thick was used to simulated the concrete diaphragm wall of 0.8 m under the acceleration of 150 g. The height of the perpex was 20 cm to simulate the prototype of 30 m. Red copper pipes of 5 mm in diameter and 1 mm in thickness were used to simulate the struts. Pre-stress was applied with screws. Micro earth pressure cells and piezometers were buried in the soil. Excavation was carried out by stopping the machine several times and excavating the soil to the required depths. The excavation continued till the bottom heaving was found in plastic deformation. In that case, only one more excavation was made. The same

technique of excavation was also used by Liu et al (1994) in simulating a major underground excavation supported with a reinforced concrete diaphragm retaining walls.

2.3.4 Closing remarks

Since 1948, there have been dozens of international or regional conferences totally or partly devoted to the problem of excavations including braced excavations. The year of 1969 seems a milestone, when Peck summarized the data collected from different sites of Oslo and Chicago and presented a method to calculate the possible maximum pressure on the sheet piles, loads in the struts and a method to estimate the possible maximum settlement of the ground surface. Indeed, textbooks have been teaching these methods and engineers have been using them in practice. However, as early as 1970, Lambe pointed out that the state-of-the-art was far from good. He also pointed out that there were a number of weaknesses in the earth pressure theory and it is difficult for engineers to predict the loads in the struts, the movement in the struts and the settlement of the ground with any accuracy according to the theory. In order to improve the situation, he suggested "the evaluation of the actual performance of thoroughly instrumented field cases" (Lambe, 1970). Since then, many contributions have been made in applying the finite element method, and some cases of field observation have been reported. Unfortunately because of the complexity of the soil deposit in the sites, the procedures of the construction and the un-estimable effect of construction technique and weather, the limited data obtained from the monitoring in the sites cannot

be interpreted with confidence. As a result, progress in this aspect of geotechnical engineering is very slow.

Chapter 3

CENTRIFUGE MODELLING

3.1 Theoretical Considerations for Centrifuge Modelling

The centrifuge is a model testing technique. This technique uses high acceleration resulting from the centripetal force in a revolving body to simulate a gravitational force. High speed revolution provides high centripetal acceleration, which may be hundreds times that of gravity. In such a way, a revolving body may be subject to an acceleration hundreds of times that of normal earth gravity in the direction of radius. If this direction is taken to be the vertical direction of a soil sample, the distribution of the stress of self-weight of hundreds of meters of soil can be simulated. This idea can be traced back to the 19th century (Craig, 1989), but the actual application was realized in this century. In the 1930's, a number of applications were carried out in the Soviet Union. In the 1960's the University of Manchester and the University of Cambridge made many new developments in

applying this technique to geotechnical engineering (Row, 1975, Schofield, 1980). Since then many centrifuge centers have been built in the United States, Canada, France, Japan, China, Singapore and other countries.

As a model is rotated horizontally at a high speed, the model will be subject to a centripetal acceleration of

$$a_i = \omega^2 r, \tag{3.1}$$

where ω is the angular velocity of the rotation and r is the centrifuge radius. If this acceleration is N times of gravity, the prototype may be simulated with a model of scale $1/N$. Usually N may be 100 to 200. Therefore, a small model can simulate a prototype of 100 to 200 times in scale.

As the geometrical ratio is $1/N$ and gravitational ratio is N, other scale relations can be derived though dimensional analysis or governing differential equation analysis. Table 3.1 shows the scaling relations of some variables.

It is noticed that the time factor can be different depending on different simulations. If the process is controlled by the consolidation of soil, the scale factor is $1/N^2$. However if the purpose of the test is to simulate a dynamic problem the scale factor is $1/N$. If both behaviors are simulated, one solution is to change the unit weight of the liquid.

For geotechnical practice, the soil and the structures are normally subject to

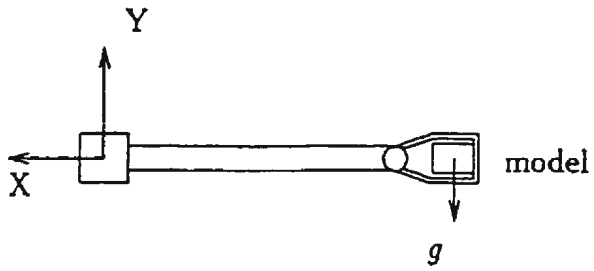

elevation view

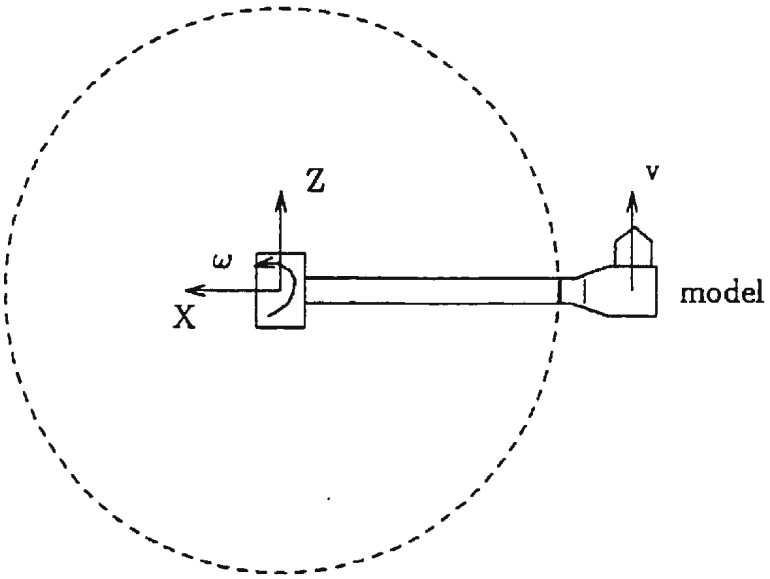

plan view

Figure 3.1: Flight of a centrifuge model

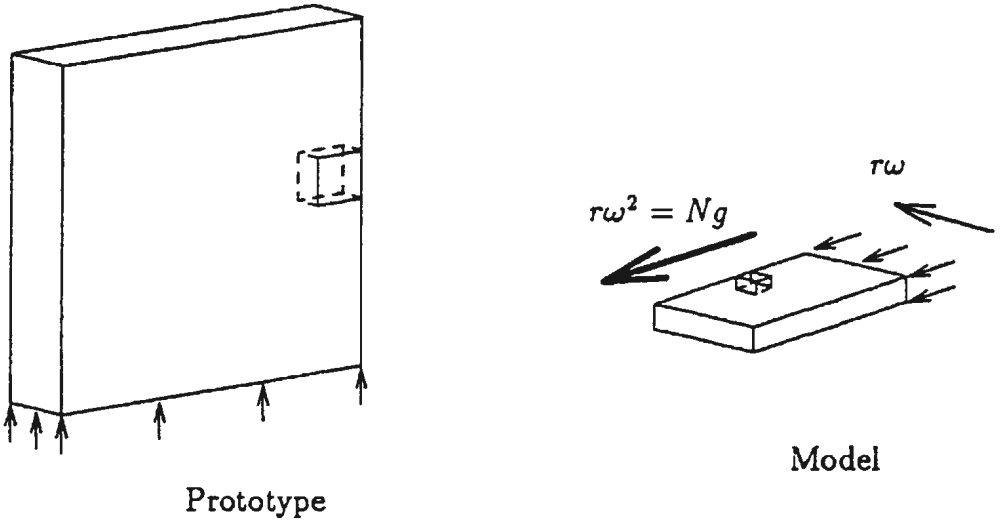

Figure 3.2: Weight; gravity effects in a prototype are identical to inertial effects in a centrifuge model, after Schofield, 1980

Table 3.1: Scaling relations, after Scott and Morgan, 1977

Quantity	Prototype	Model at Ng
Length	N	1
Area	N^2	1
Volume	N^3	1
Velocity	1	N
Mass	N^3	1
Force	N^2	1
Energy	N^3	1
Stress	1	1
Strain	1	1
Mass density	1	1
Energy density	1	1
Time		
Consolidation	N^2	1
Dynamic Events	N	1
Viscous Flow	1	1
Frequency	1	N

gravitational acceleration towards the ground. However, in centrifuge tests, while the body is rotating around the center in a plane, the body is not only subject to the acceleration along the radial direction, it is also subject to other accelerations. These accelerations imply that extra forces are applied to the model. These extra forces should be limited to as low a value as possible. Therefore it is necessary to study the extent of the impact of these accelerations (Schofield, 1980, Liang, 1985, Powrie, 1986 and Taylor, 1995).

1. In a centrifuge test, a model is subject to normal gravity in addition to the centripetal acceleration. The resultant acceleration is shown in Fig. 3.3. The model is normally designed and placed taking the bottom of the chamber as the bottom of the model. As can be seen in Fig. 3.3, the resultant acceleration is not perpendicular to the bottom of the model, in other words, the acceleration is not vertical in the prototype. The angle α between the resultant acceleration and the "vertical" direction of the model is about

$$\tan\alpha = \frac{1}{N}. \tag{3.2}$$

In this study, $N = 72$, therefore $\tan\alpha = 0.0139$ and $\alpha = 0.80°$.

For a small value of N, a special design may be made to allow the resultant acceleration to be perpendicular to the bottom of the model (not to the bottom of the chamber) and this discrepancy may be eliminated. But for a large value of N, the effect is neglected and the error still exists.

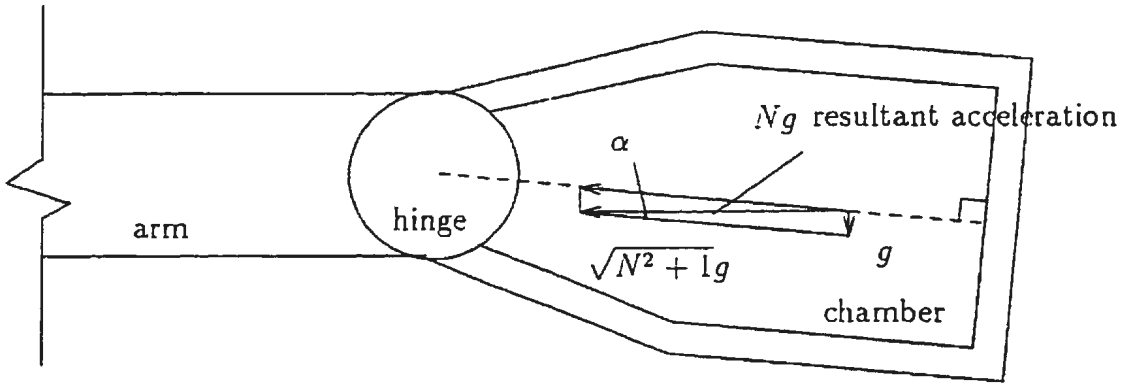

Figure 3.3: Effect of gravity in a centrifuge model

2. Along the tangential direction of the rotation, the velocity is not constant. The velocity must be increased at the beginning of the test for the model to reach the required centripetal acceleration. As a result, the model is subject to forces in the lateral direction at the beginning of the test, the magnitude depends on the time to reach the required acceleration. As this force is extra, normally the acceleration for increasing the velocity is kept below a limit.

3. Along the depth of the model, the acceleration is not the same. As the model is rotating with an angular velocity of ω, the acceleration at a radius r is shown in the equation of 3.1, that is

$$a_i = \omega^2 r. \tag{3.3}$$

Therefore, at a depth of z in the model, the acceleration is

$$a_i = \omega^2 (R_t + z). \tag{3.4}$$

where R_t is the radius of rotation at the surface of the model (or soil). In prototype, in homogenous soil, the incremental magnitude of vertical stress in a micro element at depth z is

$$d\sigma_{vp} = \frac{\gamma dV}{dA} = \frac{\gamma dx dy dz}{dx dy} = \gamma dz = \rho g dz, \tag{3.5}$$

and

$$\sigma_{vp} = \int_0^z \rho g dz, \tag{3.6}$$

where ρ is the density of the soil. Therefore in a centrifuge model, the "vertical" stress along the depth z in the soil is

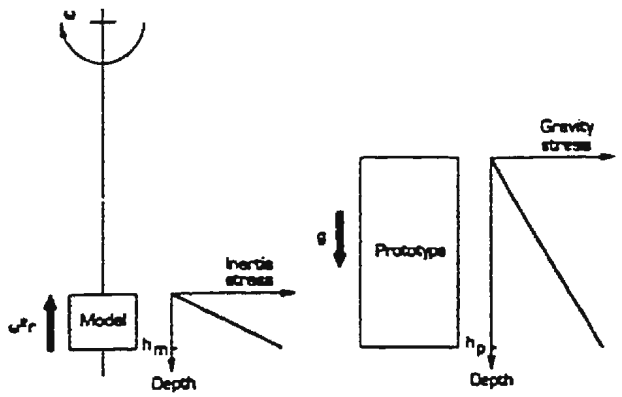

Inertial stresses in a centrifuge model induced by rotation about a fixed axis correspond to gravitational stresses in the corresponding prototype.

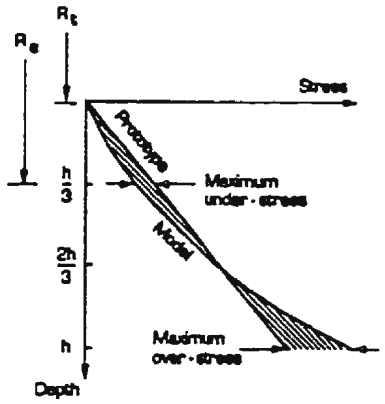

Figure 3.4: Comparison of stress variation with depth in a centrifuge model and its corresponding prototype, after Taylor, 1995

$$\sigma_{vm} = \int_0^z \rho\omega^2(R_t + z)dz = 2\rho\omega^2 z(R_t + \frac{z}{2}). \tag{3.7}$$

This is shown in Fig. 3.4. The variation of the stress along the depth is parabolalic and not a straight line as the self weight of the soil in the prototype. Therefore an effective depth of h_e for the model (or an effective radius R_e for the rotation) should be defined for applying the Ng acceleration, so that

$$R_e = R_t + h_e \tag{3.8}$$

and

$$Ng = \omega^2 R_e. \tag{3.9}$$

There are different ways to determine this depth depending on the extent of the soil of concern to the experimentalist. If the whole depth is needed, the effective depth may be determined by requiring that the maximum magnitudes of under- and over-stress are equal. As a result, the effective depth is

$$h_e = \frac{h_m}{3} \tag{3.10}$$

and

$$R_e = R_t + \frac{h_m}{3}. \tag{3.11}$$

In other words, at the depth of $h_m/3$ or radius of $R_t + h_m/3$ the acceleration Ng is applied (Taylor, 1995).

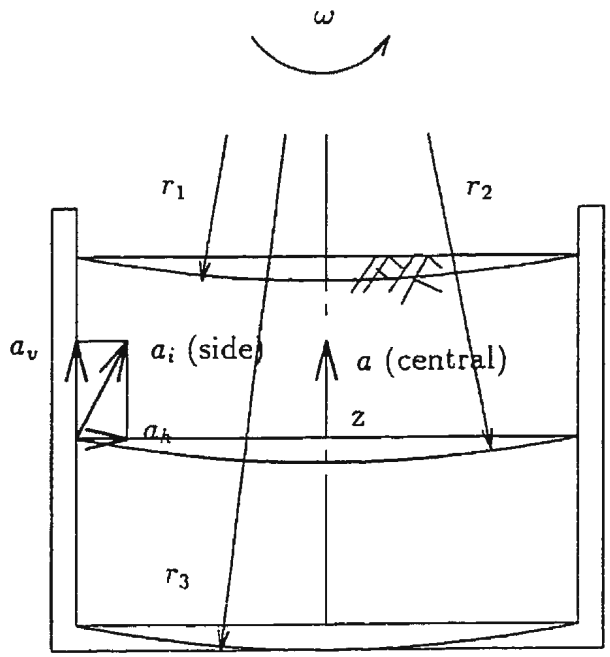

Figure 3.5: Surfaces of equal centripetal accelerations

4. As the model rotates with a constant angular velocity, the acceleration at the same radius is the same. However, at a constant depth within the model, the acceleration varies. A fixed radius traces out an arc, but in designing a model, the surface and the bottom are taken as flat surfaces rather than arcs. Therefore there is a discrepancy in the acceleration at the same depth of the model, and by default, the center section of the model is taken as representative.

At the depth of z (Fig. 3.5), in the center section, the radius is $R_t + z$, and the acceleration is

$$a_i = \omega^2(R_t + z). \tag{3.12}$$

However on the side wall, with the same depth z, the radius changes into $r_2 = \sqrt{(R_t + z)^2 + (b/2)^2}$, and the acceleration is

$$a_i = \omega^2\sqrt{(R_t + z)^2 + (\frac{b}{2})^2}. \tag{3.13}$$

This acceleration can be resolved into two components, one is "vertical" and the other one is "horizontal". The "vertical" component has the same value as the acceleration in the center section and the "horizontal" value is

$$a_h = \omega^2\frac{b}{2}. \tag{3.14}$$

There is no "horizontal" acceleration applied to the soil in the center section. For this study, the model has dimensions of width, 300 mm and depth 373 mm, the radius varies from 5065 to 5438 mm. The angular velocity is 111.4 rpm or 11.7 rad/s, the "horizontal" acceleration is constantly 20.5 m/s^2, which is 3.0% of the acceleration in the center section in the surface and 2.8% the acceleration at the bottom.

In order to reduce the effect of the horizontal acceleration, it is better to adopt the data in and close to the center section of the model for a planar strain problem. Some researchers have curved the surface of the soil and even changed the shape of the model to eliminate the effect.

5. As the soil and the structure deform during the test, there is a velocity of displacement. Normally this is small and can be neglected. However in some cases the velocity is large and cannot be neglected such as seepage in the soil and drainage in the model. As a particle moves in the plane of rotation, a Coriolis acceleration results. For a particle moving in the centrifuge chamber with a velocity of V_R, the total acceleration in the inertial frame is:

$$\mathbf{a}_I = \mathbf{a}_R + 2\omega\mathbf{V}_R + \omega^2\mathbf{r}_R, \tag{3.15}$$

where $\mathbf{a}_R$ is the acceleration of the particle in the rotating frame, $2\omega\mathbf{V}_R$ is the Coriolis acceleration and the last term is the centripetal acceleration. ω is the angular velocity of the rotation, $\mathbf{V}_R$ is the linear velocity that has the same value of the particle referring to the rotating frame but its direction perpendicular to the velocity of the particle. $\mathbf{r}_R$ is the position of the particle referring to the rotating center. The Coriolis acceleration is significant (Pokrovsky and Fyodorov, 1968), if

$$\frac{r\omega}{20} < V_R < 2r\omega, \tag{3.16}$$

where r is the radius of rotation and ω is the angular speed of rotation. Taylor said: "it is generally assumed that Coriolis effects would be negligible if the ratio

$$\frac{a_c}{a_i} = \frac{2\omega V_R}{\omega^2 R_e} \tag{3.17}$$

was less than 10%."

In this study, the radius is 5.065 m at the bottom of the soil and ω is 111.4 rpm or 11.7 rad/s, the velocity of seepage is about 1.95×10^{-7} m/s, the ratio is 1.7×10^{-7}, which is far less than 10%. Therefore the effect of Coriolis acceleration is negligible.

The centrifuge tests can be easily managed, are more reliably controlled and less expensive to operate than prototype tests. The advantages and limitations are as the followings (Liang, 1979):

Advantages:

- Boundary conditions (both deformation and drainage) are well defined;
- Spatial variations and uncertainties of material properties can be minimized by careful model preparation;
- The effects of various stress histories, stress paths, and geometry conditions can be studied;

- Time-dependent problems such as consolidation can be studied in a short period of time;
- Measurement of responses such as deformation and pore pressure variations are easy and accurate.

Limitations:

- Careful model construction procedures are required to simulate the prototype structure;
- The gravity field in the centrifuge is radial and the vertical stress distribution deviates from a straight line stress distribution;
- Boundary restraints may distort the actual behaviour of the model.

The centrifuge has been applied to the following geotechnical problems:

- landslide and slope stability;
- shallow foundations;
- deep foundations;
- earth retaining structures;
- dams and embankment;
- tunnelling;

- offshore structures;
- earthquake problems.

There are three advantages of centrifuge modelling in braced excavation:

1. Although braced excavations have been widely used in engineering practice, the design method is quite empirical. The design diagrams are based upon observational data in practical engineering. However, each project is different, not only in the properties of the soil but also in the construction technique. For example, the span of the time between the excavation of a layer of soil and the application of struts for that layer, may result in different magnitude of displacements of the sheet piles as well as the settlement of the ground. Centrifuge tests may simulate braced excavations in different conditions and the conditions could be strictly controlled.

2. Another important factor that affects the strength of the soil is the pore pressure. This data has not been systematically obtained. Yet sometimes, the pore pressure is a fatal factor for the stability of a sheet pile supporting system.

3. Although numerical methods have been applied to the analysis of the deformation and stability of braced excavations, there are still two problems they cannot solve satisfactorily. These problems are overconsolidated clay and unsaturated clay. With the help of centrifuge tests, the behavior of these soils could be simulated for braced excavations.

The items to be measured are:

- the stress in the sheet piles and the load in the struts;
- the earth pressure and pore pressure acting on the back of the sheet piles;
- the pore pressure in the soil;
- the settlement of the ground surface;

Because of the difficulties with the model, the horizontal displacement of the sheet piles and the bottom heaving are not measured.

3.2 General Considerations for Centrifuge Modelling

3.2.1 Introduction

It is a complicated task to design a centrifuge model. Not only should the geometrical dimensions be carefully selected, the physical factors should also be carefully considered. These mechanical factors include the stress field, stress history , stress path, boundary conditions, and the size of the soil particles and even the size of the centrifuge machine. Therefore it is important to know the difference between the results of the model tests and the situation in an actual site.

3.2.2 Size of soil particles

As the centrifuge may simulate a prototype hundreds of times larger than the model, a soil particle with a size of 0.1 mm would simulate a dimension of a particle of 10 mm in a centrifuge of $N = 100\ g$, which means a sand particle in the model would represent gravel in the prototype, or the clay in the model would represent sand in an actual site. However, clay, sand and gravel are in different categories in the classification of soil, in other words, their mechanical properties are totally different. This causes a contradiction for the simulation of soil particles.

It is obvious that the soils of different types cannot simulate each other. Clay should be simulated with clay and sand should be simulated with sand. If the previous rules apply, the clay and silt in actual sites cannot find a proper type of

material to simulate them. Actually no matter if the material is sand or clay, we use the same material in the model as that in the sites to obtain the same property parameters in designing the experiments, and expecting the same mechanical response. If the mechanical response of the soil in the model is the same as it is in the prototype, the scaling of the particle sizes is not important.

Bolton and Lau (1988) prepared two samples of sand: a silica flour and a flint grit, where the particle size of the silica flour ranged from 0.006 mm to 0.06 mm and that of the flint grit ranged from 0.4 mm to 3 mm. The grading curves for them were parallel to each other but the grain sizes had a factor of 50. Both samples have the same initial void ratio of 0.55. The triaxial tests showed that, during the tests, the variation of internal friction angles with the axial strains were similar to each other. Centrifuge tests of 50 g were conducted for the two sands under the action of circular footings, and the results were similar and comparable with the results of 1 g tests. This proves that if the same fabrics are prepared for the soil in the same category, the results are similar. This implies that the particle size is not a problem for the centrifuge tests and need not to be simulated to the simulation law. In other words, samples from sites can be used in the centrifuge for simulation.

For uniform sand foundations, Fuglsang and Ovesen (1988) reported that if the ratio of the model width to the average grain size is above 25 for the circular footings, there is no discernible effect resulting from the particle size. If the ratio is lower than 15, there is an obvious effect of particle size.

3.2.3 Consolidation and permeability

The speed of consolidation is increased N^2 times in the centrifuge. The reasoning begins with Terzaghi's theory of consolidation, in which the dimensionless time factor T_v is defined as

$$T_v = \frac{c_v t}{H^2}, \tag{3.18}$$

where c_v is the coefficient of consolidation, t is time and H is a distance related to the drainage path. For the same degree of consolidation in a model and prototype, T_v is the same and

$$\frac{c_{vm} t_m}{{H_m}^2} = \frac{c_{vp} t_p}{{H_p}^2}, \tag{3.19}$$

since $H_p = N H_m$, there is

$$t_m = \frac{1}{N^2} \frac{c_{vp}}{c_{vm}} t_p. \tag{3.20}$$

It is assumed that $c_{vm} = c_{vp}$ if the soil in the model is the same soil in the prototype. Thus

$$t_m = \frac{1}{N^2} t_p. \tag{3.21}$$

This is a great advantage since the required time for consolidation of a model with very low permeability is shortened.

However, in Terzaghi's theory,

$$c_v = \frac{1 + e_0}{\gamma_w a} k, \tag{3.22}$$

where e_0 is the initial void ratio of the soil, γ_w is the unit weight of the water, k is the permeability, and a is the coefficient of compression. e_0 and a may be regarded as the same in the prototype and the model. However, γ_w increases N time in the centrifuge. In order to keep c_v the same in the model and the prototype, it is necessary to increase the permeability of the soil in the centrifuge.

For a three dimensional problem, the Biot theory may be used to analyze the problem, and the problem of scaling factor is focused on the equation of continuity of flow (Wang, 1983),

$$\frac{k}{\gamma_w} \nabla^2 u = -\frac{\partial \epsilon_v}{\partial t}, \tag{3.23}$$

where u is the excess pore pressure and ϵ_v is the volume strain. This equation is the result of an application of Darcy's law. For the prototype, the equation can be written as

$$\frac{k_p}{\gamma_{wp}}\nabla^2 u_p = -\frac{\partial \epsilon_{vp}}{\partial t_p}, \tag{3.24}$$

and

$$\nabla^2 = \frac{\partial^2}{\partial {x_p}^2} + \frac{\partial^2}{\partial {y_p}^2} + \frac{\partial^2}{\partial {z_p}^2}. \tag{3.25}$$

For the model, the equation is

$$\frac{k_m}{\gamma_{wm}}\nabla^2 u_m = -\frac{\partial \epsilon_{vm}}{\partial t_m}, \tag{3.26}$$

and

$$\nabla^2 = \frac{\partial^2}{\partial {x_m}^2} + \frac{\partial^2}{\partial {y_m}^2} + \frac{\partial^2}{\partial {z_m}^2}. \tag{3.27}$$

Because

$$x_p = Nx_m, \qquad y_p = Ny_m, \qquad z_p = Nz_m, \tag{3.28}$$

and

$$u_p = u_m, \qquad \epsilon_{vp} = \epsilon_{vm}, \tag{3.29}$$

the equation of prototype can also be written as

$$\frac{1}{N^2}\frac{k_p}{\gamma_{wp}}\nabla^2 u_m = -\frac{\partial \epsilon_{vm}}{\partial t_p}. \tag{3.30}$$

If $k_m = Nk_p$, and $\gamma_{wm} = N\gamma_{wp}$, in other words, $k_p/\gamma_{wp} = k_m/\gamma_{wm}$, then from the equation of continuity, there should be

$$t_m = \frac{t_p}{N^2}. \tag{3.31}$$

The variation of permeability of soil was discussed by Taylor (1995). It is obvious that the velocity of seepage in the centrifuge is increased. This phenomenon can be recognized by examining the function of the spin drier of a washing machine. With Darcy's law, there is

$$v = ki, \tag{3.32}$$

where i is the hydraulic gradient. As to which factor makes the velocity increase, there are two opinions.

One opinion comes from the intrinsic permeability of soil, which is

$$K = \frac{\nu k}{\rho g}, \tag{3.33}$$

where K is the function of the fabric or geometry of the soil such as the shape, size and packing. ν and ρ are the dynamic viscosity and density of the fluid respectively. This implies if the soil and the pore fluid are the same, K would be the same, this requires

$$k_m = N k_p. \tag{3.34}$$

The hydraulic gradient i is a geometrical parameter and

$$i = \frac{\Delta s}{\Delta l}, \tag{3.35}$$

where Δs is the drop of the hydraulic head of pore fluid if the fluid had travelled a length of Δl. Therefore $i_m = i_p$, and

$$v_m = i_m k_m = i_p N k_p = N v_p. \tag{3.36}$$

Another point to support this opinion lies in the variation of permeability with the size of the particles. Normally permeability varies from 10^{-9} to 10^{-3} m/s if the soil changes from clay to sand. As the centrifuge simulates the particles in N times the soil in prototype, it is reasonable to believe that permeability increases with acceleration.

Some researchers argue that if k increases with acceleration, there would be no flow in the case that the gravity equals zero and the porous media becomes impermeable. This seems not acceptable, and it is suggested that k does not change with acceleration but the hydraulic gradient increases, or $k_m = k_p$, and $i_m = N i_p$, therefore

$$v_m = i_m k_m = N i_p k_p = N v_p, \tag{3.37}$$

where the argument is that the hydraulic gradient does not only mean the geometrical parameter, it represents the hydraulic pressure gradient.

It should be kept in mind that Darcy's law has its own limits. This could be a reason of the discrepancy between the cases in actual sites, the results of centrifuge tests and the results of numerical simulation. For numerical simulations, Biot's theory is always applied, in which Darcy's law is used.

3.2.4 Stress history

To simulate the soil from a real site, it is required that the behaviour of the soil in the model is the same as the soil on the site. This is because the property of the soil does not change although subject to very large accelerations. Schofield (1980) explained the reason for this as: "the force acts at the centre of mass of each atom and does not significantly affect the electron shells which determine all material properties other than selfweight."

Soil properties are affected by many factors, one being the stress history. It is impossible to let the soil undergo the same stress history in the model to obtain the same mechanical behaviour, since the stress history cannot be completely known. What can be known is the behaviour under some geotechnical tests. The solution is that according to laboratory data, one constitutive model is selected and the parameters are obtained. The purpose of preparing the soil for the model tests is not to restore the stress history but to obtain the same constitutive parameters under the same stress paths.

Undisturbed soil from a site may be used for a centrifuge test if the disturbance can be kept as small as possible. Normally the sample can be disturbed and even damaged to some degree by the process of sampling, transportation, storage and trimming. Therefore remoulded soil is more feasible and easy to handle. Sometimes special methods should be applied to make the properties of the soil as similar to the prototype as possible.

Granular soils can be remoulded by tamping and pluviation (Phillips, 1995). Tamping can prepare the samples of most soil gradings and the samples may be moist or dry. There may be some variation of the density. Pluviation can be used for preparing samples of uniformly graded dry soil.

Dickin (1988) reported using a sand-raining method to prepare dense and loose sand samples. Dense sand can be achieved by raining from a height of 1.85 m through a diffuser plate with 3 mm diameter holes in a 50 mm square grid, while loose sand can be obtained with a height of 0.35 m through 4.5 mm diameter holes in a 20 mm grid.

Silt and clay soils can be remoulded by preparing the slurries and consolidating before or during centrifuge tests or both. The initial consolidation pressure should be kept about 5-10 kP_a to prevent the slurry from extrusion.

Tsuchida et al (1991) reported using the method of consolidation at high temperature to reproduce the structure of aged clay in a laboratory. The disturbed marine clay was taken from a site. The state parameters of the clay were $w_L = 79\%$, and $w_P = 37\%$. The clay was thoroughly remolded at $w = 200\%$ and de-aired for

48 hours. The slurry was consolidated one dimensionally in a consolidation cell of 20 cm diameter. The cell was surrounded by hot water with a constant temperature of $75°C$ controlled by an electric heater. A load was applied on the plate by an air cylinder with pressures of 10, 20, 40 and 100 kP_a. After consolidation was completed, the sample was unloaded and cooled at a room temperature of $25°C$. The test results showed that the high temperature consolidation sample has similar mechanical properties to natural aged clay.

Powrie (1986) simulated the vertical stress history of the removal (by erosion) of about 150 m of overlying soil. Kaolin powder was mixed into slurry under a partial vacuum with de-aired water. The water content of the slurry was 120%, which was twice the liquid limit. The slurry was then poured into a consolidometer, and compressed one-dimensionally to a vertical effective stress of 1250 kN/m^2. The load increment was limited by the strength of the clay under the previous step. The sample was then unloaded to a vertical effective stress of 80 kN/m^2. The load was reduced gradually to control the possibility of cavitation. Therefore the final average effective stress was just below 100 kN/m^2. The clay was then cut to place in the strongbox and subjected to the centrifuge tests of 125 g.

Pepe and Renzi (1994) reported the procedure of preparing the soil samples for centrifuge tests to model the Leaning Tower of Pisa site conditions. The clay samples were prepared by the following procedure:

A 130 mm dry layer of uniform sand was pluviated into the container to simulate the bottom layer of sand and provide a drainage layer at the bottom of the container

for the clay. The sand was filled with de-aired water and then covered with a filter paper. Slurry was prepared by adding dry powder to tap water gradually to avoid clots. The slurry was mixed for about 2 hours under a vacuum after adding the required amount of powder. The final water content was about 1.5 times the liquid limit. The slurry was poured into the test container through a tube immediately. A height of 210 mm of slurry was required for the height of 124 mm of clay. The slurry was consolidated gradually with a vertical final pressure of 300 kP_a.

Before beginning of the tests, the on site soil may be consolidated to restore it to its original strength. Zhang and Zhang (1994) reported using a double-chamber centrifuge for tests with clay. Soil from a site was prepared with 80% to 120% of the water content and put into the two strongboxes on the two chambers. In one chamber the model was installed. In the other chamber, only soil of the same preparation was in the strongbox and a micro-vane was installed to test the shear strength in-flight. At the beginning of the test, the soil was consolidated to reach a consolidation degree of 90%. When the strength of the soil in the chamber reached the strength of the soil in the site, loading was applied.

Materials different from prototypes may be used in the model for stress restoration. Xie (1988) reported a centrifuge modelling for structures built on a non-uniform foundation. The foundation was a rock foundation full of weak zones and faults having a low strength and high deformability. The foundation was composed of many pieces, the moduli of the pieces of rock were different. The stresses in the tests were calculated by the photoelastic method. Photoelastic material other than the rocks from the sites were used. Therefore the scaling relations in Table

3.1 was not adhered to. Centrifuge tests of 100 g and 40 g were carried out. The models were cooled and frozen models were obtained. The stresses were calculated according to the relations of the photoelastic method. The stresses were modified and the different unit weights between the model and the site were accounted for.

3.2.5 Stress path

It is required that the stress path resulting from loading in the tests be the same as the path in the prototype. Loading seems easy work and it is normally ignored in the discussions. However it is difficult to make the stress path resulting from loading the same as the one in the prototype.

Loading such as simulating the bearing capacity of the foundation under different types of footings are routine procedures. Some loading such as simulating the scouring of icebergs on the base of the oceans (C-CORE) needs simplification in design.

The stress path also includes the results from unloading. Excavation and tunnelling are typical examples of unloading and they are very difficult to simulate. Different approaches have be carried out for excavation including stopping the centrifuge machine during tests (Zhang and Zhang, 1994, Liu et al, 1994), using heavy liquid to simulate the excavated soil (Phillips, 1982, Powrie, 1986, Powrie et al, 1994) and developing an in-flight excavator (Kimura et al, 1994). However the stress paths in these cases are not satisfactory. Tunnelling has been carried out using existing model tunnels (Bezuijen and Schrier, 1994), air bags (Schofield, 1980),

and even a miniature tunnelling machine (Nomoto et al, 1994). Again the stress paths are not the same as the prototype.

3.2.6 Boundary conditions

Boundary conditions are also important factors in a centrifuge model. The boundary may apply additional loads or deformation to the model if the effect is not correctly accounted for. Normally the boundary is regarded rigid during tests. This depends on the stiffness of the strongbox.

Friction between the soil and the side walls of the strongbox is another factor affecting the accuracy of the simulation. The problem of a braced excavation is regarded as a planar problem. It is supposed that there is no friction force on the contact and the soil may deform freely along the surface of the wall. This condition is hardly ever achieved in tests. Using some lubricating material, such as grease, is helpful in reducing friction. On the other hand, the effect of friction may be reduced by collecting the data in the middle of the model instead of close to the boundary.

The effect of the boundary may be increased if the model is too large compared to the size of the container, especially for a three dimensional simulation. Ovesen (1979) said that for simulating a circular footing, a container with a diameter 5 times the model footing diameter was found to be too small. He also pointed out that a model footing with a diameter about 15 times the average grain size was also found to be too small.

With the available strongbox, the size of the model is determined by the effect of the extent of the loading, in other words, it depends on how much extra stresses and strains would be produced on the boundary. It is desired that the extra stresses and strains would be small so as to be negligible. This is not only determined by the loading but also by the stiffness or deformation properties of soil. The effect of the boundary cannot be eliminated for most problems but it can be reduced greatly and even be negligible with a careful design.

The exact boundary effect can be investigated by the technique of "modelling of models". By performing a series of tests for the same problem with different sizes of model and accelerations, the influence of boundary conditions can be easily observed.

3.2.7 Measurement accuracy

Accurate measurement is also an important factor for a simulation. If the model is excellently built and the tests are correctly carried out, but the data are not accurately collected, it is would be a great loss to the tests.

Accurate measurement depends on several factors. The first factor is the accuracy of the equipment to be used for the measurement such as the pore pressure transducers, the LDT's and LVDT's. Large size meters are easier for a correct signal to be sent to the data collecting center. However the linear dimension in the model represents N times the dimension in the prototype. If an equipment is too large, the data would represent the average value over a long interval in the

prototype instead of a point as it was designed. Therefore when the accuracy of the equipment cannot be improved, it is helpful to reduce the value of N. This requires a large chamber on the test machine. In other words, a large rotational radius and a powerful machine would be desirable for the improvement of the accuracy of the measurement.

As it has been pointed out in a previous section, the actual stress field of the model in the centrifuge is different from that in the prototype in terms that the accelerations in the model exist in three directions and there are forces acting on the soil not only the vertical stress of self weight as in the prototype. Therefore there are some discrepancies in the results of the model tests from the prototype, and these discrepancies cannot be eliminated. Furthermore the larger the size of the strongbox in which the model is built, the larger the error. This conclusion differs from the one obtained above from the viewpoint of size of the equipment.

Chapter 4

CENTRIFUGE TEST INSTUMENTATION AND PREPARATION

4.1 Test Instrumentation

The tests are carried out in the C-CORE Centrifuge Center of the Memorial University. The center owns an Acutronic 680-2 centrifuge. It is capable of carrying loads up to 1100 kg with 100 g and 650 kg with 200 g. The effective radius is 5.5 m. Tests may be carried out in strongboxes of square, rectangular or circular sections. The square strongbox has a maximum internal area of 100 $\times$ 140 cm^2 in plan and 40 cm in height. The facility may use hydraulic, pneumatics, electric, water, refrigeration and video & CCD control. Visual monitoring during tests can also be achieved. The electrical signals from transducers are collected with a data acquisition system using a PC-compatible 486 computer.

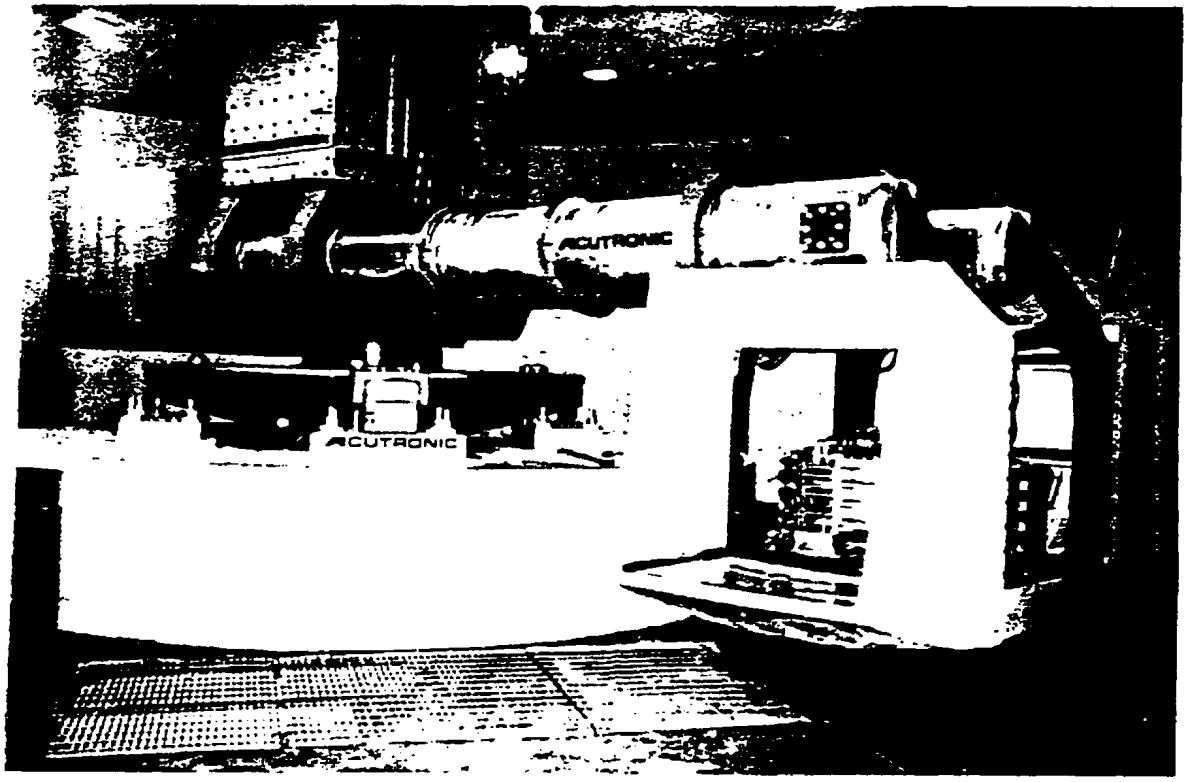

This study is carried out in a strongbox of a rectangular section, called a plane strain box. Three sides of the box and the bottom are made of aluminum, and one side is made of acrylic for the convenience of observation. The inner space is 300 · 900 mm^2 in plan and 426 mm in height. Given this space, prototype excavations of 11.5 m deep and 17.3 m wide can be modelled. The package is shown in Fig. 4.1.

Three layers of struts are used for the prototype along the depth of 11.5 m. The lateral distance between the struts is chosen as 3.6 m for the first test and 7.2 m for the rest. The popularly used value in practice is 3.6 m (or 12 feet). The vertical distance between the first three layers of struts is chosen as 4.3 m. The distance

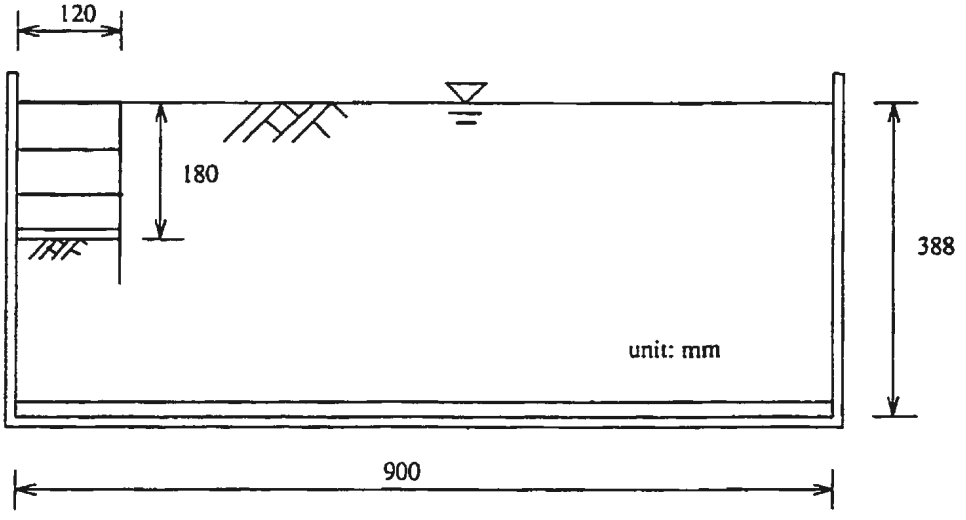

Figure 4.1: Dimensions of the centrifuge models

between the third layer and the bottom of the excavation is about 3.0 m. Both distances are much larger than practical ones, which are about 2.0 m.

Because the problem is symmetrical, only half of the prototype is simulated. According to the size of the prototype and the available dimension of the centrifuge drum, the scale factor N is chosen to be 72. Details of the design of the experiment are shown in Fig. 4.2. The sheet plates, wales and the struts are made of aluminum 6061-T10. The Young's modulus is tested and the methods are explained in Chapter 4. The designing strength of the aluminum is 110 MP_a where a safety factor of 2 is included.

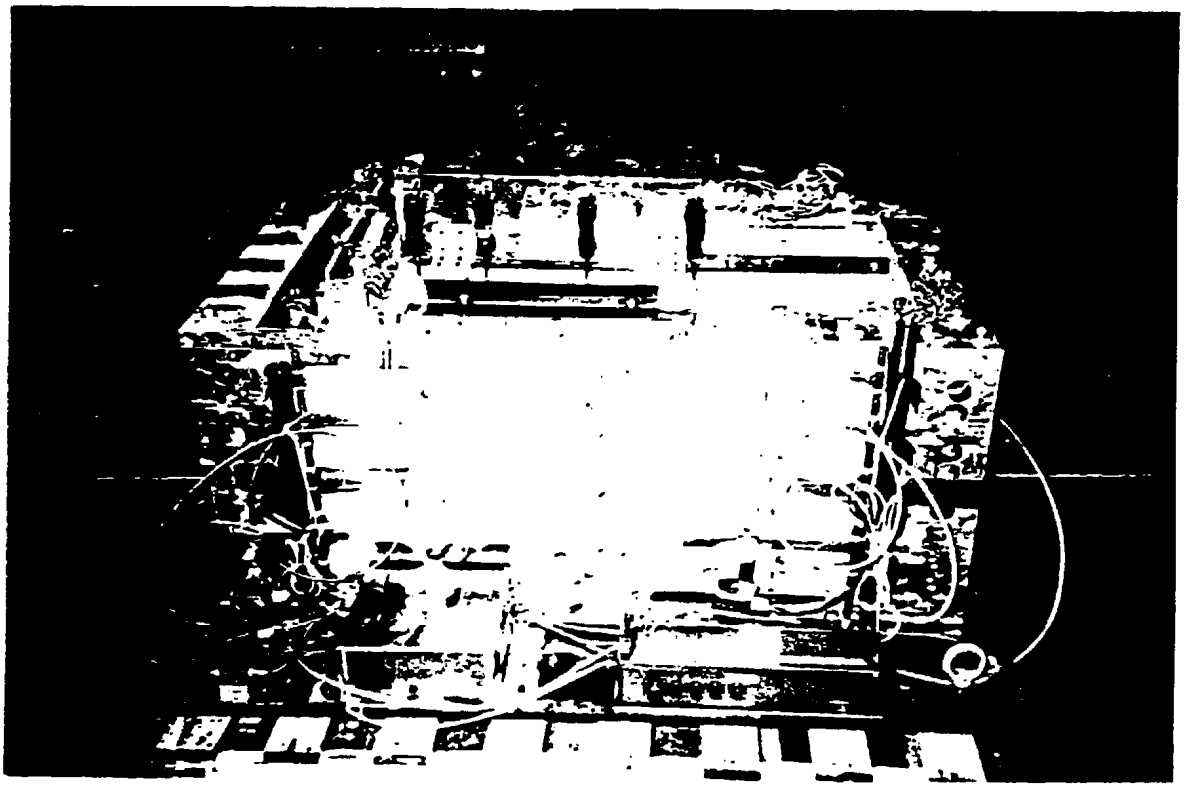

The soil in front of the sheet plate is simulated with a heavy liquid. To lower

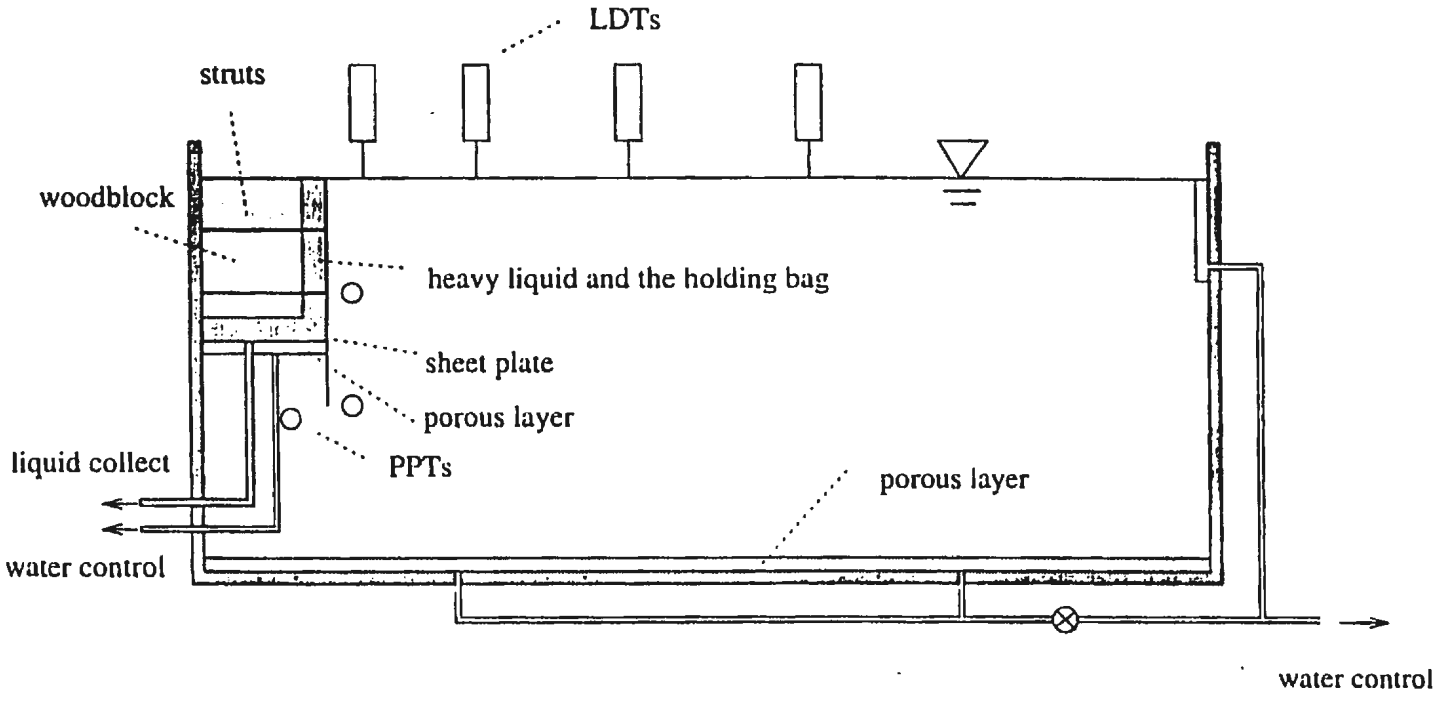

Figure 4.2: Design of the model

the cost of the heavy liquid, a woodblock is used to reduce its volume. The heavy liquid is stored in a plastic bag and is drained gradually during the tests to simulate the procedure of excavation. The woodblock is also used to fix the struts and the wales. The weight of the woodblock is supported by two angle steel beams which rest on the top of side walls of the strongbox.

The control of the water table and the drainage system of the heavy liquid are shown in Fig. 4.3. There is a porous layer at the bottom of the soil for drainage. The layer is composed of three layers of materials: at the bottom is a layer of geotextile; at the middle is a sand layer of about 15 mm; and above the sand is another layer of geotextile and filter paper. The clay lies on the filter paper. Two outlets of the porous layer are connected with a plastic pipe and this pipe is connected to a standing pipe. Another quarter inch plastic pipe is used to connect the water at the surface of the soil and the water in the standing pipe. This is achieved by excavating a semicircle reservoir in the clay at the end of the strongbox. A semi-cylinder shape of plastic pipe is used to protect the wall of the reservoir and there is a layer of geotextile and filter paper between the clay and the cylinder. The pipes are full of water and the water surface in the standing pipe is kept as high as the surface of the soil. This is achieved with a small standing pipe which is connected to the large standing pipe and the outlet is as high as the soil surface. A PPT (pore pressure transducer) is installed inside the large standing pipe to measure the height of the surface of the water inside the standing pipe. If the height is less than the required value, more water can be supplied to the standing pipe from water supply system. This design may keep the water pressure at the bottom of the soil as high as the

static pore pressure before excavation.

At the first stage of the test, the soil is consolidated under the load resulting from the self weight of the soil under centrifuge accelerations. The excess pore pressure is reduced by the consolidation and excess water is drained through the pipes. According to Terzaghi's theory of consolidation, the porous layer at the bottom reduces the required consolidation time to a quarter. At the beginning of the excavation, the connection of the water at the bottom with the standing pipe is cut off with a valve. This allows the pore pressure to vary as in actual sites.

Because the soil which would be excavated during the test is represented with the heavy liquid, the pore pressure at the bottom of excavation is not the same as actual sites. In order to simulate the pore pressure in actual sites, a porous layer is also applied at the bottom of the excavation. The layer lies just under the plastic bag. The structure of the porous layer is the same as the porous layer at the bottom of the soil. A steel pipe of a quarter inch is fixed inside the strong box in such a way that it does not block the consolidation of the clay. The steel pipe connects the water in the porous layer with another standing pipe outside the strongbox through a plastic tubing. The height of the standing pipe is the same as the surface of the soil. This keeps the maximum water table in the pipe the same as the surface of the soil, for the water head in the soil is, theoretically, the same as the surface of the soil. A small standing pipe is connected to the large standing pipe, but the outlet is much lower and the level is the same as the porous layer. This outlet is connected with a quarter inch plastic pipe and the drainage of water from this pipe is controlled by a valve. The purpose of this design is that, during excavation, as

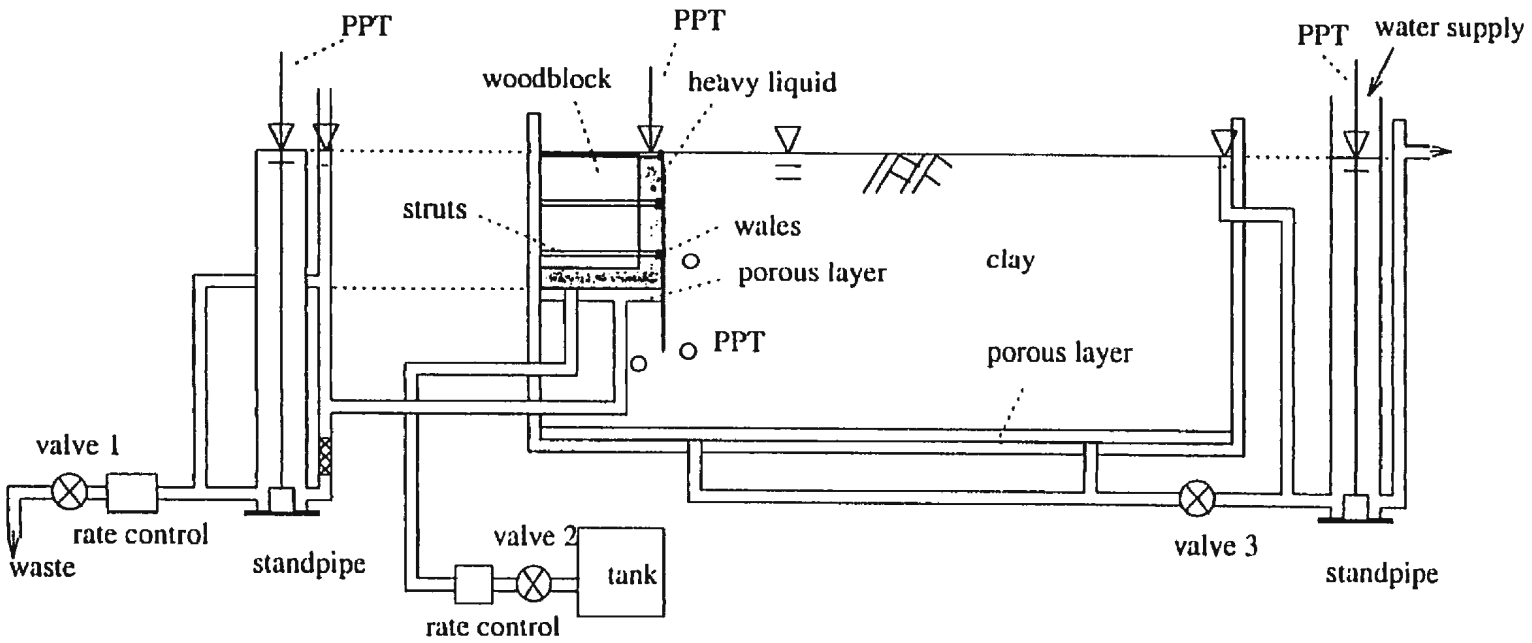

Figure 4.3: Drainage system control

the surface of the heavy liquid is reduced, the water table in the standing pipe is reduced to the same level as the liquid in the same time. Therefore a PPT is also installed in the standing pipe to read the height of the water table. Of course the pore pressure in the soil in front of the sheet piles in actual sites does not vary with the same values. After draining the heavy liquid, the valve is closed. This does not affect the water table in the drainage layer at the bottom of the excavation. However, the seepage rate of the water from the soil in the back of the sheet plate to the excavation area can be measured with the PPT in terms of the volume of the water accumulated in the standpipe.

Heavy liquid is used to simulate the soil in front of the sheet piles which would be drained during the tests. The heavy liquid is stored in plastic bag. Drainage is done with a outlet which is at the bottom of the bag and is connected to a reservoir outside the strongbox. The reservoir is made of aluminum. There is a valve in the pipe to control the drainage of the heavy liquid.

In order to avoid disturbance of the soil in installing the drainage pipe for the heavy liquid, the tube should be inside the soil during installation. However this situation would make it very difficult to connect the tube with the outlet of the bag if the soil is not allowed to be disturbed. This problem is solved by using a larger steel guide pipe (Fig. 4.4). The guide pipe is 3/8 inch in diameter and bent into an L shape. The lower end is fixed into the wall of the strongbox with a fitting and the angle part is welded onto a piece of steel also with an L shape. This piece of steel is used to support the weight of the pipe, the liquid and the force resulting from the soil. The plastic tube is connected to the outlet of the bag with a

specially designed fitting which sandwiches the bottom of the bag and may prevent the leaking of the heavy liquid through the connection. The tube is then inserted into the guide pipe from the top inlet and pulled out the strongbox from the outlet. The tube is connected to the reservoir and sealing was carried out at the outlet of the guide pipe between the pipe and the tube. This prevents the water flowing out through the space between the pipe and the tube. The pipe is fixed to the wall of the strongbox with a male connector which provides sealing between the pipe and the wall.

Pore pressure transducers (PPTs) are used to measure the pore pressures inside the soil around the sheet plate. The PPT at the bottom of excavation should be installed before the installation of the drainage layer under the bag. The maximum pore pressure would be about 283 kN/m^2.

The details and technique for the simulation are discussed below.

4.1.1 Sheet plates

In each test, the sheet piles are simulated with a flat piece of aluminum plate. Aluminum has been selected because it is lighter and has a lower Young's modulus, which makes it easier to deform during the tests. So that failure may be reached. It is possible to investigate the maximum possible deformation behaviour and a wide range of earth pressures on the sheet piles. For simulating real sheet piles, the size and the stiffness of the sheet plate depend on the mechanical properties of the actual sheet piles, such as Young's modulus and the moment of inertia of the

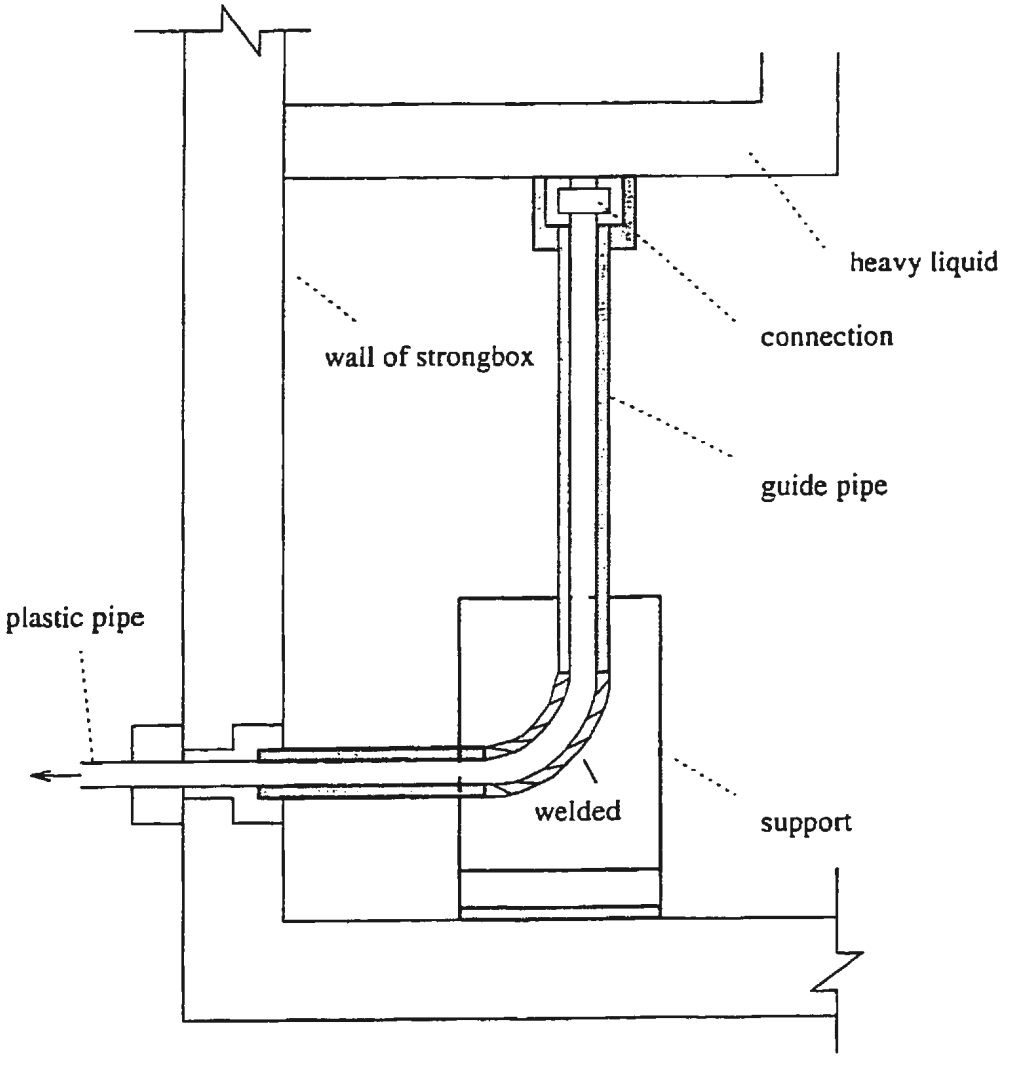

Figure 4.4: Design of the guide pipe for draining heavy liquid

sections. The selected sheet plate is a rectangular piece of aluminum plate with a thickness of 1.628 mm in design but, in fact, 1.55 mm on average. The dimensions are 290 × 298 mm^2, and the area which contacts with soil is 250 × 298 mm^2.

The aluminum sheet plate becomes very heavy during tests because of the high centripetal acceleration. This heavy weight may result in a large settlement of the plate downward to the bottom soil. In order to prevent this large settlement, the plate is attached to a steel beam. The beam is hung across the strongbox and supported by the edges of the strongbox.

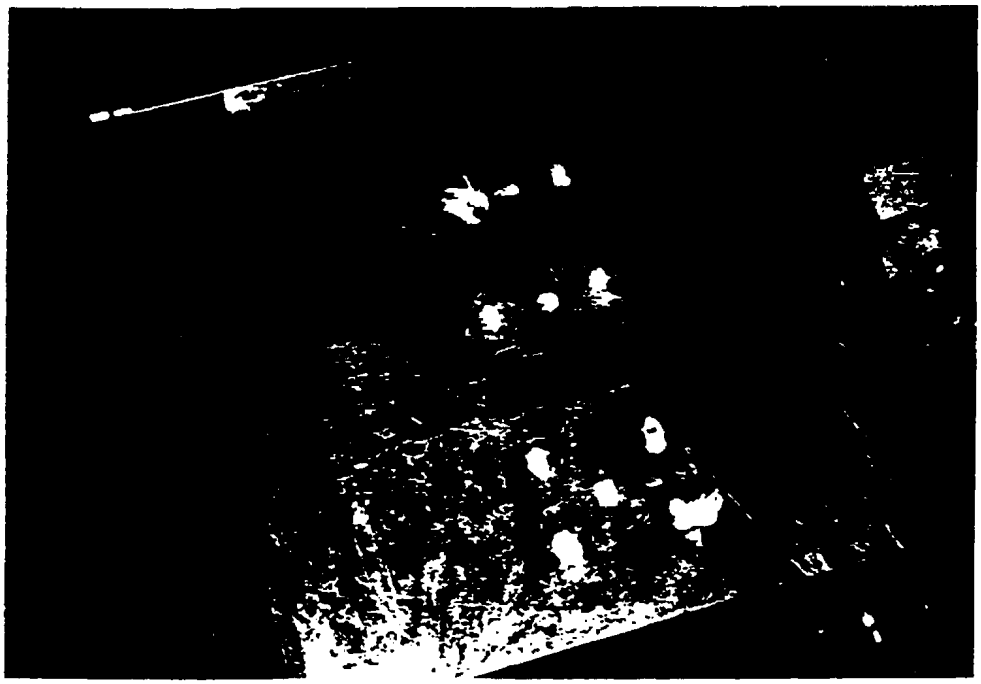

The actual irregular section of and the connections between the sheet piles are ignored. The seepage through the connections is not simulated.

One important factor which should be considered in designing the sheet plate is the seepage of the water behind the sheet plate toward the excavated area through the crevice between the sheet plate and the walls of the strongbox. The seepage should be prevented because the seepage through sheet piles in actual sites is not simulated in the model. If it is simulated, the seepage should be controlled to a reasonable magnitude.

The simplest way to cope with this problem is to reduce the crevice to be as small as possible. This is difficult to achieve because if the width of the sheet plate is almost the same as that of the strongbox, the sheet plate would not be easy to install. Even if installed, there would be friction between the plate and the strongbox, a boundary condition which does not apply to real sites. Also the sheet plate would cut into or scratch the surface of the acrylic wall (plexiglass) during installation and the tests. The beam which the sheet plate hangs on is supported by a pair of ball bearings which rest on the surface of the side walls of the strongbox. These two ball bearings would result in some unequal settlements under the load of the sheet plate during the tests. The unequal settlements make the sheet plate lean to one side and therefore it may cut into the acrylic wall, which is very expensive.

Therefore two rubber laces are applied on the edges of the sheet plate for protection. These laces are to prevent seepage of water around the sheet plate through the crevice and keep the differences of the water table after excavation. Thus the width of the sheet plate can be narrower, which reduces the possibility of cutting into the acrylic glass window.

The moment in the sheet plates is measured with strain gauges. The design is shown in Fig. 4.5. The strain gauges are applied in the vertical direction at each point and may tell the strains at that point. This study is a planar problem, and the sheet plate is regarded as a beam. By knowing the strain at the surface of the beam, the stress on the surface may be obtained by multiplying it with the Young's modulus. The moments may be known if a linear or other distribution of the stress on the section is assumed.

For the first test, 14 strain gauges are applied on two vertical lines on the back surface of the sheet plate that contacts the soil. There are 7 gauges on each line and the corresponding gauges on the two lines are at the same height. The gauges are applied in such a way to measure the vertical strain in the surface of the sheet plate at the respective points. Because this is a planar problem, the two gauges at the same height should show the same strain. In order to measure the strain at the two points, each pair of gauges form an electric bridge with two other dummy gauges. The dummy gauges are applied on a small flat piece of aluminum board and this board is fixed on an edge of the strongbox. It should be noticed that there are two active gauges in each electric bridge.

For the remaining tests, only four full bridges are used. There are four active gauges in each bridge: two are in the front side of the sheet plate and two are on the back of the sheet plate. The first bridge is in the middle elevation between the top and the middle layers of struts, and the second bridge is in the middle between the middle and bottom layers of struts. The third one is 40 mm below the bottom layer of struts and the fourth one is 40 mm below the third one and 40 mm above

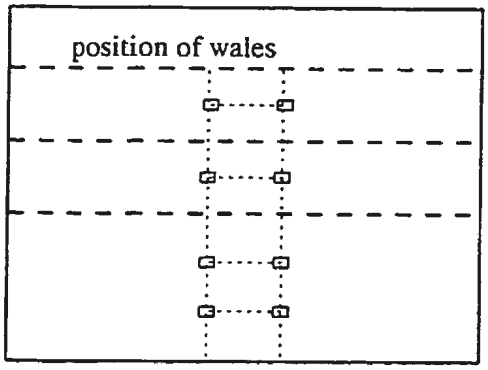

Figure 4.5: Display of the strain gauges on the sheet plates

the bottom edge of the sheet plate. In order to prevent the wales cutting the wires of the gauges in the front side of the sheet plate, two little holes are drilled between the three layers of struts and one is below the bottom layer of struts to lead the wires to the back side of the sheet plate.

The strain gauges are manufactured by Incorporation of Measurements Group. They have a resistance of $120.0 \pm 0.3\%$ Ohm at a temperature of $24°C$. Before applying the gauges, the surface is cleaned with M-PREP conditioner A together with Neutralizer 5. Gauges are installed to the position with M-Bond 200 Adhesive. The bondable terminals for the gauges on the sheet plate are applied on the top area of the sheet plate where there is no soil on the surface. The gauges are connected to the bondable terminals with small connecting wires. The length of wires applied

between the gauges and the bondable terminals is greater than required so as to allow free movement when the sheet plate bends during testing. After the wires are soldered to the gauges, the gauges are coated with M-Coat A and M-Coat D for protection. Actually this protection is not enough because the gauges would be subjected to a maximum pore pressure of 164.64 kP_a during tests. Therefore wax is applied on the surface for more protection. Because the sheet plate will rub the soil during installation, some aluminum foil is used to cover the wax for protection in the first test. For the remaining tests, plastic sheets are used. The data are transferred to the controlling center from the signal box with slip rings. The function of the signal box is to enlarge the signals.

The calibration is carried out easily by applying a resistance on two ends of a gauge, and this resistance has a value of 59,880 Ohm, which allows for a strain of 1000 microstrain (1000×10^{-6}) for the provided gauges. An extension voltage of 5 volts is applied and variation of the voltage at the signal ends can be measured. This value represents the voltage that would appear in actual tests if the extension voltage is 5 volt and the strain is 1000 micro. If the extension voltage doubles , the readings would be doubled. It should be decided according to the actual situation whether the + sign or - sign of the reading voltage represents tensile stresses on the surface of the sheet plate or compression stresses.

The horizontal displacement of the sheet plate can be measured with LVDTs. These LVDTs can be installed horizontally in the woodblock. Because the required length of the LVDT is too large for the available width of the woodblock, and the possible seepage of heavy liquid into the LVDTs, the plan of applying LVDTs is

given up.

4.1.2 Struts and wales

There are three layers of struts and six struts at each layer for the first test and three for the rest. The struts are made of aluminum with nearly square sections. The dimension of each side ranges from 6.45 mm to 6.90 mm. At each layer, one end of the struts supports the wale and the other end contacts the end beam, which is of the same dimensions as the wale. The end beam contacts the end wall of the strongbox on one side. The wales and the end beams have the same sections as the struts but the length is close to 300 mm, which enables the wales to go across the whole width of the strongbox and support the whole horizontal width of the sheet plate. The struts rest on the supporting beams, which have a length of 117.5 mm and the same sections as the struts. The purpose of using the supporting beams is to support the wales, because the weight of the wales may become too heavy during the tests. The length of the struts is 106.5 mm. Wales rest on one end of the supporting beams and the end beams on the other. There is a gap about 2 mm between the sheet plate and the supporting beams, this design avoids the contact of the supporting beams and the sheet plate, and only the wales contact the sheet plate during the tests.

The supporting beams, finally, rest on the bottom of the grooves in the woodblock. There are three layers of grooves with rectangular section to accommodate the struts and the supporting beams. There are three grooves on the back of the woodblock to accommodate the end beams.

The axial forces in the struts are measured with strain gauges. For the first test, only one strut in the middle of a layer is selected to represent the axial forces in the struts of that layer. For the remaining tests, all struts are strain gauged. There are only two active gauges for each bridge, a full bridge is formed by applying two dummy gauges which are applied on a small plate and the small plate is fixed on the top surface of the side wall of the strongbox.

The calibration of the strain gauges for the struts is different from that for the sheet plates. Struts are loaded axially with a load applier and the magnitude is obtained from the readings. A voltage of 5 volt is applied on the extension ends of the electric bridge and the voltage on the signal ends is collected for the given load. The load varies from 0 to 150 pounds, and the readings of the voltage are recorded. These data are expressed in Fig. 4.6 and a straight line is supposed to fit the points. The slope of the line gives the results of the calibration. Actually for the selected strut for the bottom layer, 1 mv represents 46.169 kg force in the strut, for the middle layer, the value is 51.215 kg and for the top layer, it is 55.350 kg.

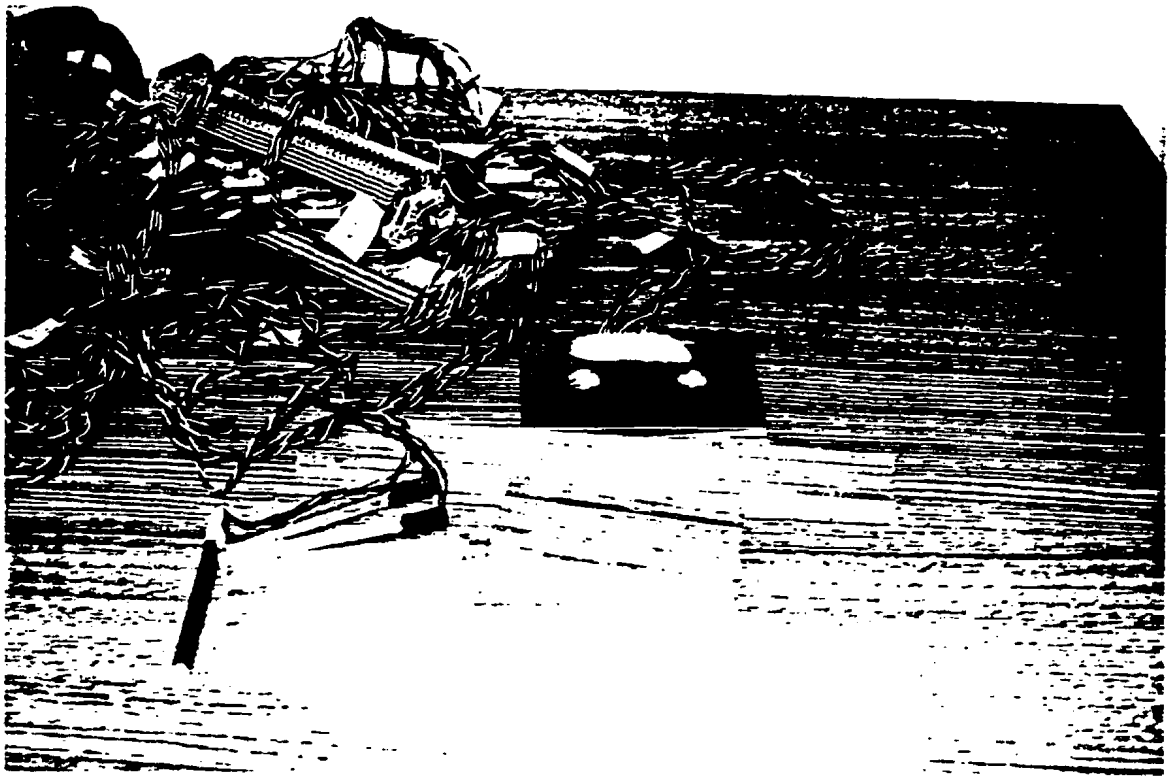

4.1.3 Heavy liquid

There are several ways to simulate the clay in front of the sheet piles. This clay would be removed in the process of excavation. The requirements of the simulation are that the simulation will apply the same amount of earth pressure on the sheet piles prior to and during the process of excavation, and the mechanical properties of the clay should be simulated, such as the deformation properties and shear strength.

Several approaches have been carried out in simulating the non-braced excavations in centrifuge tests. Craig and Yildirim (1976) used rigid supports to simulate the lateral pressure on the structure. Excavation work was simulated by the removal

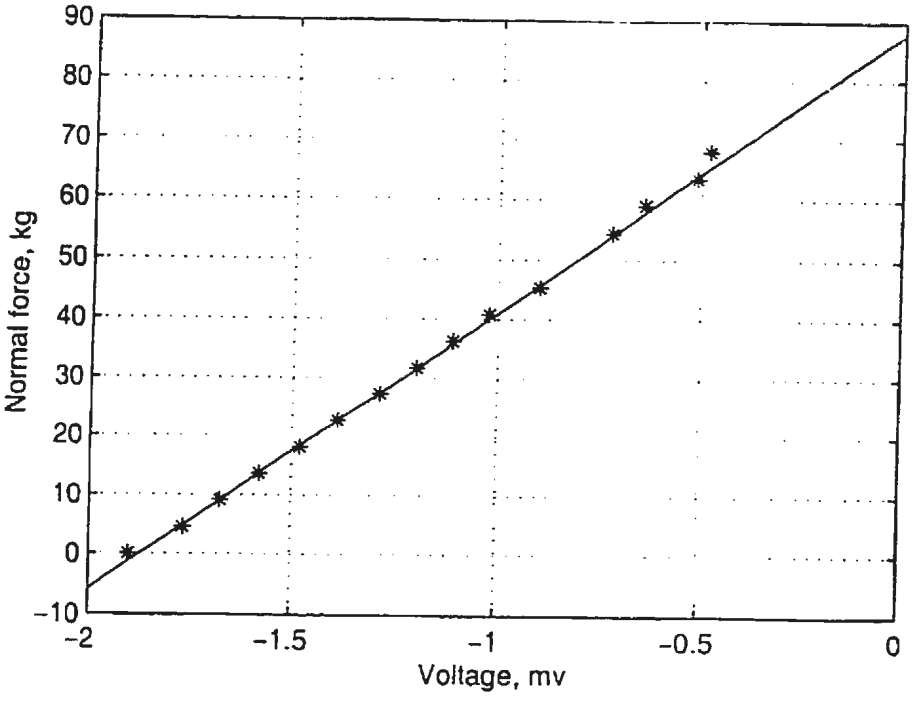

Figure 4.6: Calibration of the strain gauges

of the supports. Lade et al (1981) used paraffin oil with a density of 2.65×10^3 kg/m^3 to simulate granular soil in a K_0 state, where K_0 was calculated according to $K_0 = 1 - \sin\phi'$. Ko et al (1982) used soil which was contained in a porous fabric bag, and these bags could be winched clear by using an electric motor. Kusakabe (1982), Phillips (1982) and Bolton and Powrie (1986) used zinc chloride solution in a rubber bag to simulate clay, where the unit weight of the solution equaled to the unit weight of the clay. Powrie and Kantartzi (1993) used sodium chloride solution to simulate overconsolidated clay, the density of the solution was 1162 kg/m^3.

In simulating braced excavations, Zhang and Zhang (1994) and Liu et al (1994) reported the simulation of excavations by stopping the centrifuge machine to remove soil and then apply the struts.

Using rigid supports would be easy to employ in the tests. However, the action on the sheet piles would be very different for this case. The loading on the soil at the bottom of the excavation would not be simulated and yet the behaviour of this part of soil does affect the stability of the system greatly, especially in bottom heaving. Using soil bags would be a good simulation, but there is a great difficulty to employ them in centrifuge tests for braced excavations. When the soil bags are removed, the wales and struts are very hard to apply. Kimura et al (1994) designed an excavator to excavate the soil during the tests, but that was not for braced excavations. The method of stopping the machine for excavation is a good approach, however the stress path would be different from the actual excavations.

Using liquid to simulate the soil is a good balance between the more realistic and less difficulty. It is convenient in terms of the ease of removal. However, there are some concerns for this method.

The first concern is that, a liquid cannot be used to simulate the deformation properties and the strength of the actual soil. In fact, not only lateral pressure affects the stability of the structure, but also the mechanical properties of the soil in front of the structure. For example, in simulating the behaviour of retaining walls, the lateral pressure exerted by the soil in front of wall is not only determined by the vertical stress (usually the self weight of soil), but also determined by the mechanical properties of the soil. If the soil is hard to deform, the displacement of the wall toward the open area will be small, this will result in a small lateral stress in the soil which is transmitted to the wall. If the displacement is large, the passive earth pressure state may be mobilized, and the lateral earth pressure equals the

passive earth pressure.

The second is that it is difficult to decide the unit weight of the liquid. On the one hand, the unit weight of the liquid should equal to the unit weight of the soil. If the soil is saturated, it should be the saturated unit weight of the soil. The reason is that the liquid should apply a pressure on the soil at the bottom of excavation the same as if it were soil and not liquid. On the other hand, the lateral pressure that the liquid applies to the sheet plate should be equal to $K_0\gamma z$ in simulating the K_0 state. Normally K_0 does not equal 1 and strictly speaking, K_0 cannot be exactly known for the soil.

Because the unit weight of saturated soil is around $18kN/M^3$, it is very difficult to find a liquid which has a unit weight close to this value and has a good fluidity. Some researchers use the solution of zinc chloride which is quite toxic. The heavy liquid used in this study is a solution of the powder sodium polytungstate ($3Na_2WO_4.9WO_3.H_2O$), which is a product produced by the company of Sometu-US in Van Nuys, California. The advantage of this solution is that it is non-toxic and the density can be adjusted up to 3.10 g/ml. The solution has sufficient fluidity to satisfy the drainage requirements.

In this test, struts and wales are applied in position before draining the heavy liquid, which means the bracing system is in position before the soil is removed. This approach is not practical for actual sites, however the earth pressure on the sheet piles would be more conservative than the value for actual sites. The bottom heaving obtained from the test would be less than the actual sites. The vertical

stability of the struts is not in consideration.

4.1.4 Plastic bag

The purpose of using a plastic bag is to hold the heavy liquid which is used to simulate the soil in front of the sheet piles, the soil should be removed during excavation.

There is an outlet in the bottom to connect with a tubing to the collecting box outside the strongbox with a tubing. The bag contacts the sheet plate, the side walls of the strongbox and the surface of the drainage layer at the bottom of the excavation. The bracing system is inside the bag and soaked in the heavy liquid before draining. The wales are acting on the plastic sheet to support the sheet plate. Tests were done for the possible cutting of the plastic sheet by the wales owing to the high load in the centrifuge, and it was shown that the plastic sheet would be safe for the tests. The sheet is flat on the side contacting the sheet plate and the side wall of the strongbox but folded at the two ends to form a bag. The top parts of the bag are attached on the fixing beam and the top surfaces of the side walls. This method should make the bag loose enough so that it does not disturb the full contact of the bag with the sheet plate and the walls of the strongbox during tests.

A rubber bag was tried for holding the heavy liquid. This bag was designed to go around the strut, the wales and the woodblock. However the thickness of the bag made it too heavy and would apply some load to the soil during tests. The greatest concern was that there was a danger that the bag would slide from the

fitting connecting the bag with a tubing under the load of the heavy liquid during tests and the fitting might cut the bag. The cutting happened once during fixing the fitting onto the bag because too much force was applied on the screws. As a result, the plastic sheet bag is used instead of a rubber bag. For the safety of the tests, a new bag is made for each test.

4.1.5 Woodblock

The woodblock in the excavation area is used to hold the struts, wales and their support beams. It can also serve to hold LVDTs to measure the lateral displacement of the sheet plate and an LVDT at the dredge line to measure the bottom heaving if they are installed.

The woodblock is composed of four pieces, and the dividing surfaces are on the top sides of the grooves, this makes it easier for manufacturing and for applying the struts. To keep the struts in a real axial stress state, the woodblock should not hold the struts tight.

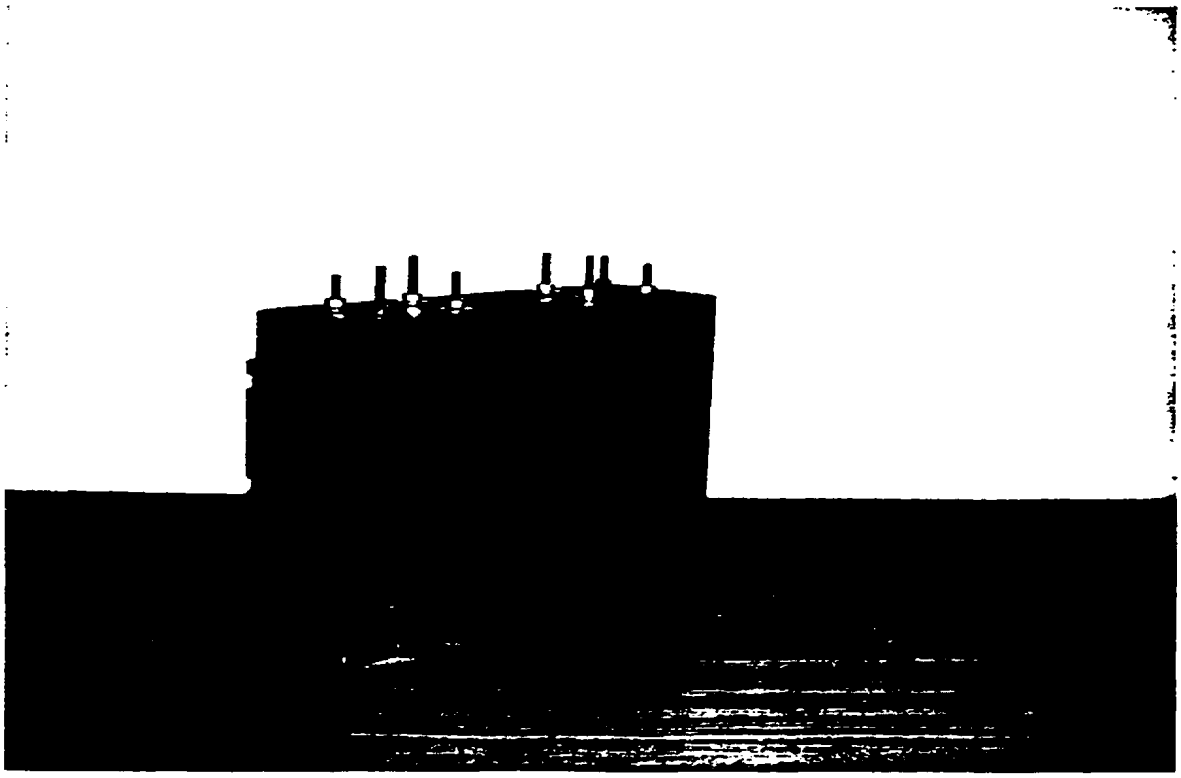

The woodblock is subjected to uplifting forces resulting from the liquid at the bottom of the woodblock before excavation. After the excavation, the woodblock is subjected to downward forces of its self weight and the weight of the struts, the wales and the beams. Therefore the woodblock should be fixed on the edges of the strongbox tightly in consideration of these two forces.

The woodblock is soaked in pure water for saturation before each test, this may prevent the heavy liquid from permeating the wood, reducing the volume of the liquid and changing the weight of the woodblock.

4.1.6 Measurement in the test

The measurements taken during the test are

- the forces in the struts;
- the stresses in the sheet plate;
- the pressures in the water in the standpipes and in the heavy liquid in the bag;
- the pore pressure distribution in the soil;
- the settlement of the surface of the soil;
- the displacement of the soil in designated points.

4.1.7 Earth pressures on the sheet plates and the loads in the struts

The display of the struts and the strain gauges on the sheet plates for test II and III are shown in Fig. 4.7.

The axial forces in the struts can be calculated with the following formula:

$$P = EA\epsilon, \tag{4.1}$$

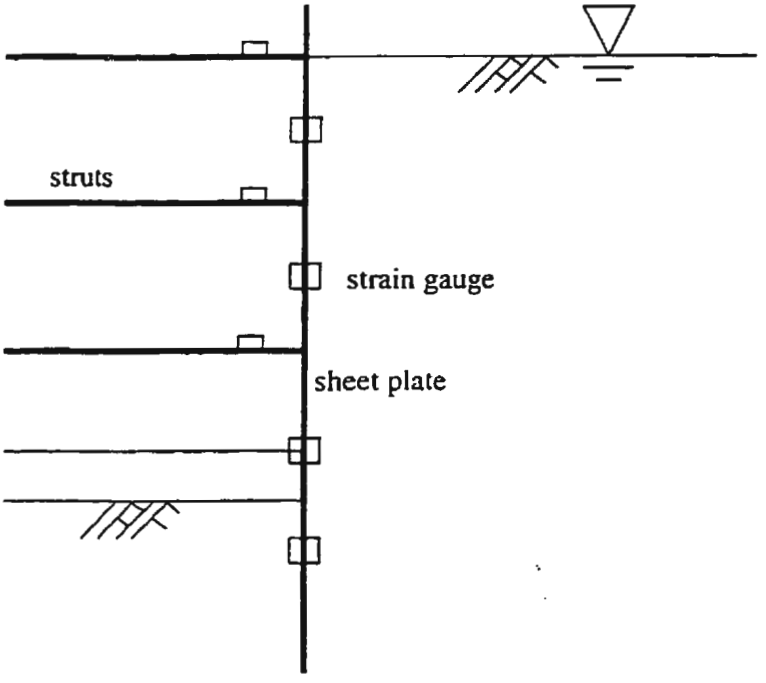

Figure 4.7: View of mechanical measurement on the sheet plates

where P is the axial force in a strut, E is Young's modulus, A is the section area of the strut and ϵ is the axial strain measured with the strain gauges.

The strains in the sheet plates are measured with the strain gauges. The sheet plates are regarded as vertical beams subjected to horizontal loads. According to the beam theory (Lardner and Archer, 1994), the stress at points on the cross section is

$$\sigma = E\epsilon. \tag{4.2}$$

The distribution of the stress on a section is linear, therefore the moment in the section is

$$M = 2\frac{\sigma_{max}}{h}I, \tag{4.3}$$

where σ_{max} is the stress at the edge of the beam, which is obtained with the measured strain, h is the thickness of the beam and I is the moment of inertia of the section.

As the axial forces of struts and the moments in the sheet plates can be found, the sheet plate can be divided into several parts and the homogeneous distribution can be assumed for the loads on each individual part. The distribution can be

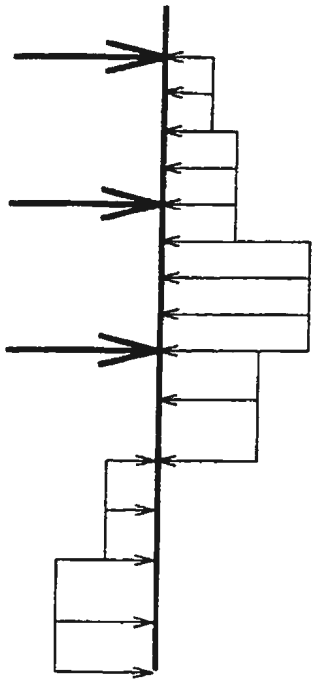

Figure 4.8: Assumed distribution of the pressures on the sheet plates

calculated from the balance of the forces and moments. The total pressures resulting from the earth and the pore pressure on the back of the sheet plates can be drawn, where the struts are regarded as the supports to the beams.

4.1.8 Pore pressure distribution in the soil

The position of the pore pressure transducers (PPTs) for test III are shown in Fig. 4.9. Two PPTs are installed in the soil on the back of the sheet piles. They are 40 mm away from the sheet plates and 125 and 240 mm deep from the surface of

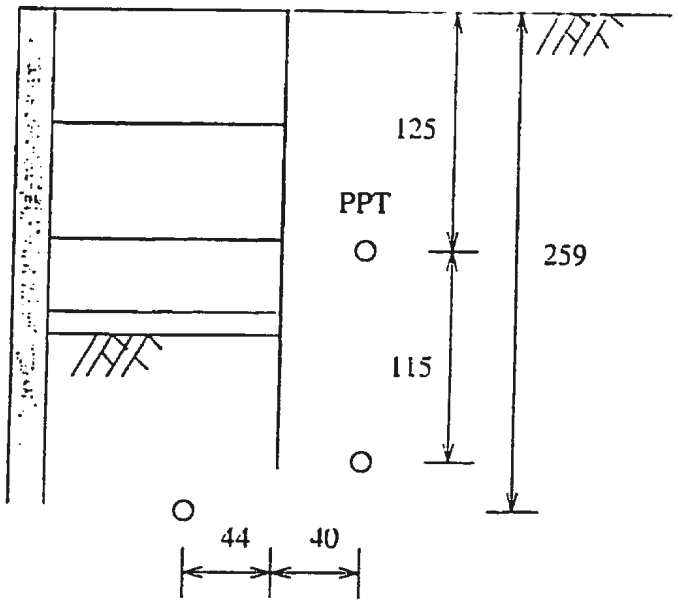

Figure 4.9: The positions of the pore pressure transducers

the soil. They are applied vertically. They are not put in one vertical line in the model for the ease of installation and to minimize interference. One PPT is beneath the bottom of the excavation and the elevation is 259 from the surface of the clay on the back of sheet plate. This PPT is applied horizontally from one side of the strongbox by drilling a hole and fixing a fitting. The purpose is to investigate the pore pressures in different areas in the soil, and because the positions are close to the sheet plate, the pore pressures on the sheet plate can be approximated. Since the pressures on the back of the sheet plate obtained with the method aforementioned are the total pressures including the earth pressures and the pore pressures, it is necessary to separate them to obtain the earth pressures and compare them with the theories and methods already used for engineering design.

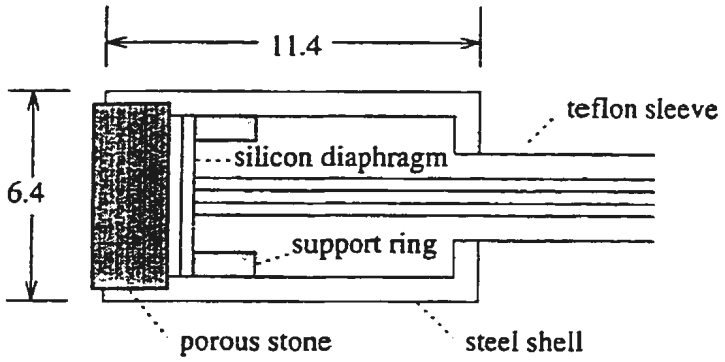

Figure 4.10: Pore pressure transducer

The pore pressure transducers used are type PDCR 1 (Fig. 4.10), made by Druck Ltd. The maximum operating pressure is 350 KP_a (35.71 m under water). The advantages are that this type is small and has a rapid response time (Lach, 1996). Its diameter is 6.4 mm and length, 11.0 mm. The response time is of the order of 0.1 seconds in saturated kaolin clay. The active face is composed of a crystal silicon diaphragm with a strain gauge bridge on its surface. The diaphragm is protected by a porous ceramic stone which resists the pressure of soil particles and the water may seep through for the measurement. For the high degree of saturation of the transducer, the porous stone is boiled in water for about 15 minutes and kept immersed before installation.

Errors resulting from the diameter of the PPT are ruled out if it is installed vertically. Since the diameter of 6.4 mm means 0.45 m in 72 g, the pore pressure would mean the average value on the face of the active side. If it is assumed that the pore pressure is almost the same at the same height around the head of the

PPT, there would be no accountable errors. However the vertical position of the PPT should be carefully measured and accuracy in installation is required.

4.1.9 Measuring the surface settlement

Four LDTs are used to measure the surface settlement of the soil on the back of the sheet plates. The LDTs are fixed on the vertical plate of aluminum parallel with the long axis of the strongbox. This plate is supported with two aluminum beams. The beams are of rectangular section and supported by the edges of the strongbox. The beams are fixed by two thin beams and the thin beams are fixed on the edge of the strongbox. This design makes it convenient to adjust the positions of the LDTs without the need of available holes on the edges of the strongbox to fix the supporting beams. The distances between the LDTs are measured on the plate and the actual positions are checked after the measuring system is fixed on the model for testing. The LDTs are calibrated before the tests.

4.1.10 Displacement field of the soil

In order to obtain the displacement field of the soil, some small plastic balls are installed on the side of soil after the steel side wall is taken off for installing the plexiglass (acrylic). Grids are made on the side surface of the clay contacting the plexiglass, then the plastic balls are applied in the crosses. After tests, the positions of the balls are measured, by comparing with the positions before the test, the displacement is determined. Some error may result from the removal of

the plexiglass.

Another method is to install some dyed spaghetti vertically in the clay at some distance from the glass. These spaghetti expand under saturation and become soft. They come into full contact with the clay, and especially deform together with the clay. After the test, by removing the glass and the clay between the glass and the spaghetti, the deformed spaghetti may give some idea of the displacement of the deformation. This technique requires that the spaghetti be installed vertically, which cannot be perfect.

The third method is not to dye the spaghetti in the previous method but glue short solder strings on the strands of the spaghetti a distance of 20 mm apart. The length of each solder string is 5 mm. The spaghetti are also installed vertically and the displacement field may be known with X-ray to measure the displacement of the solder strings after each test.

4.1.11 Mechanical parameters of the bracing system and the soil

For the purpose of analyzing the results and comparing with the numerical analysis, the properties of the soil and the structure should be obtained. The constitutive relation of the soil is determined according to these properties.

Samples of the soil are collected after the centrifuge tests. Triaxial tests and oedometer tests are carried out. Some shear vane tests are also carried out. The details and results of the tests are described in Chapter 4.

4.2 Soil Preparation

4.2.1 Introduction

The first test is used to test the reliability of the designed system. Therefore, in order to save time in consolidation, the soil for the first test is compacted clay while the remaining tests use consolidated clay.

4.2.2 Preparation I: compacting the clay

The clay for the compaction is the waste clay from other tests. The compaction is done with a hammer, made of steel with a square area of $120 \times 120\ mm^2$ and a height of 25 mm which has a 1 m handle. The total weight is 4.42 kg.

In order to check strength of the compacted clay, a trial compaction is done to test the required height of the hammer and the numbers of hitting. The shear strength is obtained with a hand shear vane. The water content is also measured.

The stability and deformation of the open cut of the clay for installing the bracing system are also tested in the trial compaction under the specific method of compaction.

The formal compaction of clay for test I is done according to the data obtained from the trial compaction. Before compaction, the strongbox is cleaned and the outlets of the bottom are cleaned and sealed. The outlets of the guild pipe and the drainage pipe are also sealed. The steps are as follows:

Drainage layer

A drainage layer is applied at the bottom of the strongbox for the purpose of increasing the speed of consolidation at the beginning of the tests. The layer is composed of a sheet of geotextile at the bottom, a layer of sand of 15 mm, another sheet of geotextile and a sheet of filter paper. The set up of the drainage layer especially the size of the geotextile should make it convenient for removing the steel side wall and applying the plexiglass. The geotextile of the upper layer should be somewhat wider than the bottom of the strongbox, and the other sides are only a little larger than the bottom. The purpose is to wrap the sand particles on that edge in order to prevent the leaking of the sand particles during replacing the side wall with the plexiglass. The geotextile should be carefully cut for the area under the guide pipe and drainage pipe at the bottom of the excavation area.

Compaction

Before compacting the clay, the side faces of the walls of the strongbox are greased with wax. The available clay is wrapped with plastic bags before compacting for keeping the water content. The clay is broken into small pieces and these pieces are displayed homogeneously on the filter paper. The clay is compacted for the bottom layer gently to avoid possible disturbance of the sand.

Compacting is applied with the steel hammer. The area around the guild pipe and drainage pipe is compacted carefully with the help of a woodblock. Two steel caps are designed for the two pipes to plug the pipes when raining the sand and

compacting the clay and to prevent the sand and clay particles from dropping in.

The remaining layers of clay are compacted in the same way. It is better to scratch the surface of the clay before compacting the next layer. The clay is compacted as high as the required surface of the clay.

4.2.3 Preparation II: consolidating the clay

Slurry

The slurry is prepared by mixing the powder of clay and silt with ratio of 1:1 in weight in the mixer. Deionized water is supplied to yield a water content of 70%. The steps are: first, fill the bottom of the mixer with 10 litres of water which would be about 10 kg; secondly, fill the mixer with a bag of clay and a bag of silt alternatively; thirdly, fill the required water; close the cover and stir the mixture for about a half an hour under normal conditions. Finally stir the mixture for about 24 hours under partial vacuum. The speed of rotation is 14 rpm. Each bag of clay is about 25 kg and each of silt is about 23 kg. In total, four bags of clay and slightly more than four bags of silt are used so that the weight of each is equal.

Consolidation device and steps

Consolidation is carried out in the strongbox. Steel wall is used temporarily for the side of the plexiglass. The cover of the strongbox is removed and the four sides of the walls are extended longer to accommodate the volume of the slurry.

The bottom of the strongbox is covered with a drainage layer. The inside surface of the box is greased to reduce friction. The slurry is gently poured into the strongbox and trimmed to a flat surface. Another drainage layer is also built up on the top of the slurry. The bottom drainage layer is connected to a reservoir outside the strongbox. The surface of the water is the same as the surface of the slurry. The initial height of the slurry is about 730 mm. The water content is about 70% and the strength should be 0.

The first load is the self weight of the piston for consolidation. Its weight is 1.079 kN and the area of the box is 0.27 m^2. The initial load in 4.0 kPa. Water in the top drainage layer may flow out around the edge of the piston.

The next step of loading is applied by a ram. The remaining loads are double those of the previous steps until the final load is reached. The loads are controlled by a loading system. The settlement of surface of the clay is recorded after each step of loading. The next load is applied after the settlement of the previous step reaches a stable value. The total process of consolidation finishes in about two weeks.

After consolidation, the loading system is removed and the water content and strength are measured for the clay in the extension part. The final height of the clay is about 500 cm, the water content is 32% and the shear strength is about 35 kPa. Then the extensions of the side walls are removed. The clay above the strongbox is cut off with a string.

4.2.4 Levelling the surface

The surface of the compacted or consolidated clay should be levelled into a smooth flat surface to simulate the ground in site. The excavation is made with a knife excavator used by C-CORE. The knife is fixed in a heavy large vertical beam and this beam is fixed in a steel frame. Two beams are used to support the frame. By moving along the beams, the clay is levelled. The position of the vertical beam may be adjusted with respect to the steel frame to change the depth of excavation.

Before levelling, the cover of the strongbox should be taken off and washed. The top surfaces of the walls of the strongbox should also be cleaned, since the residue of clay particles between the surface would make the measurement of the excavation inaccurate. For the same reason, the surfaces of the cover, the beams and the frame should be cleaned before the beams are moved to a new position.

The levelling was done in two steps, the final step cuts the clay with the surface 40 mm down from the surface of the cover. Care should be taken to avoid over-excavation. After a smooth surface is obtained, the weight of the strongbox and the clay can be measured to calculate the unit weight of the clay. The side wall of steel frame is slid off. The small plastic balls which are used to measure soil displacement are applied. A plexiglass is then installed to replace the steel wall which is on one side of the strongbox. Its purpose is to monitor the deformation of the clay during the excavation and observe the deformation after the tests.

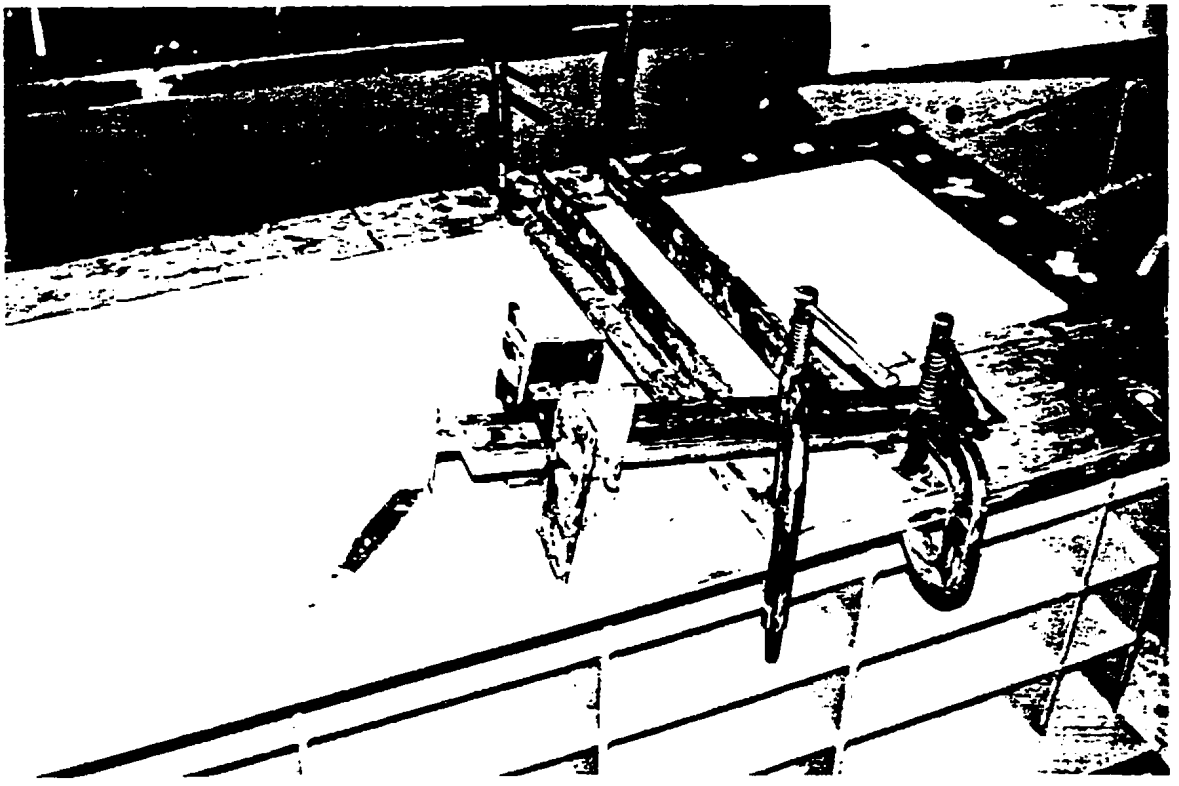

Care is taken to prevent disturbing the clay and damaging the glass. The rubber string inside the wall of the strongbox should be re-fixed with grease to prevent it from leaking. Saturation for the clay should be maintained by covering it with plastic sheets and watering it a little if necessary since the process of installation may take several days.

4.3 Test Installation

The steps and the details of installing the model in the strongbox and the centrifuge chamber are described below.

Cutting the excavation space

After the soil is compacted or consolidated in the strongbox, a small space is excavated for installing the woodblock and the bag to simulate the excavation in the tests. The difficulty in this step is that the width of the excavation should be exactly the sum of the thickness of the end beam, the wale and the length of a strut plus the thickness of the sheet plate, the plastic bag as well as the thickness of wax and the plastic sheet which covers the strain gauges on the sheet plate for water proofing. The dimensions of the cut space are about 121 to 123 mm for the different tests along the length direction of the strongbox, and 300 mm wide and 180 mm deep. It is desired that the difference would be less than 0.2 mm.

The reason that the exact length is required is that if the width is larger, the struts, wales and the sheet plate will not make contact before the excavation. The earth pressure and water pressure on the back of the sheet plate should be balanced by the liquid pressure in front of the sheet plate. However, because the exact K_0 cannot be known, on both sides of the sheet plate, the earth pressure and the pressure resulting from the heavy liquid cannot be equal. If the unit weight of the liquid is larger than the balance value, the liquid will apply a larger pressure to the sheet plate than the soil on the back. This will mobilize some passive earth

pressure in the soil which doesn't match the actual situation. On the other hand, if the unit weight of the liquid is smaller than that required, the earth on the back will apply more pressure and the sheet plate would move forward and an active earth pressure would be mobilized in the soil. Since the scale of the experiment is 72, the displacement would be 72 times in the actual prototype. This large displacement of the sheet pile should be big enough to mobilize the active earth pressures. Therefore, an exact width is preferred and the surface of the liquid and the soil should be kept the same. Unfortunately the exact value of the width cannot be achieved. In this case, it is preferred that the unit weight of the liquid should be a little bit smaller than the required value. This will prevent the mobilization of the passive earth pressure in the soil.

As the first step, a smaller space close to the end of the strongbox is excavated with a plate cutter. In the mean time the strengths are measured at different depths with a shear vane. Samples are also collected for testing the water content.

Secondly, the bottom of the space is excavated with the excavator to reach the required depth for the tests where caution should be taken to avoid cutting the drainage pipes for the heavy liquid and water, otherwise, the soil would be disturbed. Each time, only a small thickness of soil is excavated to prevent disturbance to the soil.

Finally, the width of the space is excavated with a cutter shown in Fig. 4.11. The cutter is composed of two pieces of angle beam. There is a groove in one piece and the other piece may slide along the groove. There is a long hole in the middle

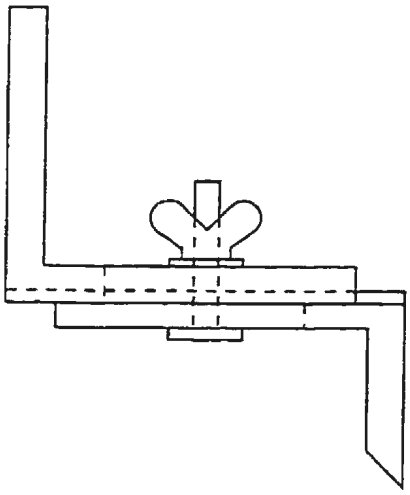

Figure 4.11: Soil cutter

of the groove. The width of excavation can be adjusted easily by sliding along the groove and fixed with a rod and screw passing through the hole. By moving the cutter downward with one end in contact tightly with one end wall of the strongbox, the excavation is carried out to the required width. For accuracy, the end wall of the strongbox should be cleaned before the excavation and the surfaces of the cutter are also smooth for the ease of sliding.

Applying the sheet plate

For each test, two rubber laces are used to prevent the water seeping from the contact between the sheet plate and the strongbox. The sheet plate should be inserted along the side surface of the soil without disturbing the soil. After the sheet plate is inserted into the soil, the wires for the strain gauges should be carefully

fixed on the sheet plate supporting beam for protection. A beam is fixed on the edges of the strongbox just behind the sheet plate supporting the sheet plate beam temporarily to prevent the possible pushing on the sheet plate toward the soil during the installation of the bag and the woodblock system.

Installing the pore pressure transducer (PPT) under the bottom of excavation

Only one PPT is applied at the bottom of the excavation for each test. The position is shown in Fig. 4.9. The PPT is applied after the sheet plate is inserted to avoid the variation of the position of the PPT. The PPT is applied horizontally. A hole is drilled horizontally from the side wall of the strongbox. The PPT is installed laterally from the hole and the hole is perfectly sealed.

Porous layer at the bottom of the excavation

The porous layer is composed of a layer of filter paper at the bottom contacting the surface of the soil, a layer of geotextile, a layer of sand of 5 to 20 mm and finally on the top a layer of geotextile. The inlet of the drainage steel pipe should be at the vertical mid-point of the sand layer, and the inlet should be wrapped with geotextile to prevent the inflow of the sand particles before and during the tests.

Installing the plastic bag

The bag is made with double layers of plastic sheet. The connection fitting between the bag and the tubing should be tight and waterproof. Pipe thread sealant (Master's PRO-DOPE with TEFLON) is used for sealing between the rubber washers and fittings. Silicone is used for sealing between the plastic sheets and the fitting. The bag should be placed evenly over all the drainage layer. The tubing should be carefully inserted into the guiding pipe and extracted out from its outlet. The connecting fitting should be correctly positioned and rest over the inlet of the guiding pipe.

The plastic sheet should be arranged to contact the sheet plate and the end wall of the strongbox, and be carefully folded at the two ends to form a cubic volume. The bag should be loose to allow the full contact with the strongbox and the sheet plate under centrifuge. There should be some folding for the bag around the connection fitting for possible stretch during tests. After the installation of the bag, the beam supporting the sheet plate is removed to slide the top cover of the strongbox out a little for the convenience of installing the bracing system. The cover and the beam should be fixed again.

Installing the bracing system and the drainage system for the heavy liquid

The bracing system includes the woodblock, the wales, the struts, the end beams and the supporting beams. Care should be taken to determine the right position

of the bottom of the wood block system, the correct contact between the struts and the wales, the end beams, and to protect the gauges on the sheet plate and the struts and wires. The bracing system cannot be totally built and then put in position but instead it is built layer by layer. Otherwise, it would damage the gauges, disturb the sheet plate, slide off the wales and make poor or no contact between the struts, the wales and the sheet plate.

The great difficulty of this installation is that a void space should be left under the woodblock for the filling of the heavy liquid, while the struts and the wales should exactly support the sheet plate in the right positions. This problem is solved with the application of four small and slender sand bags. The bags are made of cloth. One end of the bag is closed and the other end is open. Some sand is filled in the bags and the volume of the sand is only enough to go across the section of the space. The sand particles should not leak from the bags.

The four sand bags are then placed on the bottom of the plastic bag and lie across the bottom of it to support the bracing system temporarily. The open ends of the sand bags are kept handy. The aluminum plate which would be at the bottom of the woodblock is put on the top of the bags to make sure the surface of the plate is horizontal and the distance of the top of the plate to the top of the strongbox is the same as required. The bags can be reset and thus, the position of the plate can be adjusted. The plate is then taken out and the eight rods which hold the weight of the bracing system on the strong beams are applied to the plate. The plate is put back onto the top of the sand bags with one edge in contact with the end wall of the strongbox. Next the bottom piece of the wood is applied through the rods

and the supporting beams, end beams, struts and the wale for the bottom layer.

Using the same procedure, the wood pieces, the beams, struts and wales of the other two layers are also fixed in position. For each piece of wood, care should be taken for its installation. The wood should be fitted on the eight rods carefully. Disturbance of the sand bags should be avoided. The contact between the struts and the wales should be frequently checked. Different thickness and number of very think shims of aluminum are applied between the end of each strut and its corresponding end beam to improve the contact. The top piece of wood is finally applied and the beam supporting the sheet plate is free. The top cover of the strongbox is then pushed back slowly and gently into its normal position. No disturbance of the sheet plate is allowed. At last, the beams are applied across the strongbox and the rods are fixed on the beams. The beams are fixed on the strongbox with screws.

The sand in the four sand bags is pumped out with a plastic tube. The bags are removed and the installation of the bracing system is completed. The plastic bag can be trimmed and taped on the surface of the strongbox or on the fixing beams. The drainage system for the heavy liquid can also be lined up and fixed.

Installing the water control system and heavy liquid collecting system

The end of the strongbox installed with the bracing system is taken as the front side. The standpipe for controlling the pore pressure at the bottom of the excavation is fixed. The standpipe for controlling the water table in the clay is also fixed at the

end of the strongbox and connected with the tubing for draining the water from the bottom drainage layer. The valves are checked and the PPTs are installed. Some solder string should be fixed on the PPTs in the standing pipes to prevent them from floating during the test. Water is filled into the standpipes. The volume is recorded.

The tubing for draining the heavy liquid is connected to the collecting box through a rate control and a valve.

Applying the displacement identification material

One layer of dyed spaghetti may be inserted into the clay on the back of the sheet plate in this step. Care should be taken over the position and to make it vertical.

Applying the three PPTs in the soil on the back of the sheet plate

The positions are shown in Fig. 4.9, and the PPTs are not in the same vertical line. They are calibrated before installation. Before installation, the stone is boiled in water for about 15 minutes and kept in the water. The stone should be fixed onto the PPT under the water. After the position is calibrated to the surface of the clay, a tube is driven vertically into the clay. The clay in the tube is removed with a special small drill. This process proceeds alternatively until reaching the depth about 5 mm above the actual position of the PPT surface. The PPT is pushed into the bottom of the hole with the help of a guide. The required depth of installation for the PPT is obtained by inserting the PPT with reference to the mark. After a

PPT is installed, some small pieces of clay are used to backfill the hole with some compaction.

Applying the LDTs

The position of the LDT frame referring to the strongbox should be checked.

Installing the PPT in the plastic bag

The PPT in the plastic bag is used to monitor the surface of the heavy liquid during the test. The position of the active face of the PPT is measured before each test. The surface of the heavy liquid would be subjected to a lot of change during the first couple of minutes because there is some space between the bag and the strongbox.

Fix the wires, the signal box

Moving the lined up strongbox to the chamber of the centrifuge and line up all the wires

Final set up

Finally after fixing the water supply system, the wires, the cameras used for monitoring the model during the tests, the model is ready for testing.

Sheet plate strain gauge calibration

Calibrating at this time may eliminate the error resulting from the difference of temperatures between the sheet plate and the soil because the sheet plate has been put in the soil for several days.

Filling the heavy liquid

The collecting box for the heavy liquid, the tubing and the valves are fixed before filling the heavy liquid. The required volume can be estimated. The volume added and the surface of the heavy liquid are taken down for each test and can be used as reference for the next test. Before filling the heavy liquid, its specific gravity is measured.

Chapter 5

PROPERTIES OF THE SHEET PLATE, STRUTS AND CLAY

5.1 Introduction

This chapter explains the procedures of sampling and testing the clay, the sheet plate and the struts for the following parameters:

E–Young's moduli of sheet plate and the struts;

γ–unit weight of the soil;

w–water content;

e_0–initial void ratio;

k–coefficient of permeability;

ϕ–angle of internal friction;

c–internal cohesion;

c_v–coefficient of consolidation;

m_v–coefficient of volume compressibility;

C_c–compression index;

C_s–swelling index;

λ–slope of normal compression line;

κ–slope of unloading-reloading line.

5.2 Young's Moduli of the Sheet Plate and the Struts

5.2.1 Principles of the tests

The moduli were measured with a beam simply supported at the ends. Concentrated loads were applied in the middle of the beam (Fig. 5.1). According to theory, the deflections at the quarter points near the ends are:

$$y = \frac{11}{768}\frac{PL^3}{EI}, \tag{5.1}$$

where P is the concentrated load, L is the span of the beam, E is Young's modulus and I is the moment of inertia of the section of the beam. In other words,

$$P = \frac{768}{11}\frac{EI}{L^3}y. \tag{5.2}$$

This is a linear relation between P and y and can be written as

$$P = ky \tag{5.3}$$

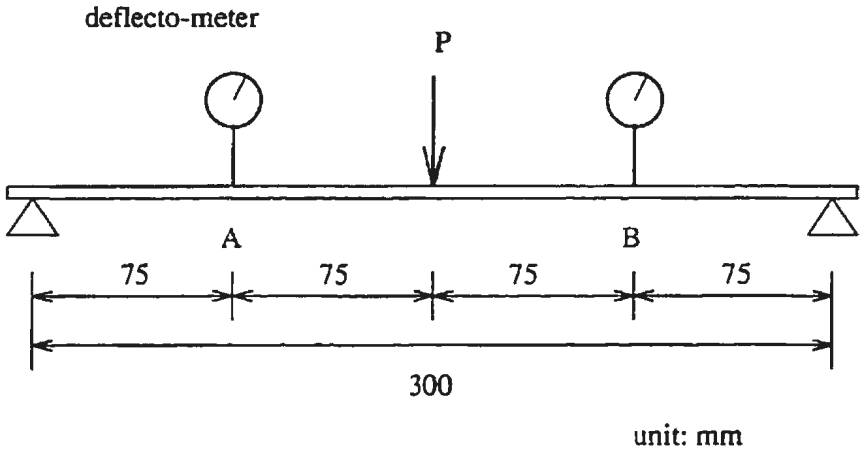

Figure 5.1: Testing Young's modulus

and

$$k = \frac{768}{11}\frac{EI}{L^3}. \tag{5.4}$$

The purpose of the tests was to find the value of k and, hence E, where

$$E = \frac{11}{768}\frac{L^3}{I}k. \tag{5.5}$$

5.2.2 Young's modulus of the sheet plate

The test assembly for sheet plate is as shown in Fig. 5.1. Two deflecto-meters were used to measure the deflection of the beam. The beam was the same material as the sheet plate. The span of the beam was 300 mm, the width was 50 mm and the thickness was 1.55 mm. Therefore the moment of inertia was 15.516 mm^4. A series of loads were applied and the corresponding deflections were measured. The parameter k is obtained by using the least squared method. For a load P_i, there is a deflection y_i, and the theoretical load P_{ti} is thus,

$$P_{ti} = ky_i, \tag{5.6}$$

and the difference is

$$\Delta_i = P_{ti} - P_i = ky_i - P_i \tag{5.7}$$

The sum of the differences squared is

$$\Delta = \sum_{i=1}^{n} (ky_i - P_i)^2. \tag{5.8}$$

For a minimum value of Δ, it follows that

$$\frac{\partial \Delta}{\partial k} = 0. \tag{5.9}$$

Therefore,

$$k = \frac{\sum_{i=1}^{n} P_i y_i}{\sum_{i=1}^{n} {y_i}^2}. \tag{5.10}$$

The results of the loading and deflection are shown in Fig. 5.2. The circle and the plus signs represent the results at A and B respectively. The figures show that the points of loading are almost in a line and there is little plastic deformation, therefore all points of the loading are used to calculated the value of k.

According to the test results,

$$k = \frac{\sum_{i=1}^{n} P_i y_i}{\sum_{i=1}^{n} {y_i}^2} = \frac{2003.49635}{0.27696145} = 7233.84 \qquad (g/in). \tag{5.11}$$

and

$$E = \frac{11}{768}\frac{L^3}{I}k = \frac{11}{768} \times \frac{(300mm)^3}{15.516mm^4} \times 7233.84(g/in) = 69.56 \qquad (GP_a). \tag{5.12}$$

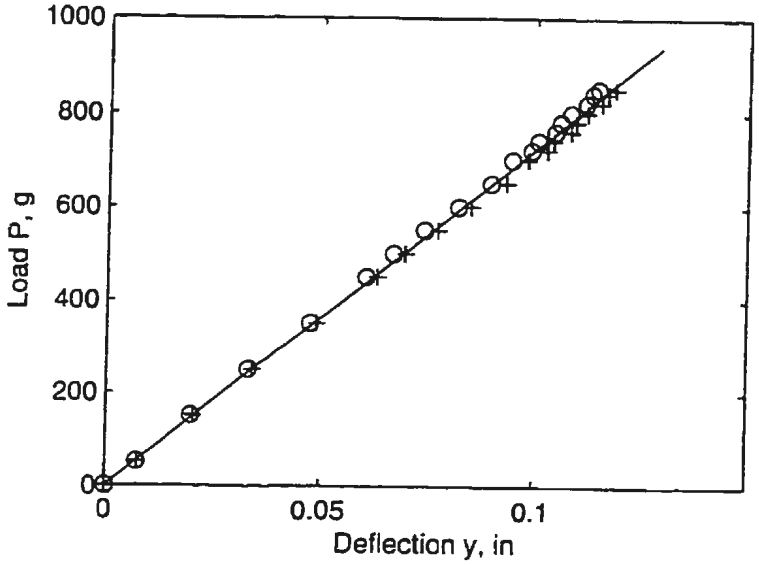

Figure 5.2: Relations between loads and deflections for sheet plate

5.2.3 Young's modulus of the struts

The struts were subjected to axial loads instead of bending and it was assumed that they were homogeneous and isotropic. The struts were also made of aluminum. Therefore the Young's modulus obtained from the bending tests may be used for axial loading. The span of the tested beam was 500 mm. The section of the struts was the same as that of the beam: the height was 6.60 mm and the width was 6.58 mm. Therefore the moment of inertia was 157.644 mm^4.

The results of the test are shown in Fig. 5.3. The points of loading can be reasonably approximated by a line passing the origin. Therefore the loading points of both A and B are used to calculated the parameter k, and

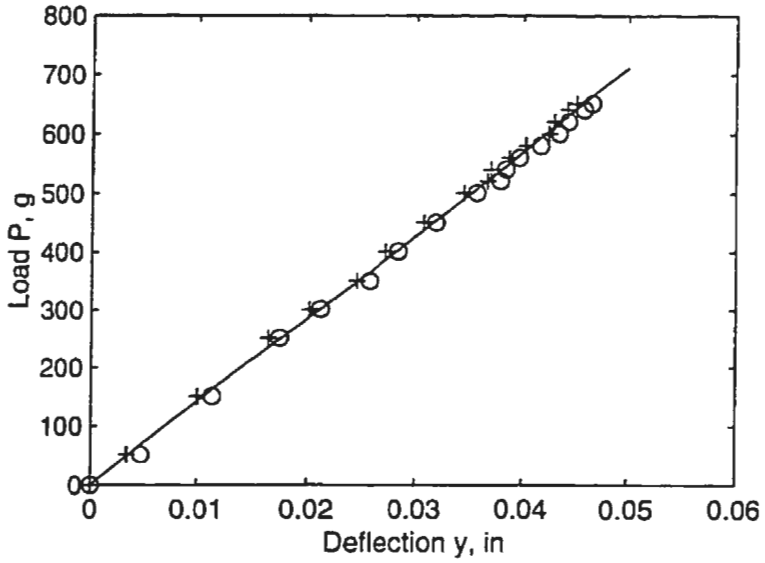

Figure 5.3: Relations between the loads and deflections for struts

$$k = \frac{\sum_{i=1}^{n} P_i y_i}{\sum_{i=1}^{n} {y_i}^2} = \frac{522.79664}{0.03673964} = 14229.77 \qquad (g/in). \tag{5.13}$$

Therefore

$$E = \frac{11}{768}\frac{L^3}{I}k = \frac{11}{768} \times \frac{(500mm)^3}{157.644mm^4} \times 14229.77 g/in = 62.35 \qquad (GP_a). \tag{5.14}$$

The normal magnitude of Young's modulus of aluminum is 71 GP_a, the results of both the sheet plate and the struts are close to this value.

5.3 Compression Tests

5.3.1 Soil samples

For the compression tests, three samples were collected with a ring sampler. The inside diameter of the ring was 63.28 mm and the height was 25.42 mm. The positions of the centers of the samples are shown in Fig. 5.4. The samples are referred to as of C1, C2 and C3.

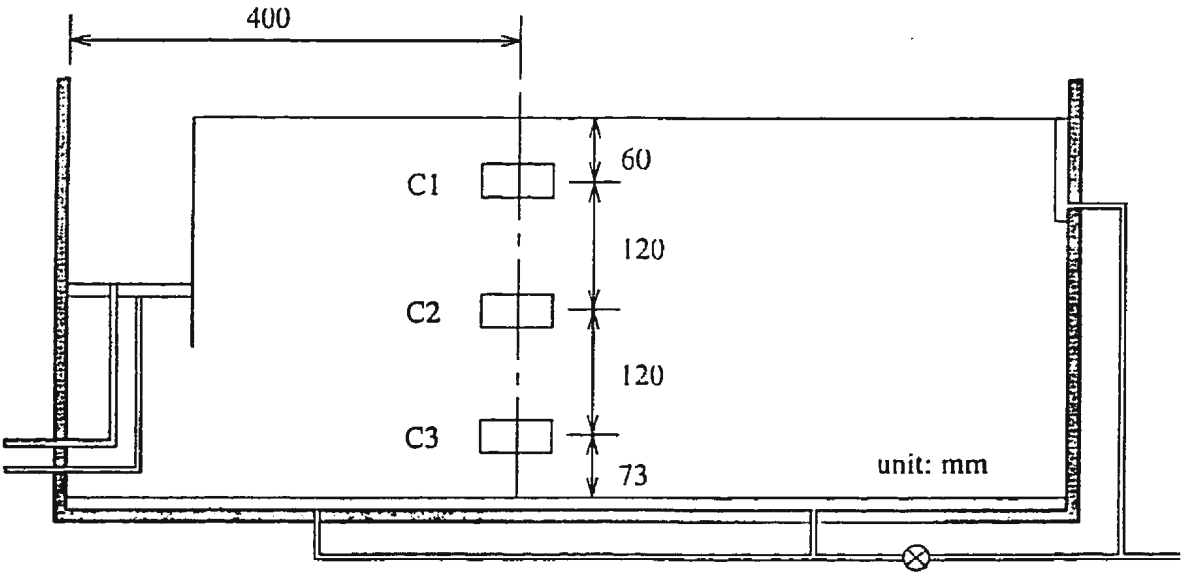

Figure 5.4: Positions of the samples

Care was taken to prevent the possible disturbance of the soil. Small samples of the clay were also collected to determine the water content. The samples were trimmed, weighed and assembled in the compression box as soon as they were collected.

5.3.2 Test procedures

The tests were done according to the procedures in ASTM D2435-90. Filter paper and sand stones were used on both ends of the sample to form a two-way drainage condition. The water squeezed out from the sample could flow out freely. The reservoirs were on both ends of the samples to keep the saturation. More water was added to the reservoirs if the water level was reduced because of evaporation. For each test, the loads were applied with dead weights through a frame which had an augment factor of 10. The settlement of the samples was measured with dial gauges. The load increment ratio ($\Delta p/p$) was kept to 1 for the first 6 steps. With the available facility, the loads were selected as 23, 47, 93, 187, 373, 746, 1243, 1741 kPa. Each load was applied for about 24 hours. The settlement of a sample under each loading was measured at 0.1, 0.25, 0.5, 1, 2, 4, 8, 30 minutes and 1, 2, 4, 8 and 24 hours after the load was applied.

The effect of unloading was also measured after the final load of 1741 kPa was applied. The decrement of unloading was the same as that for loading. Rebounding of the samples was also measured by the same procedure. After each test, the dimension and water content were measured for each sample.

5.3.3 Test results

The initial conditions of the samples such as water content ω_0, specific gravity ρ_0, void ratio e_0 and height H_0, are presented in Table 5.1. The accumulated settlement and rebounding are shown in Fig. 5.5, 5.6 and 5.7 for samples C1, C2

and C3 respectively.

The initial void ratio is calculated according to the following formula where the samples were assumed fully saturated:

$$e_0 = \frac{\rho\omega}{1-(\rho-1)\omega}, \tag{5.15}$$

$$\rho = \frac{\gamma}{\gamma_w}, \tag{5.16}$$

where ω is water content, ρ is density, γ is unit weight of soil and γ_w is unit weight of water. The height of solids is:

$$H_s = \frac{H_0}{1+e_0} \tag{5.17}$$

where H_0 is the initial height, and the void ratio after the completion of each load is

$$e = \frac{H-H_s}{H_s}. \tag{5.18}$$

where H is the height of the sample at the moment. The coefficient of compressibility, a_v, the coefficient of volume compressibility, m_v, the compression index, C_c, and swelling index, C_s, are calculated according to the following formulas:

$$a_v = \frac{e_1 - e_2}{p_2 - p_1}, \tag{5.19}$$

$$m_v = \frac{a_v}{1 + e_1}, \tag{5.20}$$

$$C_c = \frac{e_1 - e_2}{\log(p_2/p_1)}, \tag{5.21}$$

$$C_s = \frac{e_2 - e_1}{\log(p_1/p_2)}, \tag{5.22}$$

$$\tag{5.23}$$

where e_1 and e_2 are the void ratios at the beginning and the end of each step of loading for C_c and unloading for C_s.

The coefficient of consolidation c_v is defined as:

$$c_v = \frac{k}{\gamma_w a_v}(1 + e_1), \tag{5.24}$$

where k is the coefficient of permeability, γ_w is the unit weight of water. With the curves of settlement and square-root time, c_v can be calculated from:

$$c_v = \frac{T_v \bar{h}^2}{t_{90}}, \tag{5.25}$$

where $\bar{h}$ is half of the average height of the samples (double drainage layers), t_{90} is the time required for the consolidation to reach of 90%. T_v is the time factor

related to the degree of consolidation. For example, if the degree of consolidation is 90%, T_v is 0.848.

These results are listed in Tables 5.2, 5.3 and 5.4 for the samples.

From the definition of c_v, the coefficient of permeability of the clay can be estimated with

$$k = \frac{c_v a_v \gamma_w}{1 + e_1}. \tag{5.26}$$

The parameters λ and κ in the Cam-clay model can be calculated from

$$\lambda = 2.3 C_c, \tag{5.27}$$

$$\kappa = 2.3 C_s. \tag{5.28}$$

Table 5.1: Initial parameters of the samples

Samples	w_0 (%)	ρ_0	e_0	H_0 (mm)	H_s (mm)
C1	32.2	1.885	0.849	21.07	11.40
C2	32.5	1.879	0.853	20.54	11.08
C3	32.5	1.879	0.855	21.34	11.50

Figure 5.5 Accumulated settlement of sample C1

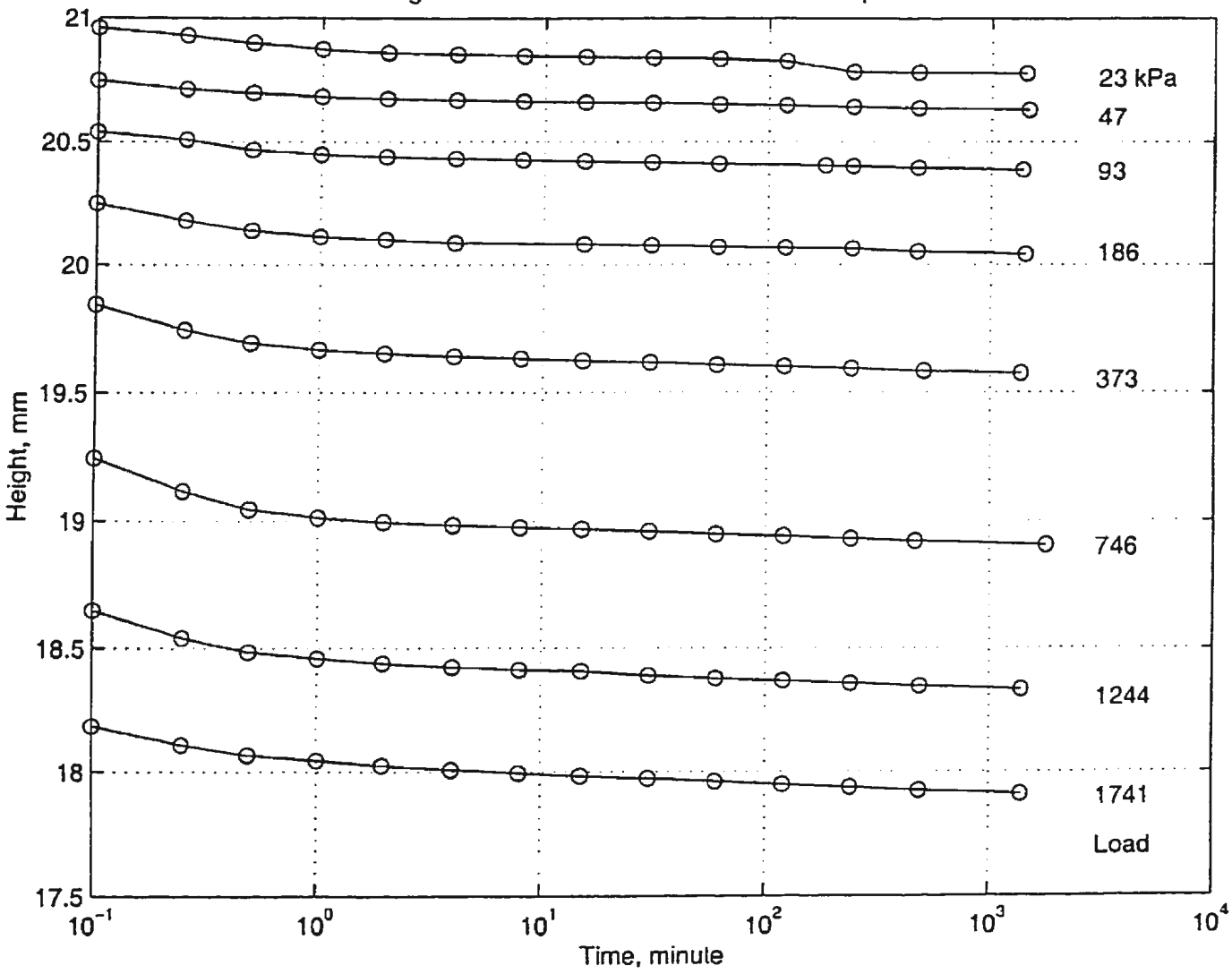

Figure 5.6 Accumulated settlement of sample C2

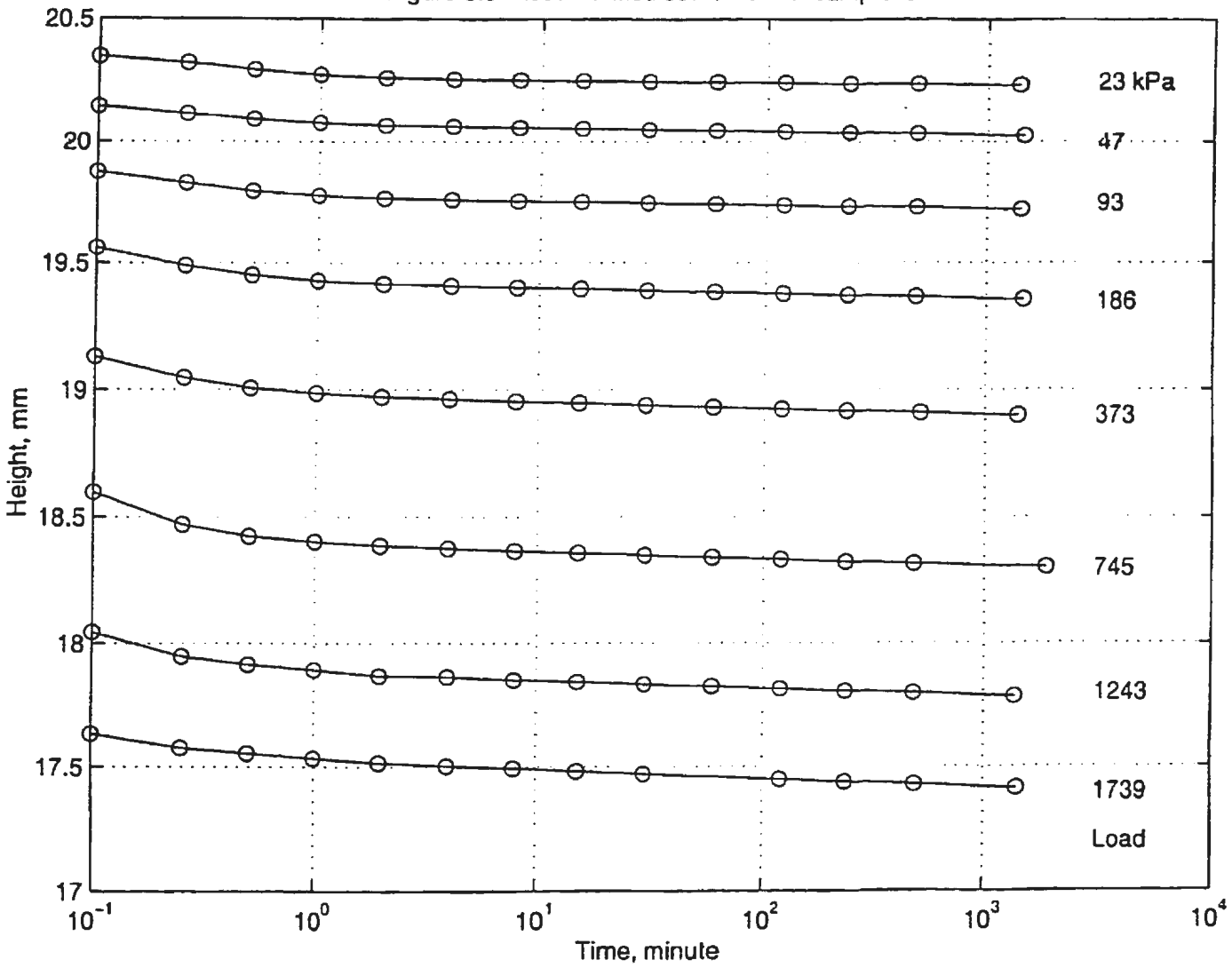

Figure 5.7 Accumulated settlement of sample C3

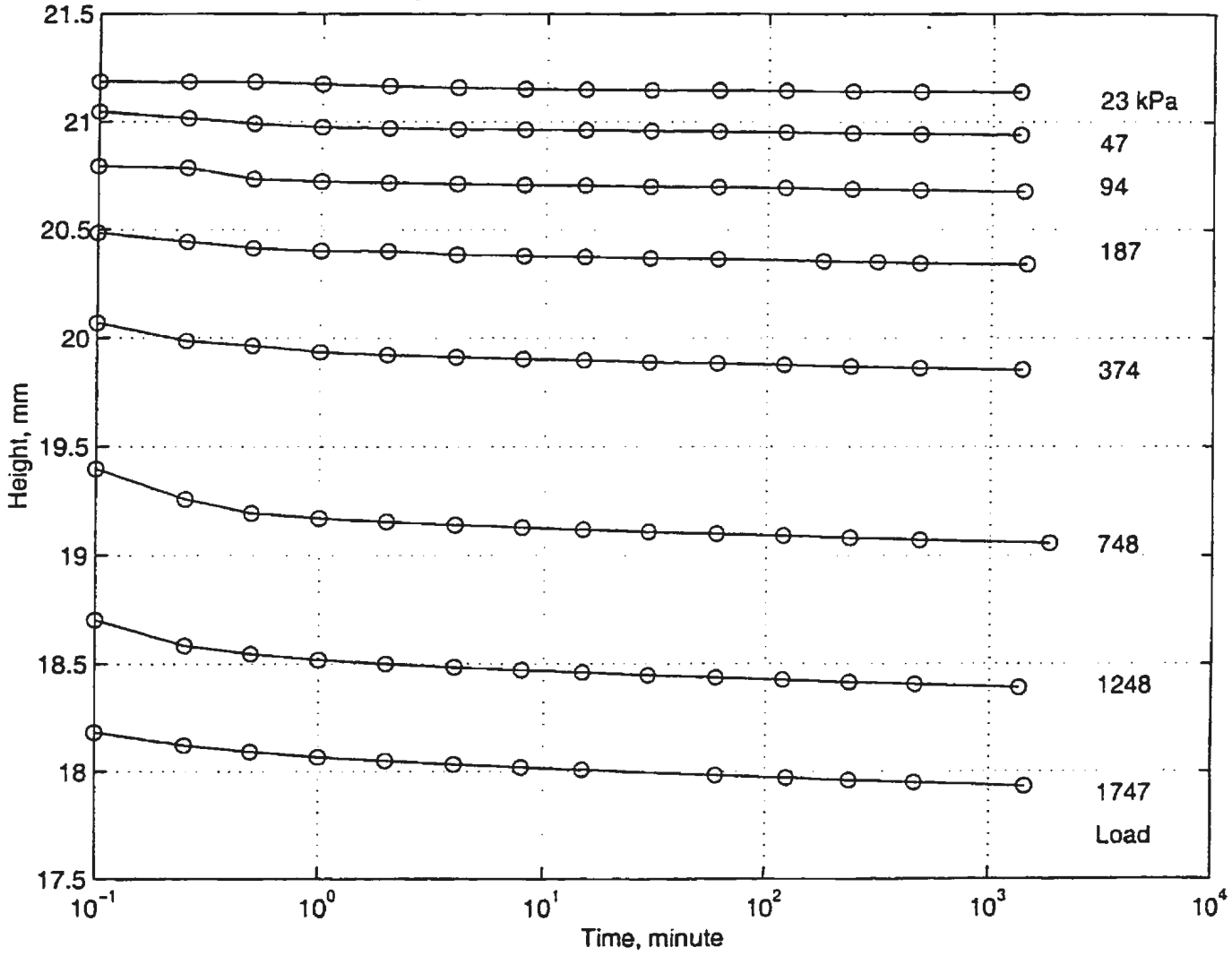

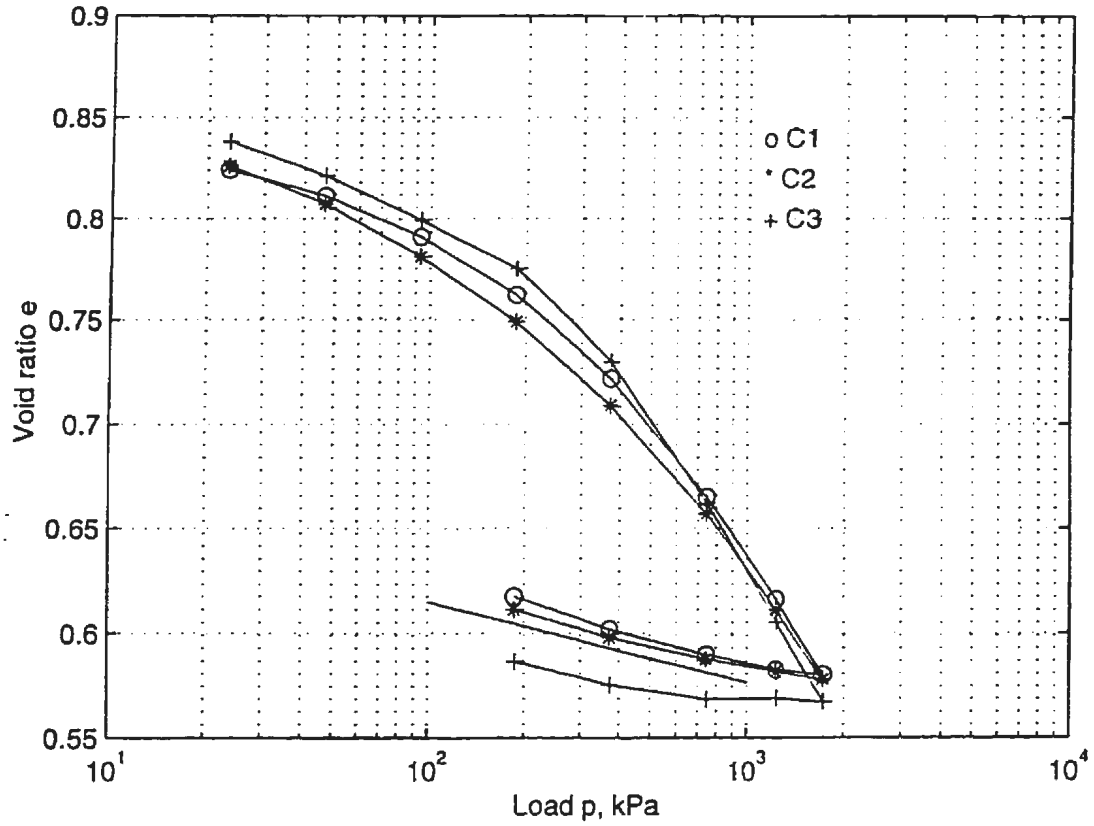

Figure 5.8: $e - \log p$ curve for samples

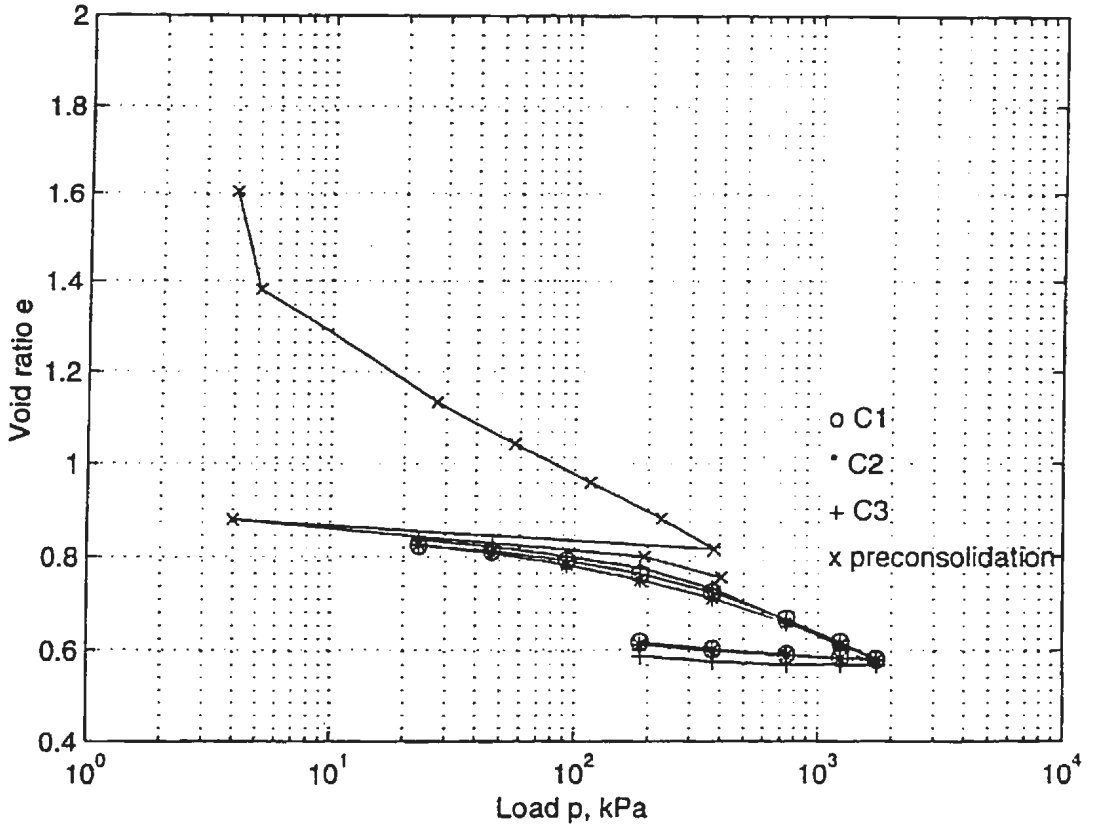

Figure 5.9: Comparison between the results of preconsolidation and the compression tests

Table 5.2: Compression parameters for sample C1

P (kPa)	H_1 (mm)	H_2 (mm)	e_1	e_2	$\bar{H}$ (mm)	t_{90} (s)	c_v (mm^2/s)	a_v (1/MPa)	m_v (1/MPa)	C_c	k ($\times 10^{-9}$ m/s)
0-23	21.07	20.78	0.849	0.824	20.92	60.0	1.5472	1.072	0.580		8.800
23-47	20.78	20.64	0.824	0.811	20.71	90.8	1.0014	0.557	0.305	0.0432	3.000
47-93	20.64	20.41	0.811	0.791	20.52	47.0	1.9000	0.429	0.237	0.0664	4.415
93-186	20.41	20.08	0.791	0.762	20.24	26.5	3.2744	0.311	0.174	0.0963	5.578
186-373	20.08	19.62	0.762	0.722	19.85	24.6	3.3952	0.244	0.138	0.1329	4.612
373-746	19.62	18.97	0.722	0.665	19.30	23.8	3.3146	0.153	0.089	0.1894	2.889
746-1244	18.97	18.41	0.665	0.616	18.69	23.8	3.1100	0.098	0.059	0.1628	1.796
1244-1741	18.41	18.00	0.616	0.580	18.21	25.3	2.7809	0.072	0.044	0.1196	1.215

Table 5.3: Compression parameters for sample C2

P (kPa)	H_1 (mm)	H_2 (mm)	e_1	e_2	$\bar{H}$ (mm)	t_{90} (s)	c_v (mm^2/s)	a_v (1/MPa)	m_v (1/MPa)	C_c	k ($\times 10^{-9}$ m/s)
0-23	20.54	20.24	0.853	0.826	20.39	55.3	1.8794	1.159	0.625		11.532
23-47	20.24	20.03	0.826	0.826	20.14	48.1	1.7871	0.816	0.447	0.0631	7.834
47-93	20.03	19.74	0.807	0.781	19.89	46.5	1.8034	0.582	0.322	0.0864	5.698
93-186	19.74	19.39	0.781	0.749	19.57	24.6	3.2992	0.343	0.192	0.1063	6.233
186-373	19.39	18.94	0.749	0.709	19.17	23.1	3.3715	0.215	0.123	0.1329	4.066
373-745	18.94	18.37	0.709	0.657	18.66	22.0	3.3541	0.140	0.082	0.1728	2.695
745-1242	18.37	17.86	0.657	0.611	18.12	21.6	3.2207	0.092	0.056	0.2072	1.754
1242-1739	17.86	17.49	0.611	0.578	17.68	22.0	3.0116	0.066	0.041	0.2260	1.210

Table 5.4: Compression parameters for sample C3

P (kPa)	H_1 (mm)	H_2 (mm)	e_1	e_2	$\bar{H}$ (mm)	t_{90} (s)	c_v (mm^2/s)	a_v (1/MPa)	m_v (1/MPa)	C_c	k ($\times 10^{-9}$ m/s)
0-23	21.34	21.42	0.855	0.838	21.24	42.3	2.2612	0.727	0.392		8.694
23-47	21.42	20.95	0.838	0.821	21.04	48.6	1.9319	0.727	0.396	0.0565	7.496
47-94	20.95	20.70	0.821	0.799	20.82	36.5	2.5185	0.470	0.258	0.0731	6.377
94-187	20.70	20.42	0.799	0.775	20.56	32.4	2.7648	0.256	0.142	0.0797	3.860
187-374	20.42	19.90	0.775	0.730	20.16	22.0	3.9230	0.240	0.135	0.1495	5.204
374-748	19.90	19.12	0.730	0.662	19.51	22.3	3.6183	0.182	0.105	0.2259	3.734
748-1248	19.12	18.47	0.662	0.662	18.79	21.6	3.4667	0.114	0.068	0.2568	2.333
1248-1747	18.47	18.02	0.605	0.567	18.25	22.3	3.1650	0.076	0.047	0.2603	1.470

The $e - \log(p)$ curves for the three samples are shown in Fig. 5.8. These results are compared with the initial consolidation curve in Fig. 5.9. It is shown that the curves match very well. The index of compression of the initial consolidation curve and the index of swelling of the samples can be used to represent the clay.

From these results, it is calculated that the index of compression of the clay is

$$C_c = 0.1213,$$

and the index of swelling is

$$C_s = 0.0167.$$

The parameters of Cam-clay model, λ and κ can be calculated according to (5.27) and (5.28) which show that $\lambda = 0.2783$ and $\kappa = 0.0384$.

The relation between the load and C_c is shown in Fig. 5.10. The data can be approximated with the function:

$$C_c = 0.0144 p^{0.3979}. \tag{5.29}$$

By using the equation (5.26), the relationship between the coefficient of permeability and the loading is shown in Fig. 5.11 for the three samples given in Table 5.2 to 5.4. These data can be used in a linear least square analysis and the relationship can be approximately described by the equation

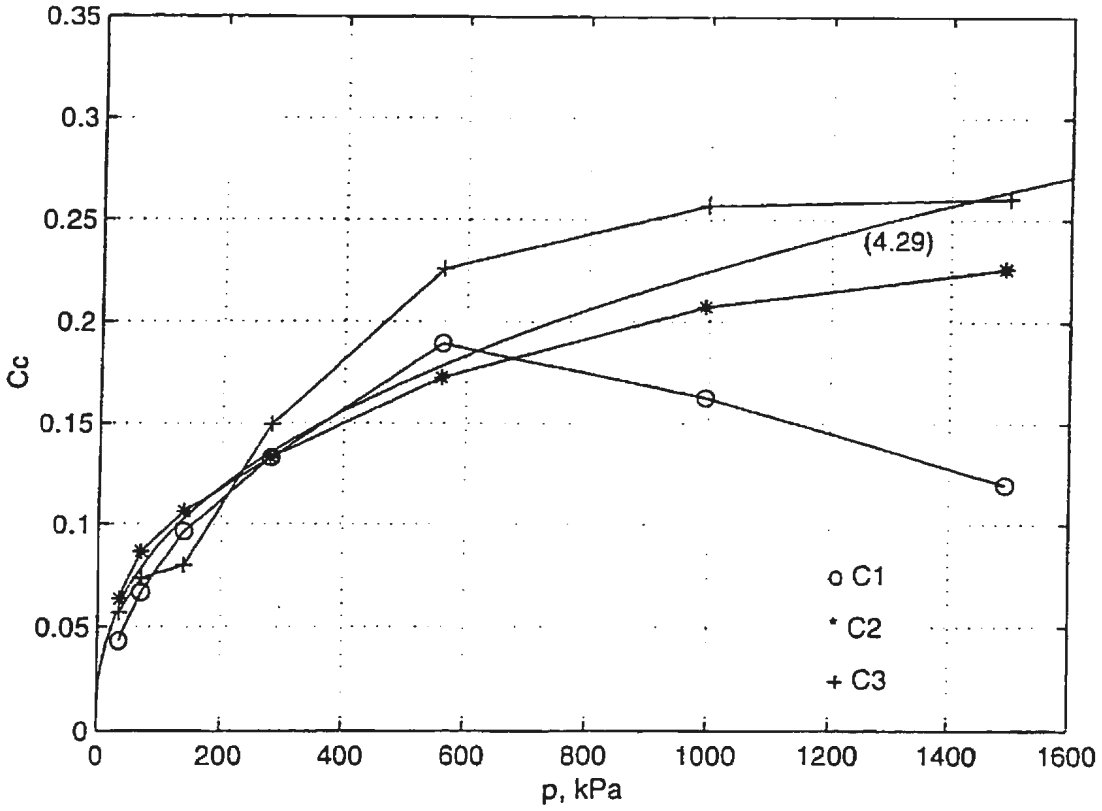

Figure 5.10: Relations between the loads and C_c

$$k = (-0.00281729p + 5.75899) \times 10^{-9} \qquad (m/s), \qquad (5.30)$$

where p is in kPa. For the actual test, the vertical stresses varied between 0 at the surface and 240.8 kPa at the bottom of the clay under 72 g. By using the pressure at the middle depth (120.4 kPa) and equation the coefficient of permeability is taken to be $k = 5.42 \times 10^{-9}\ m/s$. This value is acceptable and lies in a range normally found for clays (Cernica, 1982).

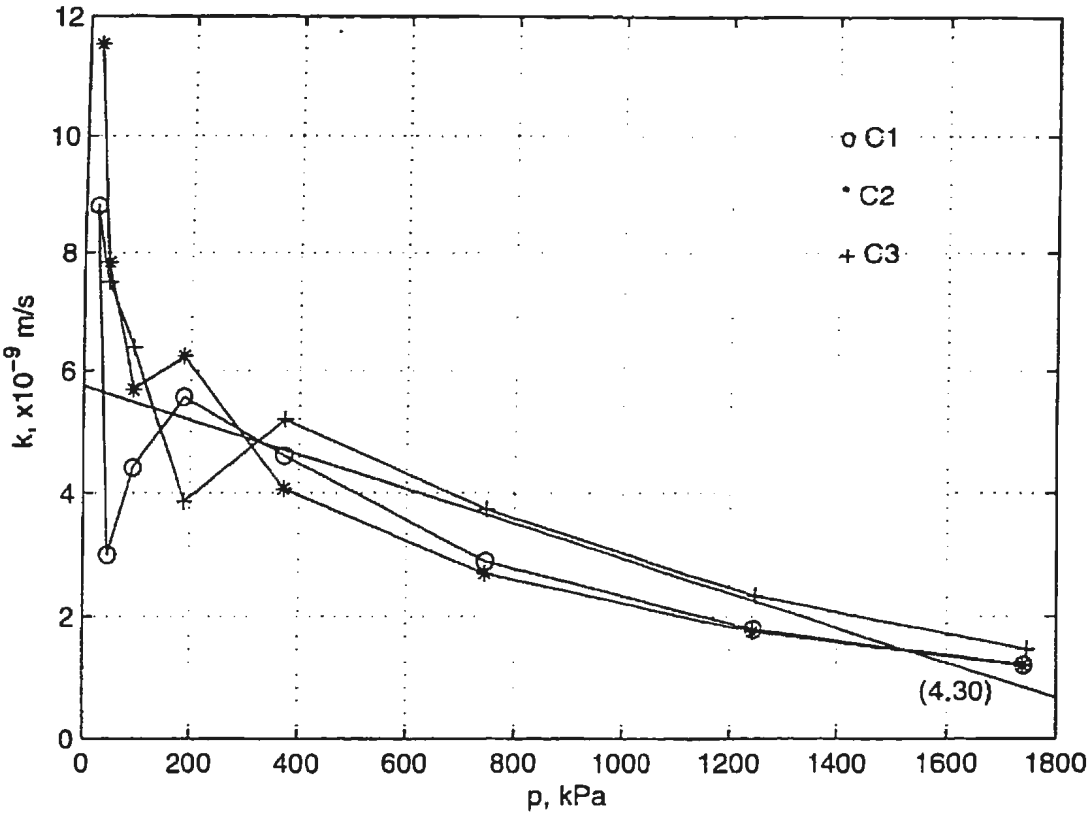

Figure 5.11: Relationship between the loads and the permeability

5.4 Triaxial Tests

5.4.1 Soil samples

Six samples were used for triaxial compression tests. The diameter of the sampler is 38 mm and the height is 170 mm. The samples were collected at the middle part of the clay in the strongbox. Samples for water content were also collected. After each sample was trimmed, the weight was measured. The collected samples were cut on both ends to make the samples 85 mm high for the tests.

5.4.2 Test procedures

The triaxial apparatus may measure the axial loads, pore pressures, cell pressures, axial strain and volume change. After a sample was assembled in the apparatus, the sample was saturated by applying a back pressure. The back pressure was applied in 50, 100, 200 or 300 kPa steps and the cell pressure was 10 kPa larger than the back pressure. It may take 3 or 4 steps for the sample to reach 95% saturation. Consolidations were carried out with 50, 100, 200, 300 and 400 kPa of effective cell pressures. The description of the samples is listed in Table 5.5.

5.4.3 Test results

The relationship between the shear stresses and the axial strains is shown in Fig. 5.12. Most relationships show the characteristics of dilation because the soil was overconsolidated. The relationship between the developing pore pressures and the

Table 5.5: Initial parameters of the samples in triaxial tests

Samples	w_0 (%)	ρ_0	e_0	H_0 (mm)	shear rate (mm/min)
T0	31.5	1.911	0.803	85.00	0.10000
T1	33.0	1.900	0.834	85.00	0.03542
T2	32.6	1.903	0.829	80.82	0.10000
T3	33.1	1.905	0.834	84.33	0.10000
T4	32.4	1.910	0.820	85.89	0.10000
T5	31.9	1.915	0.807	81.36	0.10000

Table 5.6: Parameters of the samples at failure in triaxial tests

Samples	cell pressure (kPa)	σ_1' (kPa)	σ_3' (kPa)	u_f (kPa)	ϵ_f (%)	w_f (%)
T0	54.69	192.3	59.9	-5.0	9.52	31.6
T1	123.30	281.0	89.5	24.8	12.41	28.0
T2	203.46	365.1	117.1	74.0	9.70	28.6
T3	302.84	443.5	137.5	146.0	9.50	27.4
T4	410.27	627.6	224.1	172.4	10.35	26.9
T5	449.04	619.8	202.2	224.8	10.77	26.8

axial strains is shown in Fig. 5.13. For σ_3=54.69 kPa, the pore pressure becomes negative after axial strain is more than 7%. The relationship between the coefficient A and the axial strain is shown in Fig. 5.14. It has the same characteristics as the relation between the pore pressure and axial strain. The stress paths are shown in Fig. 5.15. It shows the behaviour of overconsolidation. The details of each sample at failure are shown in Table 5.6.

The Mohr's circles for the test are shown in Fig. 5.16. The circles are drawn

according to the different effective lateral and axial stresses at failure in different samples. By fitting the circles with a tangential line, it is found that c_{cu}=4.25 kPa and $\phi = 30°$. The elastic relationship in the triaxial tests may be described by the following equations (Wood, 1990):

$$\delta\epsilon_p = \frac{\delta p'}{K'} \tag{5.31}$$

$$\delta\epsilon_q = \frac{q}{3G'} \tag{5.32}$$

where p' and q are mean and deviator stresses, ϵ_p and ϵ_q are the volumetric and shear strains. K' and G' are the bulk and shear modulus.

In undrained triaxial tests, the initial response of the soil samples is elastic. This implies that the initial slope of the curve of shear stresses and shear strains is $3G'$. However

$$\delta\epsilon_q = \delta\epsilon_a + \frac{\delta V/V}{3}, \tag{5.33}$$

and at the beginning

$$\delta V = 0,$$

therefore

$$\delta\epsilon_q = \delta\epsilon_a. \tag{5.34}$$

This implies that the initial slope of the curve of shear stresses and axial strains is also $3G'$ and the initial slope of the curve of pore pressures and the axial strain is G'. As a result, at σ_3=449.04 kPa, the shear modulus of the clay is

$G' = 2.667 \times 10^4$ kPa.

Figure 5.12 Relationship between shear stresses and axial strains

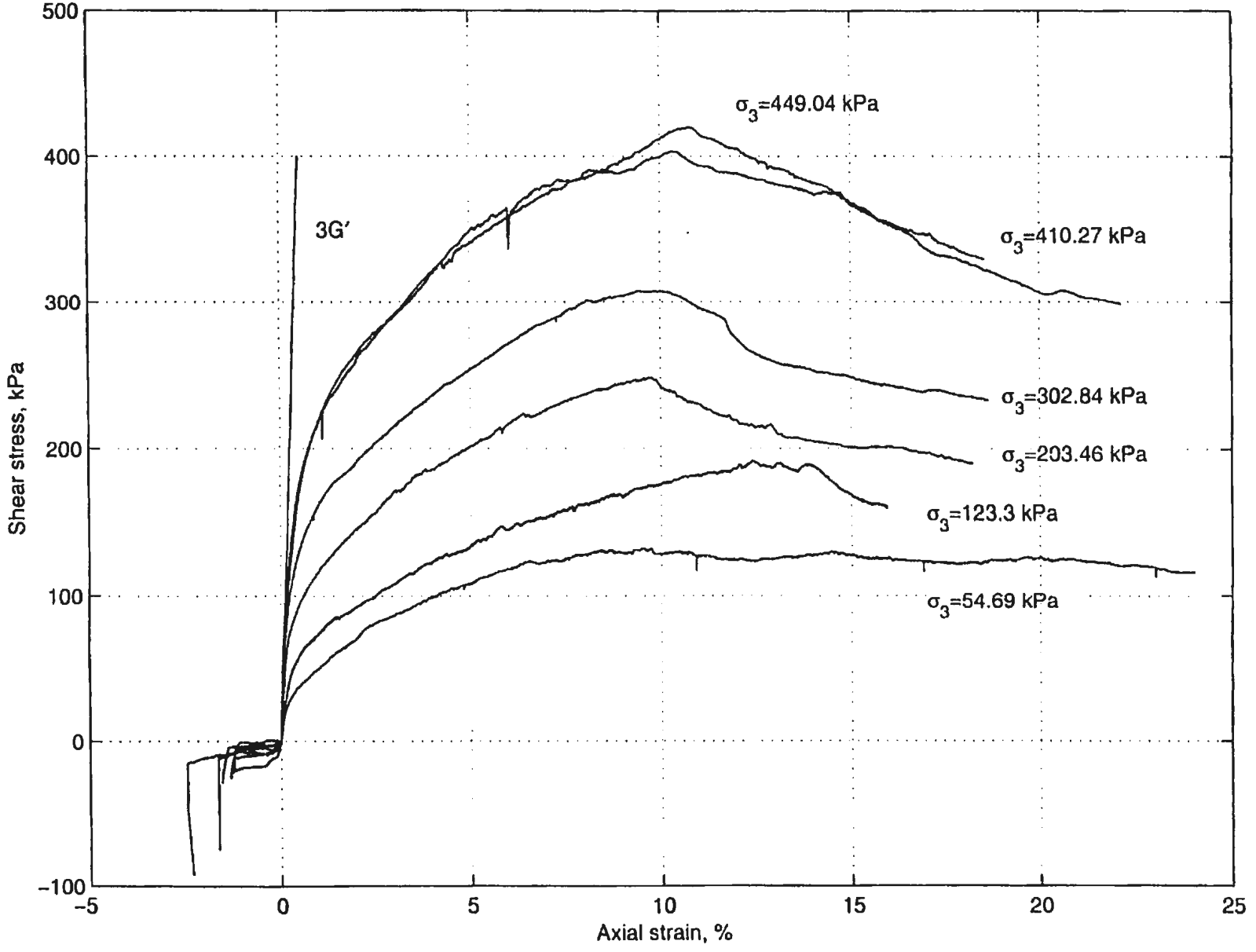

Figure 5.13 Development of pore pressures

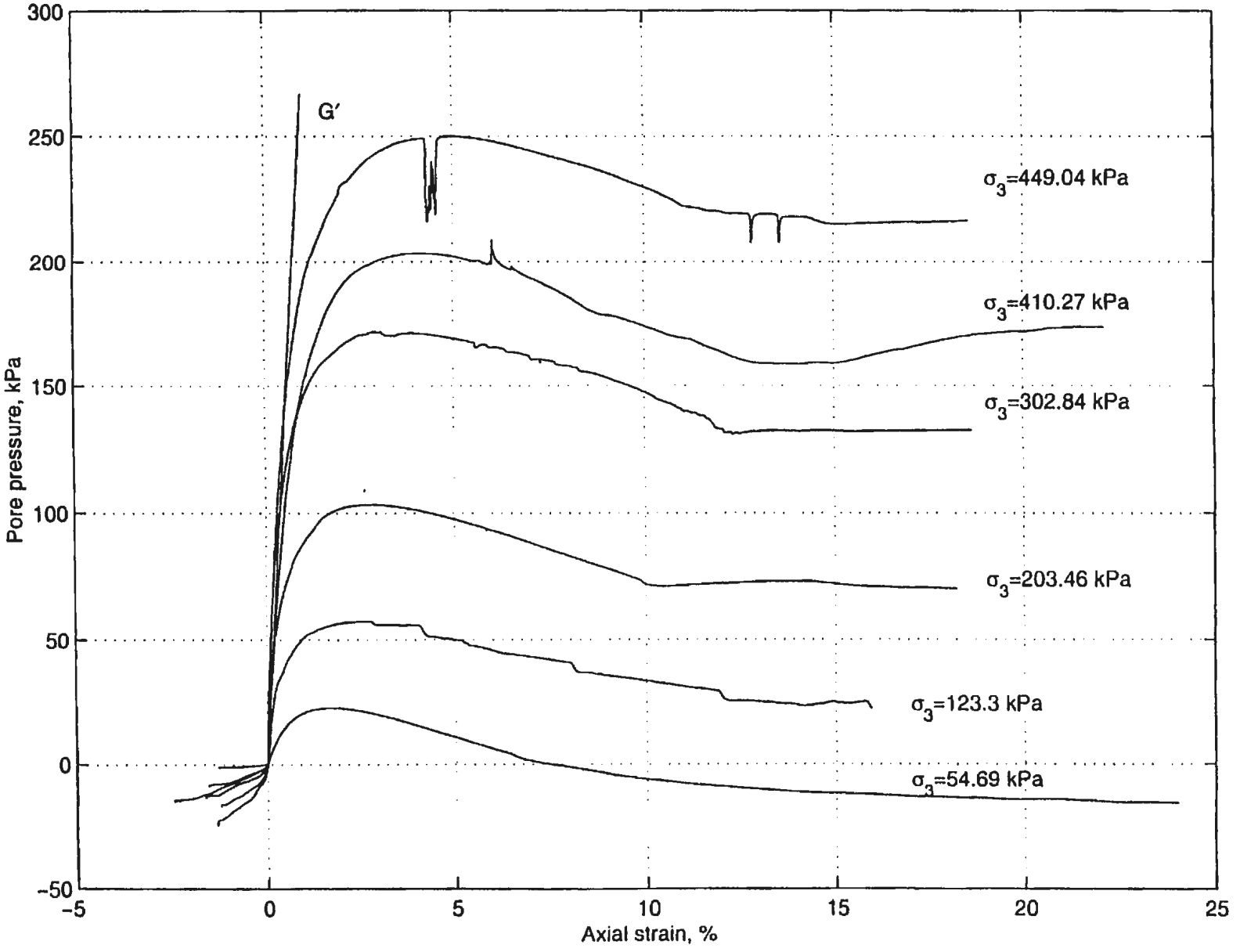

Figure 5.14 Relationship between A and axial strains

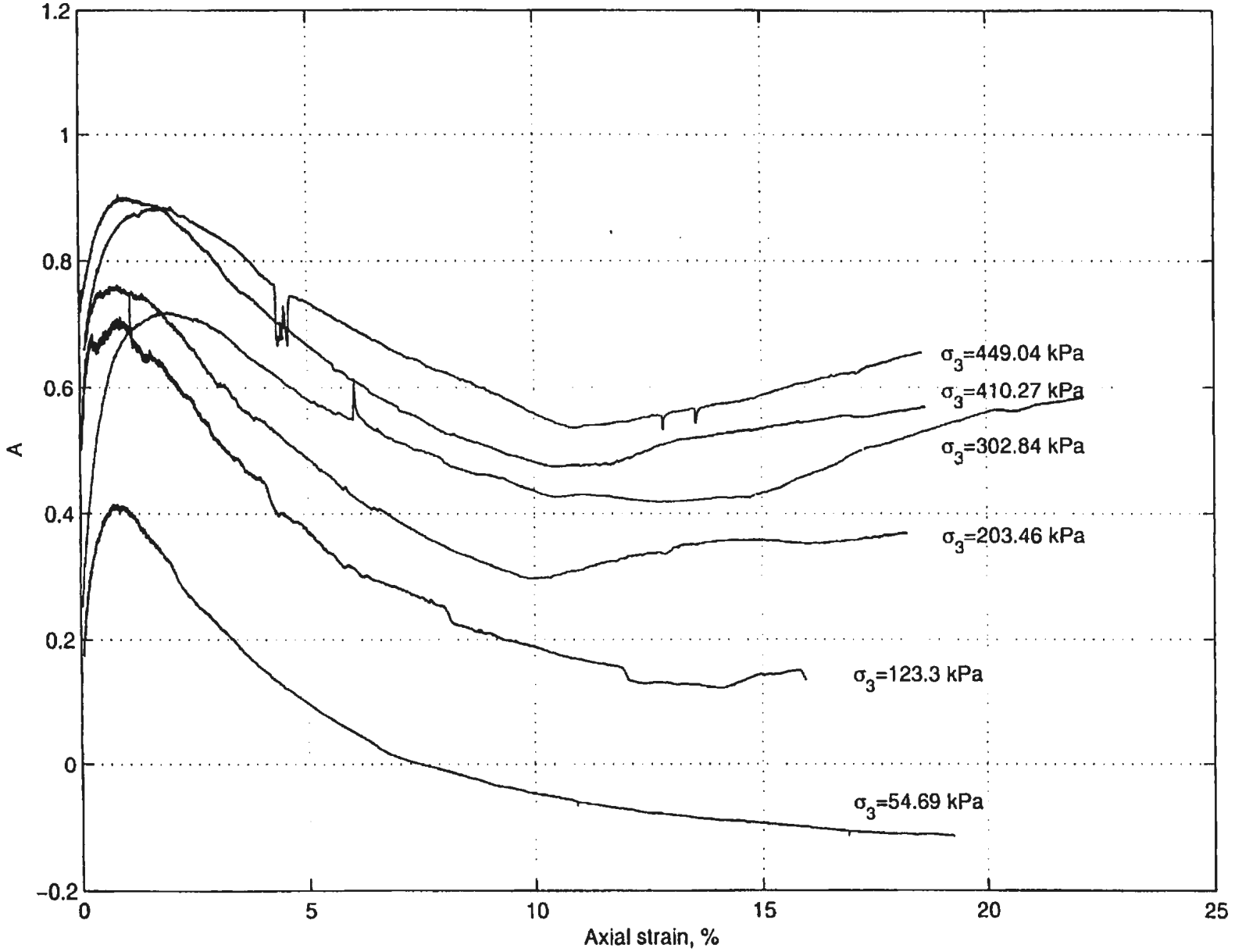

Figure 5.15 Stress paths

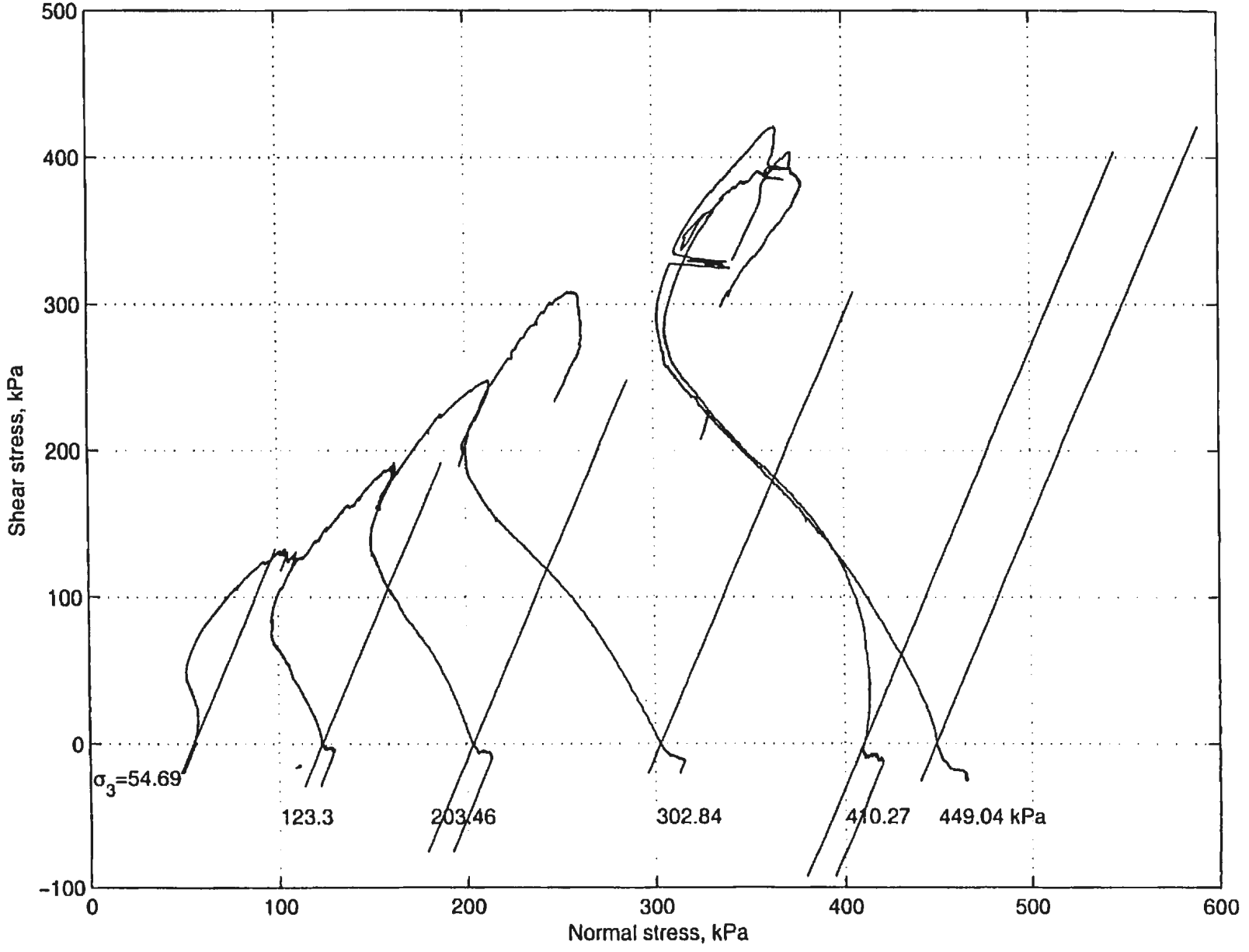

Figure 5.16: Mohr's circles

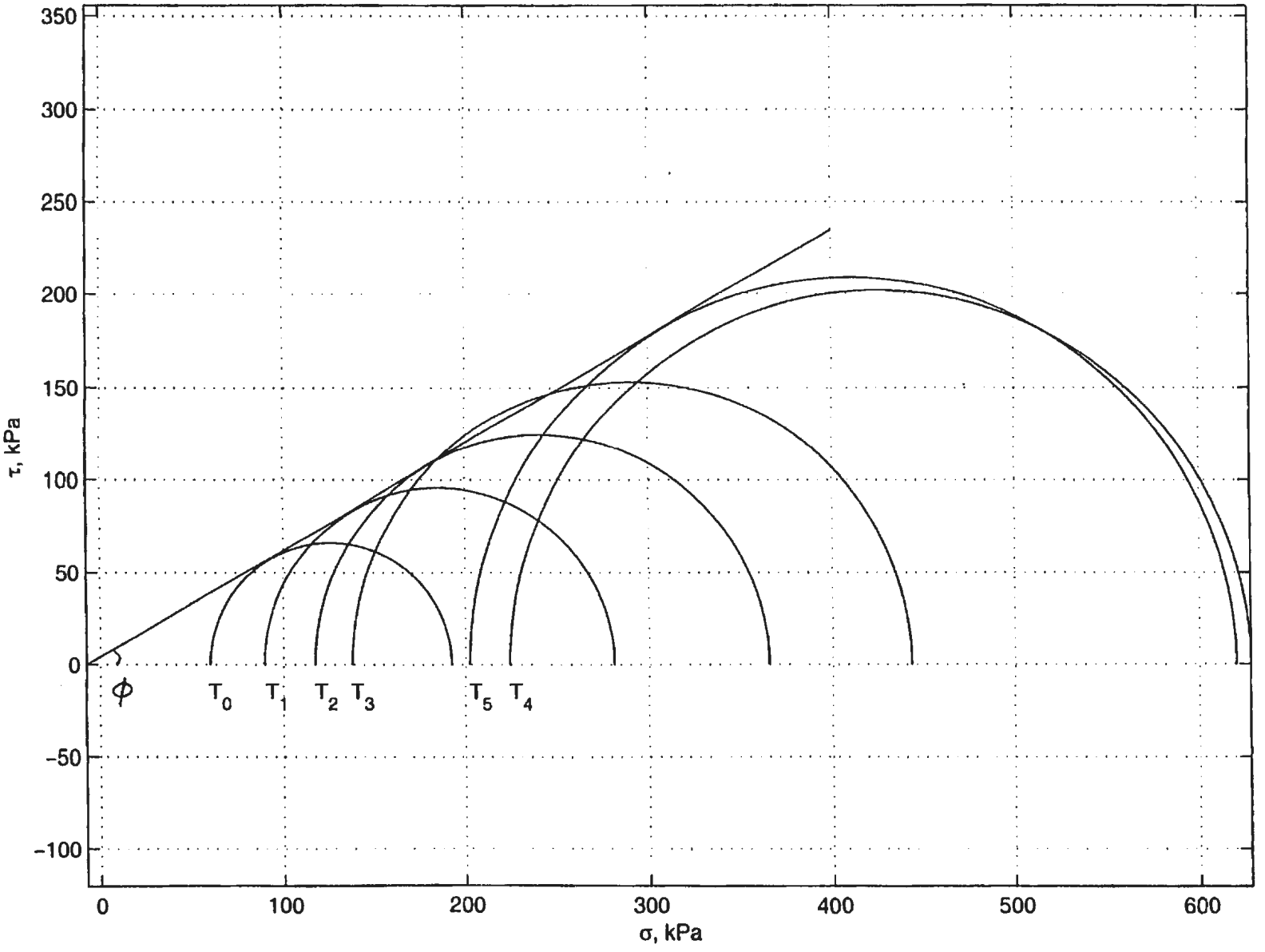

Chapter 6

RESULTS OF THE CENTRIFUGE TESTS

6.1 Test Operation

For the first test, stress calculations should be carried out for each item of the package under the proof test acceleration, which is 86 for this experiment. For each test, the data such as the centroid, the load, the disposition of the items and the test procedures should be filed and the tests are carried out under approvals.

The data of the test is acquired by a computer and stored. The data and the curves for specific channel are also shown on the monitor of the computer. It is required to take the data down by hand frequently during the test in spite of the fact that the data are also recorded by the computer. The speed of rotation of the centrifuge should also be recorded frequently.

The acceleration of 10 g is picked up first for each test whose acceleration is

larger than 10 g. The package is rotated under this acceleration for about 10 minutes. The acceleration is picked up step by step for proof tests until it reaches the proof acceleration and stays with that speed for a while to check the safety. Other tests may go to the testing accelerations directly from 10 g.

The first part of the test is to re-consolidate the clay under centrifuge. This is a process of monitoring the surface settlement of the soil. As shown in Fig. 4.3, valve 1 and valve 2 are closed and valve 3 is opened during re-consolidation. Water supply to the end standpipe should be open during all the tests. When the settlement does not change, it is implied that consolidation is completed.

For carrying out the actual simulation, valve 3 is closed. Valve 2 and valve 1 can be opened together to simulate the process of excavation. However, the rate of draining the heavy liquid should be controlled according to the required process. In the first test, this rate is controlled by frequently opening and closing the valves. The rate of the drainage is not smooth. For the remaining tests, special rate control fittings are made for the heavy liquid and the water in the front standpipe. It is required to drain the heavy liquid in more than 5 minutes under the test acceleration of 72 g according to the actual rate of site excavations. Therefore a fitting with an inner diameter of 0.35 mm is made to connect the bag and the collecting box.

After the simulation, the centrifuge is kept in motion until the stable flow is formed in the package from the clay in the back of the sheet plate to the excavated area, in other words, until the pore pressures in the PPTs in the clay are stable. At the final step, the speed is slowed down to 1 g in time as the procedure requires.

After the machine stops, the package is unloaded and the parts are taken off. The plexiglass is slid off and the profile is measured. The strength is obtained with a hand shear vane and the clay samples are collected for water content. The profile of the soil surface is measured.

Other work can be done at this time such as measuring the displacement of the small plastic balls to obtain the displacement field, or gently remove the clay and taking pictures of the displaced spaghetti. Clay samples may be collected at this time for the laboratory tests to obtain the mechanical parameters.

Finally the data of the test can be processed to obtain the results of the simulation, improvements in design may be made for next tests.

6.2 Difficulties in the Centrifuge Simulation

Three major centrifuge tests were conducted for this thesis. As may be appreciated by the description of these tests in earlier chapters, they are quite difficult to perform. There are many details which must be carefully monitored.

The experience of this study shows that following four aspects are the most difficult problems to cope with:

- water-proofing for the strain gauges;
- keeping full contact between the sheet plate with the clay on the back of the plate;
- leaking of the plastic bag;
- maintaining the level of the heavy liquid.

Water can seep into the gauges through the wires or directly from the surface of the gauges, especially since the water is under high pressure during the acceleration of 72 g. This problem happened in the first test. After careful design and a couple of isolated tests, this problem was solved by painting wax on the gauges and the plate, and then covering the plate with a plastic sheet. The silicone was used to water-proof the struts.

Full contact between the sheet plate and the clay is hard to achieve for a number of reasons. First, the struts are applied on the wales and the end beams. The wales

are not directly applied to the sheet plate, while the end beams are not directly applied to the end wall of the strongbox. In both cases, plastic sheets are placed inbetween. Although the sheets are applied without wrinkles, these sheets may deform under a high load. The same plastic sheets are also applied on the both sides of the sheet plate for protecting the strain gauges.

Secondly, the wax applied on the sheet plate, which is used to protect the gauges, cannot be perfectly flat. The thickness of the wax may result in a lack of contact between the plate and the clay. This wax may also deform during test because it is soft. Therefore the degree of contact may be reduced because of this deformation.

While the degree of contact may be increased by increasing the preloading in the struts, high preloading may damage and disturb the soil. Actually some preloading was applied in the tests.

The previous factors make the degree of contact lower and the state of K_0 was not achieved. As a result, there is some difference between the results of the finite element analysis and the tests.

However, in practical excavations, the struts are applied after the corresponding layers of soil are removed. This implies that the active state of earth pressure indeed has been mobilized to some degree before applying the struts. Therefore from the view point of a practical design, the lower degree of contact may give a result closer to actual excavations.

The leaking of the plastic bag was of the greatest concern during the tests.

Actually, two layers of plastic were used for the tests. The outside layer is thicker than the inside layer. However leaking still happened in the second test. It was found that there was a very small pin hole at the bottom of the bag. This hole can only be detected under high air pressure applied to the sealed bag full of water. In this case the water seeped out from the bottom of the bag. The cause of this hole was unknown. Possible damage to the bag may have resulted from a scratch during installation, or some very small sharp materials in the soil or geotextile.

It is hard to keep the level of the heavy liquid the same as the surface of the clay. This is because the folded plastic sheets on the end of the bag make some space between the walls of the strongbox and the bag. This space reduces the volume the heavy liquid may occupy during filling. In the third test, the surface of the heavy liquid during the filling was as high as the surface of the strongbox. This means that the maximum possible volume of liquid was filled in the bag. However under acceleration, the pressure of the heavy liquid pushed the bag to make full contact with the walls of the strongbox and the space disappeared. As a result, the surface of the heavy liquid fell lower than the surface of clay. The possible solution to this problem is to install a small reservoir of heavy liquid so that surface of the heavy liquid in the bag could be raised if required. This, of course, further complicates the design of the experiment.

6.3 Test Measurement

This chapter only presents the results of the third test. The first test was used primarily to "prove" the experimental design. The second test was conducted successfully but the results were marred by a leak in the plastic bag.

The clay was consolidated from a slurry, which was a mixture of Kaolin and silt with the ratio of 1:1. The initial water content and void ratio of the slurry were 68.1% and 1.77, while the final values after consolidation were 28.9% and 0.754. The maximum load was 404.6 kPa. The shear strength after consolidation was 41 kPa. The consolidation curve is shown in Fig. 6.1.

The density of the clay was 1.914, and the test was run under 72 g. The over-consolidation ratio versus elevation is shown in Fig. 6.2, where the elevation is referring to the inside bottom of the strongbox. The test instrumentation is listed in Table 5.1 and shown in Fig. 6.3.

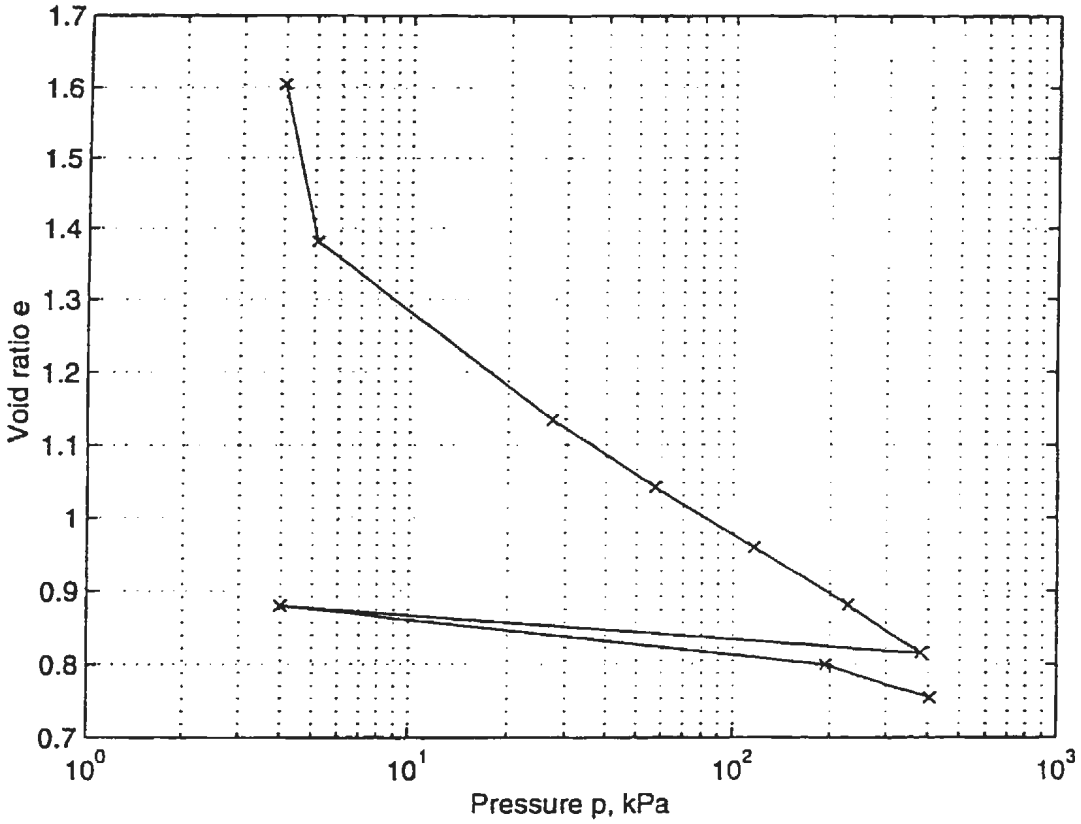

Figure 6.1: Consolidation curve

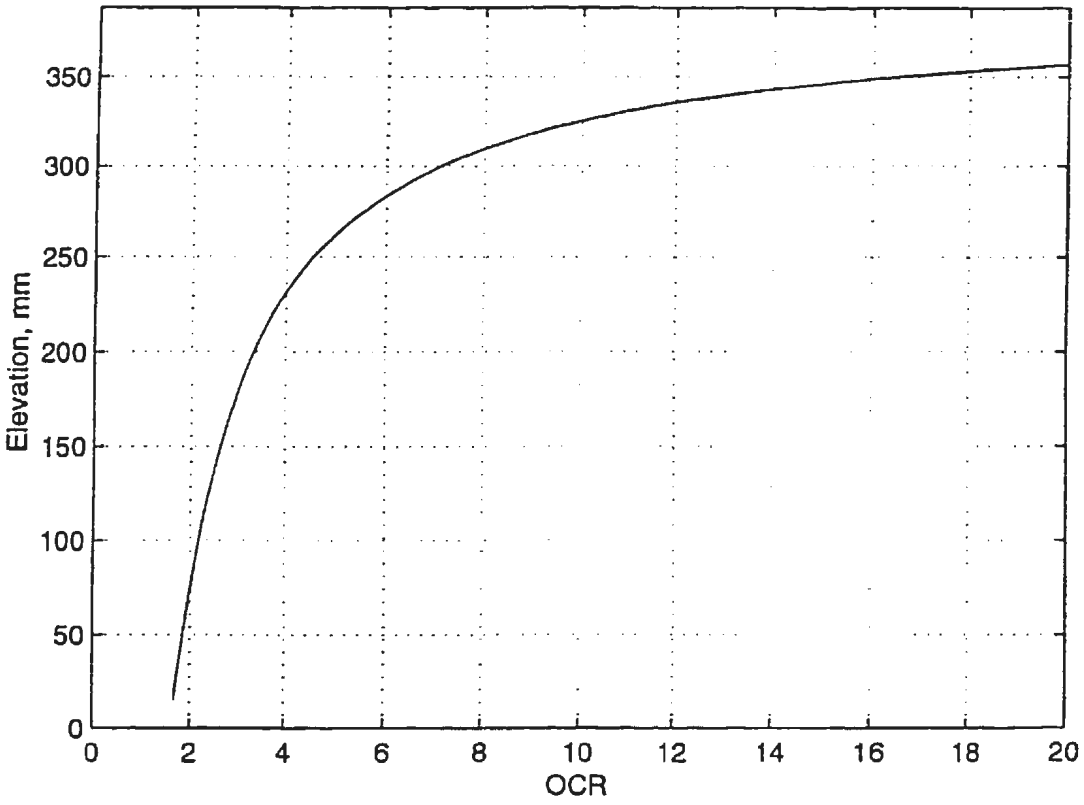

Figure 6.2: Over-consolidation ratio

Table 6.1: Test instrumentation (output of signal box)

Channel	Facility	Short name	Measurement
A1	PPT	Front PPT	Water pressure at the bottom of the front standing pipe
A2	PPT	Bag PPT	Liquid pressure in the bag at 150 mm from the surface of the soil
A3	PPT	End PPT	Water pressure at the bottom of the end standing pipe
A4	Strain gauge		These strain gauges measuring the stress
A5	Strain gauge		on the sheet plate from the top to the bottom
A6	Strain gauge		
A7	Strain gauge		
A8	Strain gauge	Bottom	The load in the bottom layer struts
A9	Strain gauge	struts	
A10	Strain gauge		
A11	Strain gauge	Mid	The load in the middle layer struts
A12	Strain gauge	struts	
A13	Strain gauge		
A14	Strain gauge	Top	The load in the top layer struts
A15	Strain gauge	struts	
A16	Strain gauge		
A17	LDT	LDT 1	These LDTs are used to measure the settlement on the
A18	LDT	LDT 2	surface of the soil starting from close to the
A19	LDT	LDT 3	sheet plate along the middle section of the soil
A20	LDT	LDT 4	
A21	PPT		Pore pressure at the bottom of excavation area
A22	PPT		Pore pressure on back of the plate
A23	PPT		Pore pressure on back of the plate
A24	Monitor		

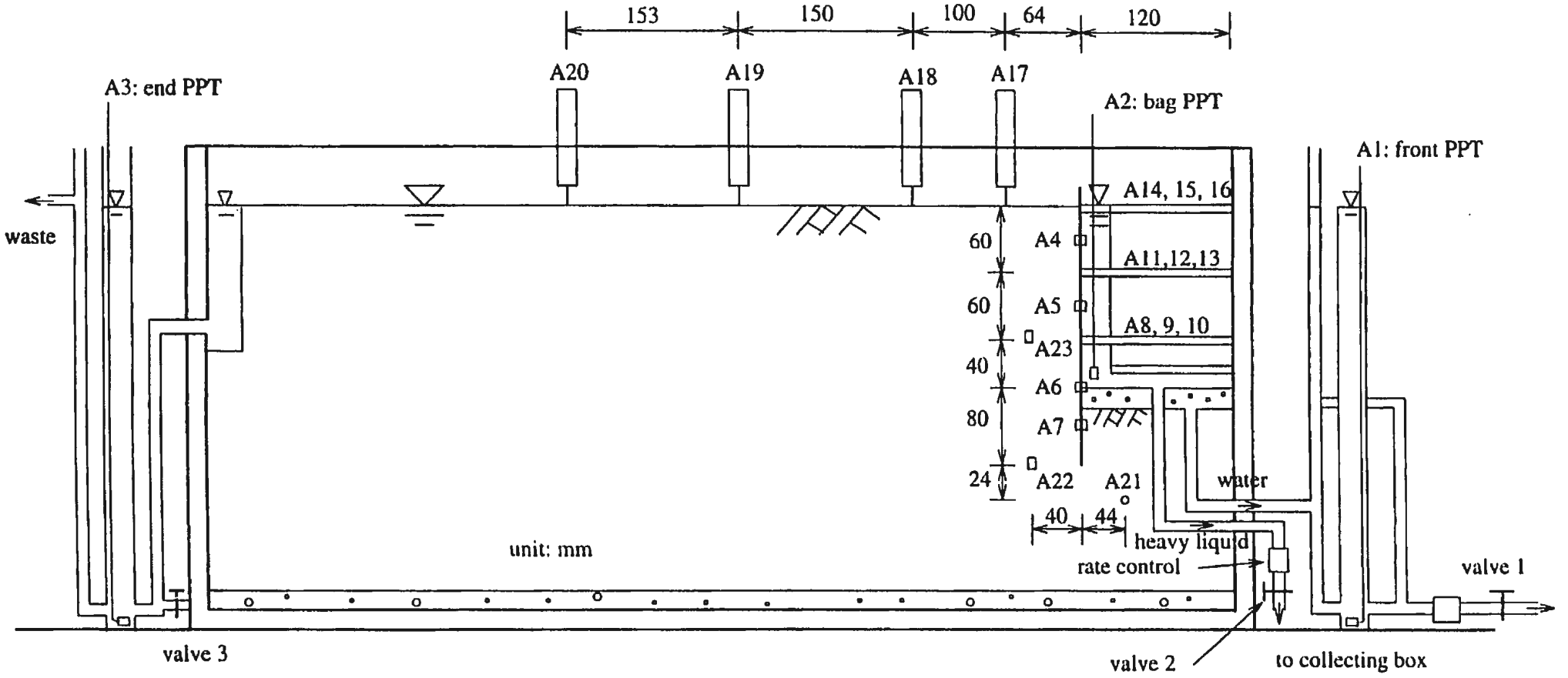

Figure 6.3: Test instrumentation

6.4 Pressures in the Bag and the Standpipes

The pressures on the PPTs in the front standpipe, bag and end standpipe are shown in Fig. 6.4. The bag was filled with a heavy liquid with a specific gravity of 1.629. This value of specific gravity was kept the same during the test as there was not any extra water in the bag before filling the heavy liquid and no water was allowed to flow into the bag. The steps in the figure show increases of the acceleration of the centrifuge, from 1 g to 10 g, 20 g, 40 g, 50 g, 60 g and 72 g. The acceleration was increased in about 82 minutes to 72 g which is the acceleration for testing. After 183 minutes of consolidation it was found that the settlement of the surface of the clay reached the stable profile. This indicated that the consolidation was completed. Therefore the excavation test was carried out.

The process of excavation was simulated by opening the valve which controlled the drainage of the heavy liquid. The valve which controlled the water table in the soil at the bottom of the excavation was also opened at the same time. It took 15 minutes to totally drain the heavy liquid. The water table reduced faster because of the larger diameter the rate control. The pore pressure in the front standpipe was 0 after the water in the pipe was totally drained. However the water table in the bottom of the excavated area was the same as the surface of the bottom because of the design. After the heavy liquid was totally drained, the valve which controlled the drainage of the water in the front standpipe was closed to monitor the rate of seepage in the soil. The acceleration of 72 g was kept for about 45 minutes in order to reach the stable state of seepage of the water from the back of the sheet plate

to the excavated area. The excess water drained into the standpipe and the pore pressure in the stand pipe kept increasing. The test was finally stopped after 330 minutes.

Fig. 6.5 shows the detail of the variation of the pressures during the process of draining the heavy liquid, in the period of T=260 minutes to T=285 minutes. The drainage began about 265 minutes and the heavy liquid was totally drained at T=280.5 minutes.

The levels of the water in the front and end standpipes and of the heavy liquid in the bag are shown in Fig. 6.6. The height is referred to the bottom of the strongbox. The levels reduced somewhat during the process of increasing the acceleration to 72 g, and kept stable during consolidation. The level of the end standpipe was kept the same during the draining of the heavy liquid and the subsequent consolidation. The level of the heavy liquid reduced sharply during drainage, which was because of the small area of the section of the heavy liquid. However, the flat curve of the level of the bag does not represent the actual level of the heavy liquid, because the PPT which was measuring the pore pressure of the heavy liquid was not at the bottom of the bag. The level of the water in the front standpipe kept increasing because of the inflow of the excess water from the bottom of the excavation resulting from seepage. The water content of the clay at the surface after the test was 29.7% and the shear strength was 46 kPa.

Figure 6.4 Pressures in the bag and the standpipes

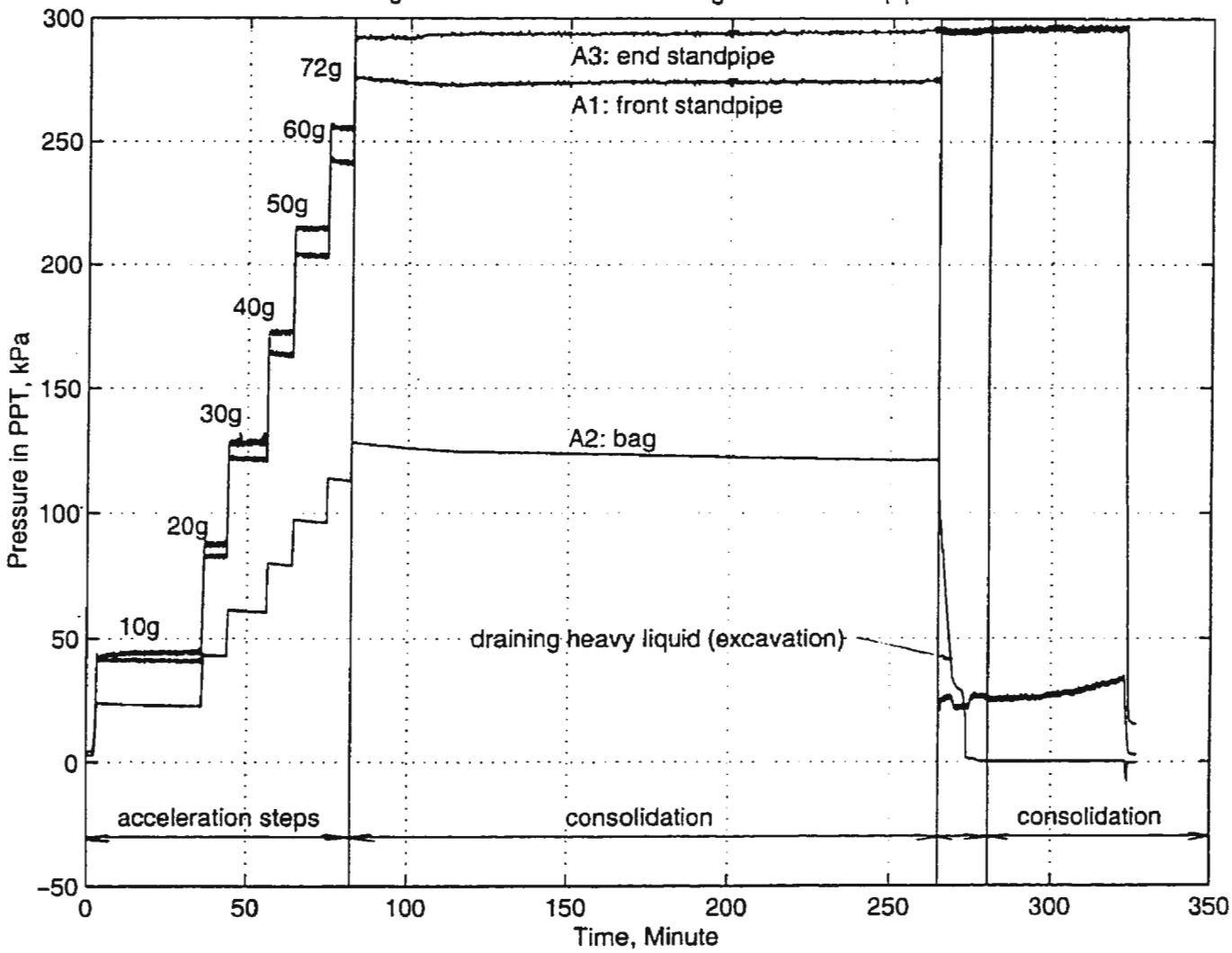

Figure 6.5 Pressures in the bag and the standpipes

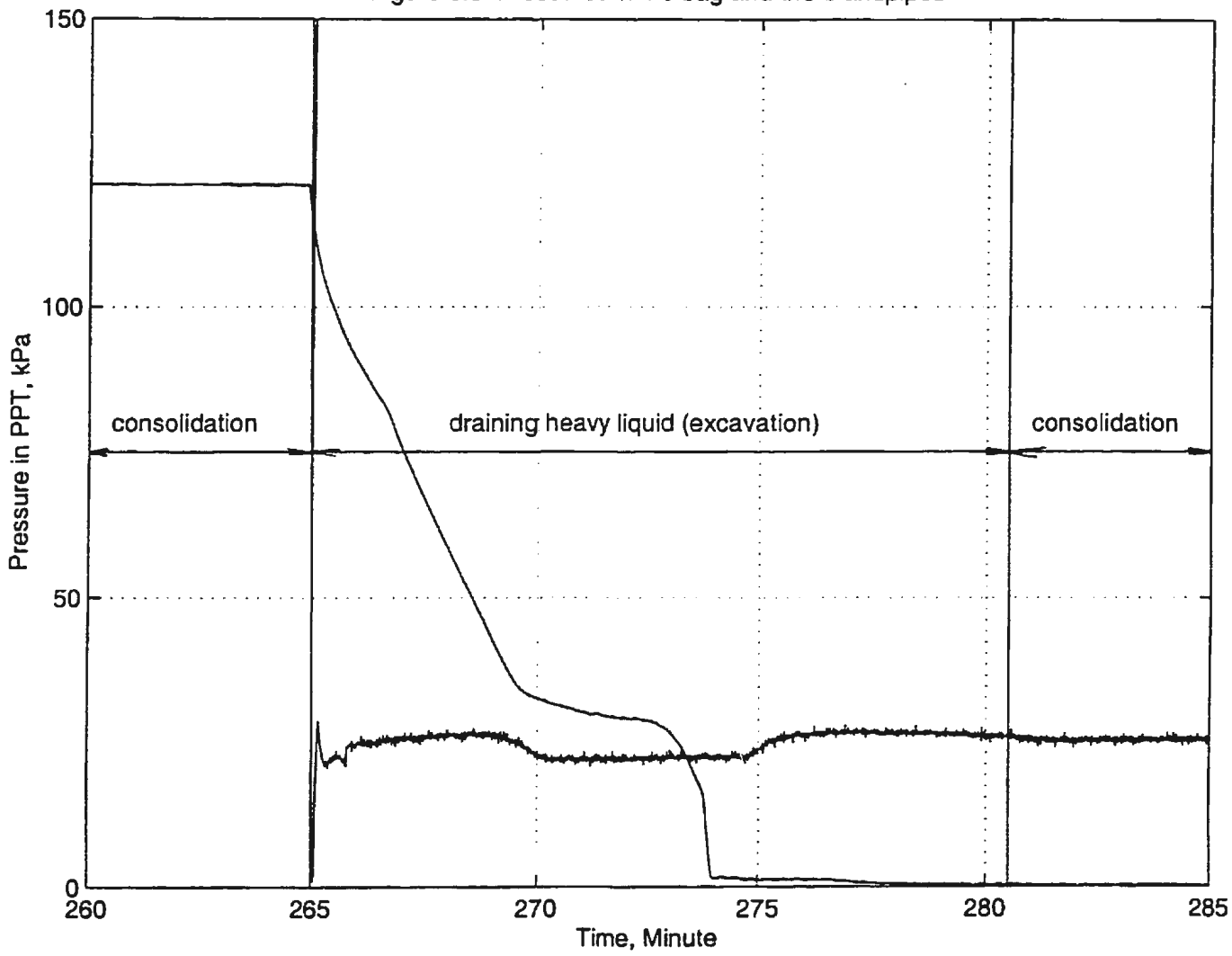

Figure 6.6 Levels of the heavy liquid in the bag and the water in the standpipes

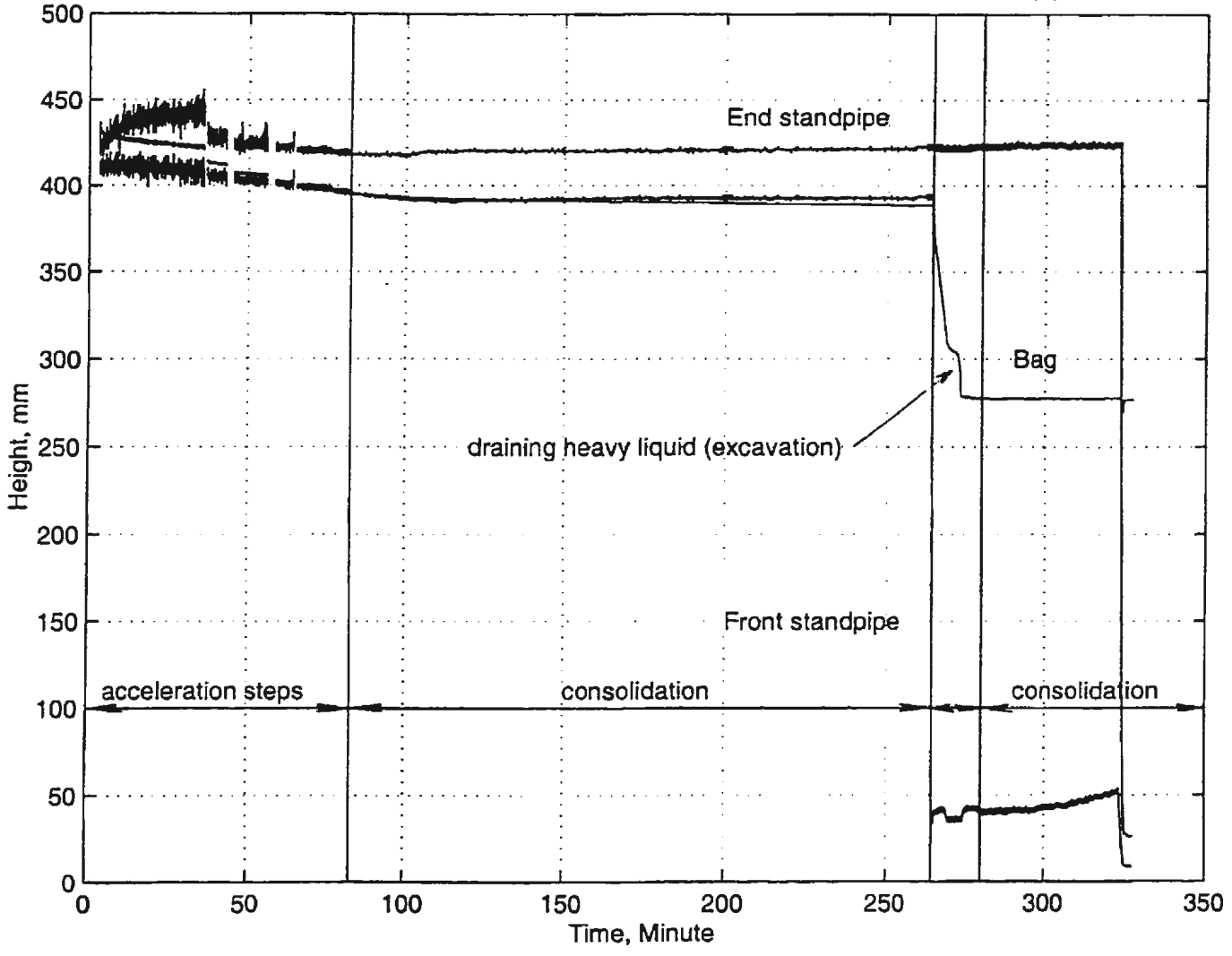

6.5 Stresses in the Sheet Plate

The stresses in the sheet plate according to the output are shown in Fig. 6.7. A4 shows the stresses on the surface of the sheet plate midway between the top and the middle layers. A5 shows the stresses midway between the middle and bottom layers. A6 is 40 mm below the bottom layer of struts and A7 is the 40 mm lower than A6 and 40 mm from the bottom of the sheet plate. It is assumed that at the same elevation, the bending stresses on the surface of the front side of the sheet plate are the same value as the back side with one in tension and the other in compression. There were four active gauges forming a full bridge with two on the front side and the other two on the back side. All of the full bridges were formed the same way.

Fig. 6.8 shows the history of the stresses in the sheet plate during the draining of the heavy liquid. There was a flat curve for A4, which began at 267.5 minutes and ended at 274 minutes. At 274 minutes, A4 began to increase steeply until the end of the draining. A5 changed from minus at the beginning of the draining to plus at the end. It reached its maximum value at 270.8 minutes, and reduced to about 0 after the draining. A6 began to increase sharply at the beginning of the draining, and reached the maximum value at 273 minutes. A7 reduced some at the beginning of the draining and increased a little in the process of draining, but the variation was small comparing with the variations of the other three points.

The curves reflect the variation of the acceleration and the process of consolidation and drainage. When the acceleration reached 72 g, the order of the higher

stresses were A6, A7, A5 and A4. After consolidation, A6 reduced sharply. At the end the new order was A7, A6, A4 and A5. It should be noticed that A4 and A5 were negative before the acceleration reached 40 g. A4 was almost 0 during consolidation, but A5 was -3.5 MPa after consolidation. However during the draining of the heavy liquid, A6 jumped to the highest value, A5 was second, followed by A7 and A4. Moreover, this order of value was maintained only for a while. With the total draining of the heavy liquid, in the subsequent process of consolidation, A4 jumped from the lowest to the highest, followed in order by A7, A6 and A5. A5 changed its sign back to negative about 23 minutes after the beginning of draining the heavy liquid.

The variation of the sign of the stresses represents the change of the direction of the bending of the sheet plate, and implies a variation of the loads and the subsequent adjustment of the sheet plate. The bending directions are shown in Fig. 6.9 and 6.10. A7 bent toward the excavating area all the time.

Before 30 g, A4, A5 and A6 bent toward the back. Between 30 g and the first part of the consolidation, all parts bent toward the excavating area. This was because of the load resulting from the high pore pressure. With the completion of the consolidation, this load greatly reduced. While in the last period of consolidation, A4 and A6 still bent toward the excavating area, but A5 bent backward. With the drainage of the heavy liquid, all parts bent toward the excavating area again. This time it was not because of the increase in load on the back of the sheet plate, but because of the reduction of the load in front of the sheet plate. However, during the subsequent consolidation, A5 bent backward again.

Figure 6.7 Stresses in sheet plate

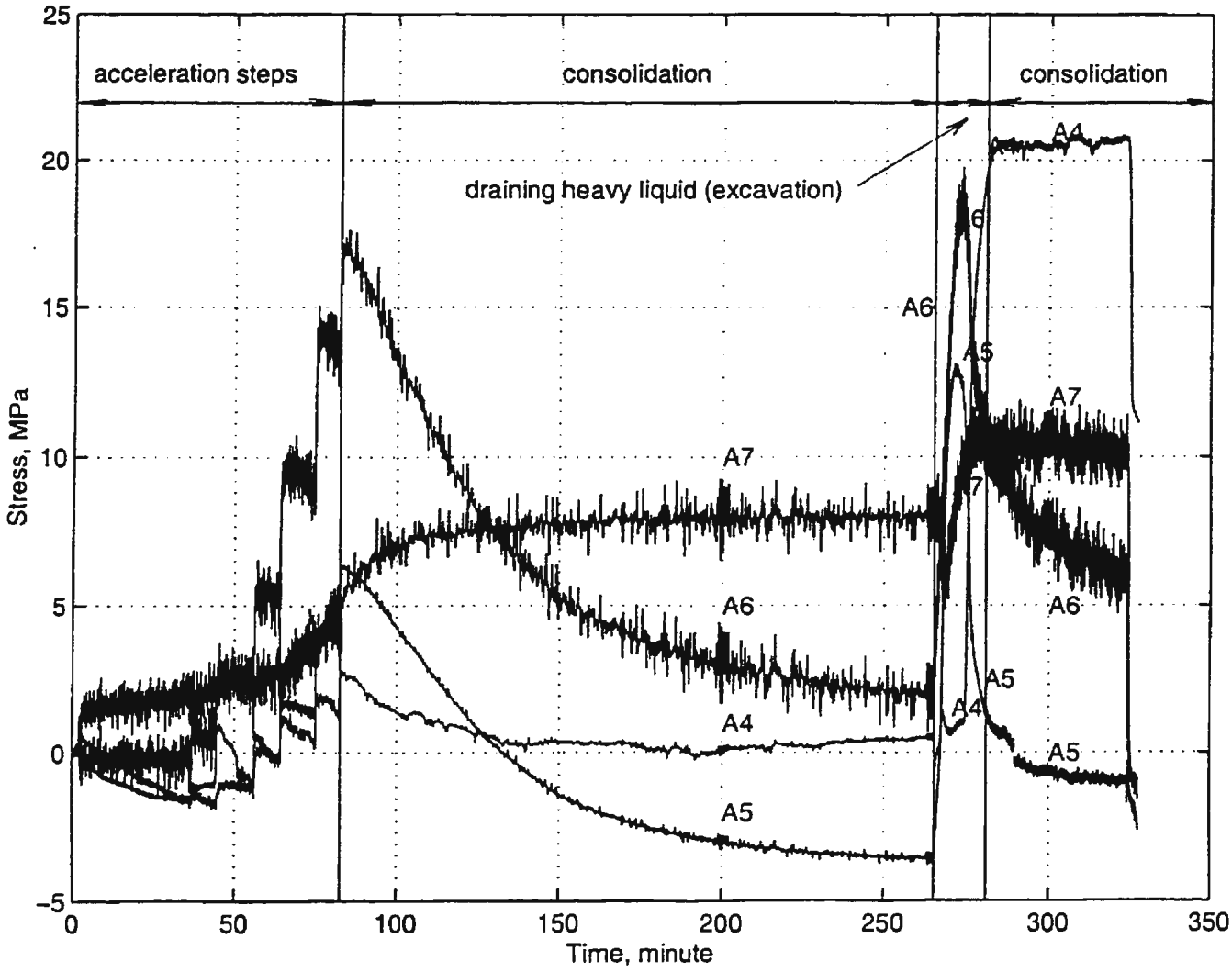

Figure 6.8 Stresses in sheet plate

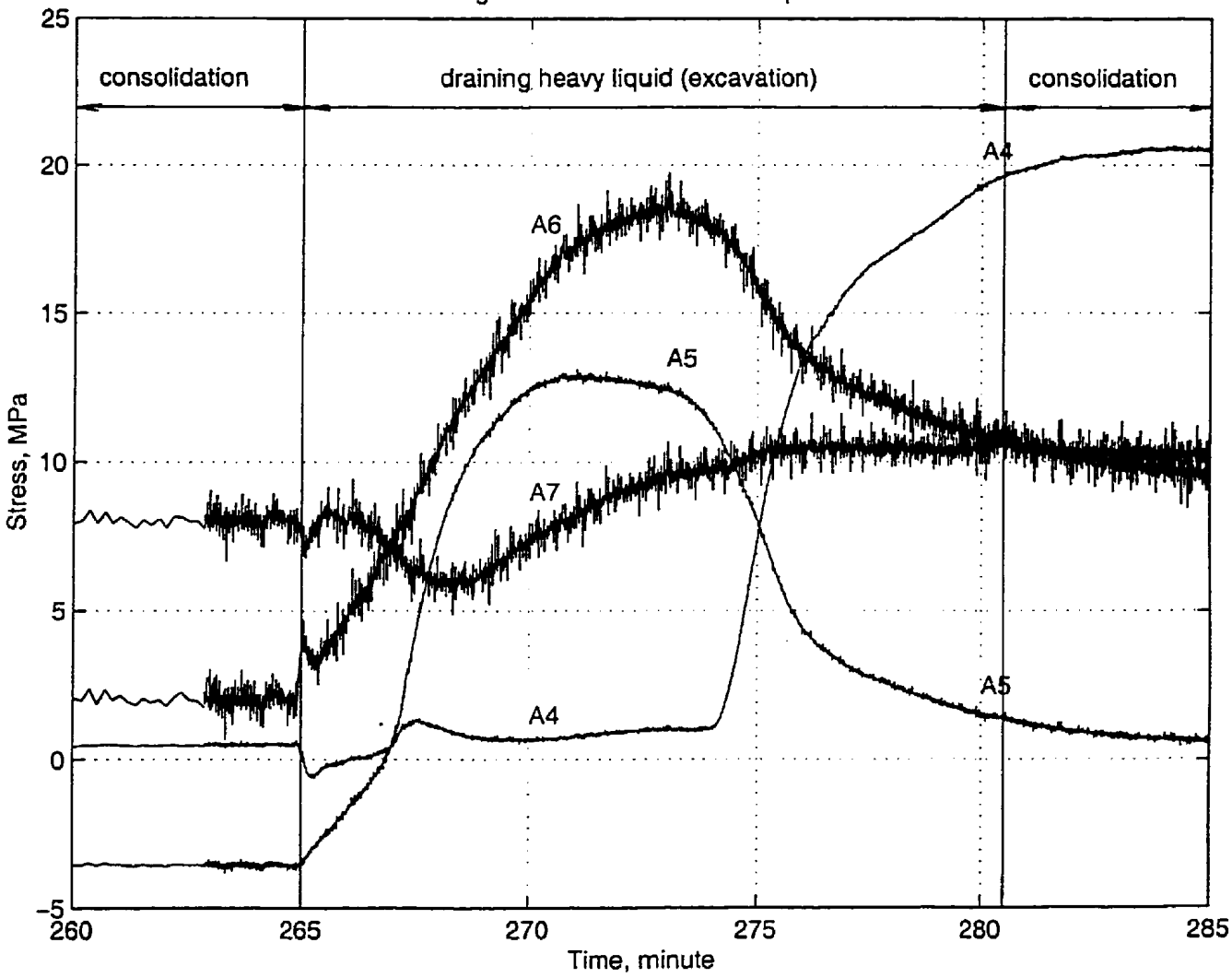

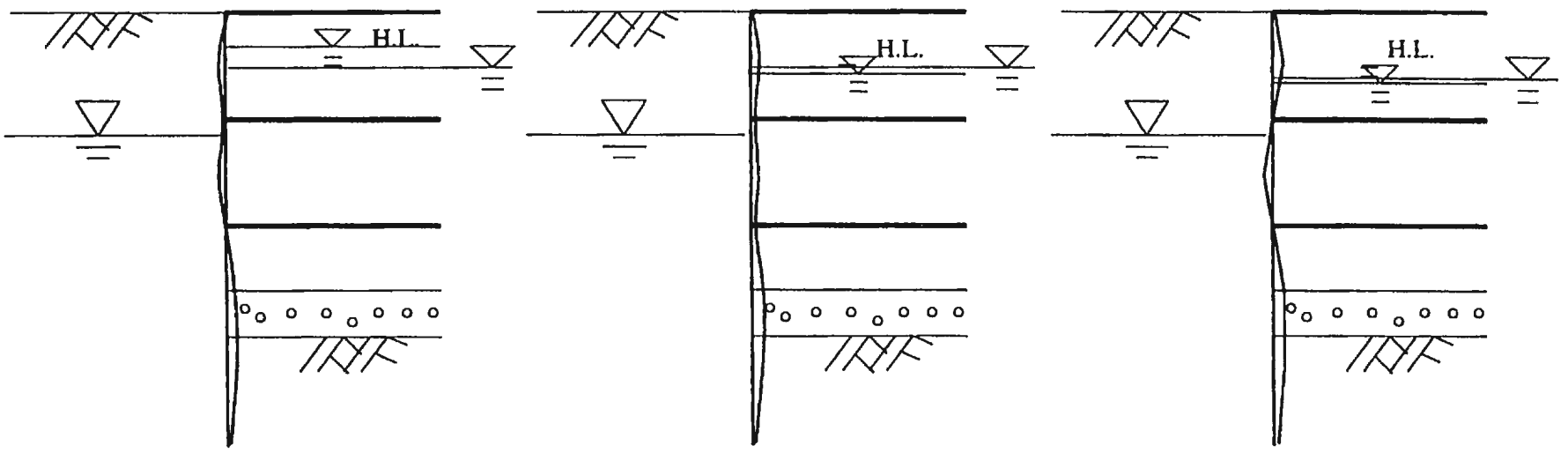

T=50 minutes T=100 minutes T=250 minutes

Figure 6.9: Bending directions prior to draining heavy liquid (excavation)

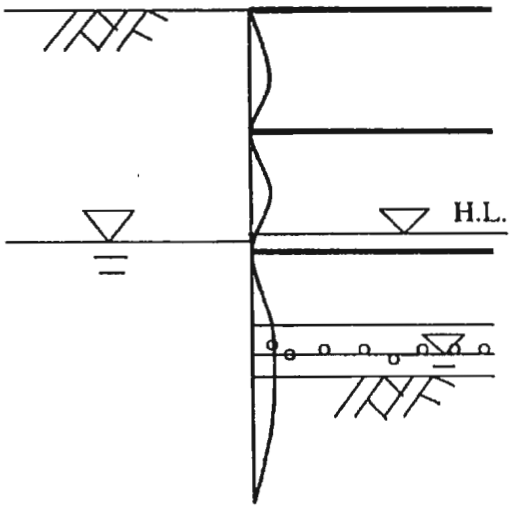

T=270.8 minutes

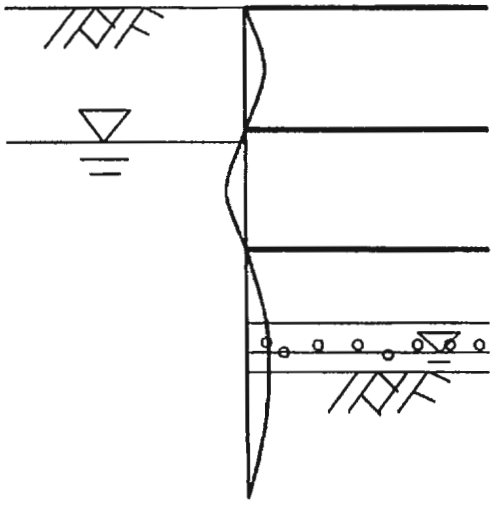

T=320 minutes

Figure 6.10: Bending directions after draining heavy liquid (excavation)

6.6 Loads in the Struts

The load history on the bottom layer struts is shown in Fig. 6.11 and 6.12. Unfortunately A9 did not work. There was a considerable load on A8, but almost no load on A10 before draining the heavy liquid. The loads in the middle layer struts are shown in Fig. 6.13 and 6.14. These curves show that the gauges worked very well, and there was good contact between the struts and the wales. The three gauges gave almost the same value before the drainage with the maximum load appearing at the beginning. The loads in the top layer struts are shown in Fig. 6.15 and 6.16. There was some difference between the magnitudes with some preloading in the struts before the test. The comparison of the loads in the three layers of struts are shown in Fig. 6.17 and 6.18, which show that the loads are highest in the bottom layer and lowest in the top layer.

Figure 6.11 Loads in the bottom layer struts

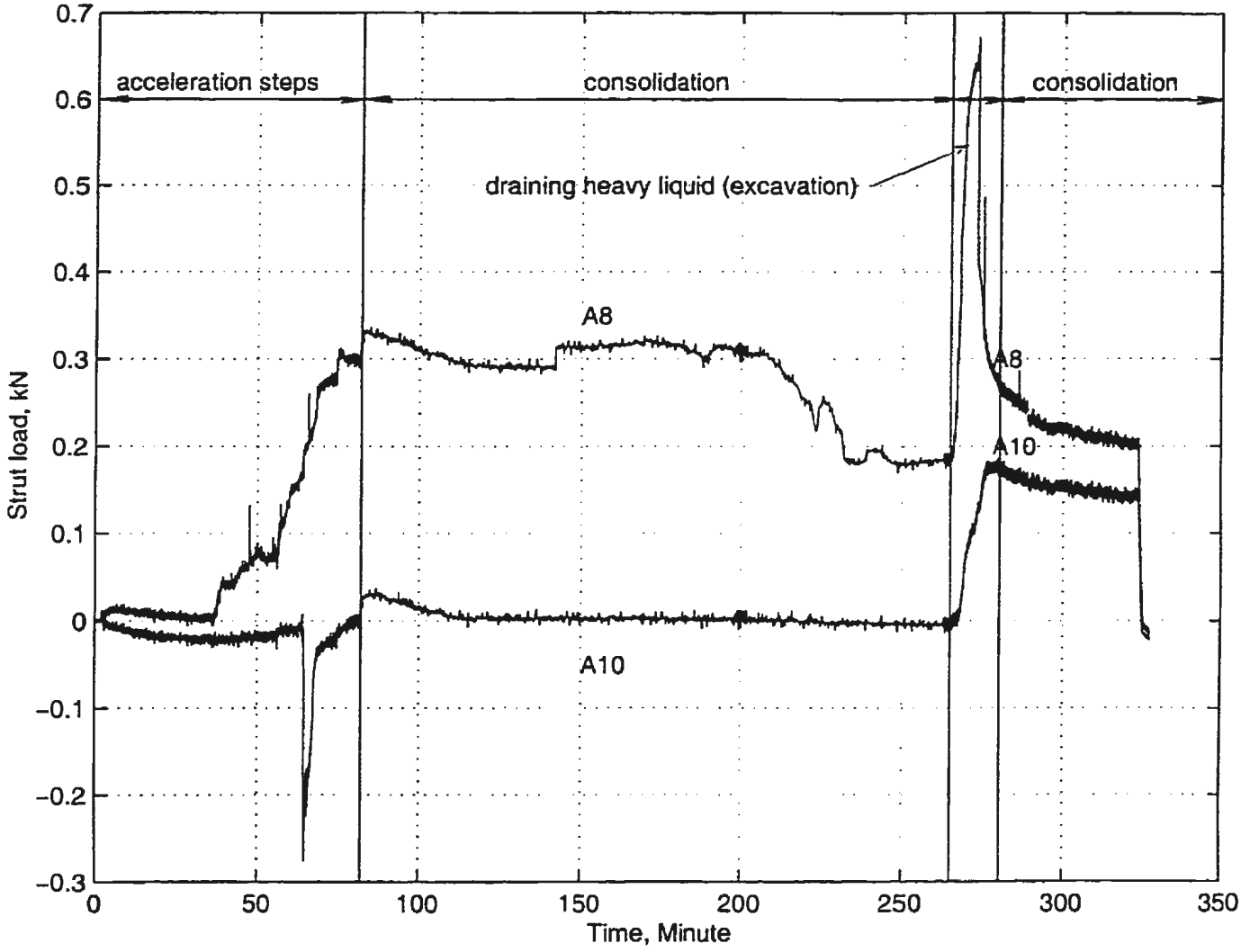

Figure 6.12 Loads in the bottom layer struts

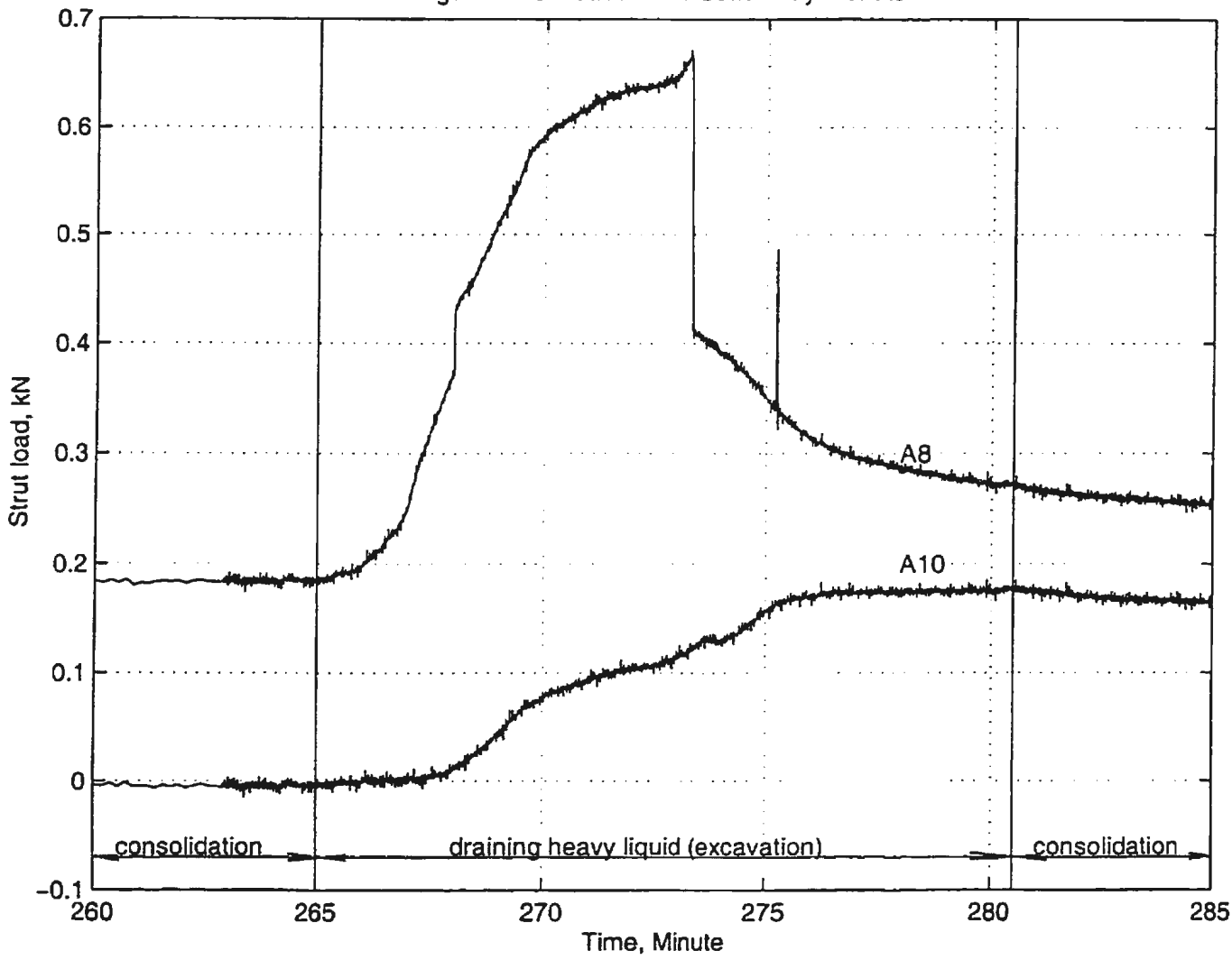

Figure 6.13 Loads in the middle layer struts

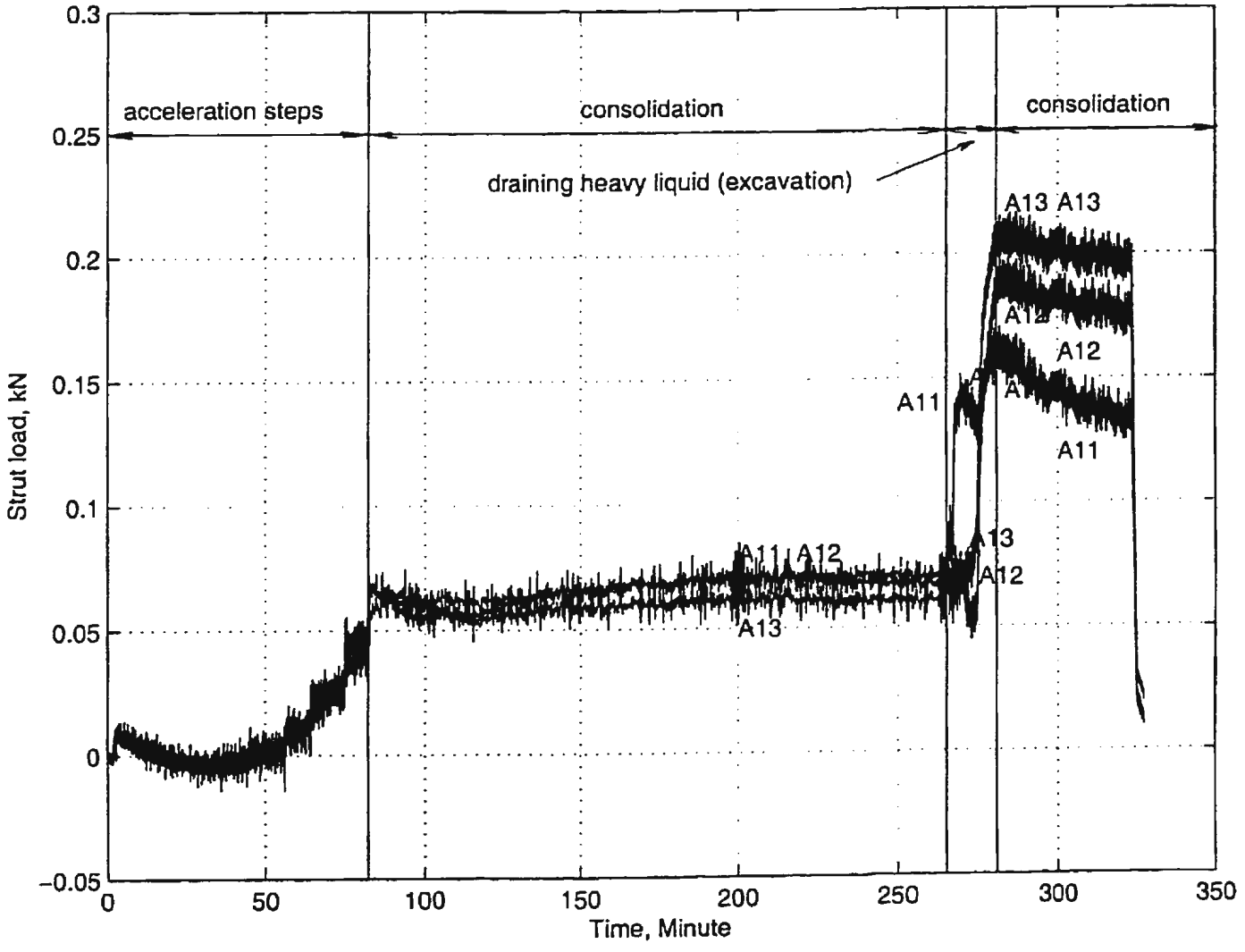

Figure 6.14 Loads in the middle layer struts

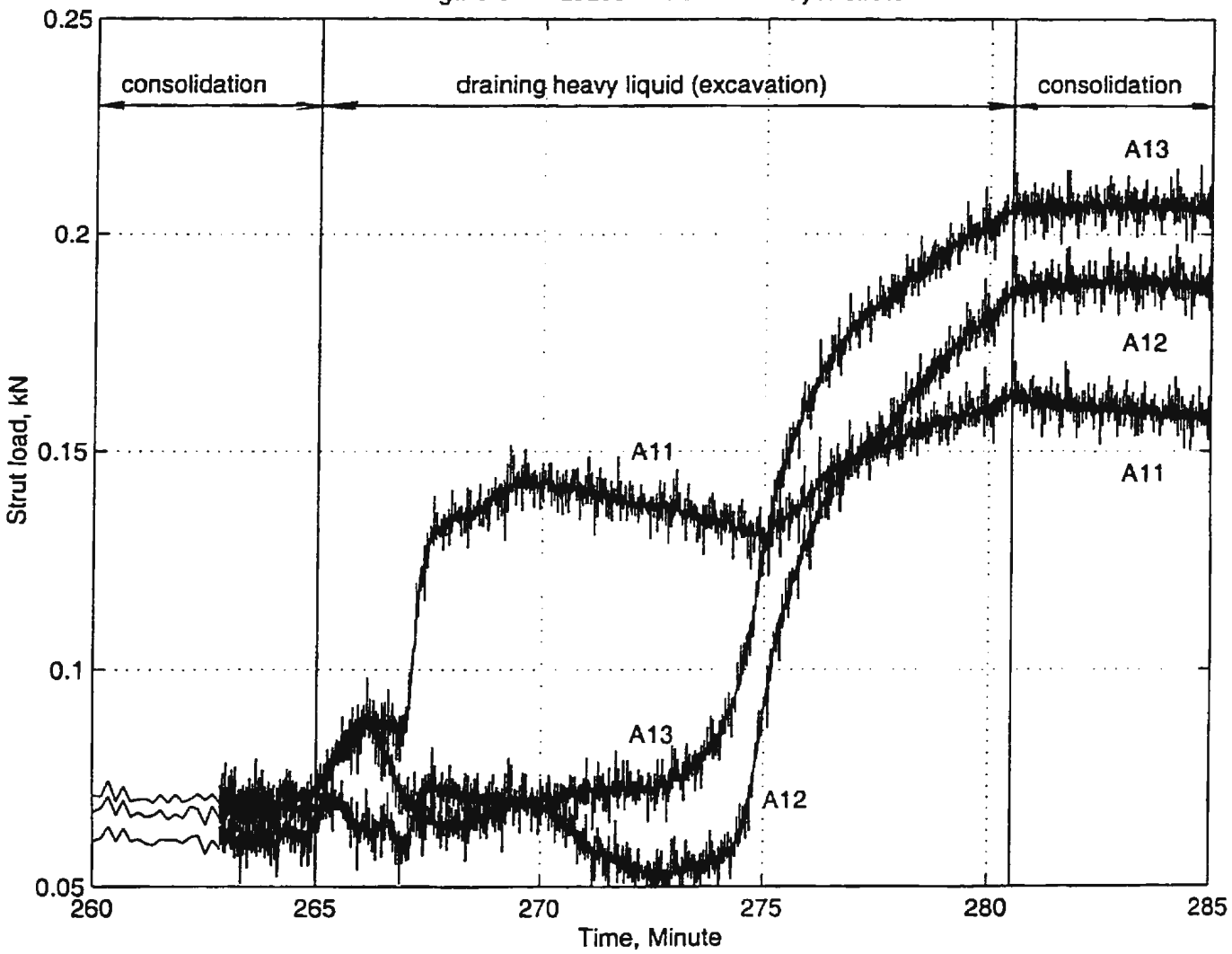

Figure 6.15 Loads in the top layer struts

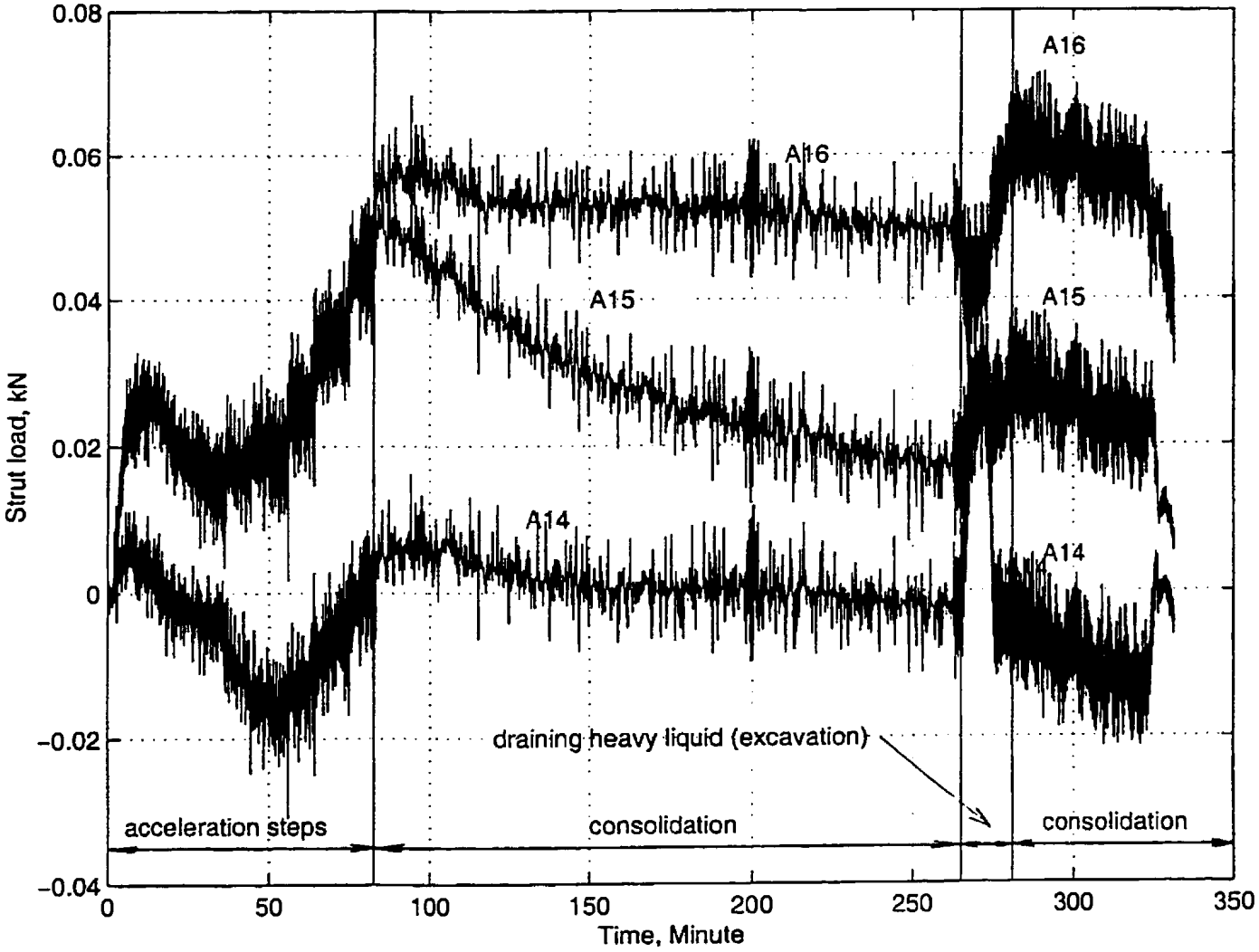

Figure 6.16 Loads in the top layer struts

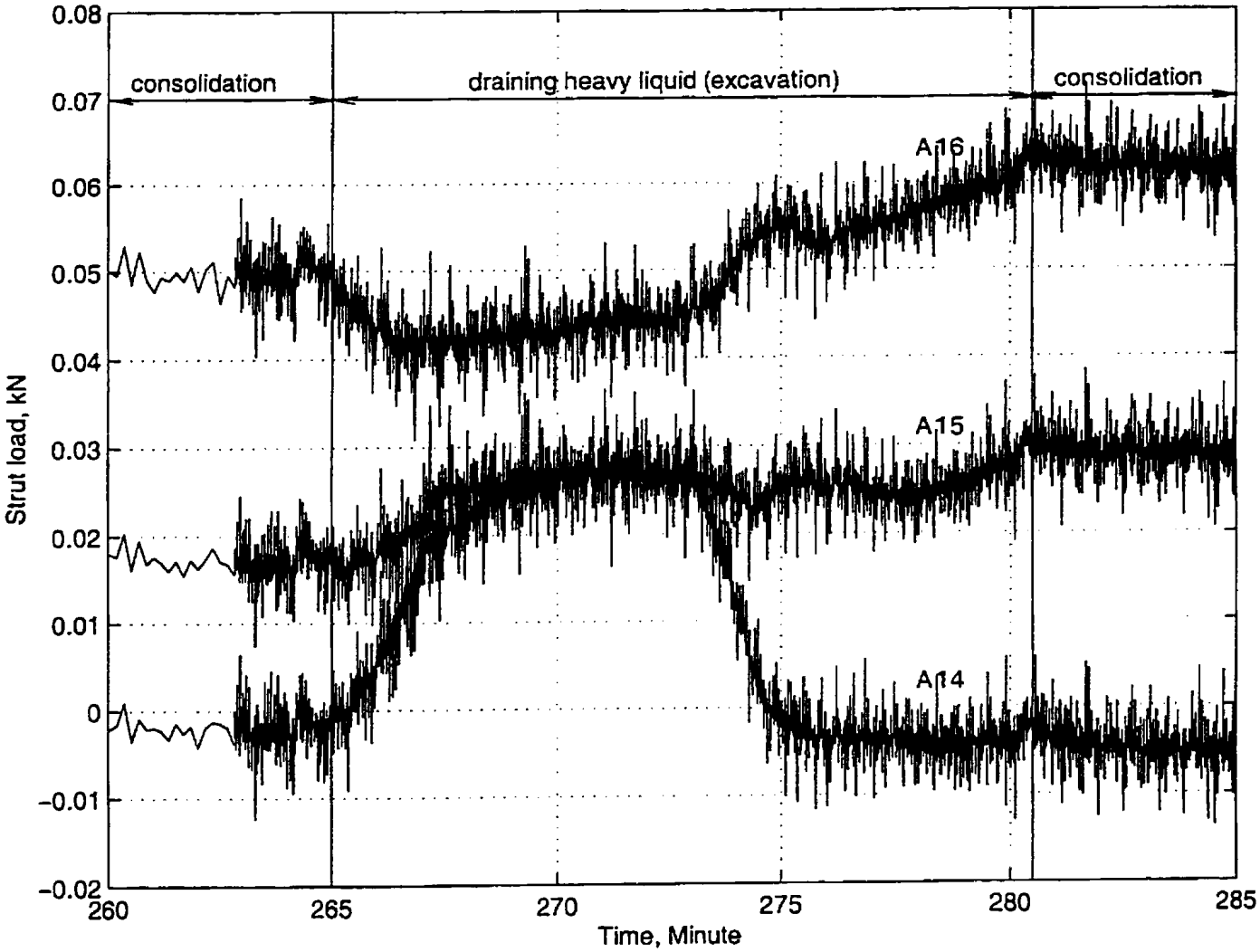

Figure 6.17 Comparison of the loads in the struts

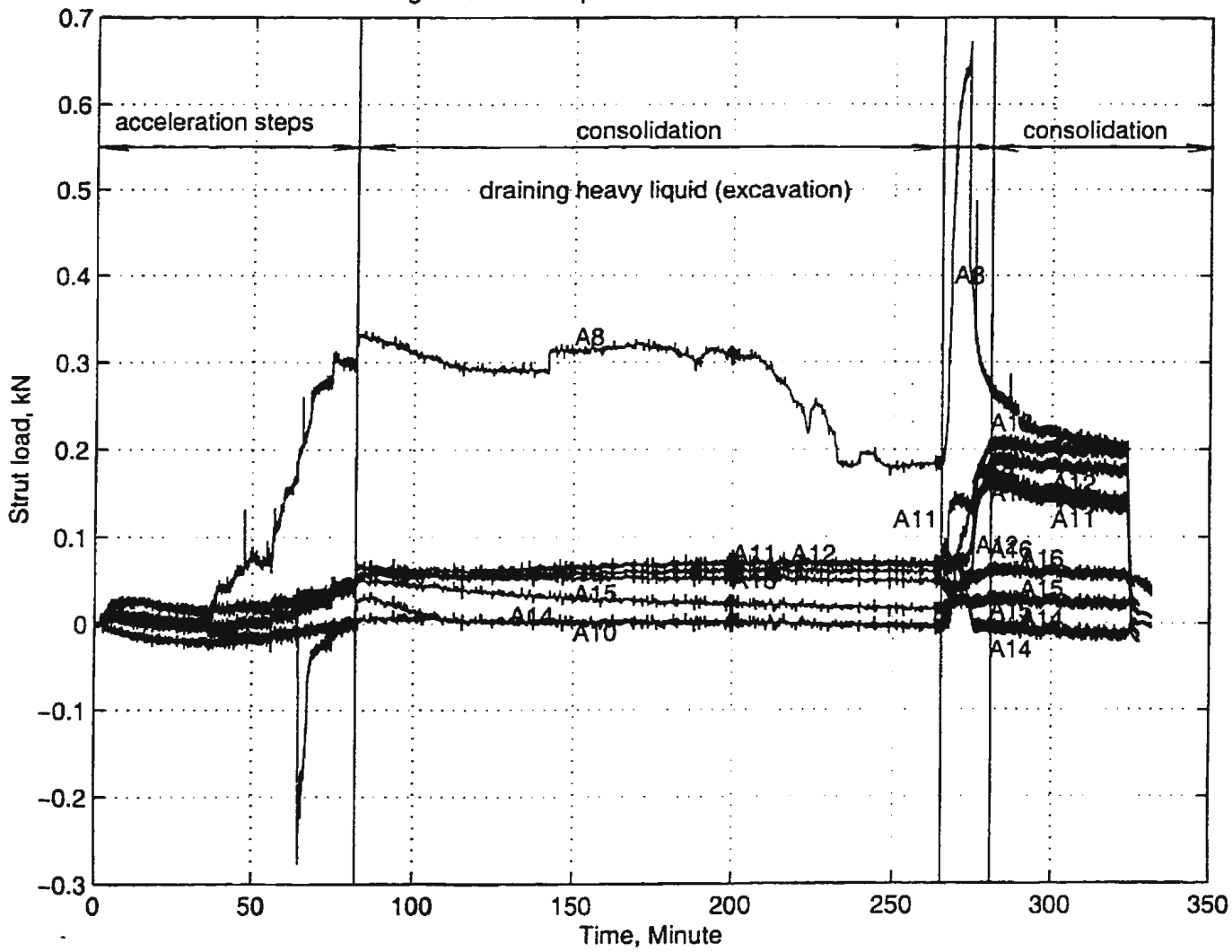

Figure 6.18 Comparison of the loads in the struts

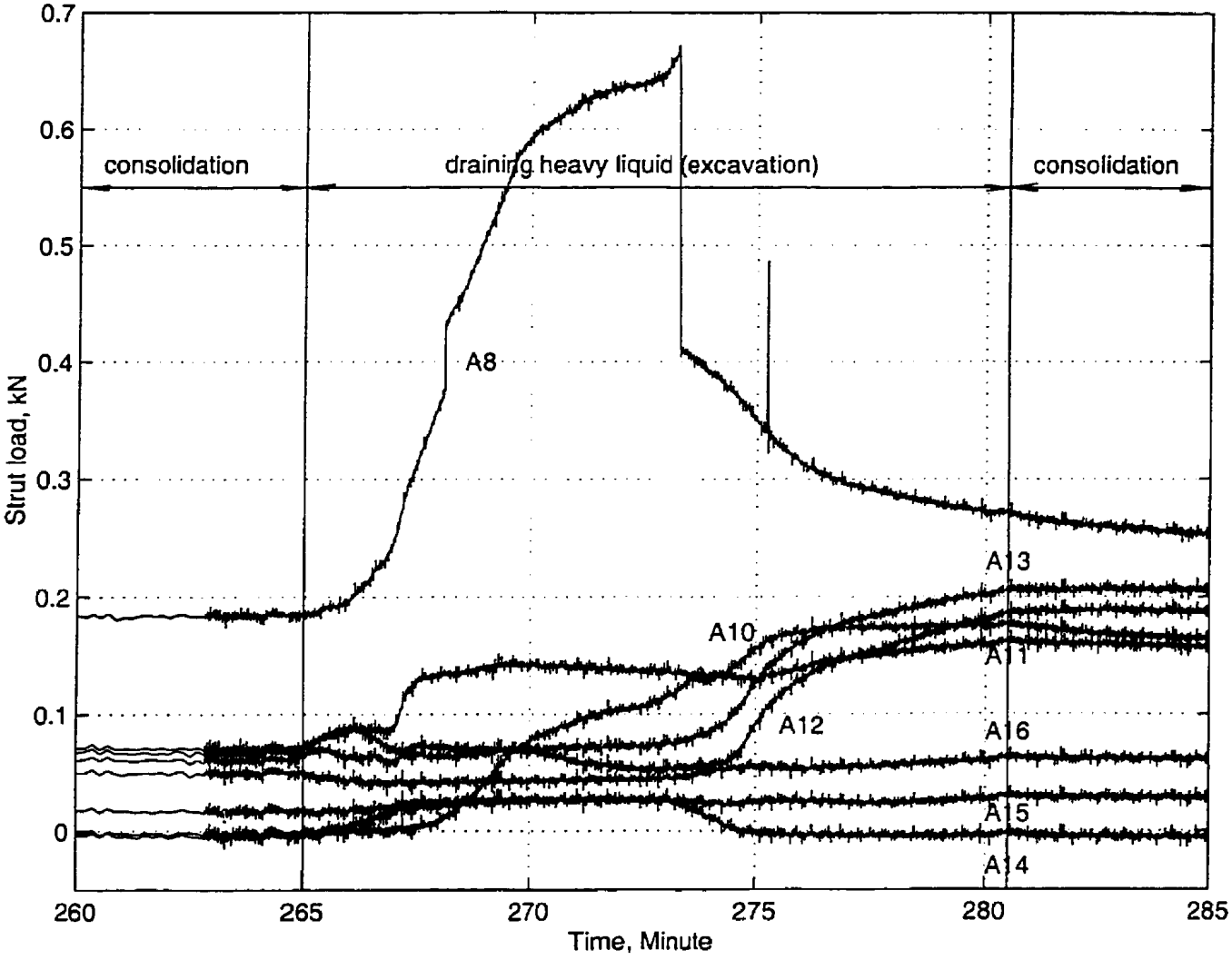

6.7 Surface Settlement

The surface settlement is shown in Fig. 6.19 and 6.20. LDT 1 is the closest to the sheet plate and LDT 4 is furthest from the sheet plate. The curves show similar patterns of settlement of the surface. LDT 1 settled the least before draining and LDT 4 settled the most. During draining and consolidation, the settlements increased, and the middle two points had close values.

LDT 4 had a higher settlement than LDT 1 because at the end part of the strongbox, the clay may deform laterally, while close to the sheet plate, the plate cannot move much because the strong support of the struts. Therefore the clay in the middle part deformed less in the horizontal direction than the clay in the end part of the strongbox.

The settlements resulting from the draining are shown in Fig. 6.21. These settlements are obtained by deducing the settlement resulting from consolidation of the total settlements. The fact that the surface of the heavy liquid was lower than the surface of the soil can be interpreted as part of the draining (excavation) had been completed during consolidation. However the settlement resulting from this "draining" cannot be separated from the total settlement during consolidation. As a result, the settlement resulting from "net" consolidation is over-estimated. This is the reason the "net" settlement resulting from the actual draining is negative. The numbers in the figure represent the different states and are shown in Table 5.2. This figure also shows the level of the heavy liquid of each state. Fig. 6.22 shows a comparison between the final profile of settlement in this test and the summary

Table 6.2: Selected states

Number	Total time (Minutes)	Time from draining (Minutes)	Time in prototype (Days)
(1)	265.0	0.0	0.0
(2)	267.5	2.5	9.0
(3)	270.8	5.8	20.9
(4)	274.0	9.0	32.4
(5)	280.5	15.5	55.8
(6)	320.0	55.0	198.0

given by Peck in 1969. The settlements of the first two points are within the line of Zone I, which is for the soil with higher strength. It is defined as the zone of "sand and soft to hard clay". This matches the clay of this test, because after preconsolidation and before the test, its shear strength was 41 kPa. Meanwhile Zone II and III are for soft to very soft clay. For this test, points 3 and 4 drop into the top parts of these zones. This shows that the settlement happened in a larger area than the definition of Peck's zones.

Figure 6.19 Surface settlement of varying distance from back of sheet plate

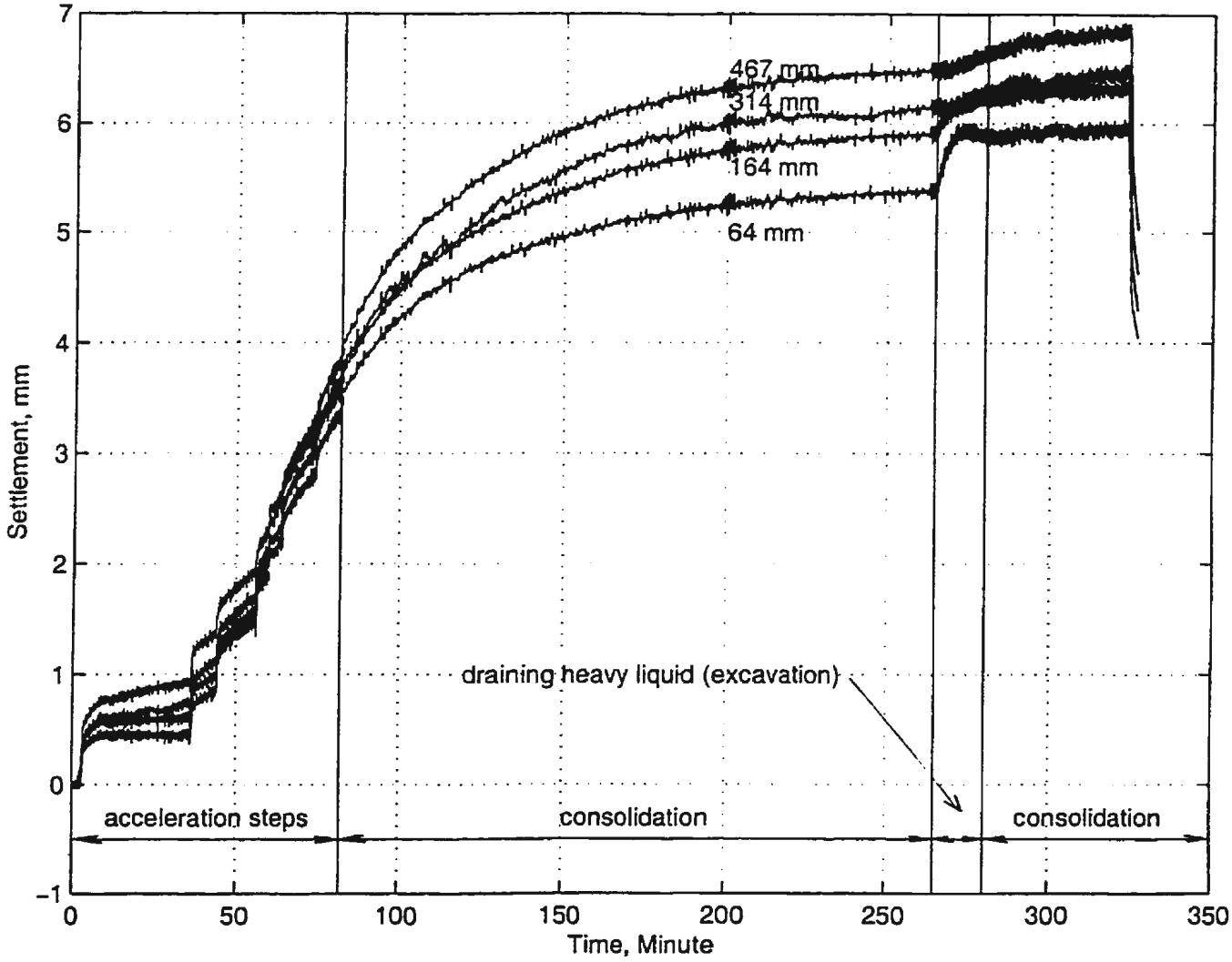

Figure 6.20 Surface settlement of varying distance from back of sheet plate

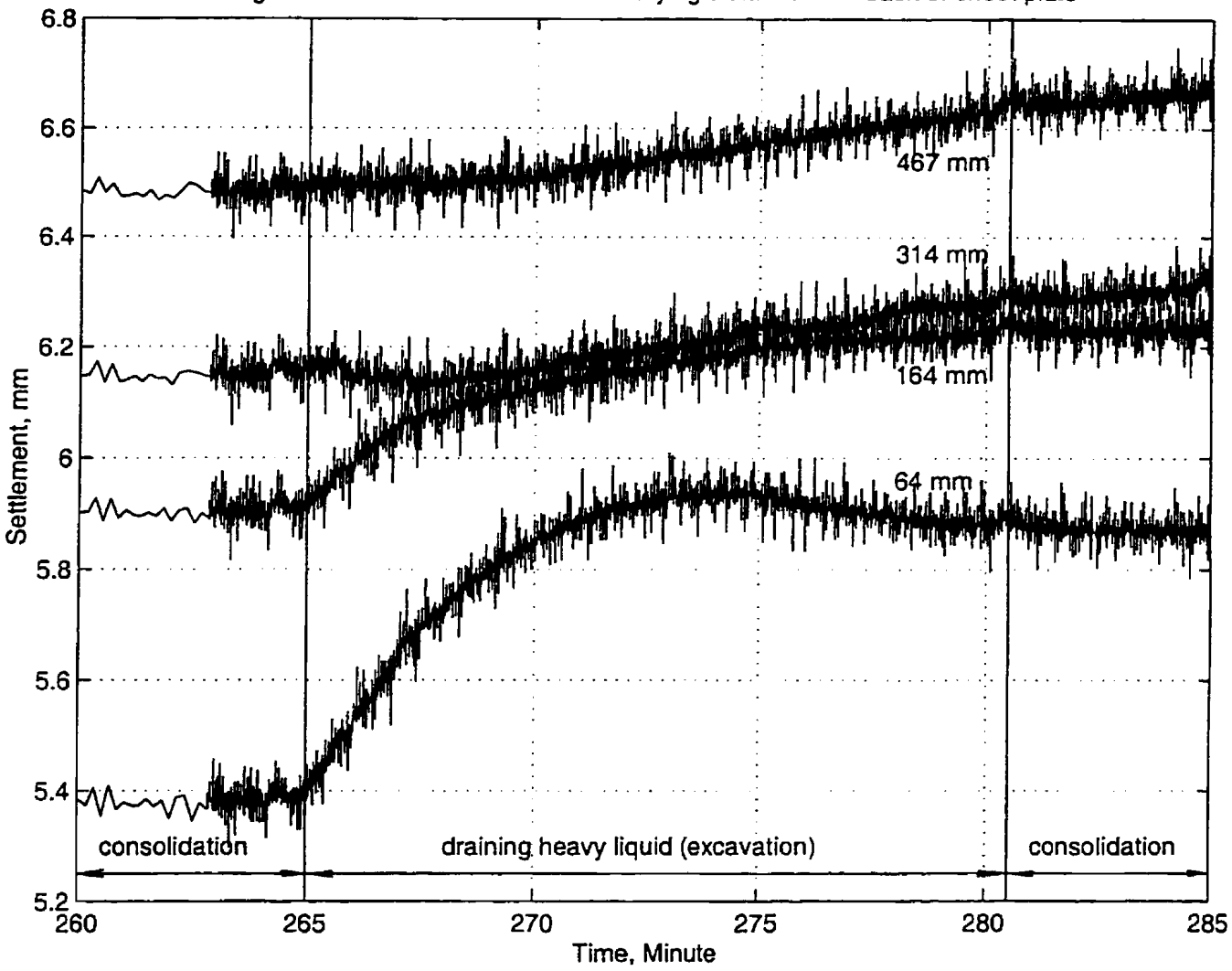

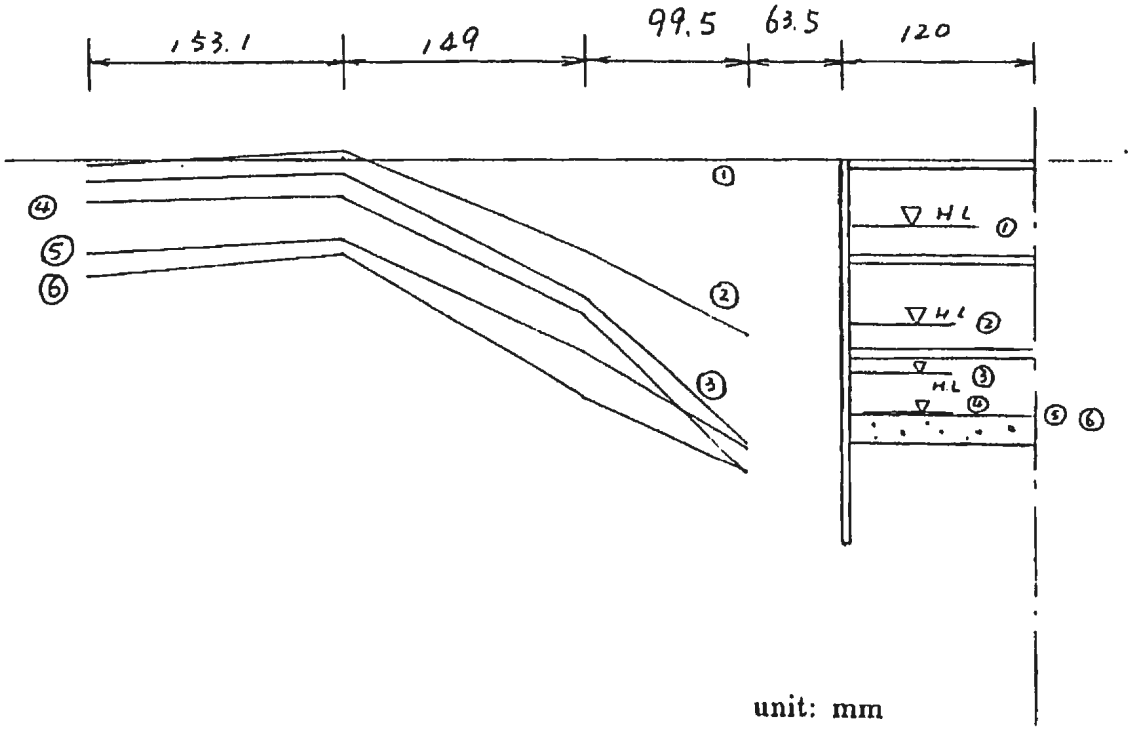

Figure 6.21: Surface settlement resulting from draining the heavy liquid

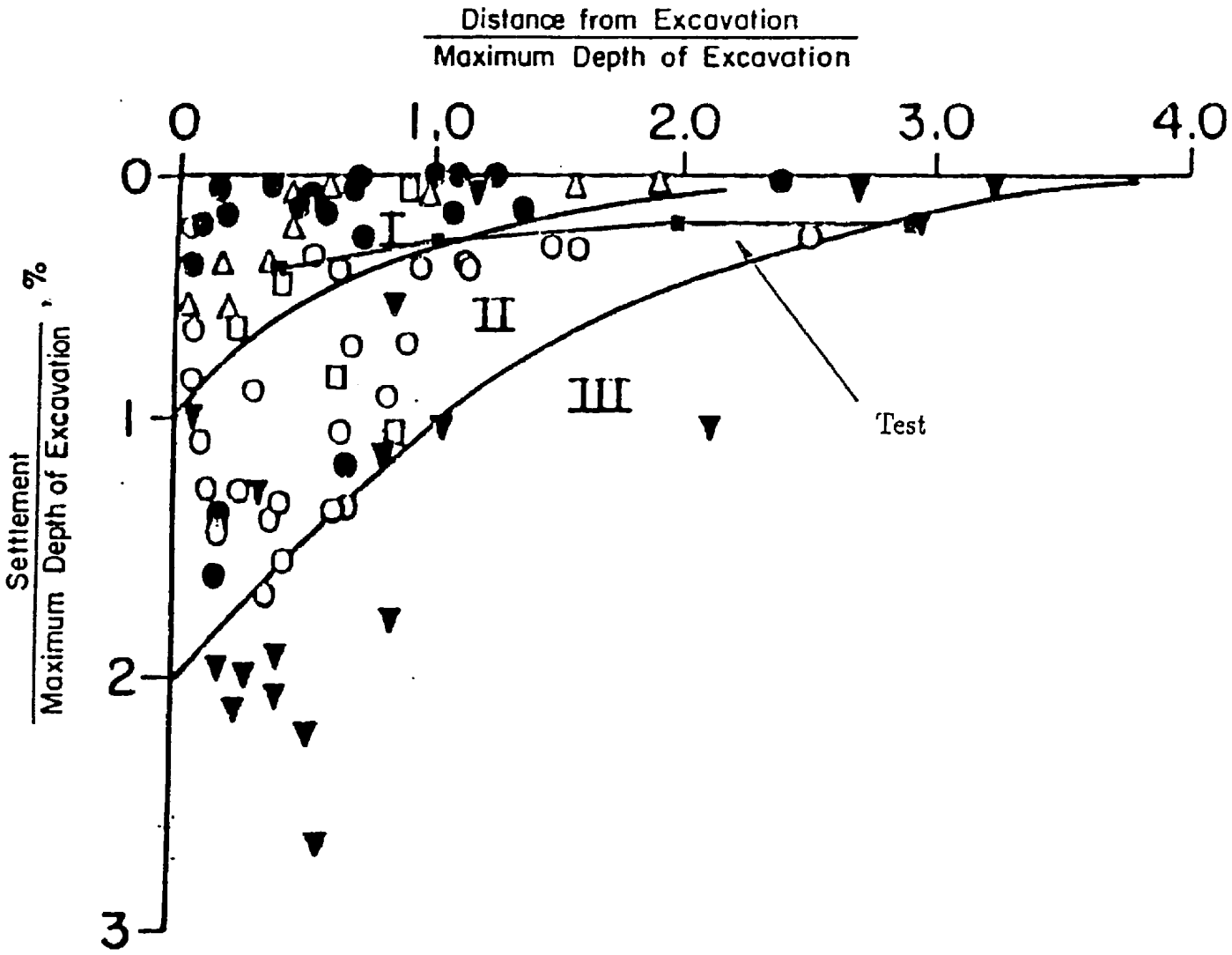

Figure 6.22: Comparison of the surface settlement between the results of the test and the statistical results given by Peck (1969)

6.8 Pore Pressures in the Clay

The development of pore pressures in the clay is shown in Fig. 6.23 and 6.24. After the acceleration reached 72 g, the consolidation began and the pore pressures kept reducing, all three curves have the same pattern. The drainage of the heavy liquid made the pore pressures reduce somewhat but recovered during the subsequent consolidation and remained stable.

Figure 6.23 Soil pore pressures

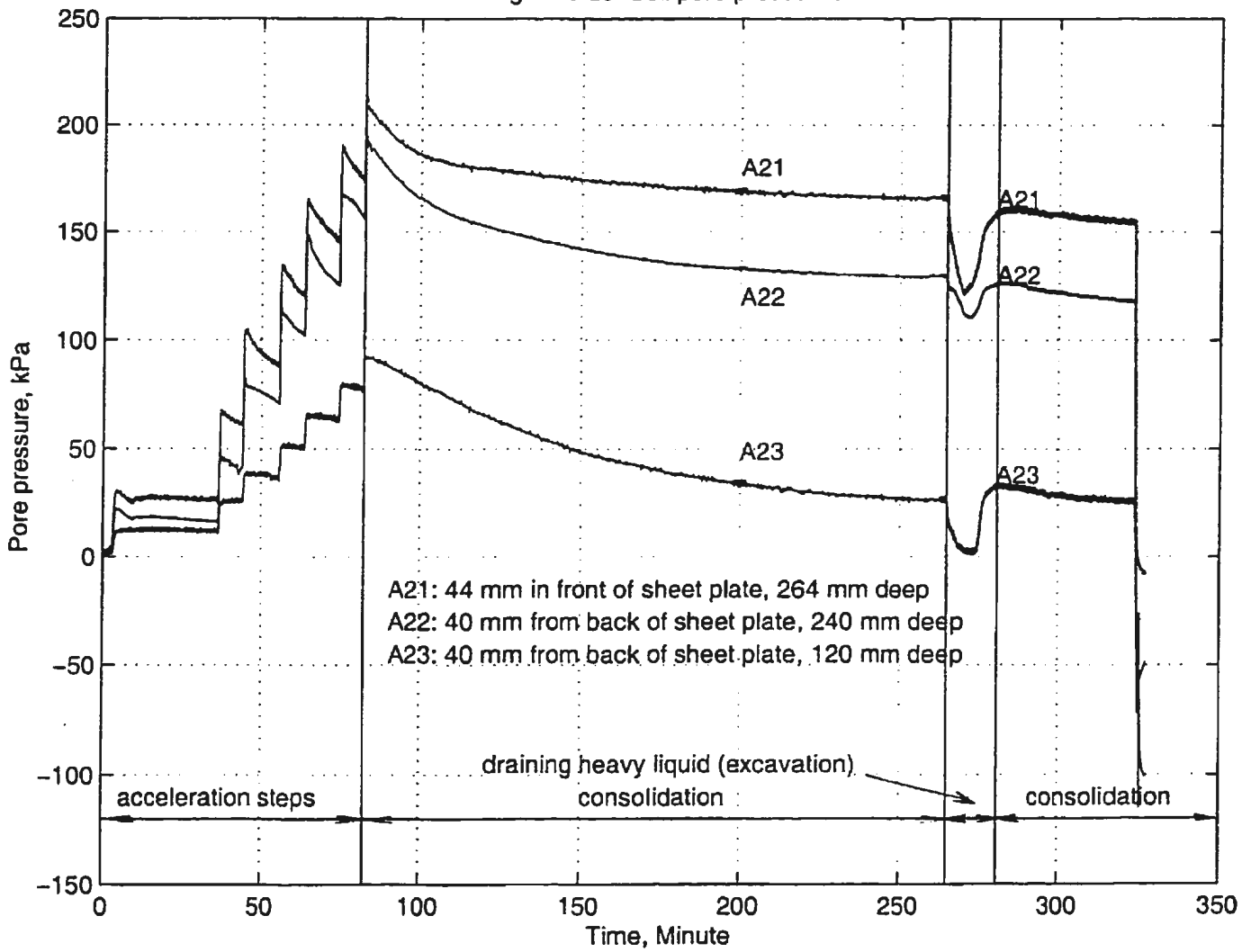

Figure 6.24 Soil pore pressures

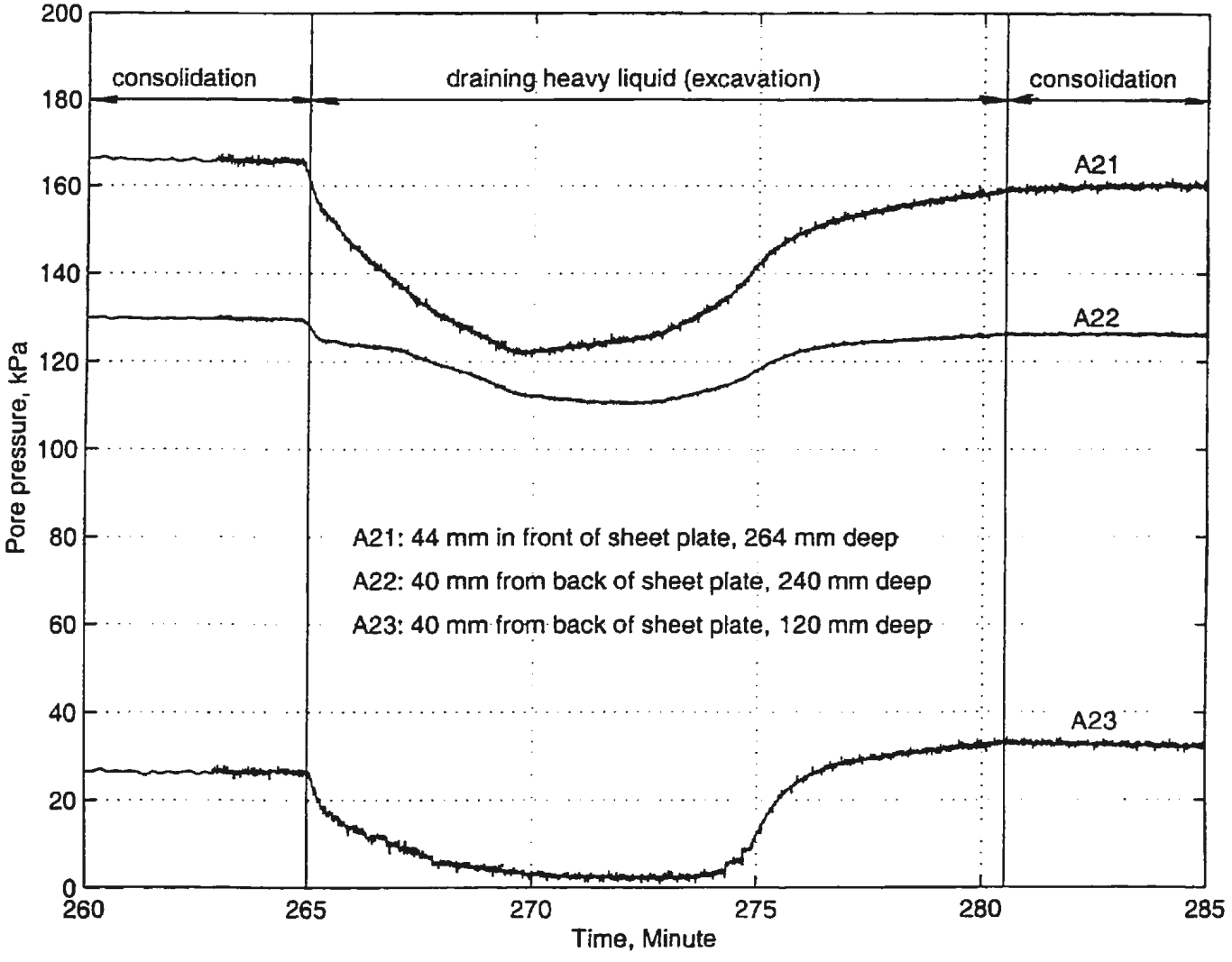

6.9 Earth Pressures

The effective earth pressures, the water tables in the clay at the back and in front of the sheet plate, and the levels of the heavy liquid in different states are shown in Fig. 6.25, 6.26 and 6.27. All the effective earth pressures are drawn together in Fig. 6.28. The height of the sheet plate is divided into five parts from the top (part 1) to the bottom (part 5) according to the positions of the strain gauges. The numbers represent the states shown in Table 5.2. The results of prediction with Peck's method for medium and stiff clay, and the the results of prediction with Tschebotarioff's method for medium and stiff clay are compared with the results of the test in Fig. 6.28. It should be noted that these methods assume that the sheet piles are simple beams supported by the struts. The shear strength of the clay is 47 kPa after the test, and the clay can be considered as medium clay.

The earth pressures at T=264.4 minutes had their maximum value in the middle part of the sheet plate supported by the last layer of struts. Normally the pressures increase with depth. However, the earth pressures at the bottom part of the sheet plate are less than the pressures at the middle part. This is because the earth pressures are reduced by the displacement of the sheet plate.

As the draining of the heavy liquid proceeds, the distribution of pressure at the first part jumps on both sides of the plate, (although the pressure on the excavation side was not significant). This shows bending directions of the middle parts of the plate changed frequently.

The pressure at part 2 is stable during draining (except when T=267.5 minutes, which is negative, may be error resulted from the possible friction between the sheet plate and the walls of the strong box). Actually this value at part 2 is the largest earth pressure on the back of the plate at the final stage of draining the heavy liquid. In practice this value may be used to represent the actual maximum earth pressure on the sheet piles. The difference between this test and an actual excavation is that the struts were already installed before "excavating" the "soil" in the test. However, as mentioned before, because the contact between the struts, wales and sheet plate was not very tight, the active earth pressure was mobilized somewhat. Therefore there was some similarity between the test and an actual excavation.

The pressure in the middle part keeps reducing during draining. The final value of the pressure is negative. This implies that some friction of the sheet plate with the side walls of the strongbox has not been considered. The pressure in the fourth part changes its direction after the first step and reached its maximum value at the final step. This pressure keeps increasing with the draining of the heavy liquid, and tends to mobilize the passive earth pressure. The pressure in the bottom part of the plate has a similar distribution as the fourth part. This value is quite stable during the whole process of draining.

By comparing the predictions of the methods and the results of the test, it seems that Peck's methods for stiff clay may provide a good prediction if the largest value at the first step is not considered. Tschebotarioff's prediction for medium clay may give the similar results but the distribution pattern does not match. Peck's

prediction for medium clay gives too large a value and Tschebotarioff's prediction for stiff clay does not give a safe value for practical designs.

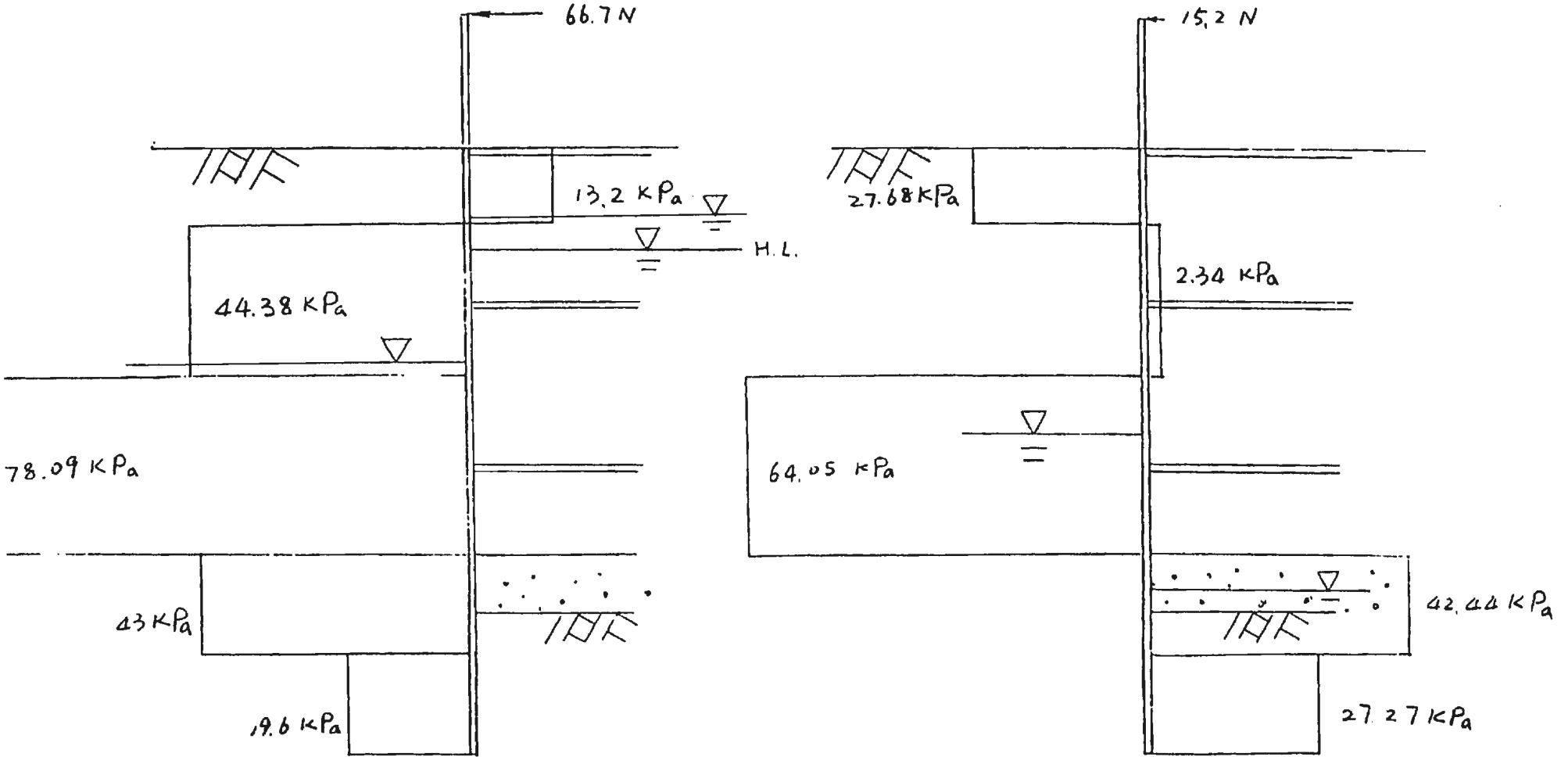

(1) T=264.5 min (just before draining)

(2) T=267.5 min (just after draining)

Figure 6.25: Effective earth pressure on the sheet plate

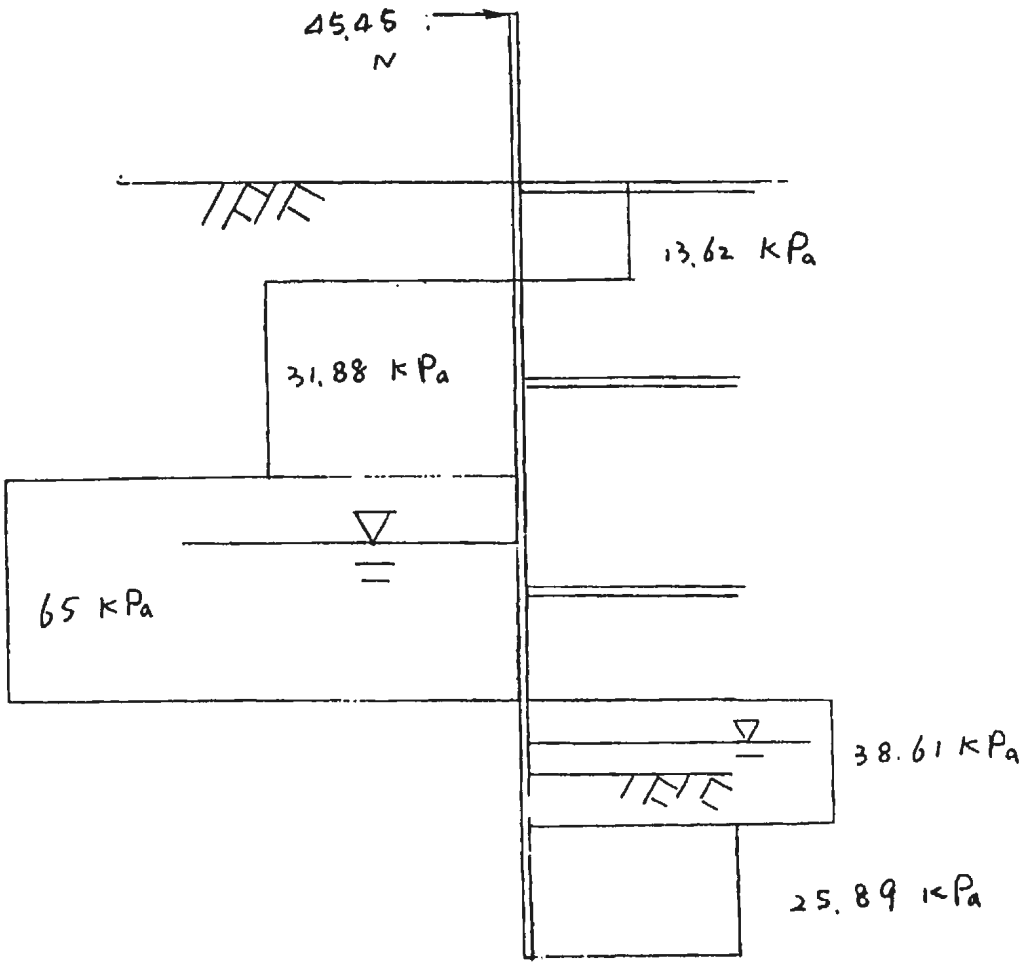

(3) T=270.8 min

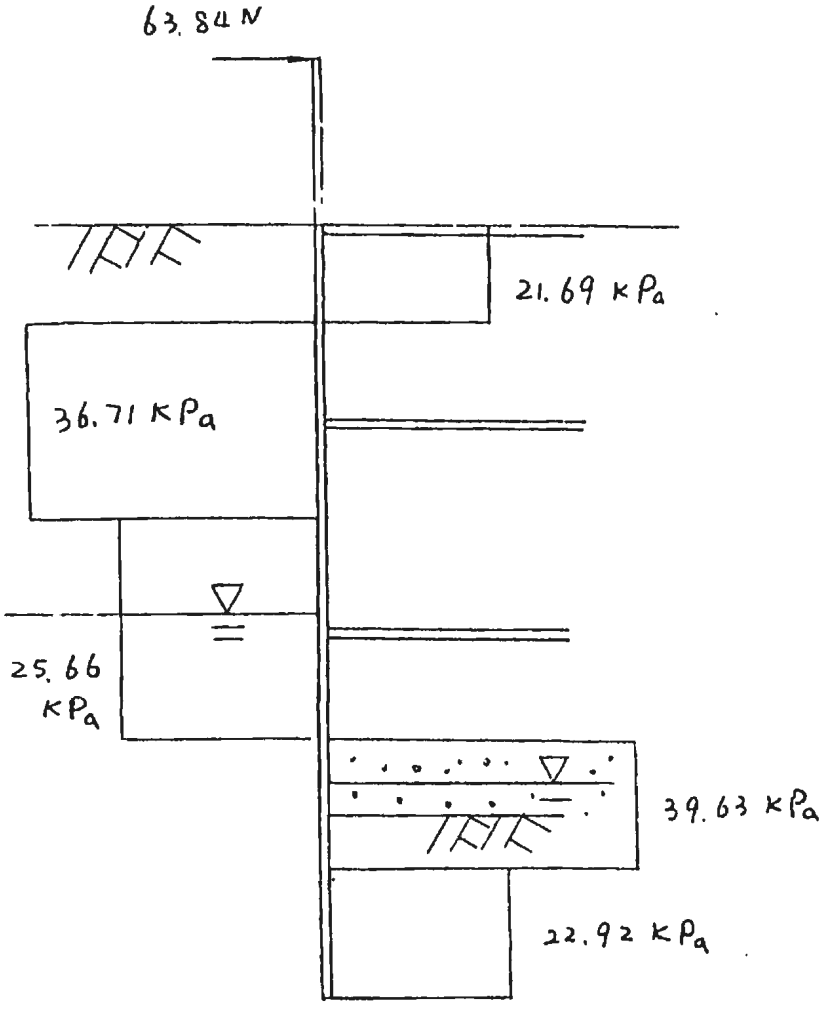

(4) T=274 min

Figure 6.26: Effective earth pressure on the sheet plate

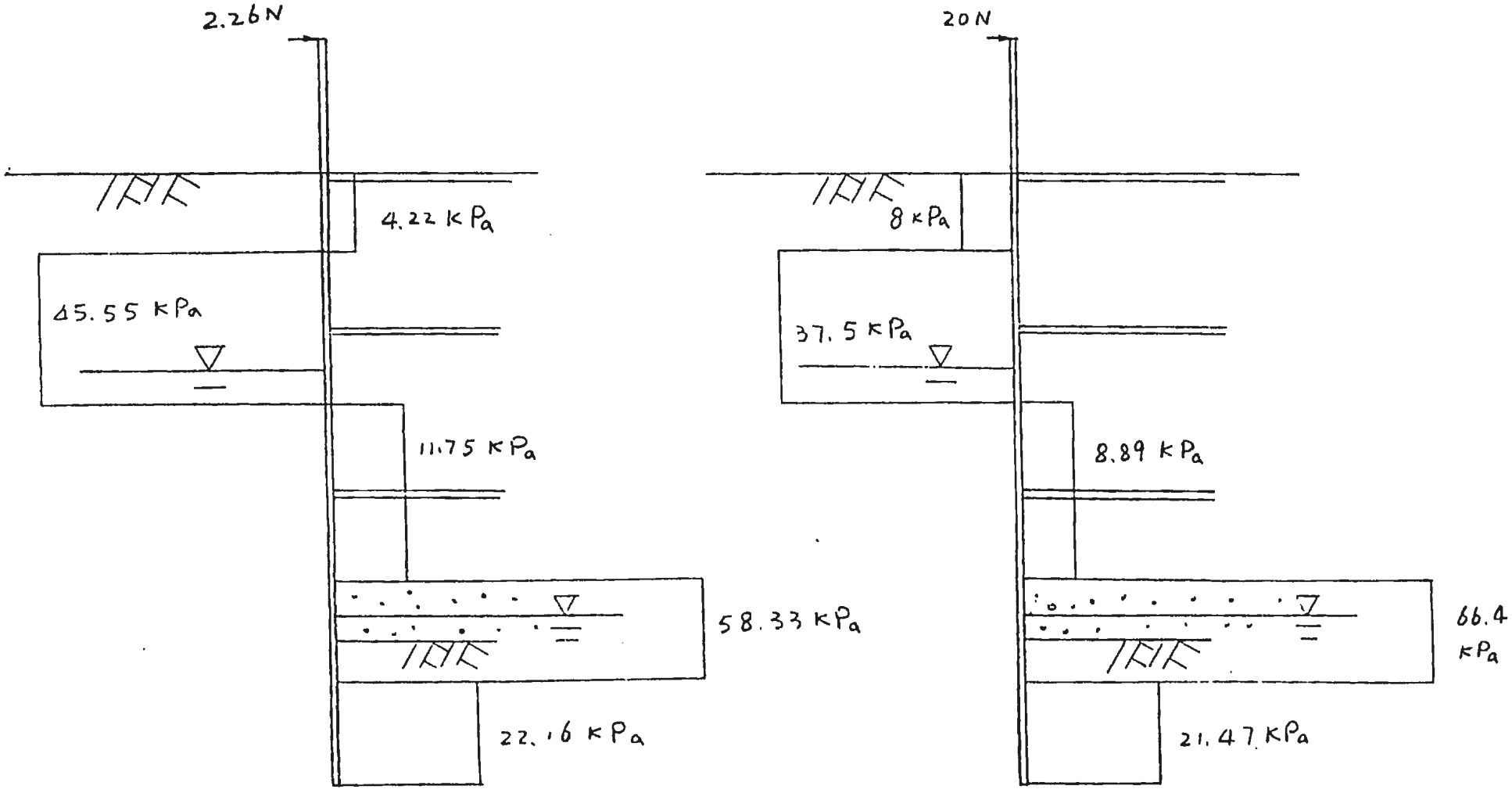

(5) T=280.5 min

(6) T=320 min

Figure 6.27: Effective earth pressure on the sheet plate

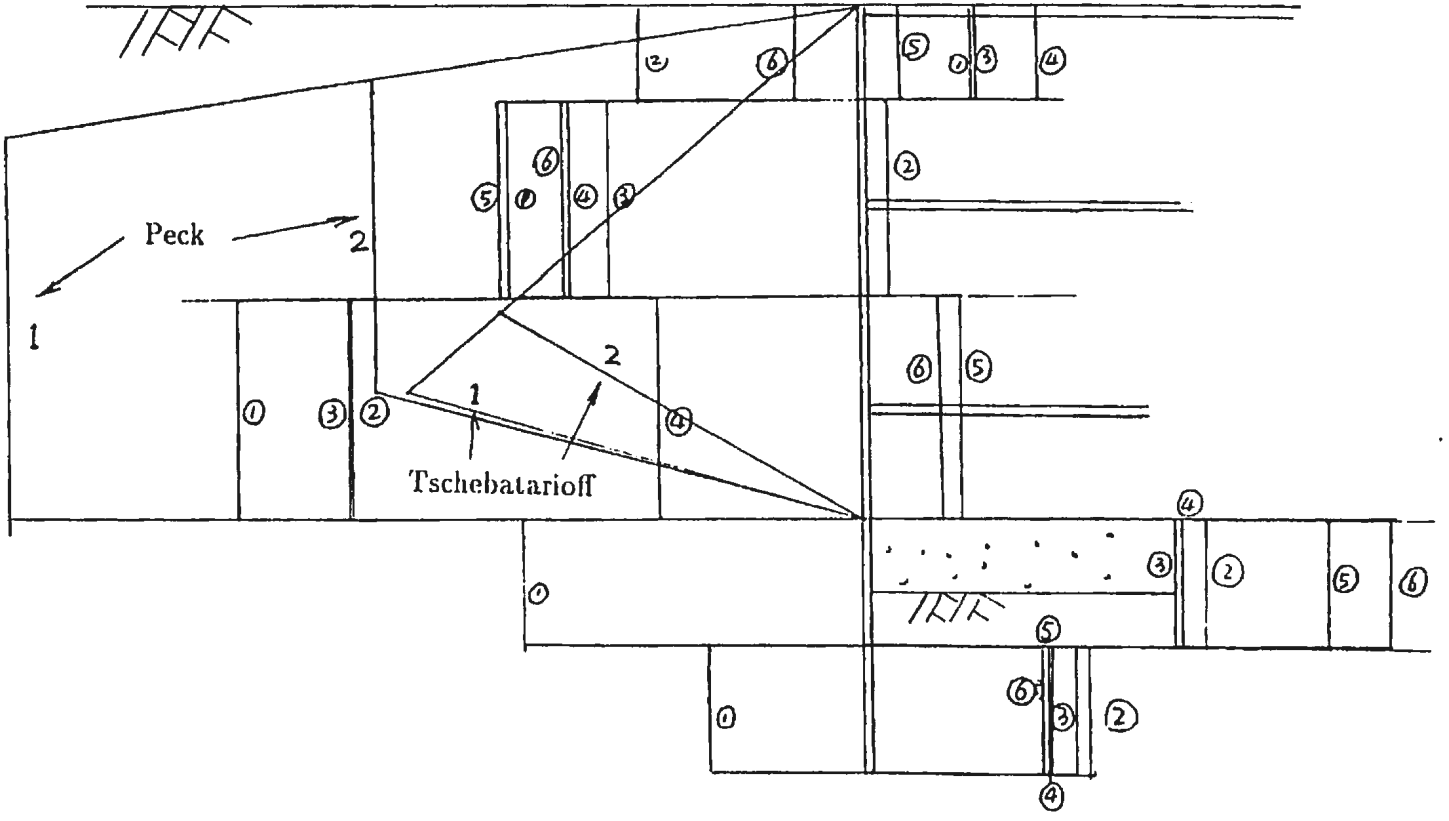

Figure 6.28: Prediction of the established methods and the test results of the effective earth pressures on the sheet plate ([1]medium clay, [2]stiff clay)

6.10 Residual Displacement

The plastic displacement is shown in Fig. 6.29. The displacement may be disturbed a little because of sliding off the plexiglass. However, a general idea of the displacement may be obtained from this figure. The final profile of the surface of the clay is shown in Fig. 6.30. The residual bottom heaving after the test was 2.34 mm.

model scale 1:3.3
displacement scale 1:0.5

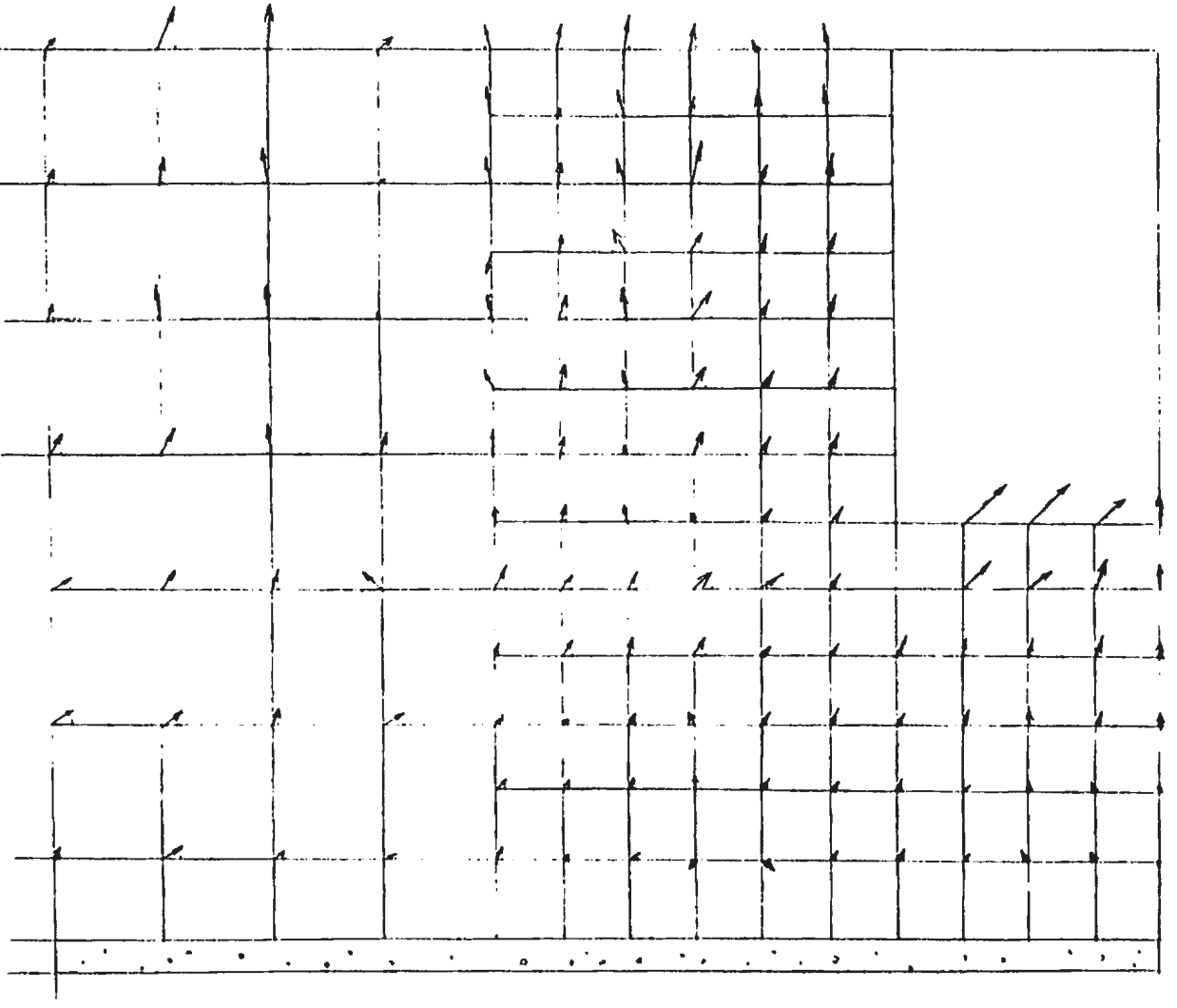

Figure 6.29: Residual displacement

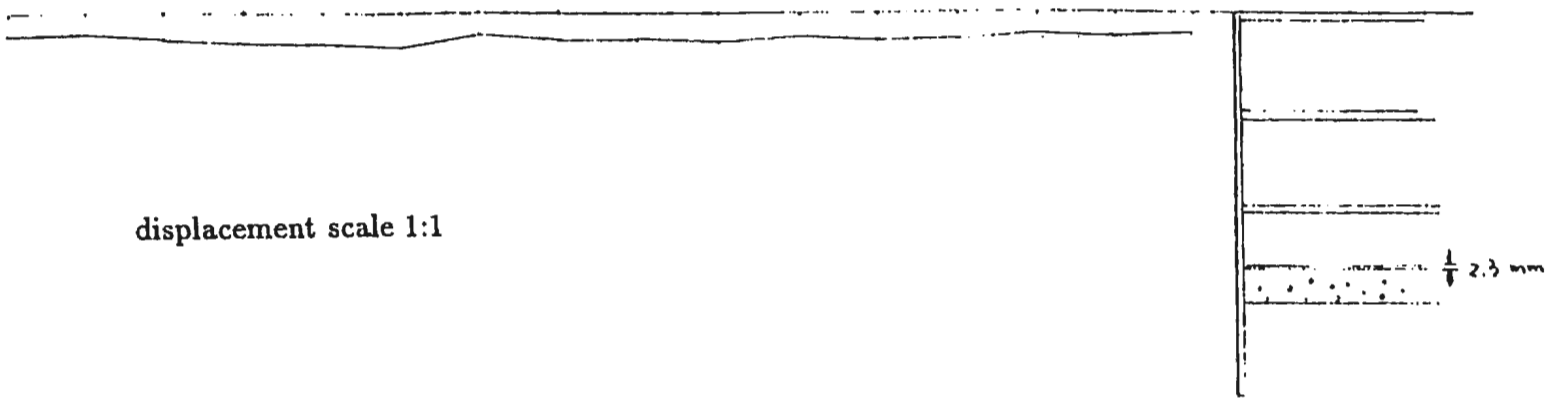

Figure 6.30: Final profile of the model after test

Chapter 7

FINITE ELEMENT ANALYSIS

7.1 Introduction

While the centrifuge tests provide a method to obtain experimental data which simulate real data, the finite element method may easily simulate complicated situations as long as the procedures are correctly defined and the correct values of the parameters are used. Therefore, in approaching the problem of excavation, the centrifuge tests and numerical analyses combine to be an excellent tool to study complex problems. The results can be checked against each other and corrections can be made according to the comparison and contrast.

Braced excavations may be analyzed with Biot's theory of porous-elasticity (Biot, 1943). The major assumptions of Biot's theory are that

- the deformation of the skeleton of the soil particles is linear and elastic;

- the deformation is small;
- seepage adheres to Darcy's law;

The equations of equilibrium, Hooke's law, the relation between stress and strain, and the equations of continuity are applied in the finite element analyses.

Plastic deformation is analyzed by continuously changing the stiffness matrix at each increment. The behaviour of plastic deformation is governed by the constitutive relations of the soil. This study uses the Cam-clay model to simulate the plastic properties of the soil. The parameters were tested in the lab by collecting soil samples from the strongbox after the centrifuge test. The process of obtaining the parameters for the analysis is described in Chapter 4.

The analysis for the excavation problem is carried out using the finite element package ABAQUS. This package has been developed by Hibbitt, Karlsson and Sorensen.

7.2 Introduction to the Analysis

The dimensions of the model in prototype are shown in Fig. 7.1. The excavation area is put on the left side of the model for convenience of plotting the results. The finite element mesh for the model is shown in Fig. 7.2 which is composed of 1197 nodes and 363 elements. 346 CPE8RP elements are used for the soil, 14 continuous CPE8R elements are used for the sheet piles and 3 spring elements are used for the struts. The CPE8RP is the 8-node biquadratic displacement element with bilinear pore pressure and reduced integration. The CPE8R is the 8-node biquadratic displacement element with reduced integration. It was proposed to use interface elements to simulate the interface between the sheet piles and the soil. However there was a convergence problem when the interface elements were used.

Day and Potts (1993) pointed out that "beam elements are more accurate for modelling thin section walls such as sheet pile walls". However because of the difficulties in coping with different pore pressures on either side of the sheet piles, two-dimensional block elements are used for the sheet plate (sheet piles). Its Young's modulus is 6.956×10^7 kPa and Poisson's ratio is taken as 0.3. The actual thickness of the sheet plate in the centrifuge experiment was 1.55 mm. According to the similarity law, this thickness of aluminum plate can simulate an actual aluminum sheet pile of a thickness of 111.6 mm in 72 g. This thickness of sheet pile has the sectional moment of inertia of $1.158 \times 10^{-4}\ m^4/m$. The value of EI is $8.057 \times 10^3\ kNm^2/m$.

The struts and wales are represented with springs. Because the simulation is

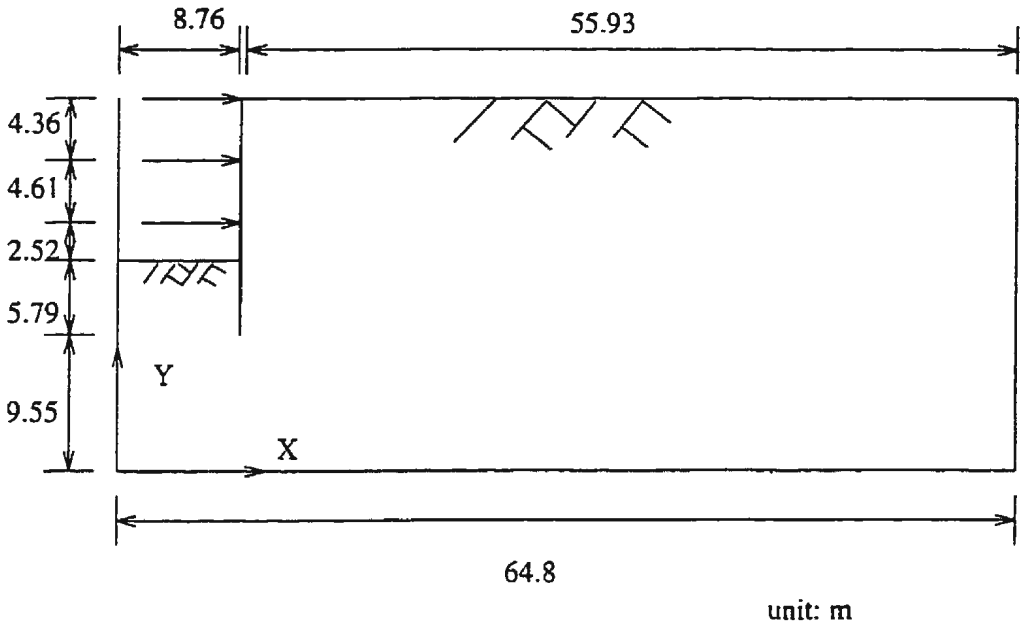

Figure 7.1: Dimensions of the model in prototype

Figure 7.2: Finite element mesh for simulating the test model

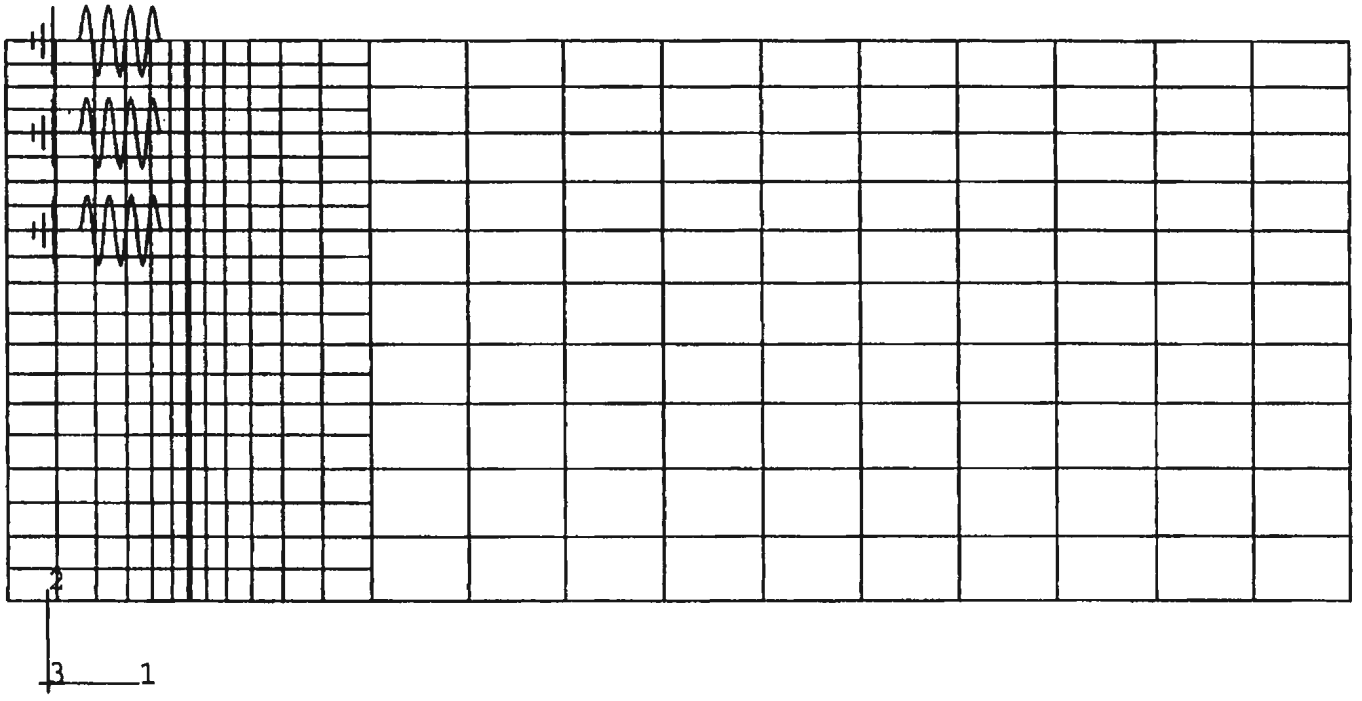

carried out as a planar problem, the springs would not be only a spring acting on one point but represent springs acting in a line in space, in which the struts and the wales are acting. Therefore the spring stiffness is calculated per linear meter along a horizontal line of 7.2 m between the struts. The unit is kN/m/m. From the test data, the stiffness for the spring is taken as 2.256×10^5 kN/m/m.

Preloading the struts is a common technique to promote the stiffness of the bracing system and reduce lateral displacement. The effect of preloading in practical sites has been reported by several researchers. This research will not study the effect of preloading.

Before excavation, initial effective stresses are assigned to each soil element and initial pore pressures are assigned to each soil node. The vertical stress is given according to the buoyant unit weight of the soil and the depth of the element. Whereas, the lateral stress is given by the effective vertical stress times K_0, the coefficient of static lateral earth pressure. The initial pore pressures are given according to the hydrostatic pore pressure at each node, and the water table is the same as in the test.

The properties of the soil, the sheet piles and the springs are also given before loading (excavating). These parameters which include the parameters for a Cam-clay model and the shear stiffness are shown in Table 7.1. K_0 takes the value of 1, because the soil is overconsolidated. The physical meaning of the parameters are shown in the List of Symbols.

The following describes how the shear modulus of soil G' is obtained.

Assuming the soil is fully consolidated under a vertical effective stress p_0', the lateral effective stress is $k_0 p_0'$, and there is no excess pore pressures. In a consolidated undrained triaxial test, the sample is tested and failed at a total axial stress σ_1 and cell pressure σ_3. The increment of principal stresses are $\Delta\sigma_1$ and $\Delta\sigma_3$. Therefore,

$$\sigma_1 = p_0' + \Delta\sigma_1, \tag{7.1}$$

$$\sigma_3 = K_0 p_0' + \Delta\sigma_3, \tag{7.2}$$

and the increment of excess pore pressure is

$$\Delta u = \Delta\sigma_3 + A_f(\Delta\sigma_1 - \Delta\sigma_3), \tag{7.3}$$

where A_f is the coefficient of pore pressure at failure. As a result,

$$\sigma_1' = p_0' + (1 - A_f)(\Delta\sigma_1 - \Delta\sigma_3), \tag{7.4}$$

$$\sigma_3' = K_0 p_0' - A_f(\Delta\sigma_1 - \Delta\sigma_3). \tag{7.5}$$

Referring to Fig. 7.20, the undained shear strength is

$$s_u = \frac{1}{2}(\sigma_1 - \Delta\sigma_3) = \frac{1}{2}(1 - K_0)p_0{}' + \frac{1}{2}(\Delta\sigma_1 - \Delta\sigma_3), \tag{7.6}$$

$$\Delta\sigma_1 - \Delta\sigma_3 = 2s_u - (1 - K_0)p_0{}'. \tag{7.7}$$

Therefore

$$\sigma_3{}' = K_0 p_0{}' - A_f(2s_u - (1 - K_0)p_0{}'). \tag{7.8}$$

From the same figure (Fig. 7.20),

$$\sin\phi = \frac{s_u}{(\sigma_1{}' - \sigma_3{}')/2 + c\cot\phi}. \tag{7.9}$$

It follows that

$$s_u = \frac{c\cos\phi + p_0{}'\sin\phi(K_0 + A_f(1 - K_0))}{1 + 2(A_f - 1)\sin\phi} \tag{7.10}$$

In the triaxial test for the sample T5 as shown in Section 5.4, cell pressure σ_3=449.04 kPa, A_f=0.535, c=4.25 kPa, $\phi = 30°$, and K_0=1. Therefore

$$s_u = 0.483 p_0' + 3.556 \qquad (kPa). \tag{7.11}$$

From Harahap (1990) (Table 7.3), $G' = 300 s_u$, therefore,

$$G' = 1066.84 + 144.9 p_0' \qquad (kPa). \tag{7.12}$$

In this test, $p_0' = \sigma_3'$=449.04 kPa, it follows $G' = 6.613 \times 10^4$ kPa according to (7.12). The result from the test is $G' = 2.667 \times 10^4$ kPa, therefore the expression for G' is

$$G' = \frac{2.667 \times 10^4}{6.613 \times 10^4}(1066.84 + 144.9 p_0') \tag{7.13}$$

or

$$G' = 430.25 + 58.395 p_0'. \tag{7.14}$$

In the analysis, p_0' is written as σ_z'. This gives the expression in Table 7.1.

Table 7.1: Summary of the parameters of the clay for finite element analysis for the model

Soil parameters	value	units
ρ_d	1.434×10^3	kg/m^3
γ'	8.776	kN/m^3
e_0	0.817	/
κ	0.0384	/
λ	0.2783	/
M	1.2	/
ϕ	30	degree
K_0	1	/
k	4.683×10^{-4}	m/day
G	$430.25+58.395\sigma'_z$	kPa

The excavation procedure is to make a sequence of load increments. The soil between two levels of struts is divided into 4 layers and each layer consists of 6 elements. Each of the first two layers is removed in 21 increments in 10.01 days. The removal of an element is accomplished in two steps: the first step is to fix the boundary of the element at the nodes and remove the element; the second step is to remove the boundary and apply the loads on the nodes, where the loads were applied by the element to the nodes before it was removed. These loads are removed gradually during the whole step of consolidation. For the first two layers, 0.01 day is used for the first step and the remaining time is used for the second step. This effort is to bring the excavation into a fully stable state of seepage. The reason is that the surface of the heavy liquid in the centrifuge test was two layers below the surface of the clay and full consolidation was reached before draining the heavy liquid.

Each of the remaining layers is removed in 11 increments, where 1 increment is also used to remove the elements and fix the boundary. The rest are used to gradually remove the loads applied by the elements. The elapsed time for removal of each layer is calculated according to the rate of draining the heavy liquid during the test. The elapsed time is equally distributed among the loading increments at each step. The complete loading steps for simulating the test are given in Table 7.2.

Table 7.2: Steps for simulating the centrifuge test with FEA

steps	total days	elapsed days	max. inc.	used inc.	excavated depth (M)	total depth (M)	remarks
1	1.	1.	1	1	0.	0.	Create static equilibrium
2	1.01	0.01	1	1	1.09	1.09	remove layer 1
3	11.01	10.	20	7	/	1.09	remove layer 1
4	11.02	0.01	1	1	1.09	2.18	remove layer 2
5	21.02	10.	20	7	/	2.18	remove layer 2
6	21.03	0.01	1	1	1.09	3.27	remove layer 3
7	23.396	2.366	10	7	/	3.27	remove layer 3
8	23.407	0.01	1	1	1.09	4.36	remove layer 4
9	25.773	2.366	10	6	/	4.36	remove layer 4
10	25.774	0.01	1	1	1.1525	5.5125	remove layer 5
11	30.228	4.454	10	7	/	5.5125	remove layer 5
12	30.238	0.01	1	1	1.1525	6.665	remove layer 6
13	34.055	3.817	10	8	/	6.665	remove layer 6
14	34.065	0.01	1	1	1.1525	7.8175	remove layer 7
15	38.292	4.227	10	8	/	7.8175	remove layer 7
16	38.302	0.01	1	1	1.1525	8.97	remove layer 8
17	53.715	15.413	10	10	/	8.97	remove layer 8
18	53.725	0.01	1	1	1.26	10.23	remove layer 9
19	58.715	4.99	10	10	/	10.23	remove layer 9
20	58.725	0.01	1	1	1.26	11.49	remove layer 10
21	63.715	4.99	10	10	/	11.49	remove layer 10

7.3 Results of the Finite Element Analysis

This section presents some results of the finite element simulation of the test model. These are results at the final step of the simulation.

Fig. 7.3 shows the deformed mesh of the analysis. The magnitudes of the displacement are magnified 20 times. It shows that a large settlement at the surface of the soil is close to the sheet plate. However settlement at the nodes very close to the plate is close to 0, this is because contact elements are not used. The displacement of the nodes contacting the plate are restricted by the displacement of the plate. Therefore the displacement at these nodes is very small. The bottom heaving in front of the plate is also shown in the figure.

Fig. 7.4 shows the horizontal displacement of the clay. Most of the horizontal displacement is towards the excavation area. The largest horizontal displacement is about the middle of the model. The small displacement of the clay close to the plate is because of the bracing system, while the small displacement on right boundary of the model is because of the distance from the excavation area.

Fig. 7.5 shows the vertical displacement. It also shows that the largest settlement is behind the plate. Fig. 7.6, 7.7 and 7.8 show contour plots of the lateral, vertical and shear stresses respectively. Actually the largest stresses are inside the sheet plate. In order to show the stresses in the clay, the maximum and minimum values of the stresses are limited. The lateral stresses increase gradually from the surface to the bottom of the model. The same conclusion can be used for vertical

stresses. However, the large variation of shear stresses is limited in area and close to the tip of the sheet plate.

Fig. 7.9 shows the pore pressures. The pore pressures increase gradually from the top to the bottom of the model. Although the water table was set under the surface of the clay in the input of the analysis, the results show that the water table is in the surface of the model. One possible reason is that the Cam-clay model is for fully saturated clay.

Figure 7.3: Deformed mesh of the model

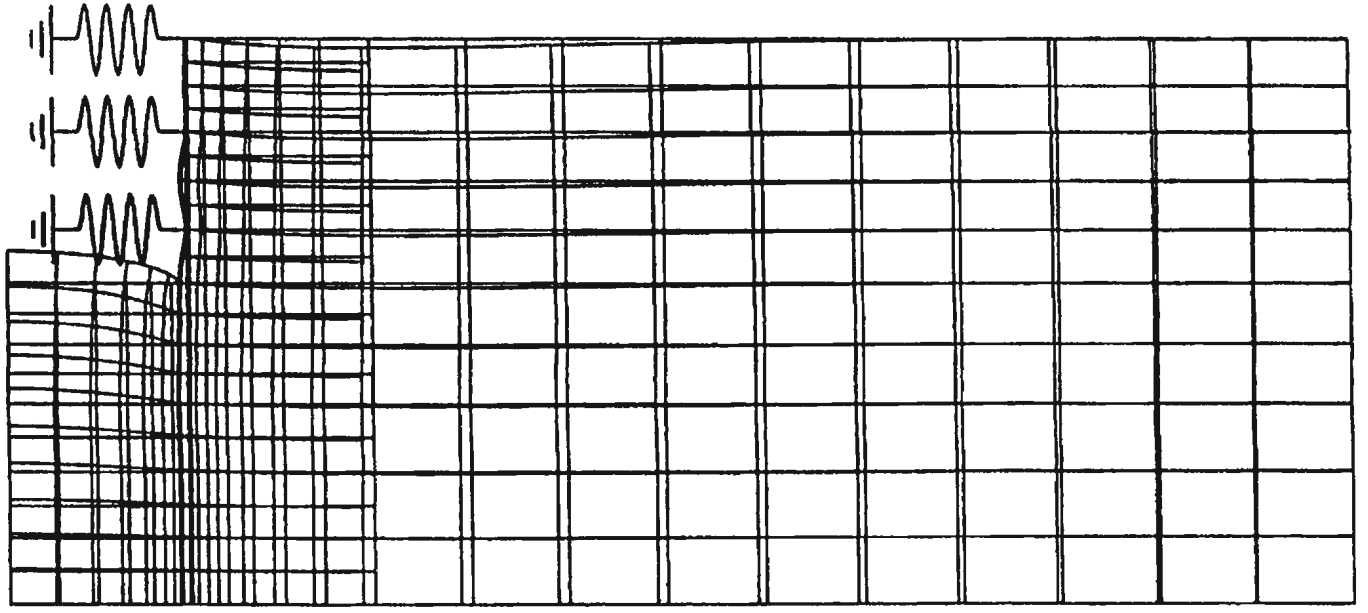

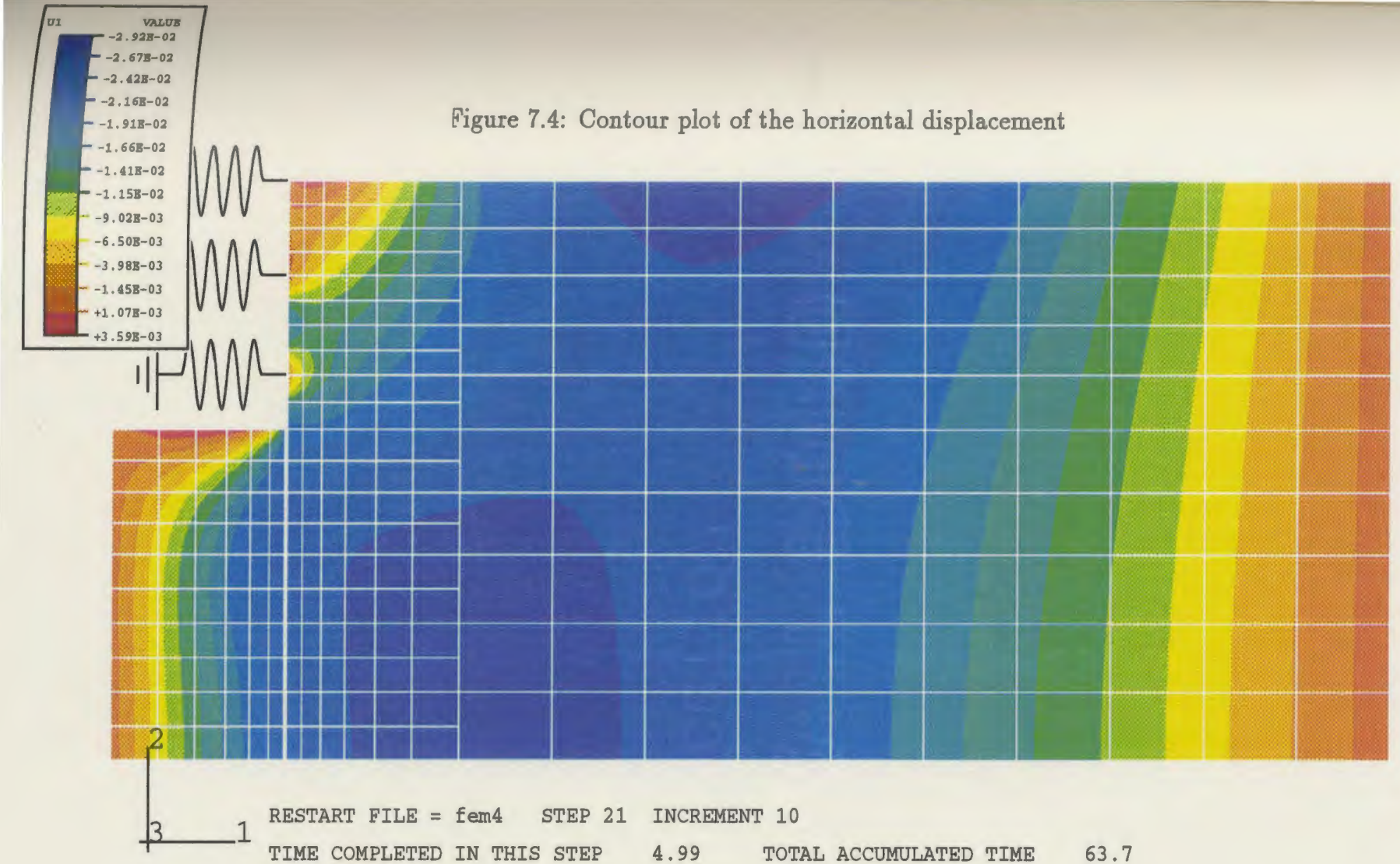

Figure 7.4: Contour plot of the horizontal displacement

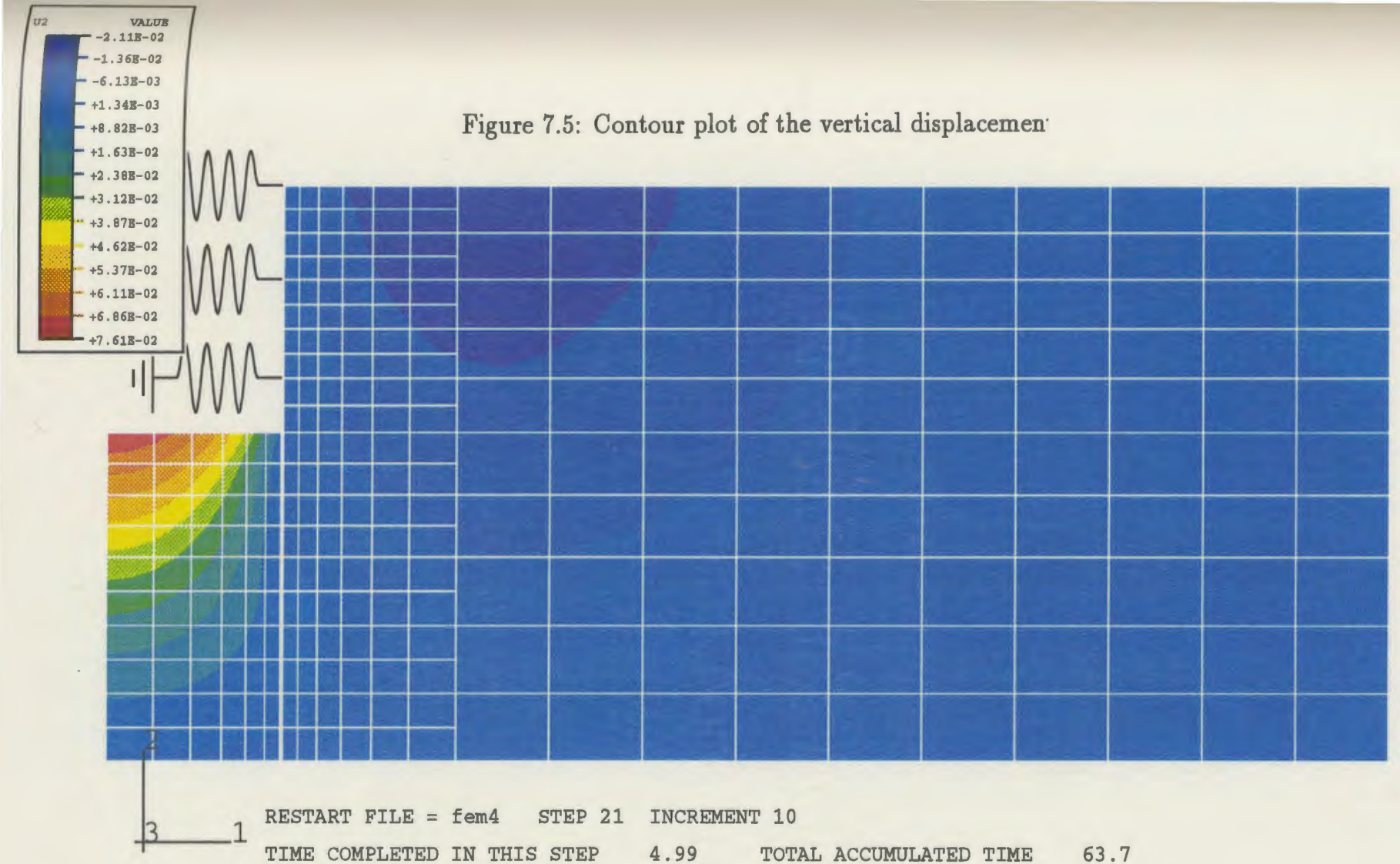

Figure 7.5: Contour plot of the vertical displacemen

Figure 7.6: Contour plot of the horizontal stresses

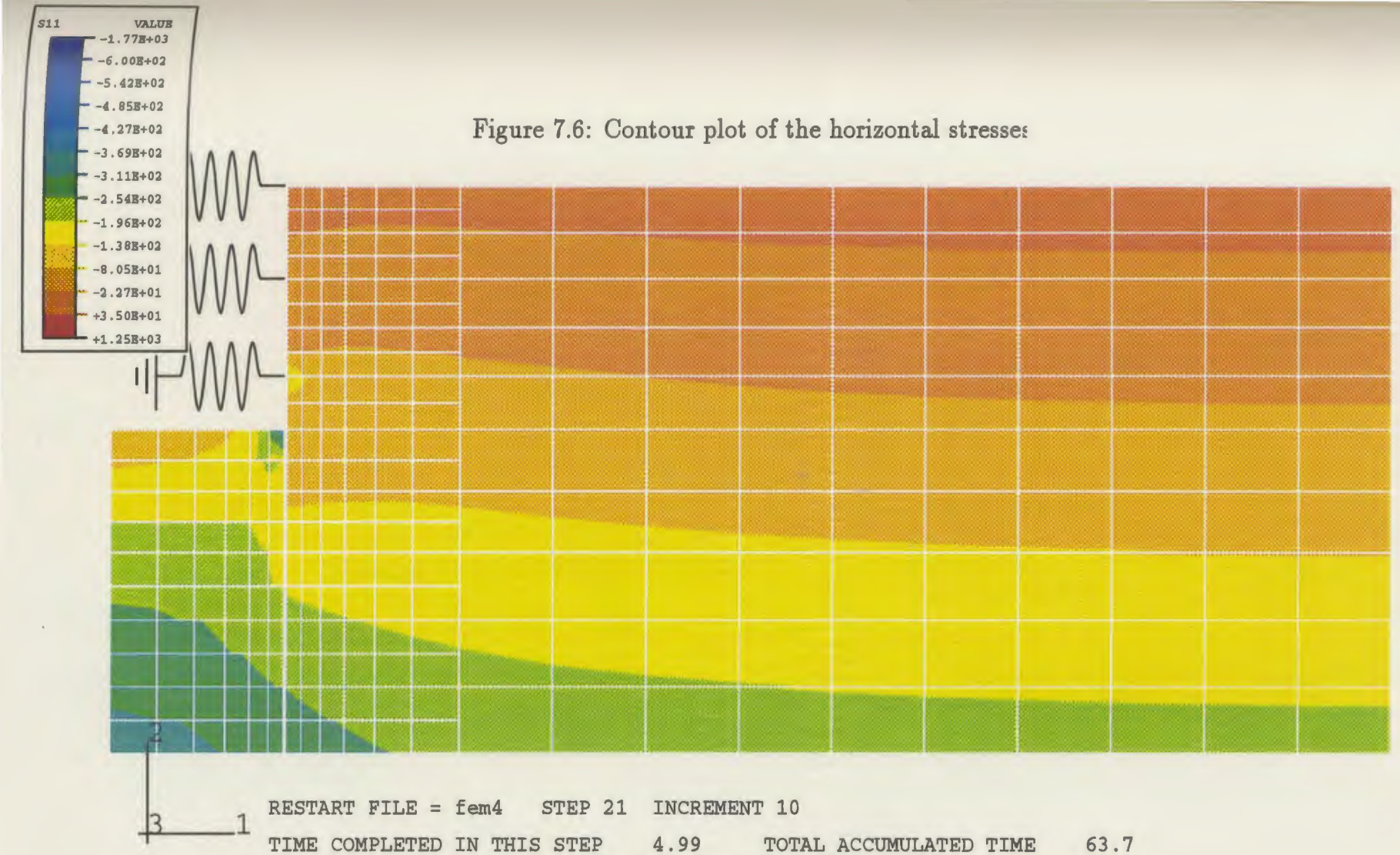

Figure 7.7: Contour plot of the vertical stresse:

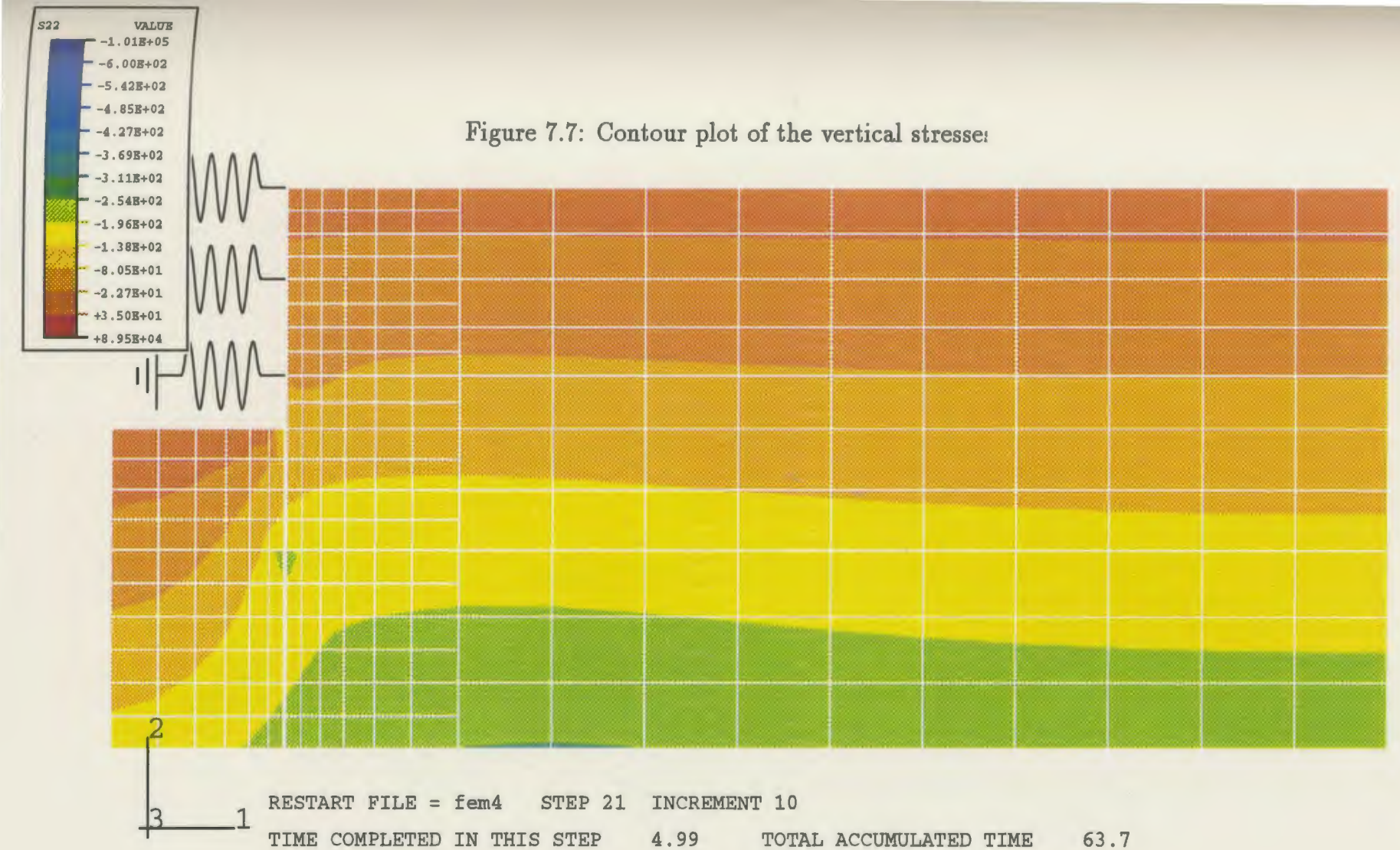

Figure 7.8: Contour plot of the shear stresses

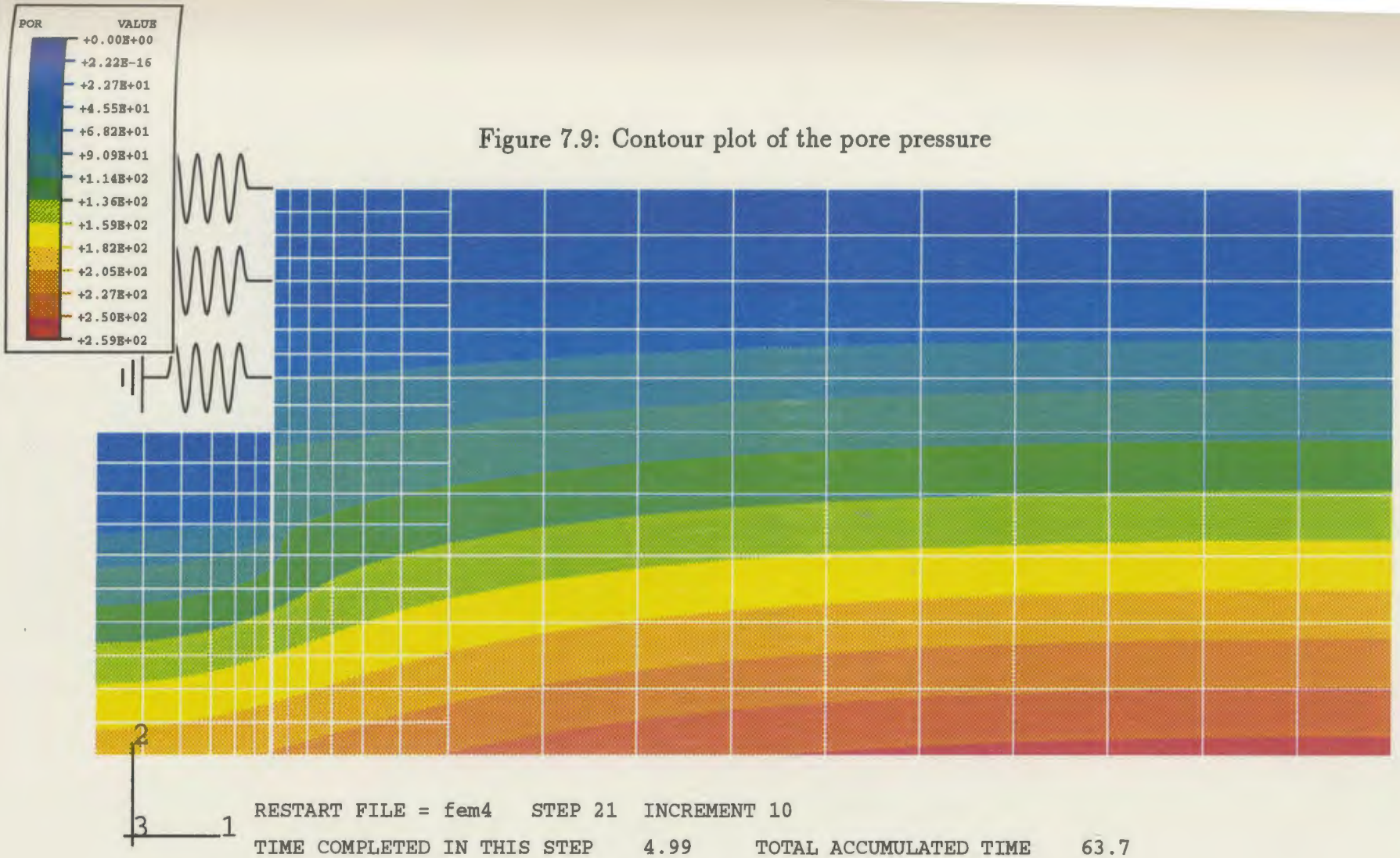

Figure 7.9: Contour plot of the pore pressure

7.4 Comparison Between the Results of FEM Analysis and the Centrifuge Test

The results of finite element analysis are compared with the results of centrifuge tests. The parameters are the same as stated in the previous parts of this chapter and calculations are performed for two values of K_0, 1.0 and 0.5. K_0 is defined as the ratio of lateral earth pressure to the vertical earth pressure at the initial state at a point. If it is not the initial state, the ratio is defined as K.

7.4.1 Earth pressures on the sheet piles

The calculated earth pressures in front of and on the back of the sheet plate before and after the excavation of each layer are shown in Fig. 7.10 and 7.11. These pressures are the effective earth pressures. The numbers beside the curves represent the steps of the analyses. Step 1 is for the static equilibrium. The line 1 represents the static earth pressures according to K_0=1. The front earth pressures grow larger than the static earth pressure. It tends to mobilize the passive earth pressure. Lines p_{p1} and p_{p21} show the passive earth pressures at step 1 and step 21. The results of the analysis are between these two lines. It seems that at each step, the front earth pressures are too larger in the top couple layers. The earth pressures on the back of the sheet plate develop different sizes of S-shape curves on the line of static lateral pressures. The earth pressures decrease somewhat in the middle of the excavation. Therefore there is an effect of arching in the clay on the back of the plate. The actual active earth pressure line is line p_a, it is shown that the back pressures are

more than the active pressure. This implies that the active pressure is not fully mobilized. It may be because of high degree of the stiffness of bracing. Most of the deformation is elastic. Therefore it does not reach limit equilibrium.

The total earth pressures at the final step are compared with the results of the centrifuge test in Fig. 7.12. The distribution of the earth pressures on the back of the plate have two maximum values. This is because of the high stiffness of the bracing system in terms of the support before excavation. The lower maximum value will disappear when the struts are applied after the corresponding layers have been excavated. This is shown in Section 8.2.5.

The distribution of the earth pressures on the upper part shows that the measured maximum earth pressures on the back of the plate are between the results of K_0=0.5 and 1 in the finite element analysis. This implies that the results of the finite element analysis and the centrifuge tests can match each other with respect to the distribution of earth pressures. However, for the lower part above the dredge line, the earth pressure is negative. This may result from the errors in the test, such as friction between the sheet plate and the walls of the strongbox. In the same region, the results of the finite element analysis give a maximum value. This may result from the strong support of the bracing system because the sheet plate cannot move at the support position at the bottom layer of struts.

The comparison of the results of the analysis with the predictions according to Peck (1969) is shown in Fig. 7.13 and the comparison with the method of Tschebotarioff (1951) is shown in Fig. 7.14. The upper extremum value for K_0=1

at A is close to the maximum values predicted by Tschebotarioff's method for medium clay and Peck's method for the stiff clay. While Tschebotarioff's method for stiff clay and Peck's method for medium clay give larger prediction than the upper maximum but smaller than the lower extremum.

For K_0=0.5, Tschebotarioff's and Peck's predictions give larger values than the maximum value at B. For the lower part, only Peck's prediction for medium clay gives a value between K_0=0.5 and 1. Other predictions give smaller values.

The actual values of K calculated for the test at the end of consolidation were between 0.544 and 0.583 for the soil above the dredge line according to back analysis. For the soil below the dredge line, the values were even smaller. It seems that for the soil above the dredge line, the values of K were reduced. For overconsolidated soil, the value of K_0 is normally larger than 1. The internal friction angle is 30°. The coefficient of active earth pressure is 0.33. Therefore the actual value of K is between K_0 and the coefficient of active earth pressure. This implies that the soil developed some degree of active earth pressures before draining the heavy liquid.

For the centrifuge tests, the bracing system was not able to keep the clay in natural state since there was a small lateral displacement. This was caused by the fact that there was not full contact between the clay and the sheet plate. As a result the value of K is reduced from K_0 to a number less than 1.

The K values for the soil below the dredge line are smaller than 0.5 according to back analysis. This implies that the clay was mobilized closer to the state of active earth pressures. At the same time, the soil below the excavation should develop

some passive earth pressures. But the calculated values of K accounted for soil on both sides of the plate, and, therefore K is an average value. In order to achieve the K_0 state, the stiffness of the bracing system should be stronger and the density and level of the heavy liquid should have proper values.

It is shown that Tschebotarioff's method could be used to predict the maximum value of the earth pressures on the back of the sheet piles, however Peck's method for stiff clay is closer to the distribution of the earth pressures.

7.4.2 Loads in the struts

The comparisons of the variations of loads in the struts with time are shown in Fig. 7.15, 7.16 and 7.17 for the top, middle and bottom layer of struts, respectively.

Taking into account that the surface of the heavy liquid was lower than the surface of the soil before draining (excavating), the results of the finite element analysis and the results from the test are drawn in such a way that the excavation of the third layer in the analysis is finished at the same time when the heavy liquid drained to the same level.

The loads in the top layer struts are close to the measured values in the test. The loads in the bottom layer match the development of the measured values in the test in most steps. But in the final steps, the values of the analysis are higher. There are large differences between the measured and predicted values for the middle layer of struts. This may result from two aspects: first, the water tables on the back of

the plate are not the same; secondly, the stiffness of the bracing resulting from the contact between the clay and the plate is not the same.

7.4.3 Surface settlement

The comparison of the final surface settlements are shown in Fig. 7.18. It shows that the values of the middle parts match each other. The settlement curve for K_0=0.5 is almost the same as the settlement curve of K_0=1. The nodes close to the sheet plate are restricted in their motion. Therefore there is a large difference between the measured values and the calculated ones. However, the measured values for the middle two points are very close to the calculated curves. The difference is larger if the difference of the surface of the heavy liquid and the clay is taken into account. The value for the last test point is out of line with the calculated curves.

The bottom heaving at these steps are shown in Fig. 7.19. The nodes close to the plate are restricted in their motion.

7.4.4 Pore pressures

The comparison of the pore pressures in the clay are shown in Fig. 7.20, 7.21 and 7.22. The curves with words of "Reduced" are the result of subtracting the original curves by the value of 60.616 kPa. This value is the result of the difference of the water tables between the model and the analysis.

For the analysis, the curves of the pore pressures for K_0=1 and 0.5 are the same.

It is shown that the pore pressures of the test are in the middle between the curves of analyses and the "Reduced" curves, except that for A23, which is a point on the back of the plate about the middle elevation of the excavation. The "Reduced" curve is much closer to the test results.

7.4.5 Displacement field

Fig. 7.23 shows the displacement field of the analysis at the final step for K_0=0.5. Most points on the back of the plate move toward the excavation area. The points behind the plate move toward the bottom of the excavation, while the points at the bottom of the excavation move upward.

7.4.6 Summary

The results of finite element analysis match the results of the test in the upper part of the sheet plate. For the lower part, the results do not match. This may result from the high stiffness of the bracing system used in the finite element model and relatively lower stiffness in the centrifuge model (the stiffness here refers to the degree of contact between the sheet plate and the soil).

The loads in the struts match the results of the test in the top and bottom layers. But for the middle layer, there is a difference. This difference matches the difference between the finite element analysis and the test results for the earth pressures on the sheet plate. While the earth pressure in the middle part of centrifuge model is close to 0, the pressure from the analysis is at maximum.

The surface settlement in the finite element analysis matches the results of the test, except that the nodes close to the plate are restricted in their movement since no contact elements were used.

Figure 7.10 Front earth pressures

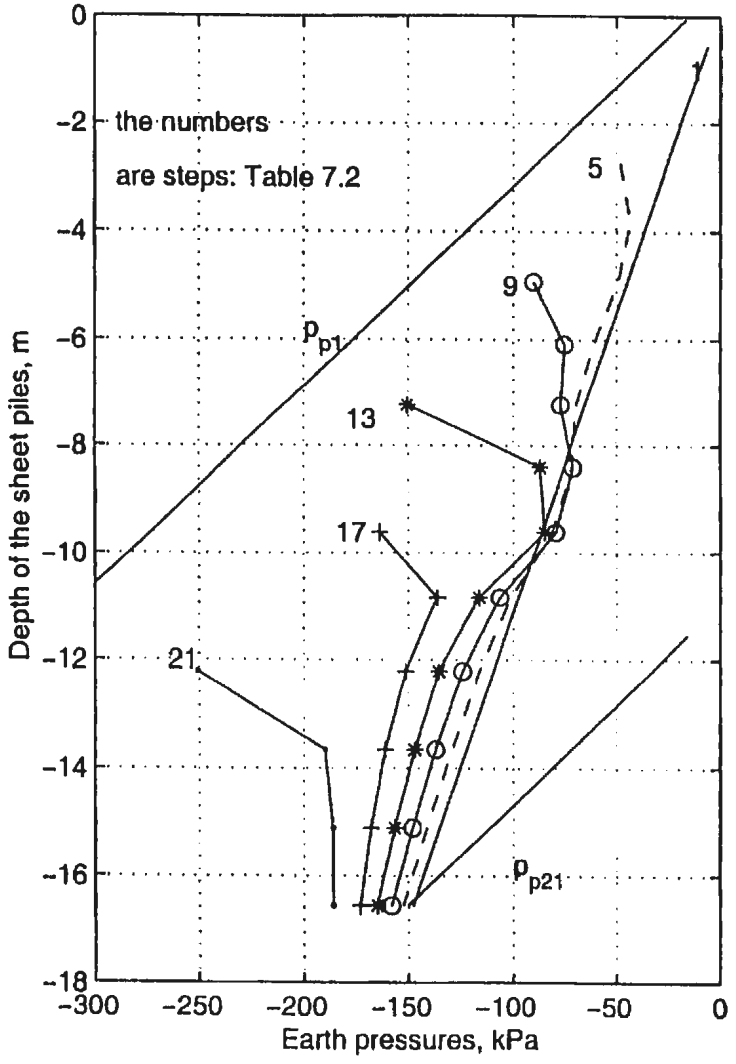

Figure 7.11 Back earth pressures

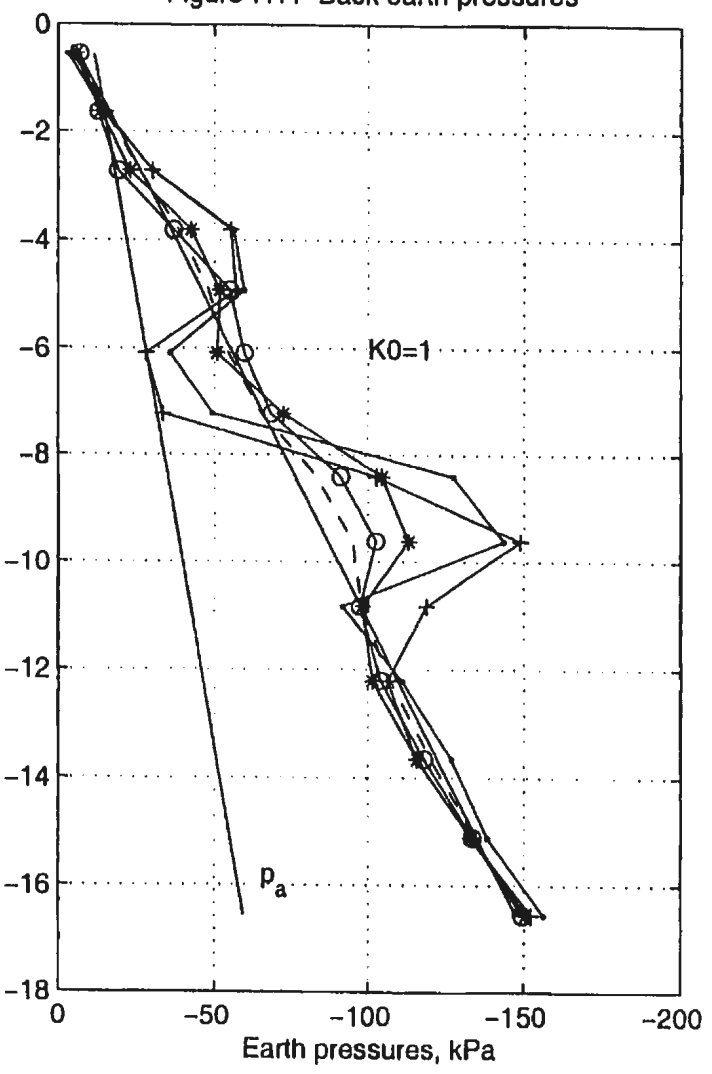

Figure 7.12 Total earth pressures on the plate in FE analysis

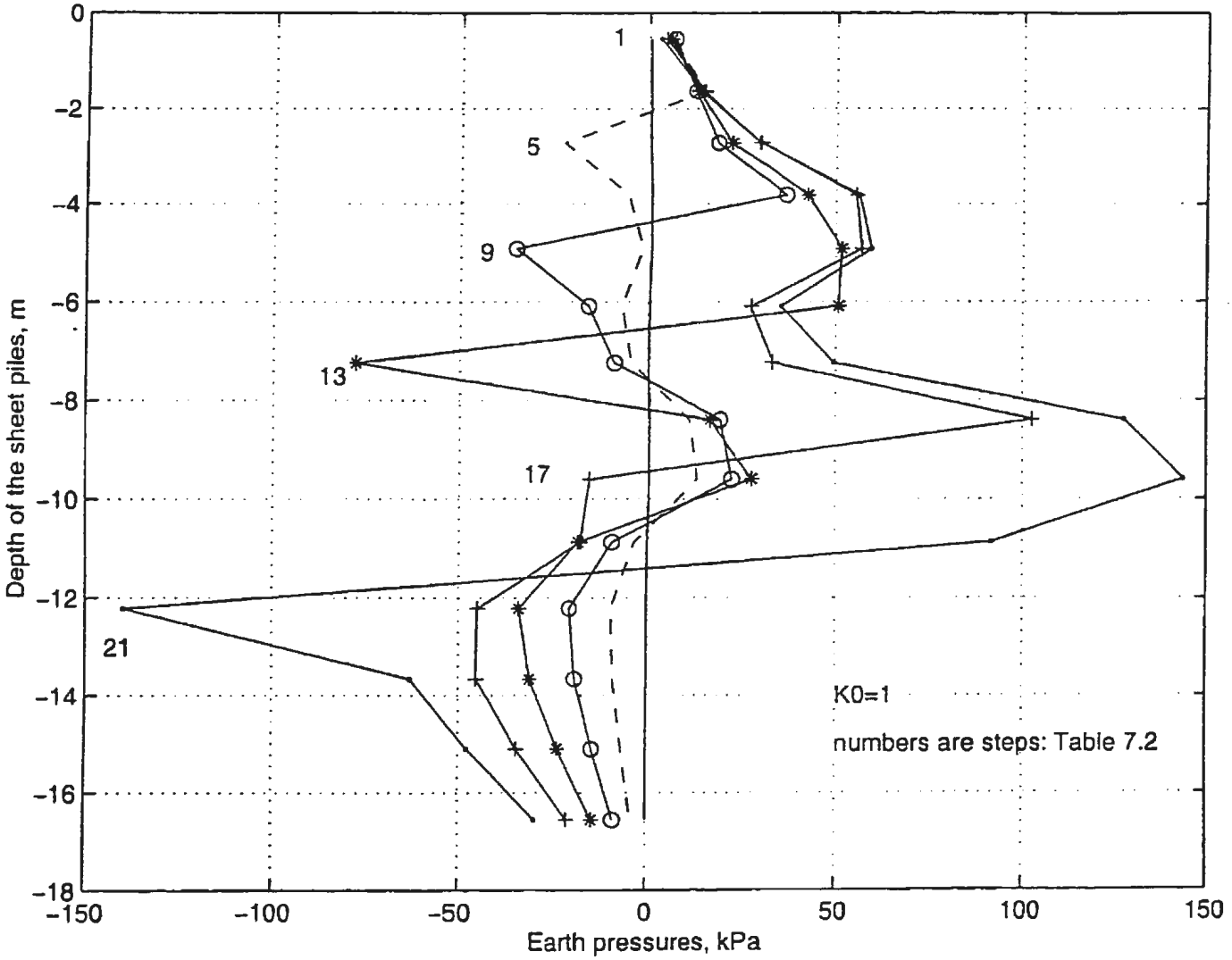

Figure 7.13 Comparison of the final earth pressures of the test and FE analysis

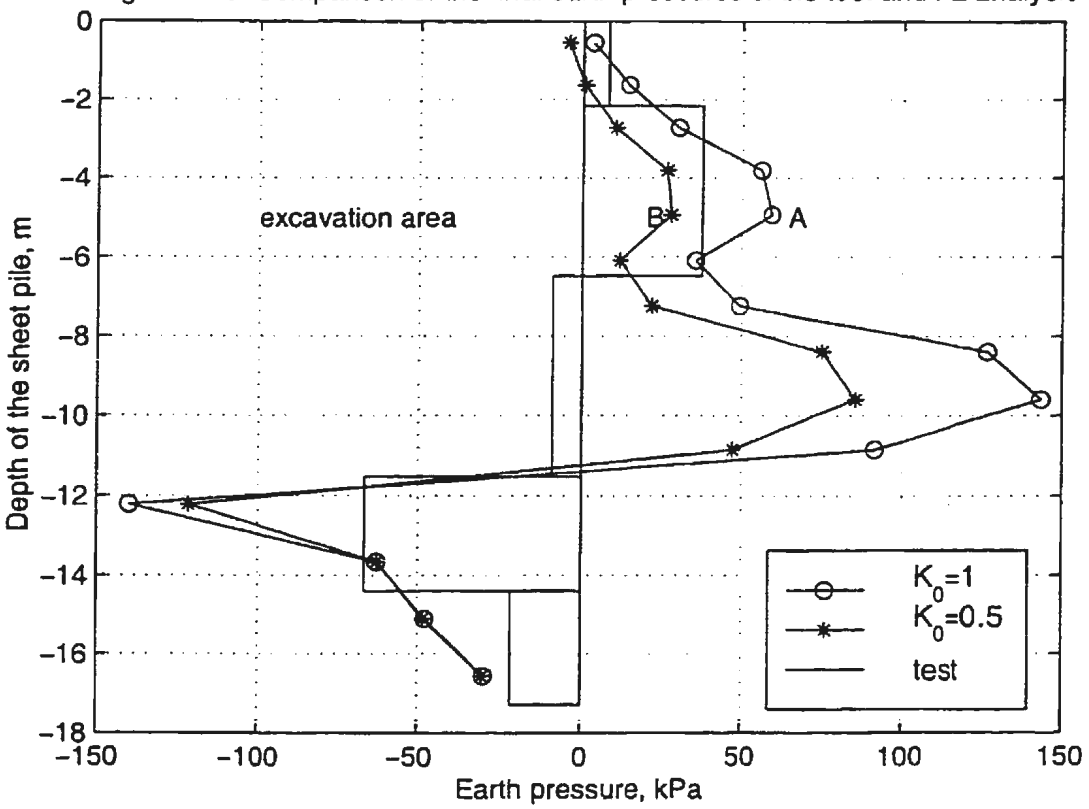

Figure 7.14 Comparison of the final earth pressures of FE analysis with Peck method

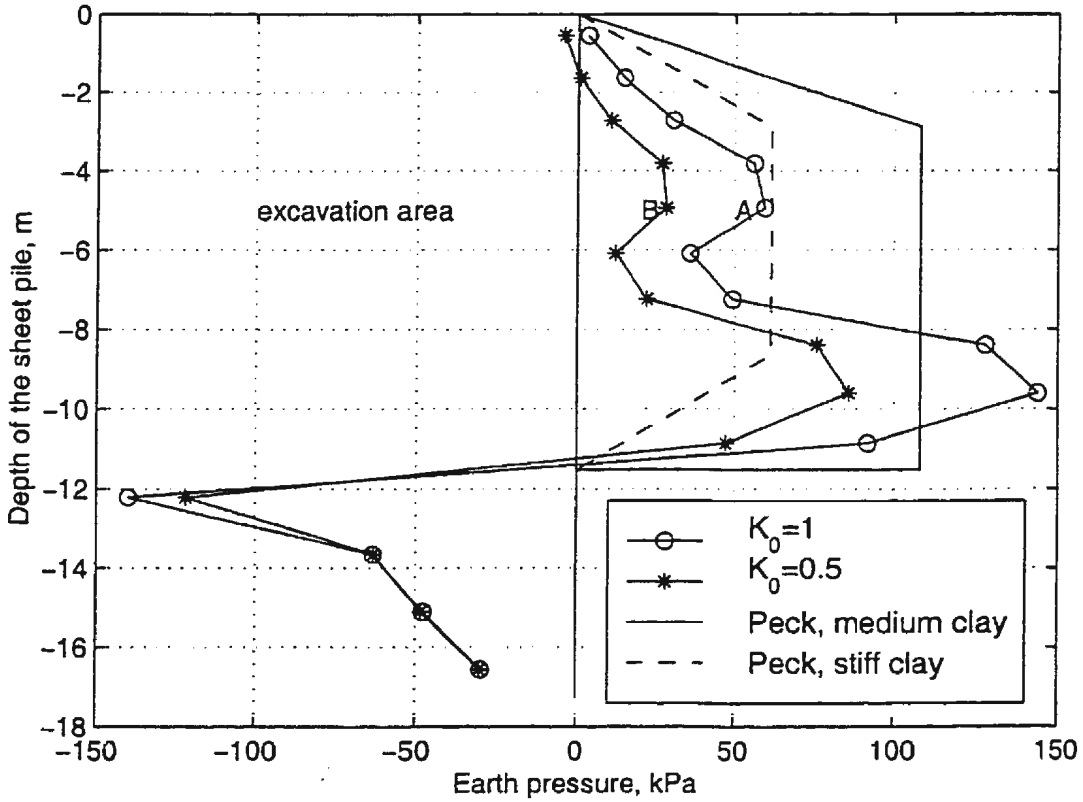

Figure 7.15 Comparison of the final earth pressures of FE analysis with T method

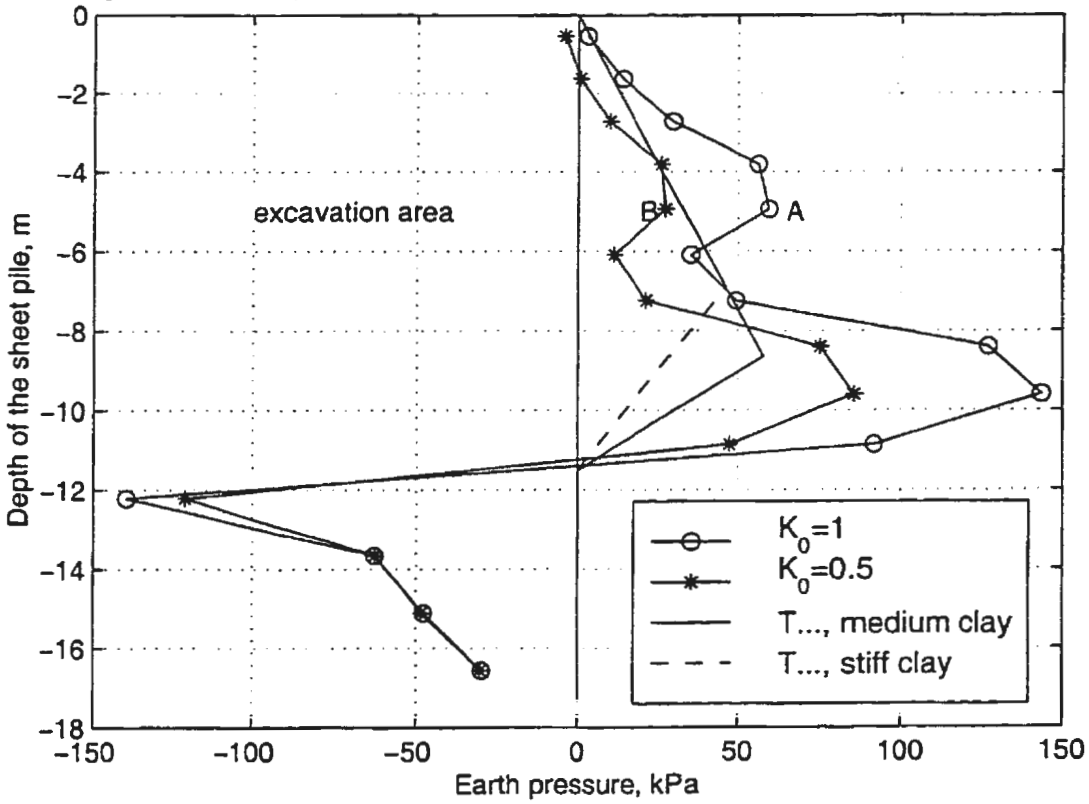

Figure 7.16 Comparison of the loads in the top layer struts

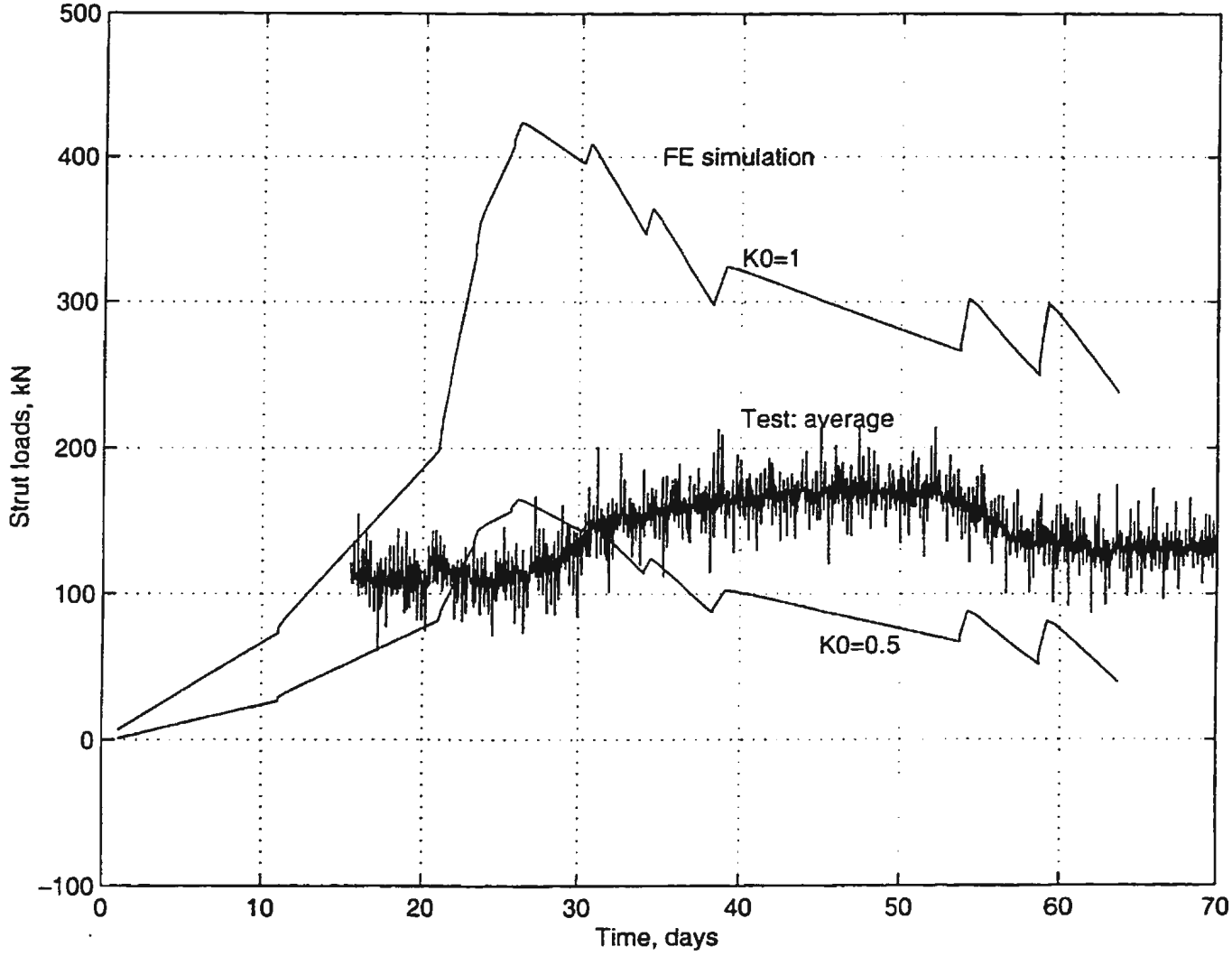

Figure 7.17 Comparison of the loads in the middle layer struts

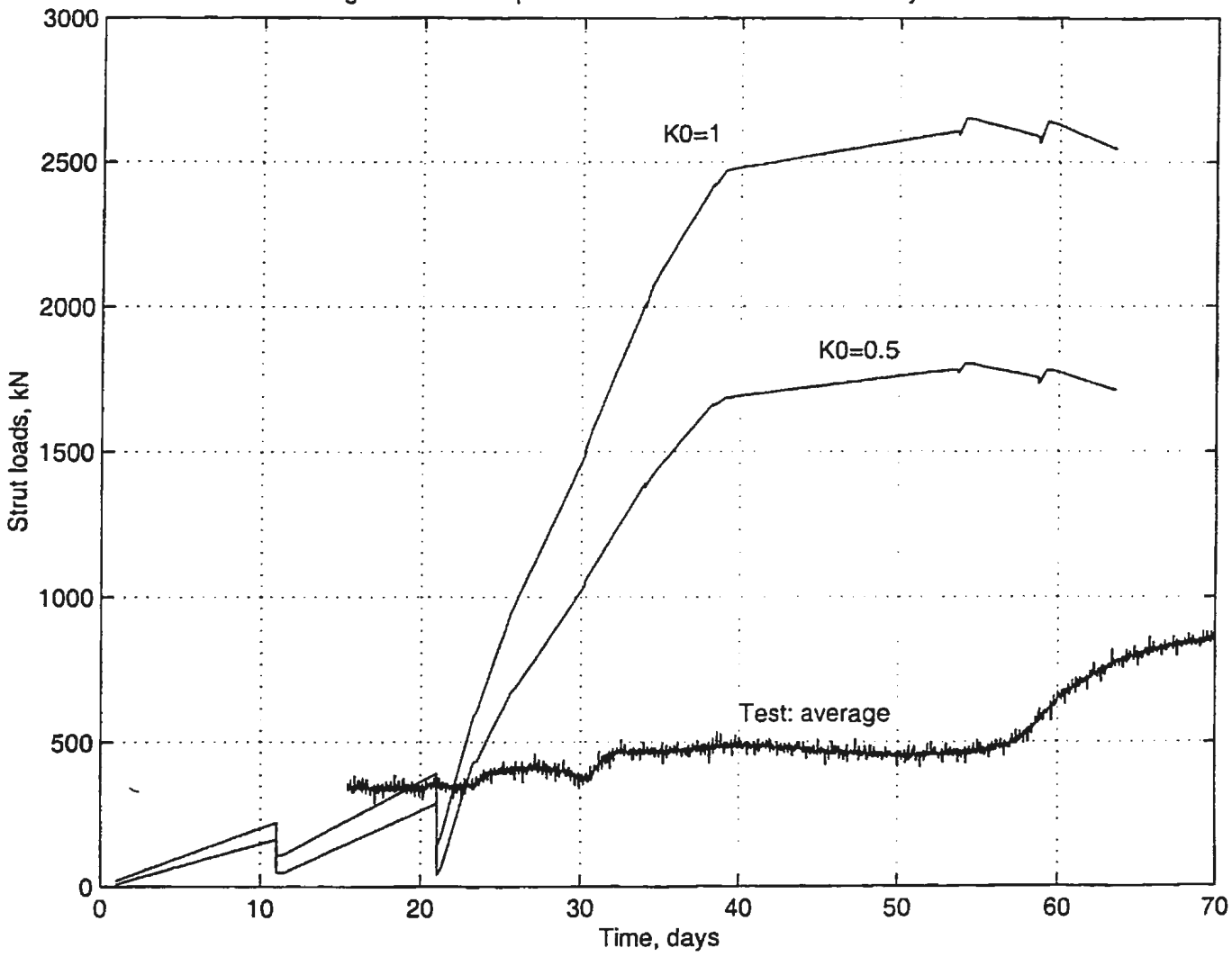

Figure 7.18 Comparison of the loads in the bottom layer struts

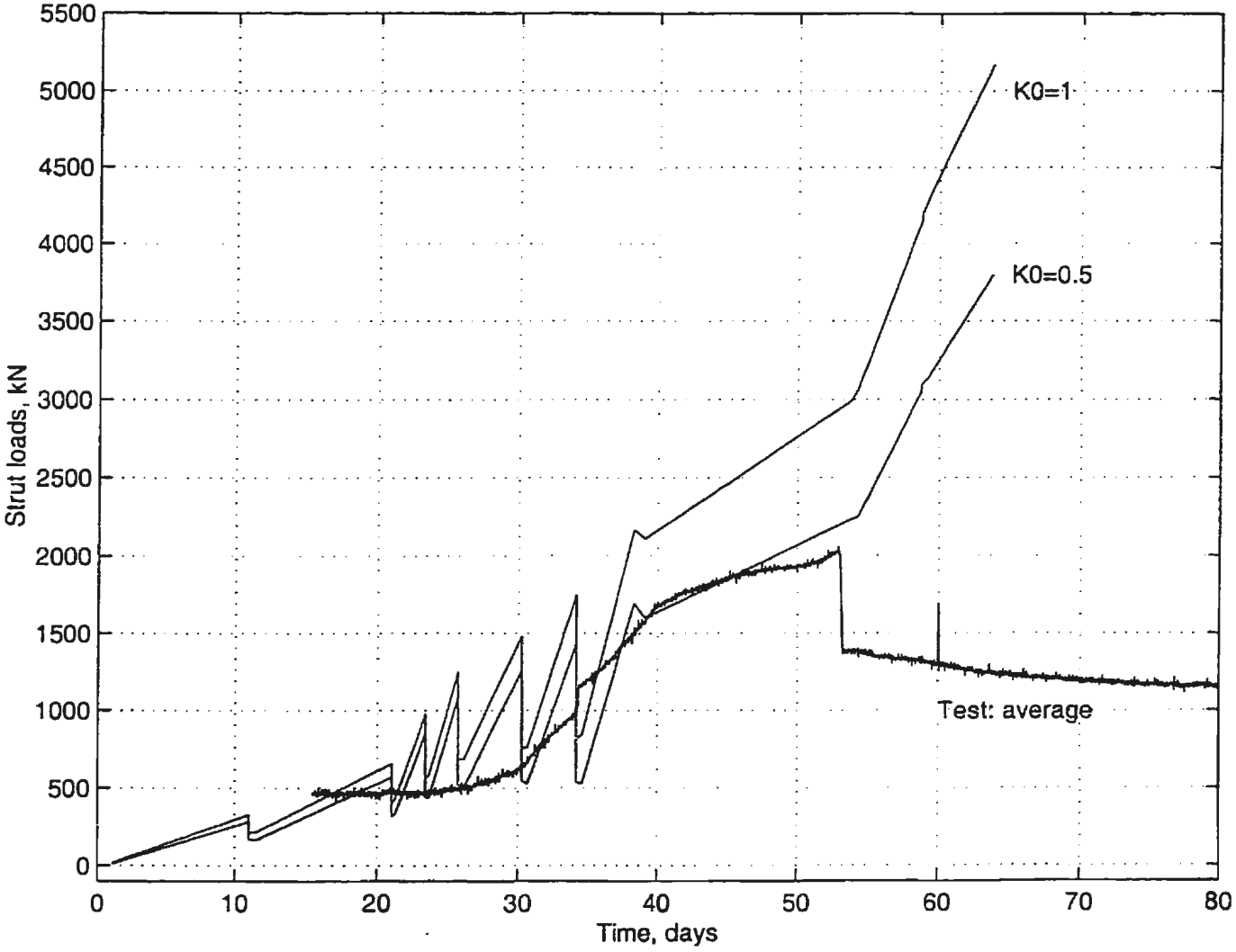

Figure 7.19 Comparison of the ground settlements

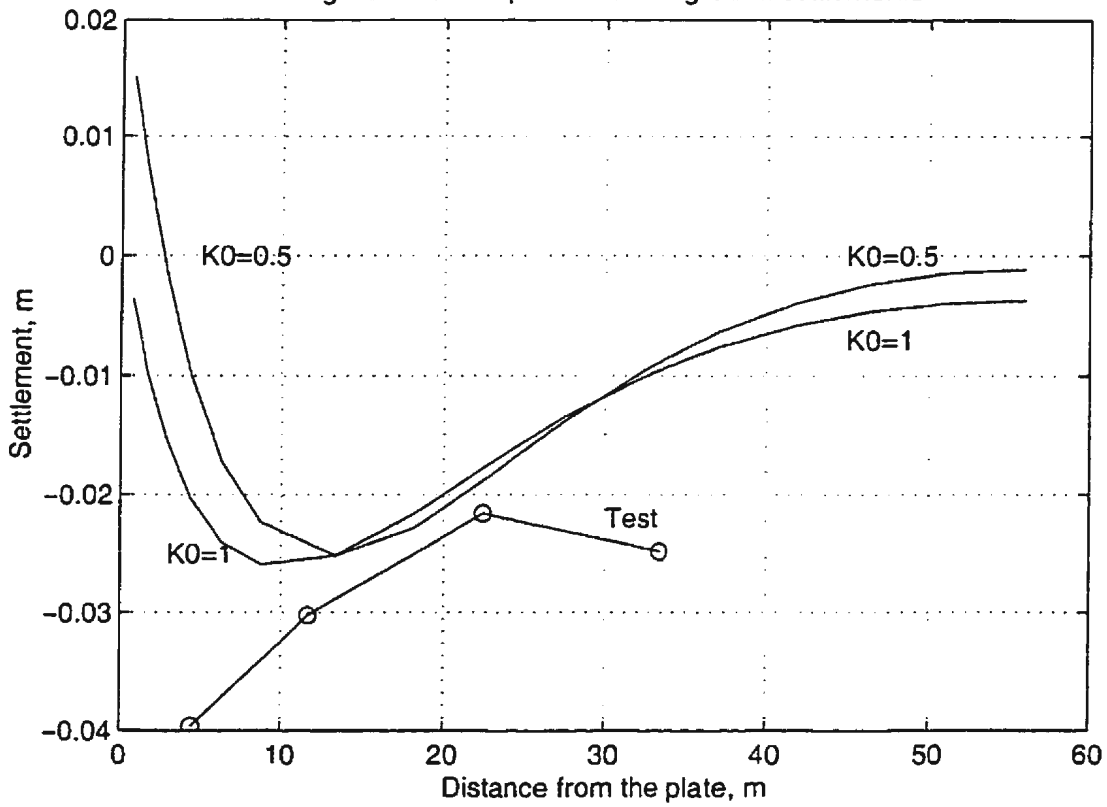

Figure 7.20 Bottom heaving of FE simulation

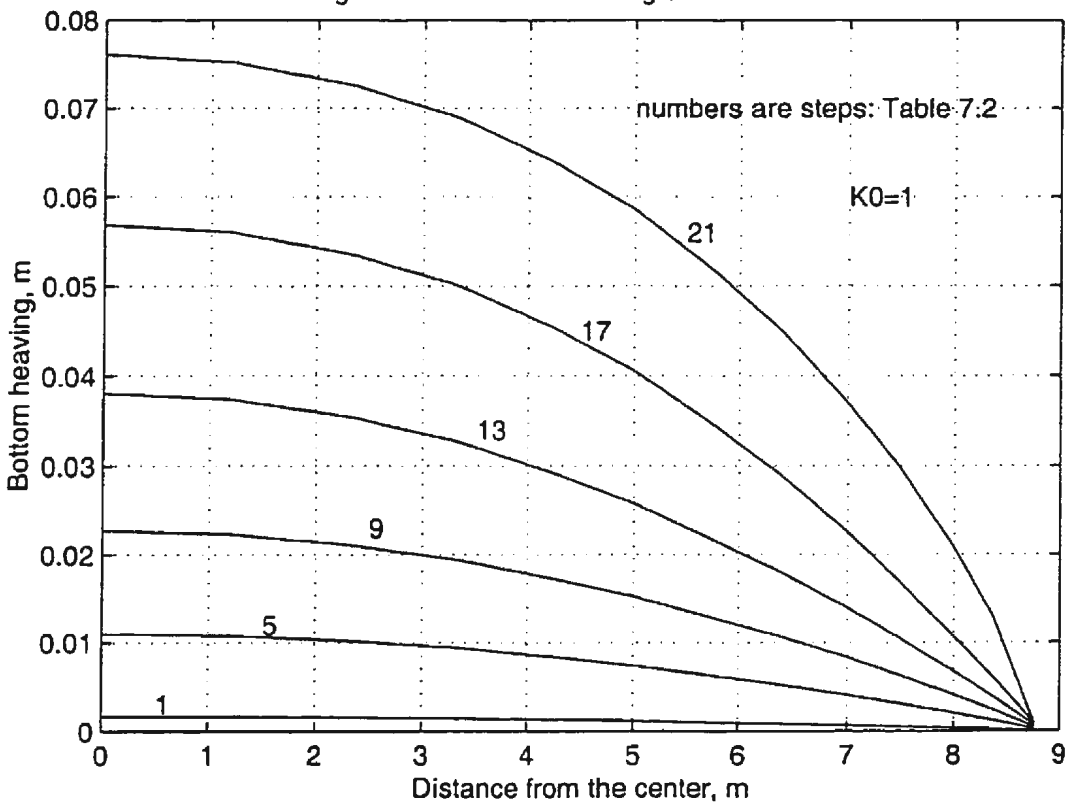

Figure 7.21 Comparison of pore pressures: A21

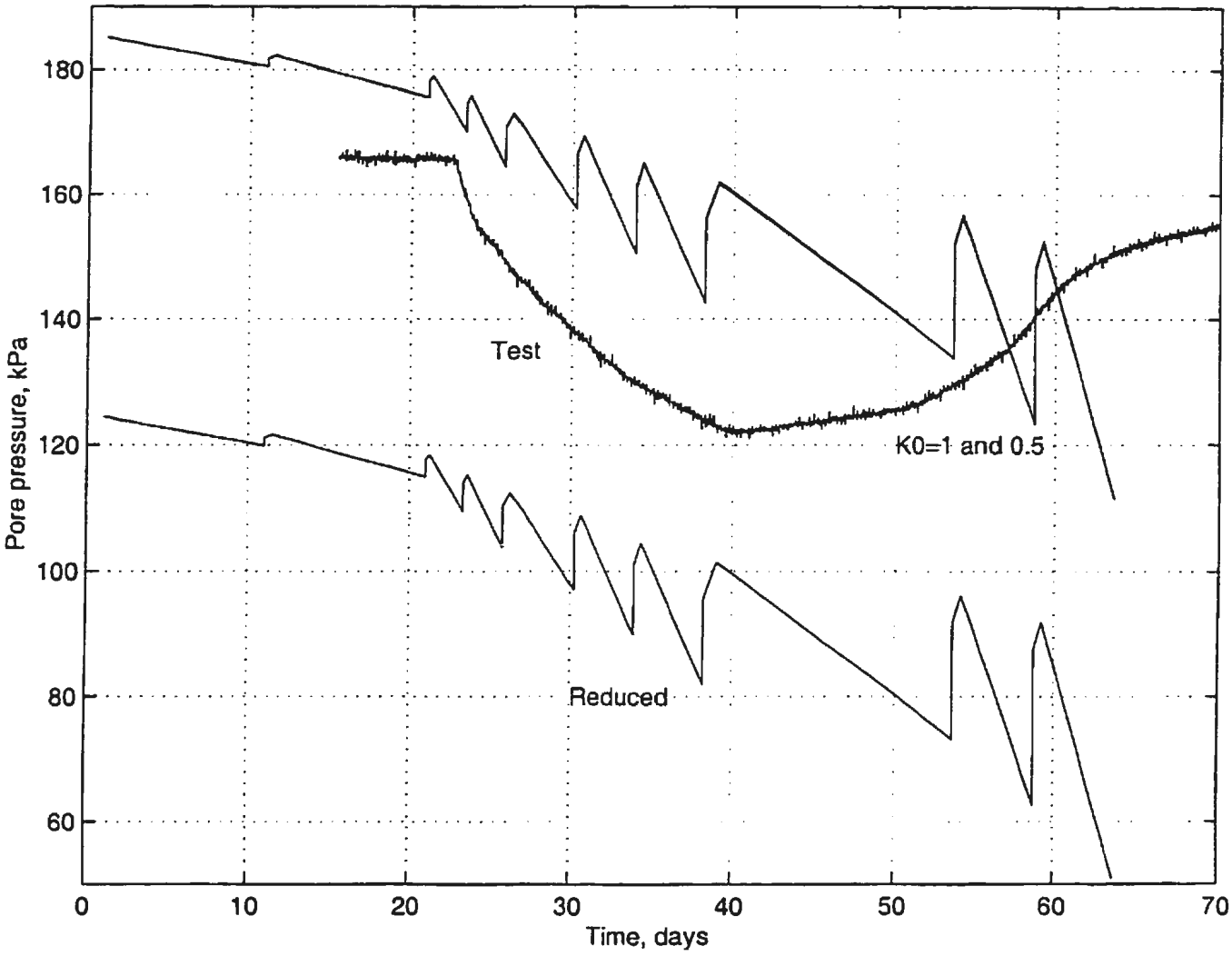

Figure 7.22 Comparison of pore pressures: A22

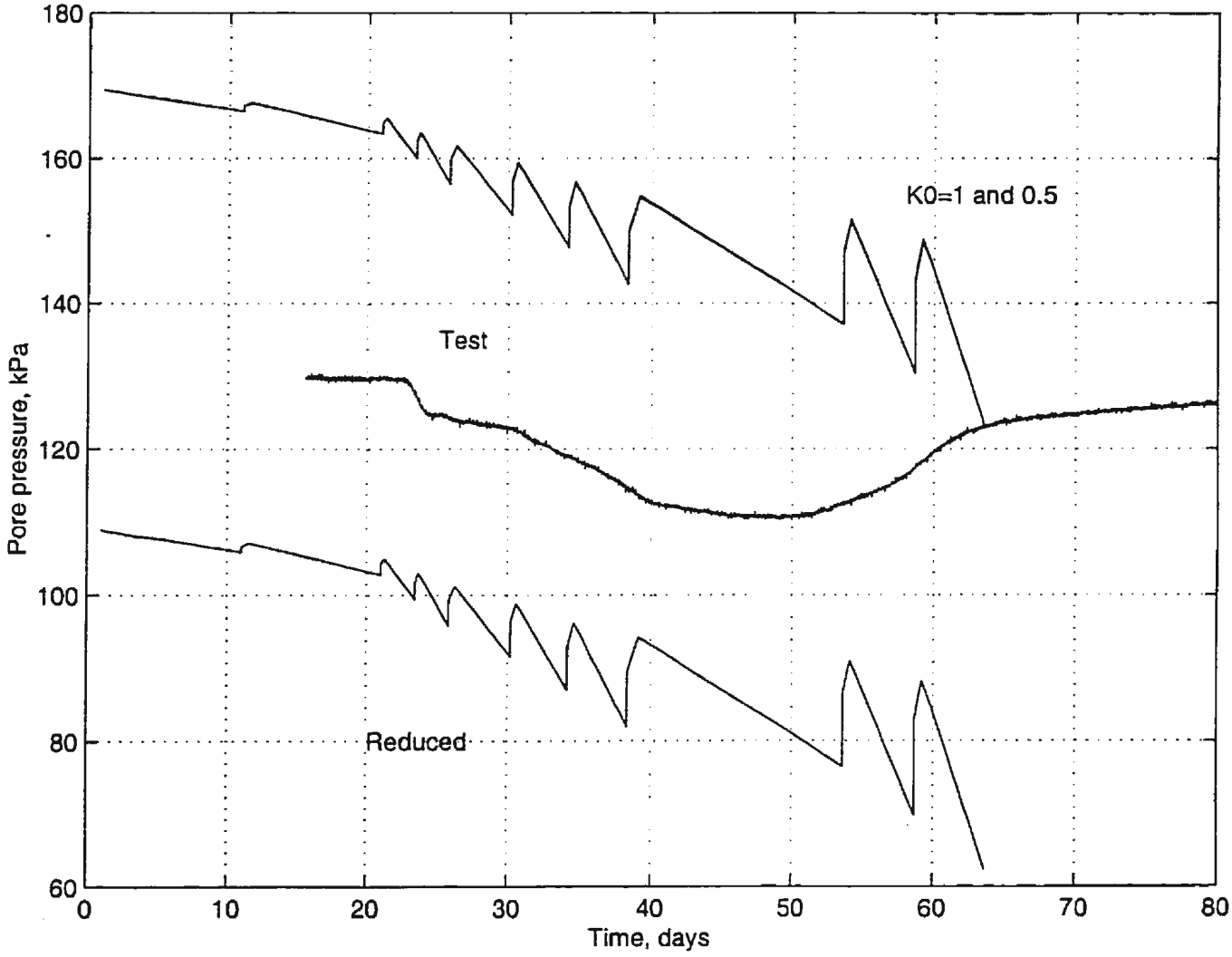

Figure 7.23 Comparison of pore pressures: A23

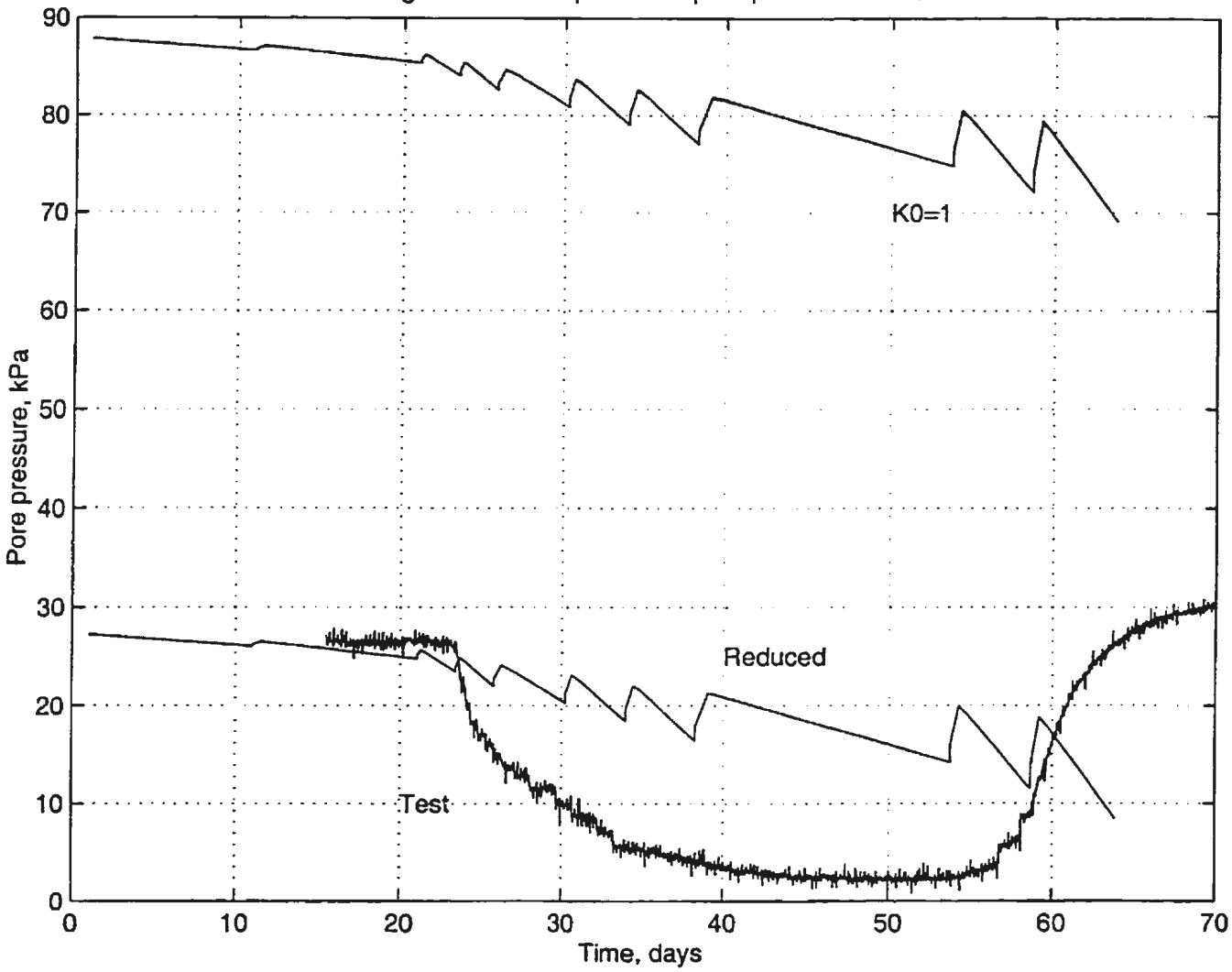

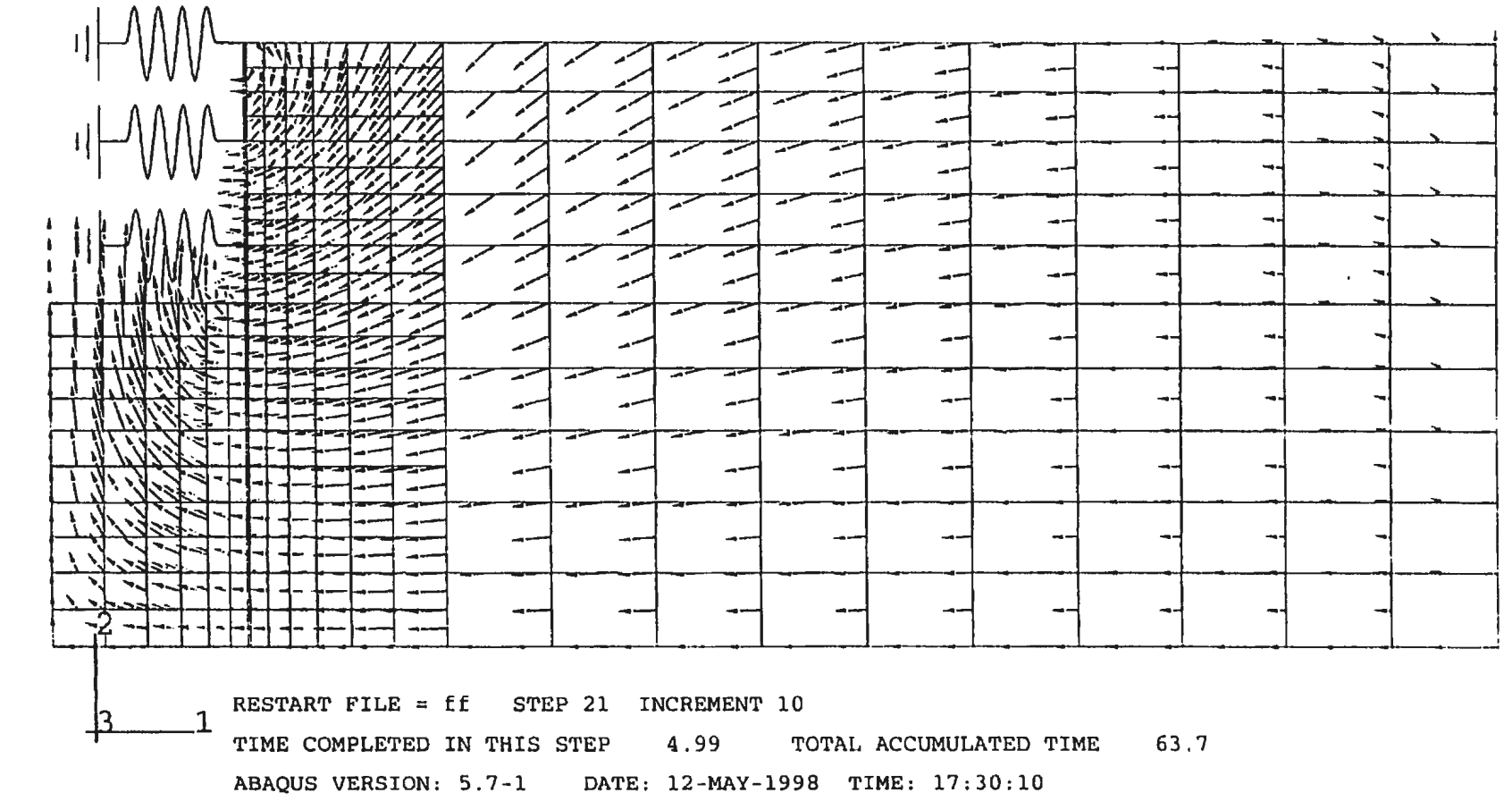

Figure 7.24: Displacement vectors at final step

Chapter 8

Parametric Studies

8.1 Introduction

8.1.1 General consideration of the parameters

This chapter presents the parametric studies for braced excavations. In each case, the procedures of practice are simulated, which means the wales and the struts are applied after the soil of the corresponding layers is excavated. Generally, the stability of a braced excavation is affected by many factors, which include:

- type of bracing system;
- stiffness of bracing system;
- degree of wall embedment;
- degree of preloading;

- method of constructing the bracing system;
- time period for the construction;
- methods of constructing the structures within the excavation;
- size of surcharge loads;
- weather;
- subsoil condition and properties;
- surrounding structures; and
- excavation shape and depth.

These factors may be divided into two parts. The first part includes those factors the designers may control and the second part includes those factors designers cannot control. In this study, the following factors will be investigated:

1. soil parameters in the Cam-clay model to evaluate their effect;
2. support system to evaluate the effect of the stiffness of the wales and struts and the vertical distances between the layers of the struts.

Table 8.1: Types of sheet piles

designation	height (m)	section modulus m^3 per lin m of wall	m. of inertia (m^4/m)	thickness (m)
PZ22	0.229	9.73×10^{-4}	1.113×10^{-4}	0.110
PLZ25	0.343	17.63×10^{-4}	3.024×10^{-4}	0.154
PZ40	0.409	32.63×10^{-4}	6.675×10^{-4}	0.200

8.1.2 Parameters considered in this study

Sheet piles

There are many types of sheet piles. In this study, the sheet piles listed in the *Foundation Engineering Handbook* will be chosen for analysis. The data are listed in Table 8.1. Column 6 shows the representative thickness of flat sheet piles which have the same moment of inertia of their corresponding designations. The depth at which the sheet pile penetrates the soil below the dredge line will be fixed as 6 m. Young's modulus is $2 \times 10^8\ kN/m^2$ and Poisson's ratio is 0.3.

Wales and Struts

Because the problem is a two-dimensional problem, the deflections of the wales will be ignored, and the function of the wales and struts will be simulated with springs distributed linearly along the length direction. The stiffness of the springs will be selected according to the stiffness of the struts. The available data of H piles in the *Foundation Engineering Handbook* is shown in Table 8.2. The stiffness is shown in Column 3. They are calculated using the following values:

Table 8.2: Types of H piles used for struts

designation	area m^2	stiffness kN/m/m	stiffness (doubled) kN/m/m
HP14 × 117	2.219×10^{-2}	6.658×10^4	1.332×10^5
HP13 × 100	1.897×10^{-2}	5.615×10^4	1.123×10^5
HP12 × 84	1.587×10^{-2}	4.697×10^4	9.394×10^4

Young's modulus of steel: E=2×10^8 kN/m^2;

Length of the struts: L=18.768 m;

Horizontal distance between the struts: D=3.6 m (about 12 ft).

Soil

The unit weight of the saturated soil is 19 kN/m^3. The soil is considered as normally consolidated. The coefficient of lateral earth pressure is calculated according to $K_0 = 1 - \sin\phi$. The coefficient of permeability is 2.56×10^{-4} m/day. The properties of the soil are simulated with the Modified Cam-clay model. The parameters adopted by Harahap for Chicago glacial clay are taken as a reference. These parameters are shown in Table 8.3. These parameters were obtained from a number of experiments with undisturbed clay from construction sites.

Table 8.3: Parameters of Cam-clay model, Harahap, 1990

Soil Parameter	Blodgett Till Field	Deer Ridge	Park Tinley Till	
κ	0.025	0.014	0.003	0.005
λ	0.180	0.065	0.0650	0.012
e_{cs}	2.050	1.500	1.120	0.30
M	0.941	1.030	1.030	1.500
G/S_u	300.0	300.0	600.0	600.0

Other considerations

The width of the excavation will be fixed at 24 m. The depth of excavation is 12 m. The vertical distance between the struts will be chosen as 2.0, 3.0, 4.0 m.

Section 2 gives the detail of the results of the finite element simulation for a basic case. The following sections deal with the variation of different parameters. These results are compared with the results found for the basic case.

8.1.3 Summary

In summary, the parameters for the basic case are listed in Table 8.5. In the following sections, the parametric studies are conducted according to the parameters listed in Table 8.6.

Table 8.4: Cam-clay parameters for the basic case

Parameters	M	λ	κ
Magnitude	0.941	0.18	0.025

Table 8.5: Bracing parameters for the basic case

Parameters	Sheet pile stiffness	Strut stiffness	Strut distance
Units	m^4/m	kN/m	m
Magnitude	6.675×10^{-4}	9.394E4	2.0

Table 8.6: Parametric study

Parameters	units	Magnitude 1	Magnitude 2	Magnitude 3
M	/	0.689	0.772	0.941
ϕ	degrees	18	20	24
K_0	/	0.691	0.658	0.593
λ	/	0.06	0.12	0.18
κ	/	0.01	0.02	0.03
sheet pile thickness	m	0.11	0.154	0.20
strut stiffness	kN/m/m	4.696E4	6.568E4	9.394E4
strut distance	m	4.0	3.0	2.0

8.2 Simulation of the Construction Technique in Practice

8.2.1 Introduction

The object of this section is to simulate the actual construction technique in practise where the wales and the struts are applied after the soil of the corresponding layers is removed. The case is regarded as the basic case, which is provided for the purpose of comparison. In the following sections, the variation of different parameters referring to the basic case is studied to investigate their effects on the pressures on the back of the sheet piles, the displacement of the sheet piles, the bottom heaving and the surface settlement of the ground.

The depth of the excavation is 12 m. The width is 24 m. Sheet piles of PZ40 are used and the moment of inertia per meter length is $6.675 \times 10^4\ m^4/m$. There are six layers of struts distributed equally along the depth. The vertical distance between adjacent layers is 2 m. The horizontal distance between two neighbouring struts is 3.6 m. Each strut is composed of two HP12×84 H piles.

8.2.2 Finite element simulation

The problem is considered as a plane strain problem. Only half of the model will be simulated on account of symmetry. The finite element mesh is shown in Fig. 8.1 step 1. The mesh consists of 1413 nodes and 438 elements. These elements includes 412 CP8RP elements which are used to simulate the saturated clay, 18

CP8R elements simulating the sheet piles and 6 SPRING1 elements simulating the struts.

The complicated shape of the sheet piles is simulated with flat block elements with a thickness of 0.200 m depending on the equivalent moment of inertia per meter length. Each layer of struts is simulated with a spring of stiffness of 9.394×10^4 kN/m/m. Both the sheet piles and the struts are made of steel where the Young's modulus is $2 \times 10^8\ kN/m^2$. Poisson's ratio is taken as 0.3.

The soil is normally consolidated clay. The clay is fully saturated. The unit weight is γ_{sat}=19 kN/m^3. The seepage coefficient is $k = 2.56 \times 10^{-4}$ m/Day. The coefficient of lateral static earth pressure is adopted according to $K_0 = 1 - \sin\phi$, where ϕ is the internal friction angle.

The soil is simulated with a Cam-clay model using the parameters from Harahap (1990) as shown in Table 8.3:

$\kappa = 0.03$,

$\lambda = 0.180$,

M=0.941 or $\phi = 24°$,

$G = 75\gamma z$.

The loading (excavating) sequences are shown in Table 8.7. At each step, the activities simulated and the increments used are also presented. The excavation

procedure is carried out by a sequence of load increments. The soil between two layers of struts is divided into two layers. Each layer is removed in 11 increments, where the first increment is used to remove the layer and fix the boundaries, the rest of the increments are used to remove the loads applied by the soil of that layer. The elapsed time for each step is calculated according to the time required to remove the area of the section required in a practical excavation. The elapsed time is equally distributed among the loading increments at each step. The standard is that an area of 4.8 m^2 of soil is removed in one day on the site. 12 increments are used to apply the struts, where 10 increments are used to actually apply a layer of struts and 2 increments are used for consolidation. In total 5 days are required to remove the soil between two layers of struts and one day is used to apply a layer of wales and struts.

Table 8.7: Loading sequence for the finite element simulation

stage	construction days	elapsed days	maximum increments	actual used increments	excavated depth (M)	total depth (M)	remarks
1	1-5	5	11	7	1.0	1.0	Excavating soil layer 1
2	6	0.75	10	10	/	1.0	applying strut layer 1
3	6	0.25	2	2	/	1.0	consolidation
4	7-11	5	11	7	1.0	2.0	Excavating soil layer 2
5	12-16	5	11	7	1.0	3.0	Excavating soil layer 3
6	17	0.75	10	10	/	3.0	applying strut layer 2
7	17	0.25	2	2	/	3.0	consolidation
8	18-22	5	11	7	1.0	4.0	Excavating soil layer 4
9	23-27	5	11	7	1.0	5.0	Excavating soil layer 5
10	28	0.75	10	10	/	5.0	applying strut layer 3
11	28	0.25	2	2	/	5.0	consolidation
12	29-33	5	11	7	1.0	6.0	Excavating soil layer 6
13	34-38	5	11	7	1.0	7.0	Excavating soil layer 7
14	39	0.75	10	10	/	7.0	applying strut layer 4
15	39	0.25	2	2	/	7.0	consolidation
16	40-44	5	11	7	1.0	8.0	Excavating soil layer 8
17	45-49	5	11	7	1.0	9.0	Excavating soil layer 9
18	50	0.75	10	10	/	9.0	applying strut layer 5
19	50	0.25	2	2	/	9.0	consolidation
20	51-55	5	11	7	1.0	10.0	Excavating soil layer 10
21	56-60	5	11	8	1.0	11.0	Excavating soil layer 11
22	61	0.75	10	10	/	11.0	applying strut layer 6
23	61	0.25	2	2	/	11.0	consolidation
24	62-66	5	11	10	1.0	12.0	Excavating soil layer 12

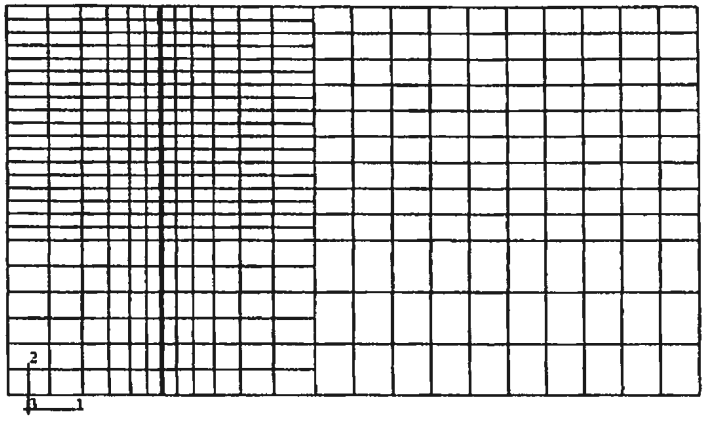

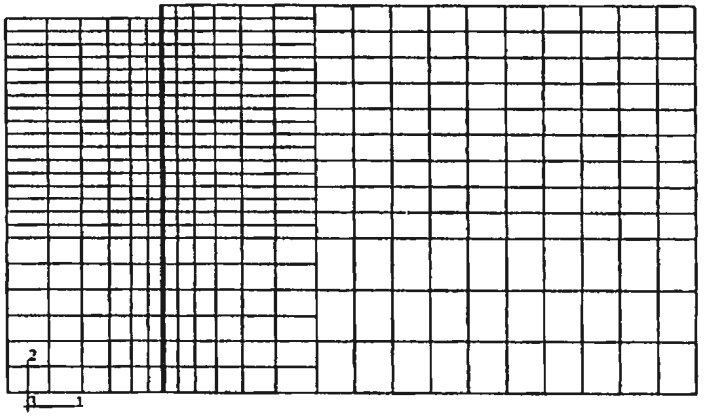

Figure 8.1(a): Steps in finite element analysis

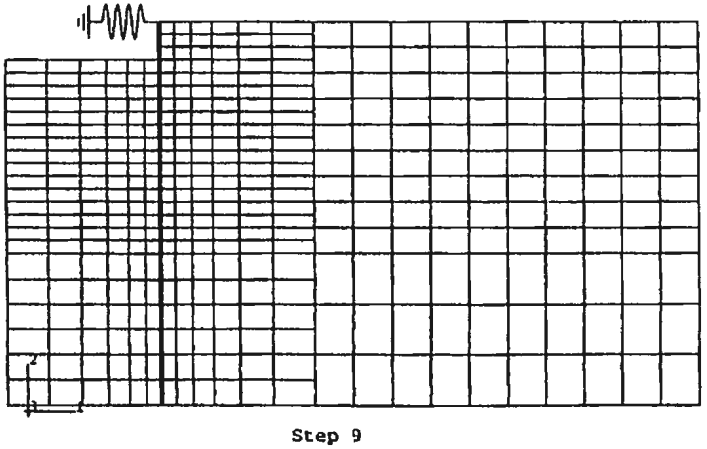

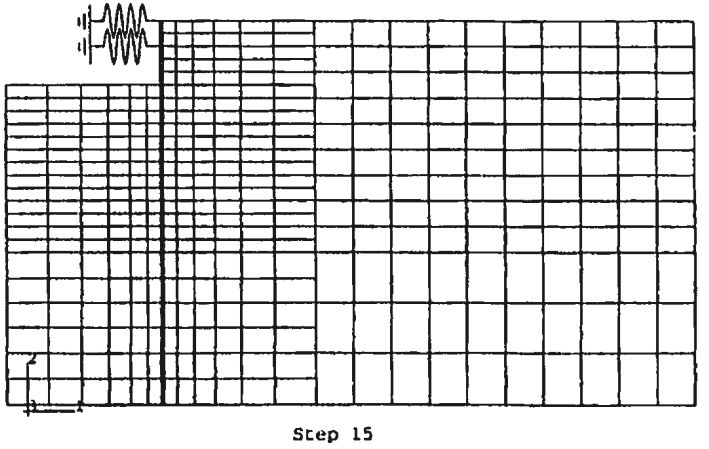

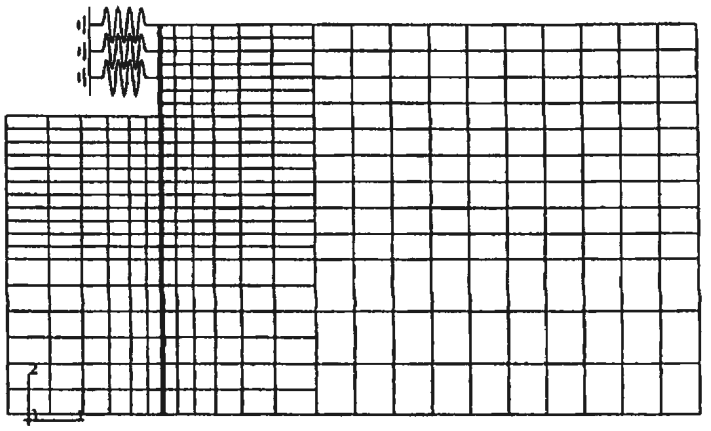

Step 21

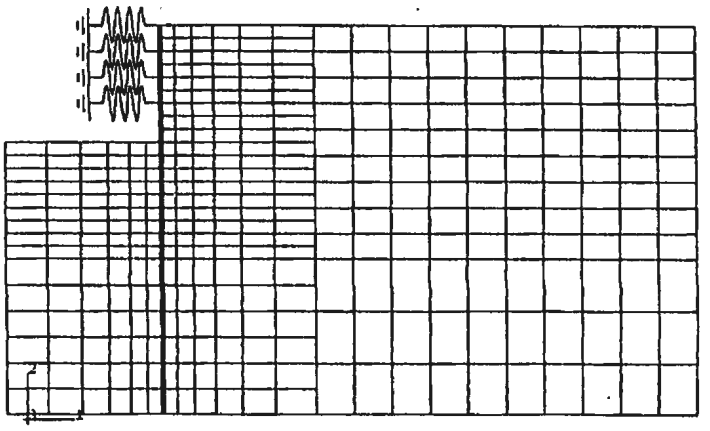

Step 27

Figure 8.1(b): Steps in finite element analysis

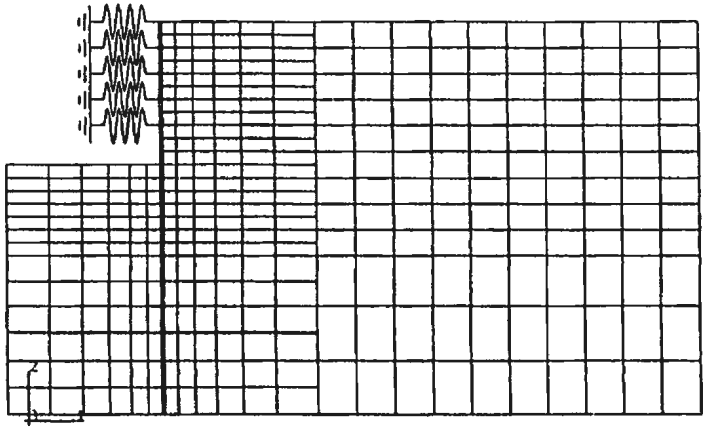

Step 33

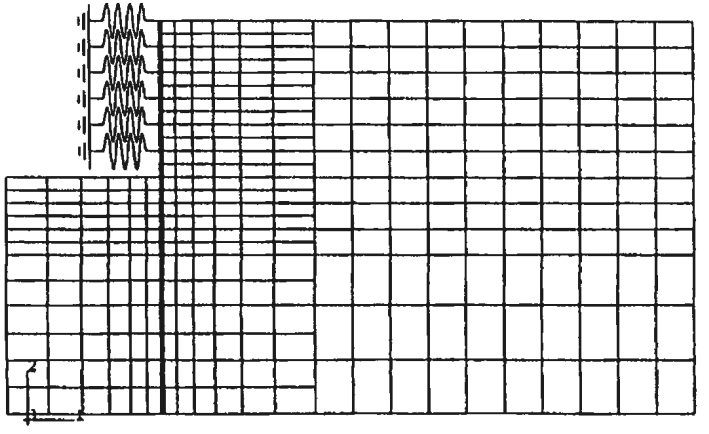

Step 37

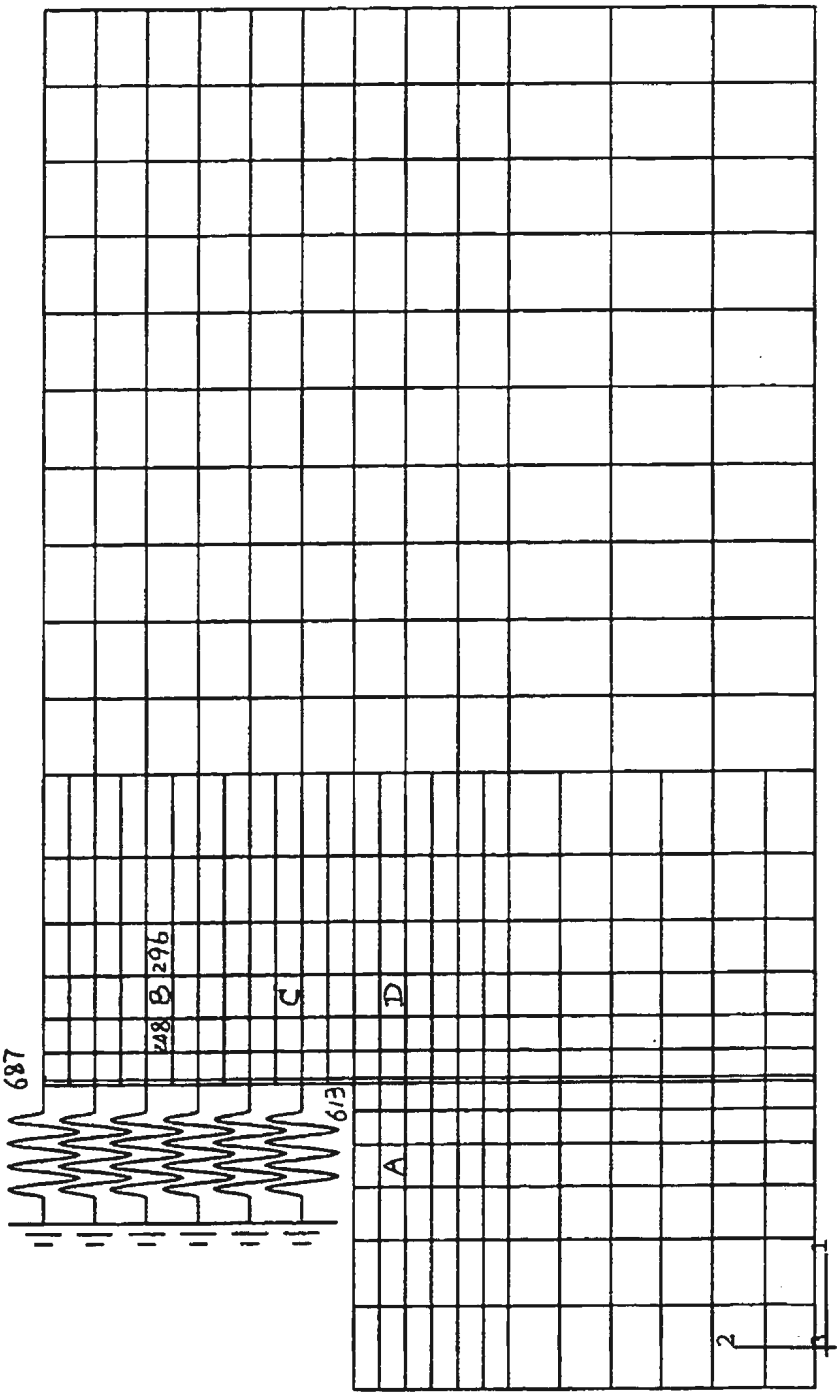

Figure 8.2: Positions of the selected elements and points

8.2.3 Plots of the results at the final excavation step

Displacement

The deformed mesh is shown in Fig. 8.3. The elements close to the sheet piles are subject to large horizontal and vertical displacements. For those elements far from the excavation, the predominant displacement is settlement, and for the elements under the excavation, the major displacement is bottom heaving.

The vector plot of the displacement is shown in Fig. 8.4. The arrows show the direction of the displacements and the length of the arrows indicates the magnitude of the displacement. This figure conveniently gives the displacement trend of the nodes.

A contour plot for horizontal displacement after excavation is shown in Fig. 8.8 and the vertical displacement is shown in Fig. 8.9. It can be seen that the displacement is highly inhomogeneous. The maximum horizontal displacement is toward the excavation area at the support position of the last layer of struts. One may expect a large earth pressure on the sheet piles. However, this is not true. From Fig. 8.40, one may see that the earth pressure at this position is very small. This may result from arching which is explained later in this section.

The maximum vertical displacement is the settlement behind the sheet piles.

Strains

The contour plot of horizontal strains, vertical strains and shear strains are shown in Fig. 8.10, 11 and 12. Except for elements close to the sheet piles, there is not very much variation in the horizontal strains and shear strains. For vertical strains, the value decreases gradually from the surface to the bottom, with the surface subjected to a large settlement. For the elements close to the sheet piles, the strains in the soil vary gradually, except at two points. The first point is at the surface close to the sheet piles. Here the contours vary greatly. In the process of excavation, with the element subjected to a large vertical downward strain, the element also deforms toward the excavated area at first and later toward the unexcavated area. The studies of other researchers reveal that the element at this point settles greatly. In fact, contact elements should be used for the contact between of the soil and the sheet piles. Because of the limitations of the finite element program, the contact element seems to diverge at this point. This rules out the applicability of the contact element in this study. The reason for the divergence may come from the possible large sliding and large separation between the sheet piles and the soil.

The second point of large variation of strains is at the bottom of the excavation on the corner between the soil and the sheet piles. At this position, the soil tends to heave greatly. Without contact elements this heaving is retarded, and the strain varies rapidly. However the restriction on the deformation is limited to the local elements. The deformation of other elements is not affected very much because of soil deformation properties.

The vector plots of the principal strains, the principal elastic strains and principal plastic strains are shown in Fig. 8.5, 8.6 and 8.7. It is seen that the principal strains and the principal plastic strains are distributed around the sheet piles, and the principal elastic strains are distributed all over the elements with a higher density around the sheet piles. If we notice the actual value of the strains, we may find that the elastic strains only contribute a little portion to the total strains in the elements around the sheet piles. Take node 613 and node 687 for examples; node 613 is located at the right corner of the bottom of the excavation as shown in Fig. 8.2. The minimum total principal and plastic strains at this point are, -7.6940E-02 and -7.1963E-02, respectively. Thus the principal plastic strain is the 93.5% of the principal strain and consequently the elastic strain contributes very little.

Node 687 is located at the right corner of the top of the sheet pile, with the maximum total principal and plastic strains. The total principal strain is 5.6963E02 and principal plastic strain is 5.7861E02. In this case, the principal plastic strain is the 102% of the total strain. This implies that the direction of the elastic deformation is opposite to the direction of the principal strain and the elastic deformation contributes very little to the total principal strain.

The plastic strain occurs around the sheet piles because of the large deformation and stresses. The area not close to the sheet piles is in a state of elastic deformation. This is helpful in the limit analysis for assuming the area of limit equilibrium. However it should be noticed that for some elements on the back of the sheet piles and close to the surface, there is no or very little plastic deformation, while in the figure of displacements, these elements are subject to very large vertical

settlement. The explanation may be that the elements settle evenly in the state of elastic deformation. Therefore when assuming the area of limit equilibrium, it should be noticed that this area is in a state of elastic deformation.

Stresses

The contour plots of normal and shear stresses are presented in Fig. 8.13, 14 and 15. It should be observed that, for the purpose of drawing the contours of stresses in the soil elements, the maximum and minimum stresses inside the sheet pile elements are not presented. From these figures, it can be seen that the distribution of the stress does not possess large gradients. The distribution of pore pressures are shown in Fig. 8.16. The analysis of the state of stress at some typical elements is presented in the following part.

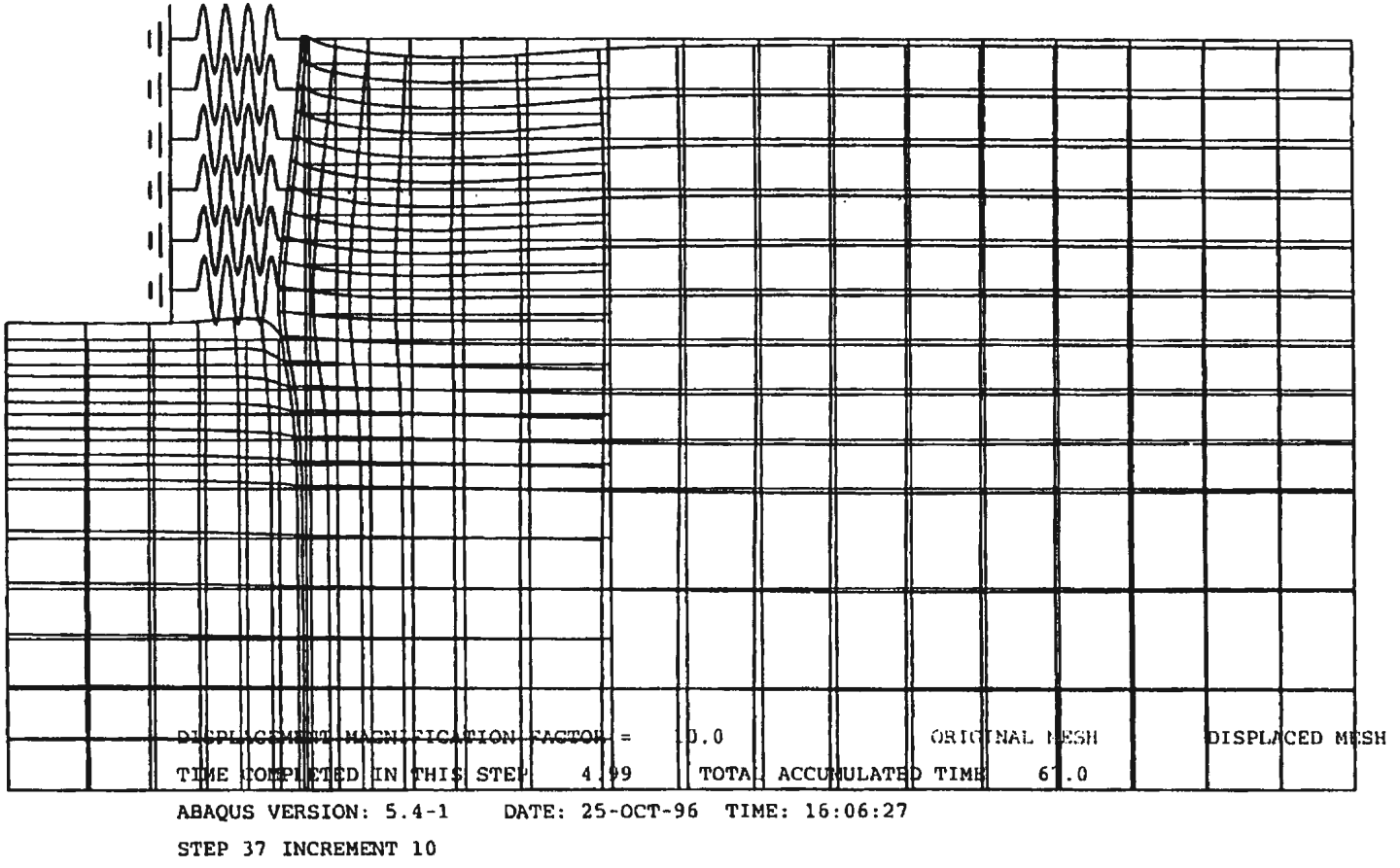

Figure 8.3: Deformed mesh of the excavation

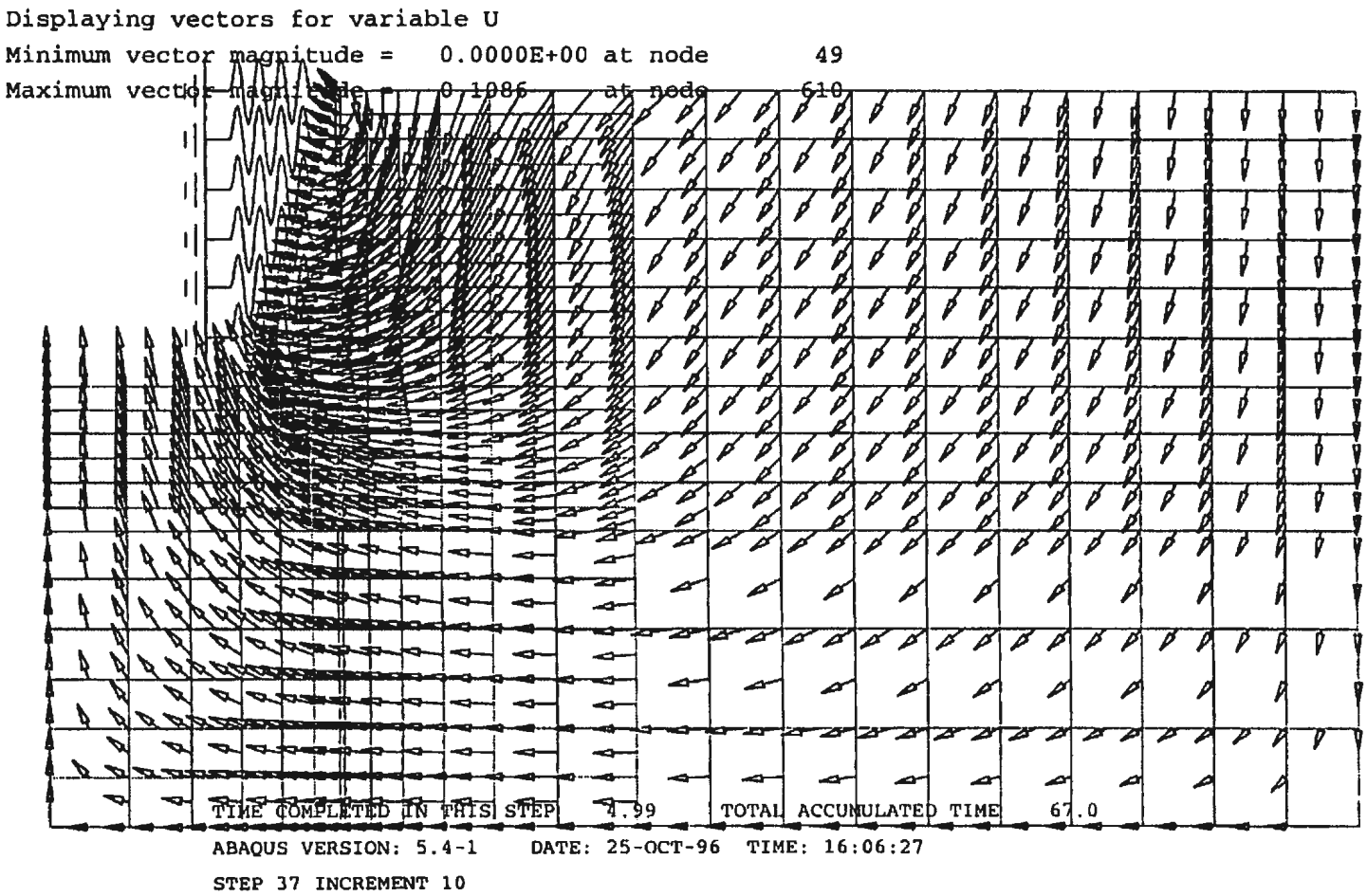

Figure 8.4: Vector plot of the displacement

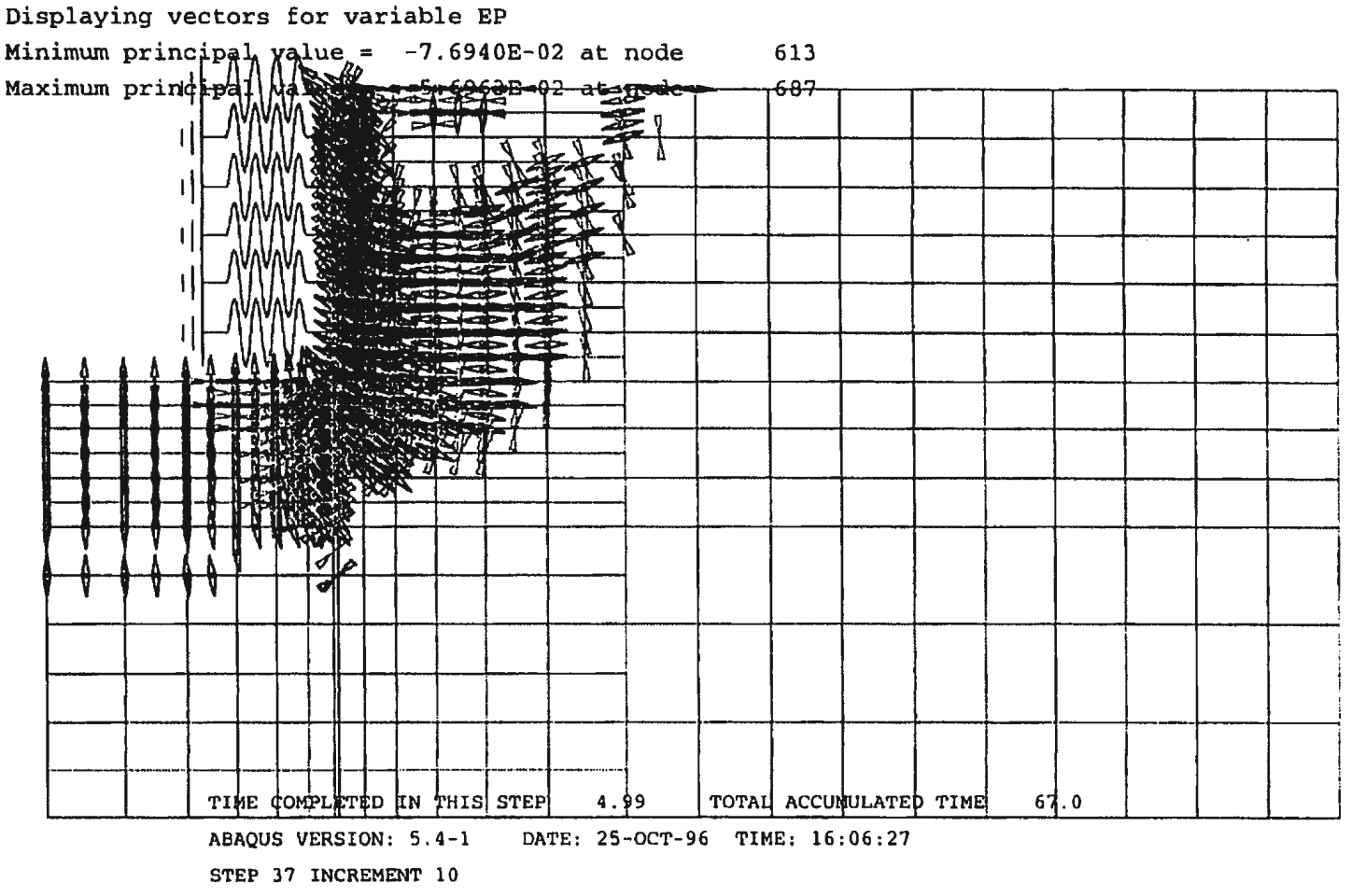

Figure 8.5: Vector plot of all principal strains

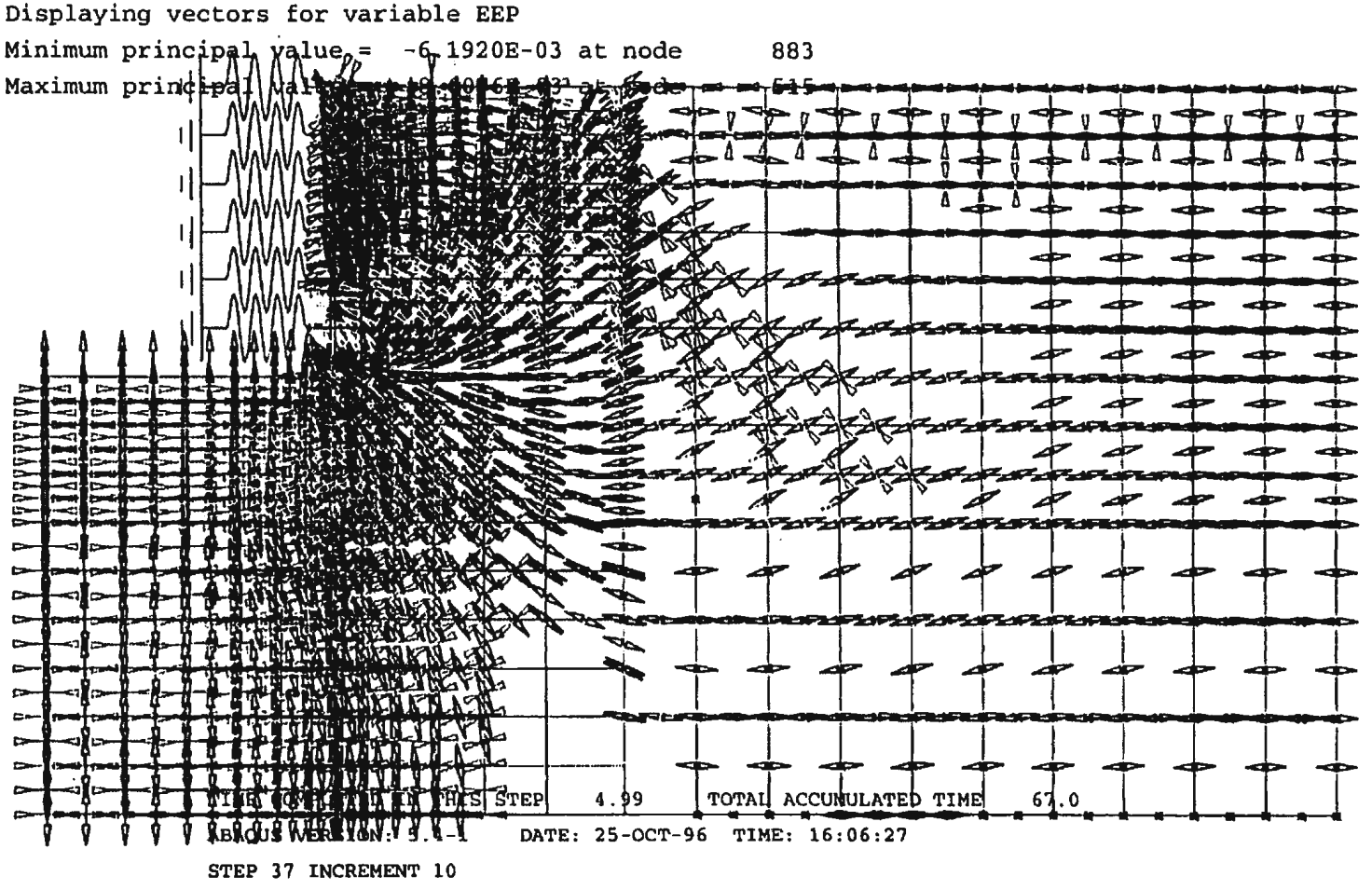

Figure 8.6: Vector plot of all elastic strains

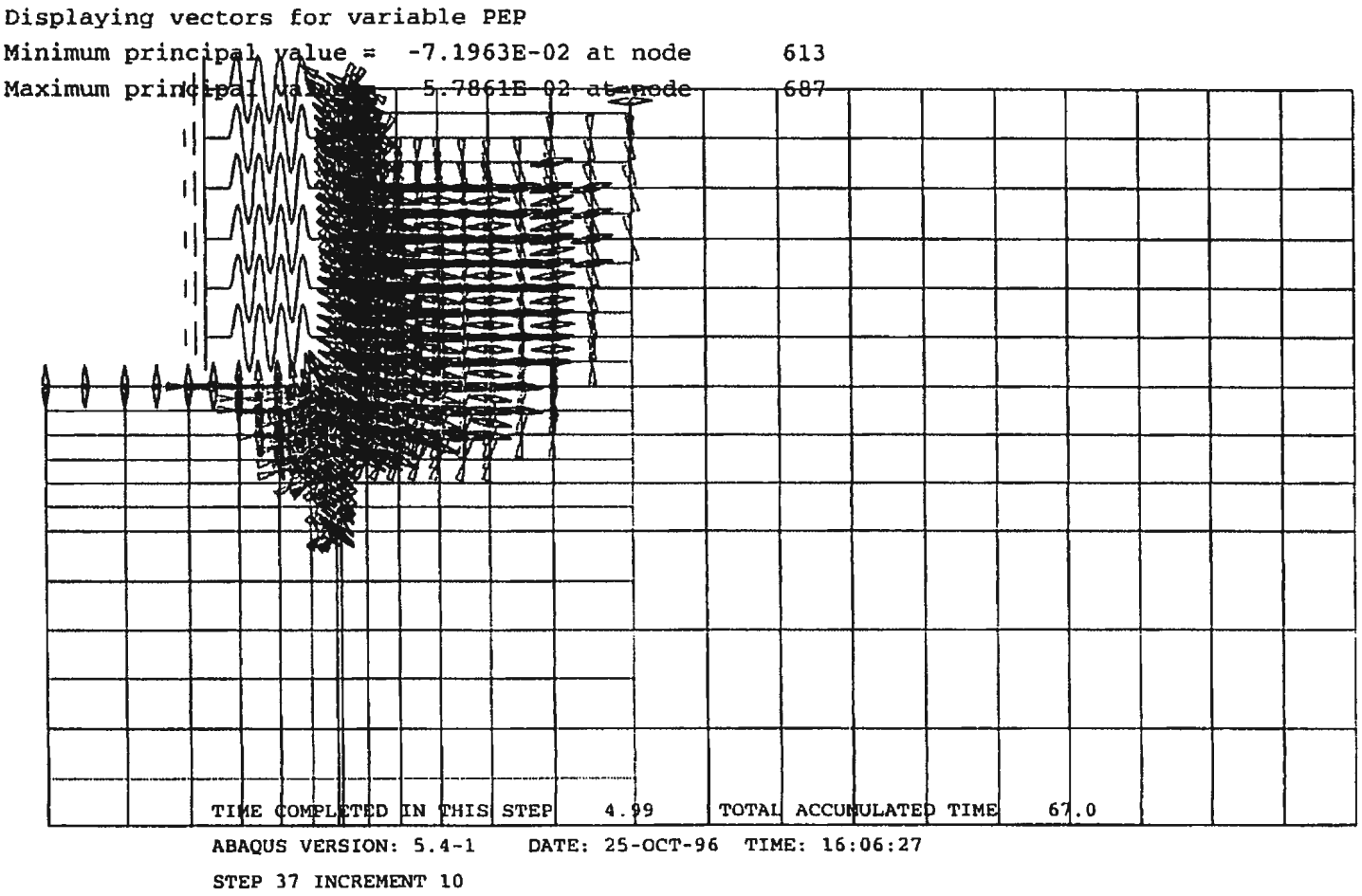

Figure 8.7: Vector plot of all plastic strains

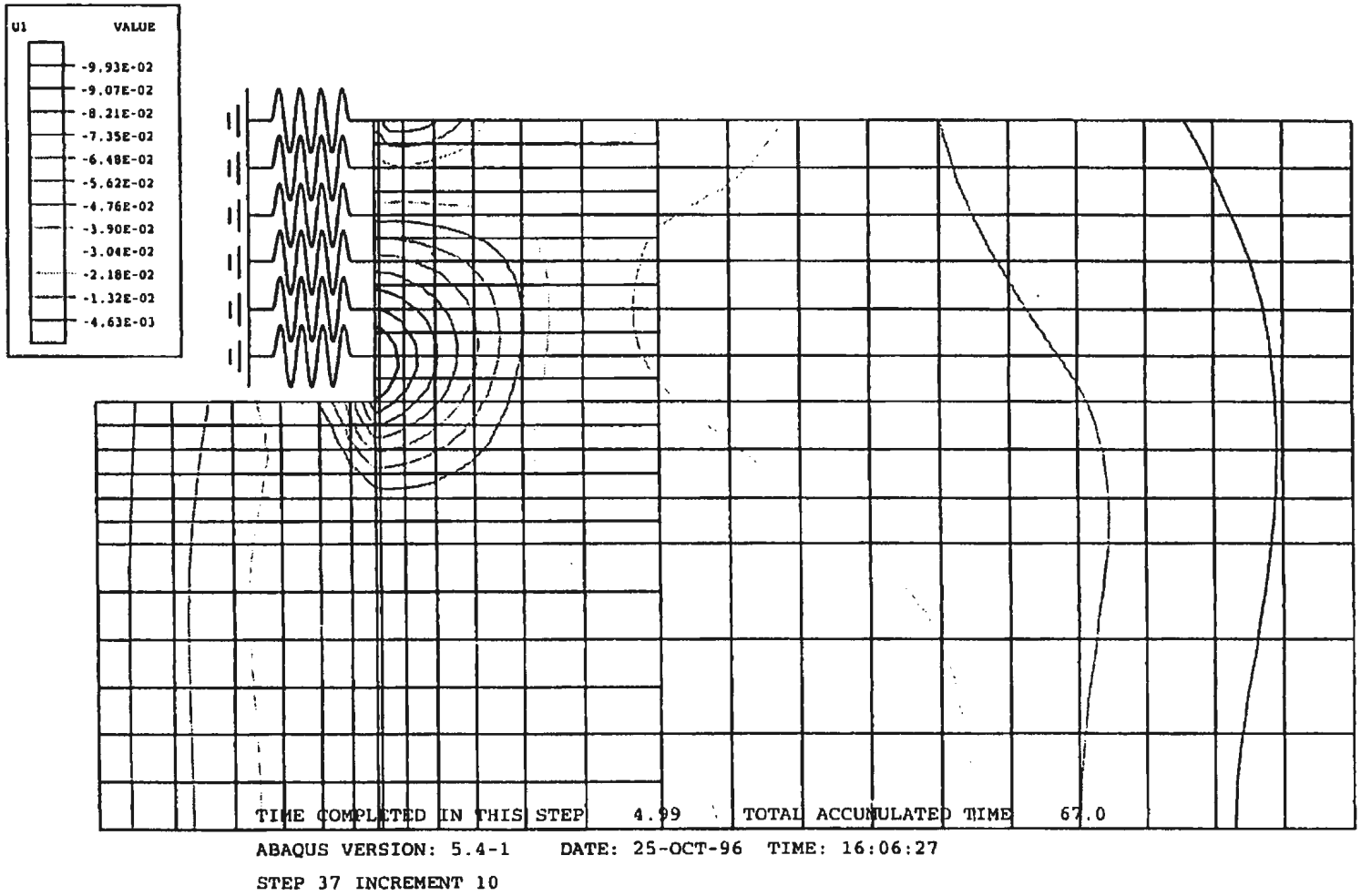

Figure 8.8: Contour plot of the horizontal displacement

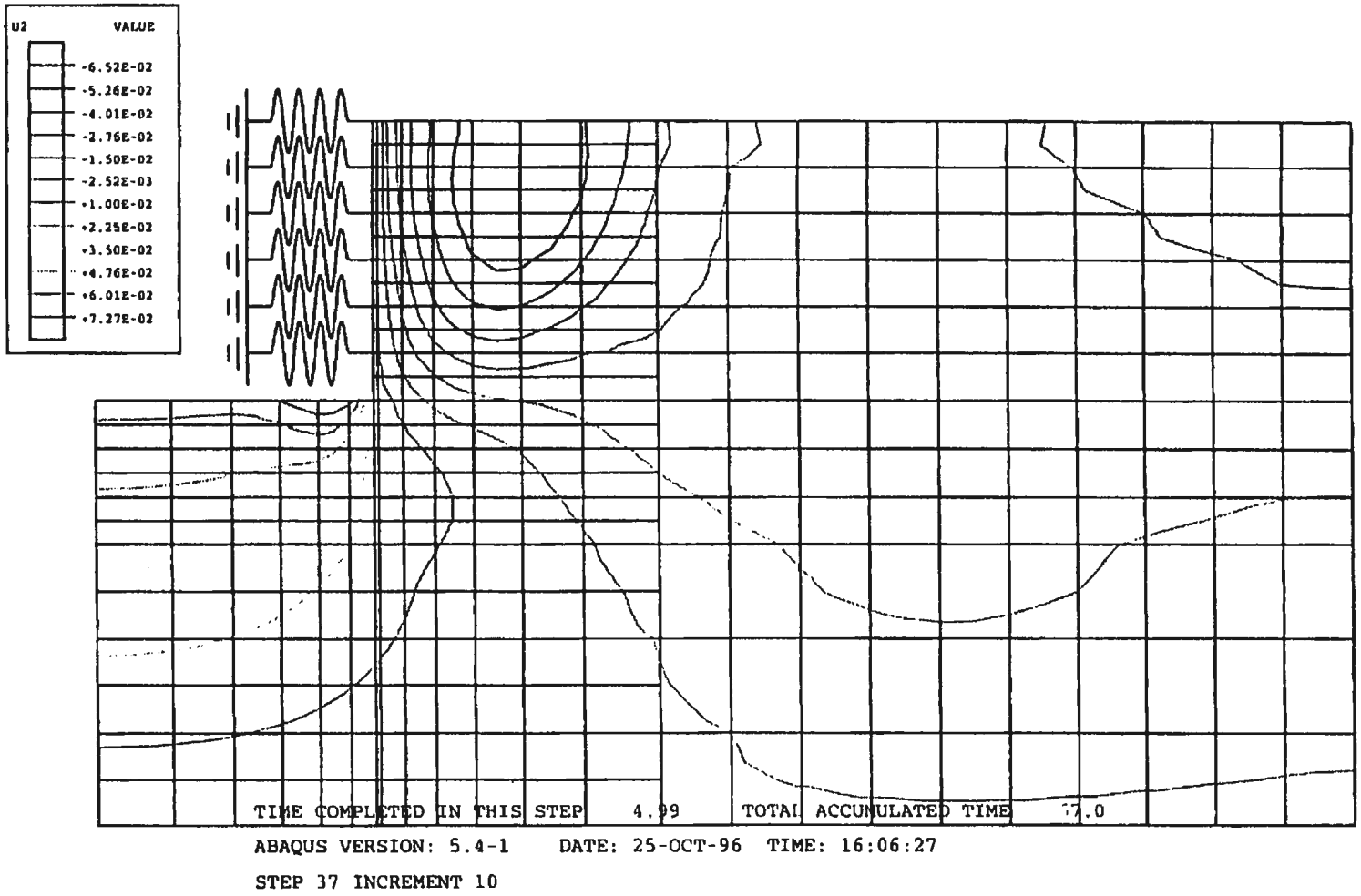

Figure 8.9: Contour plot of the vertical displacement

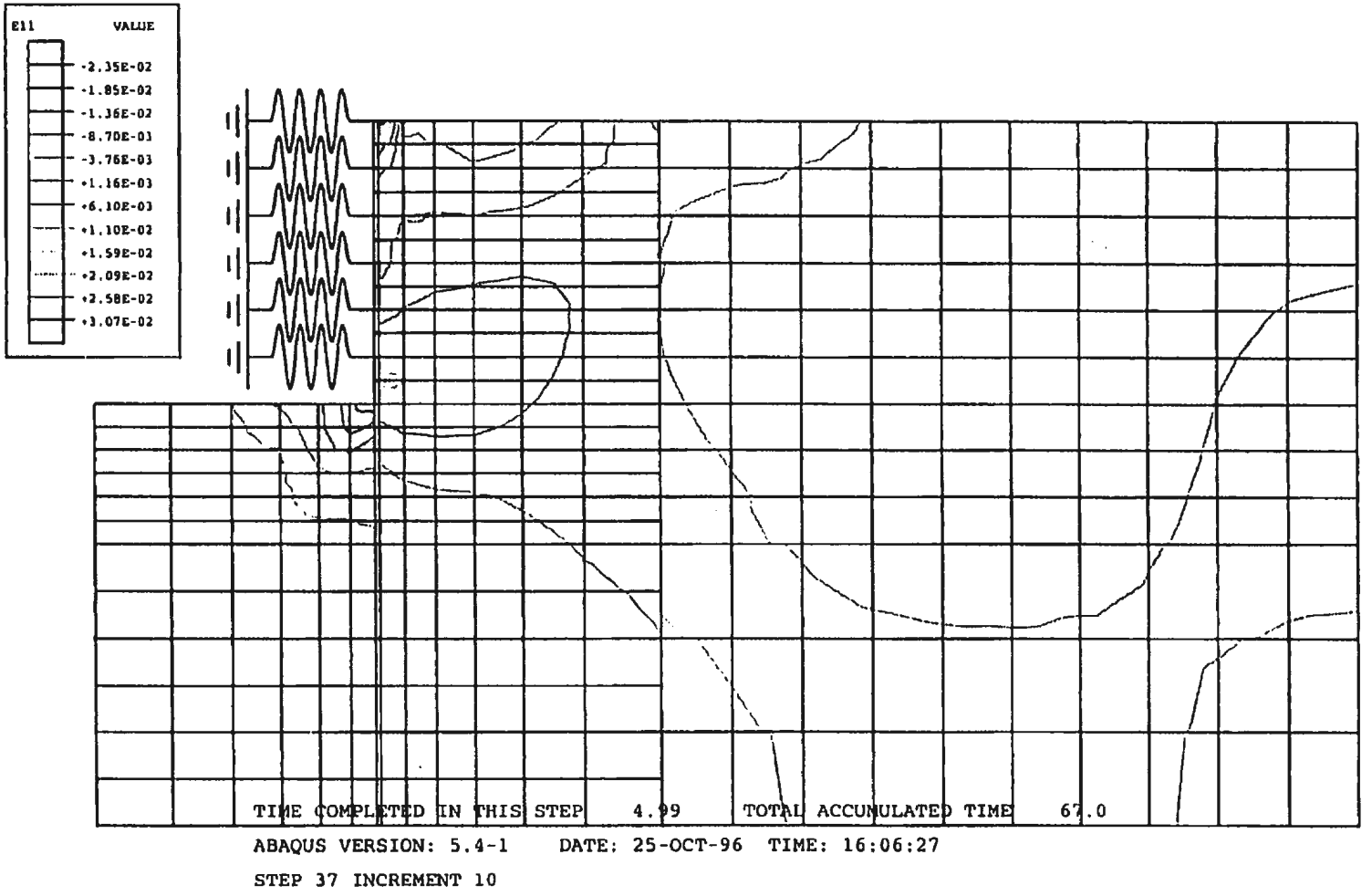

Figure 8.10: Contour plot of the horizontal strains

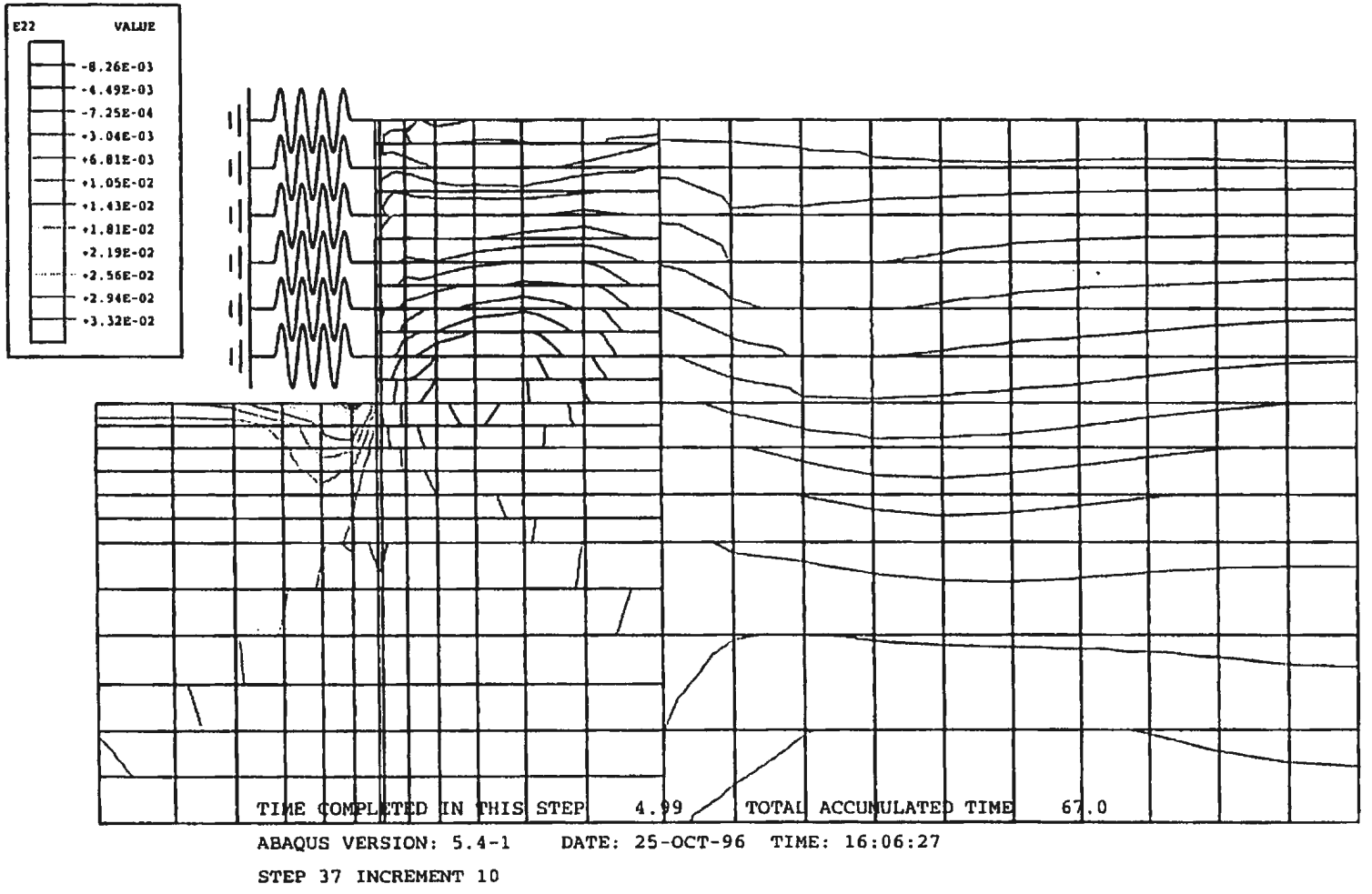

Figure 8.11: Contour plot of the vertical strains

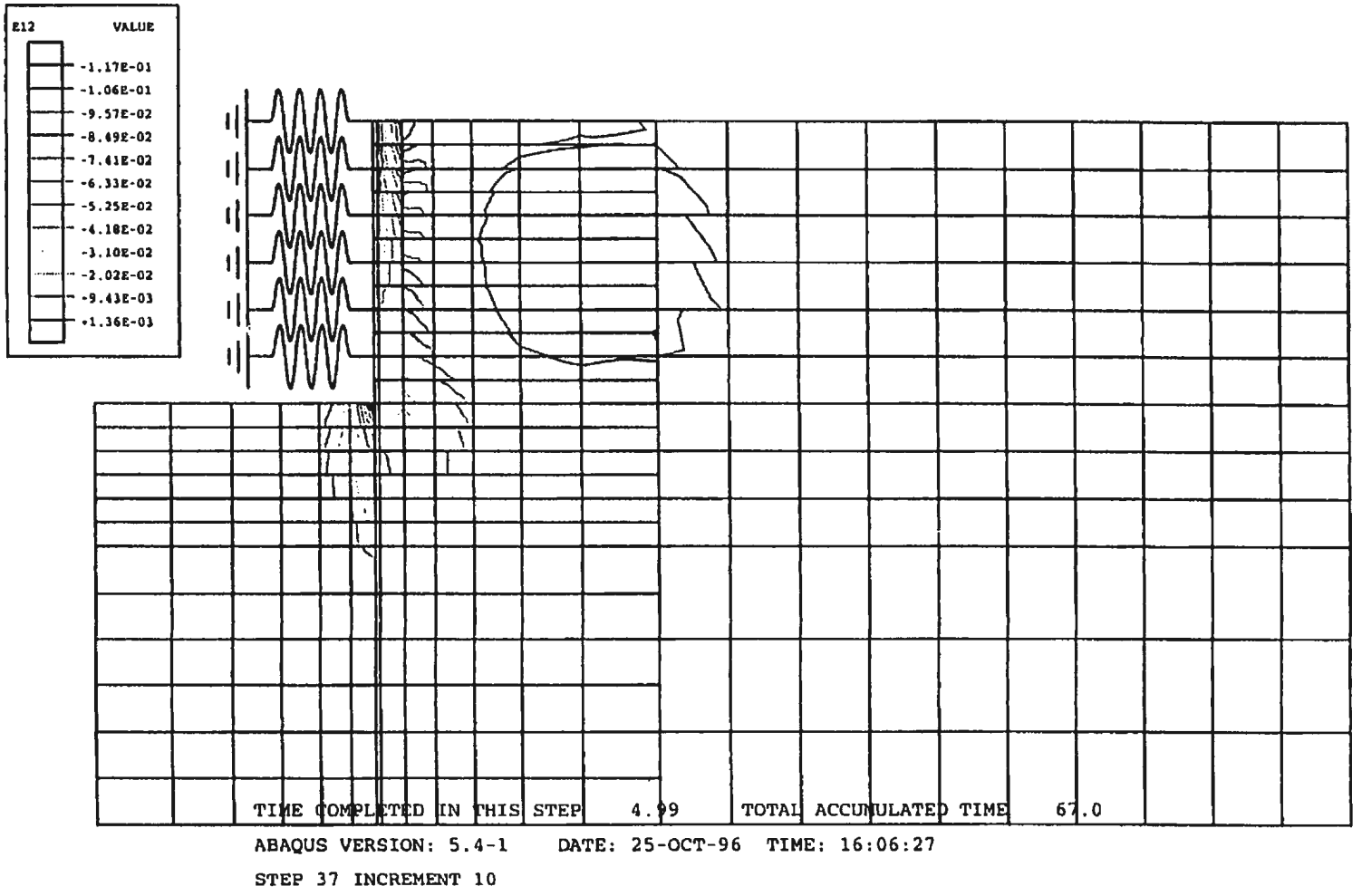

Figure 8.12: Contour plot of the shear strains

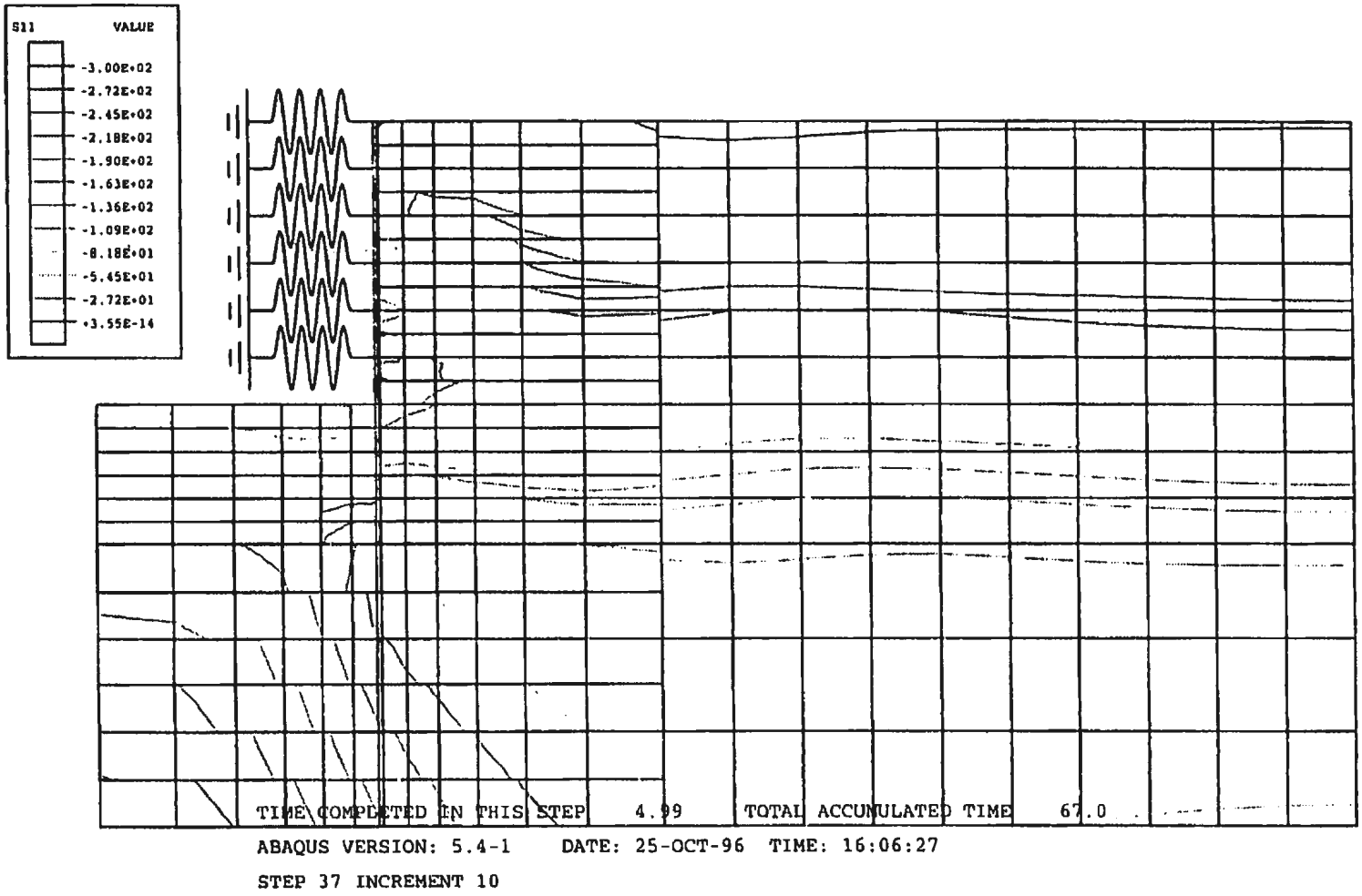

Figure 8.13: Contour plot of the horizontal normal stresses

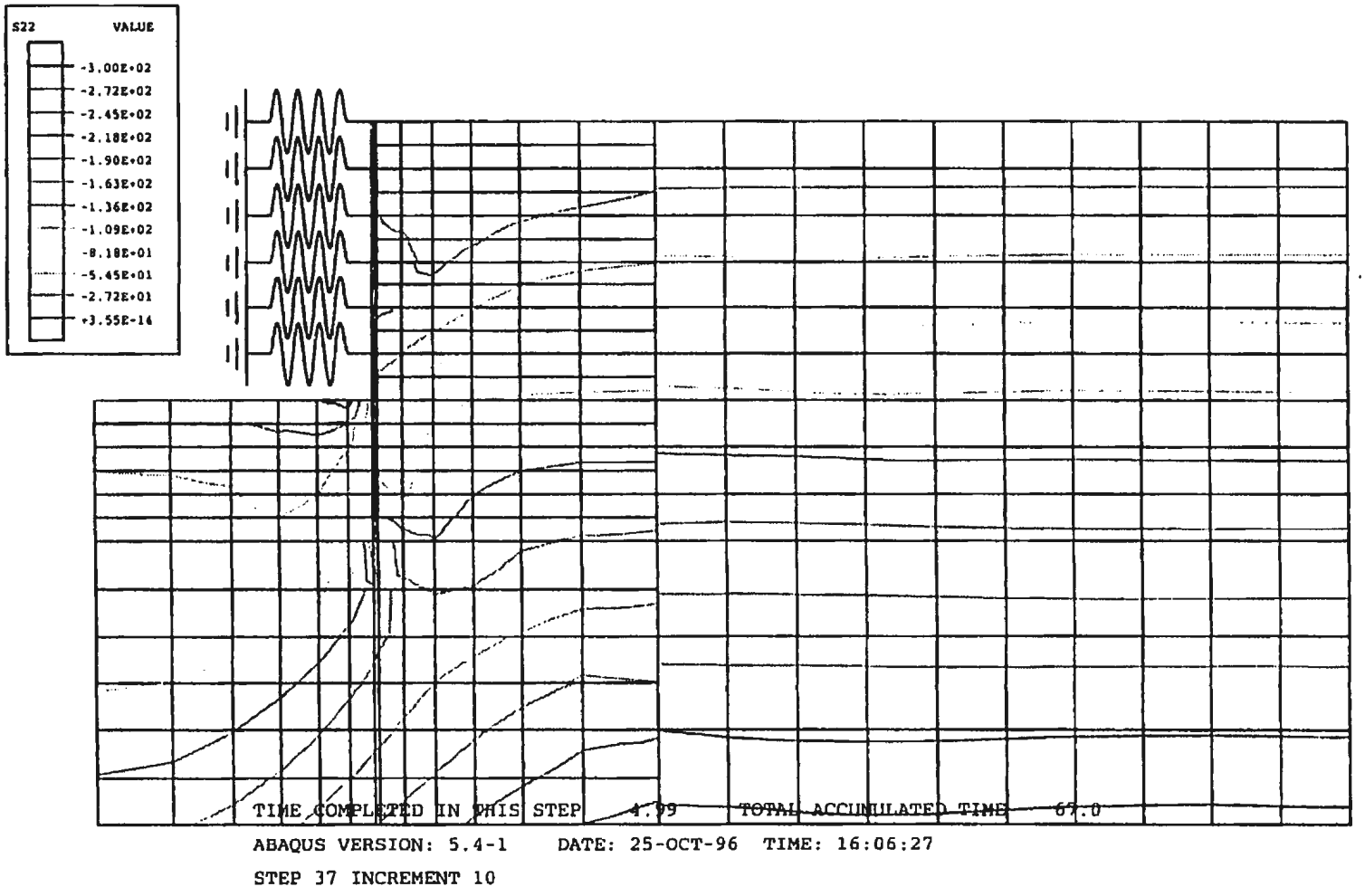

Figure 8.14: Contour plot of the vertical normal stresses

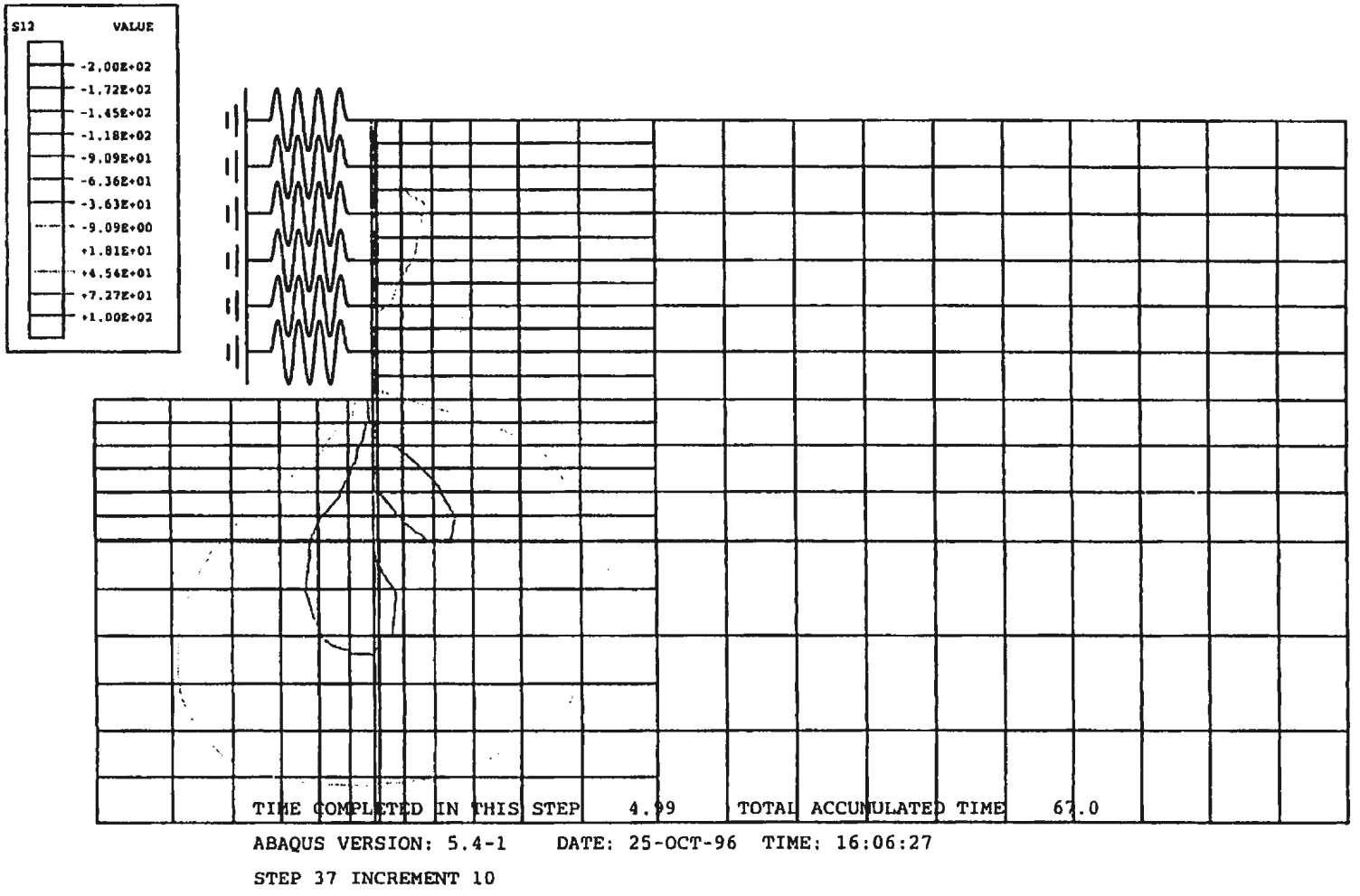

Figure 8.15: Contour plot of the shear stresses

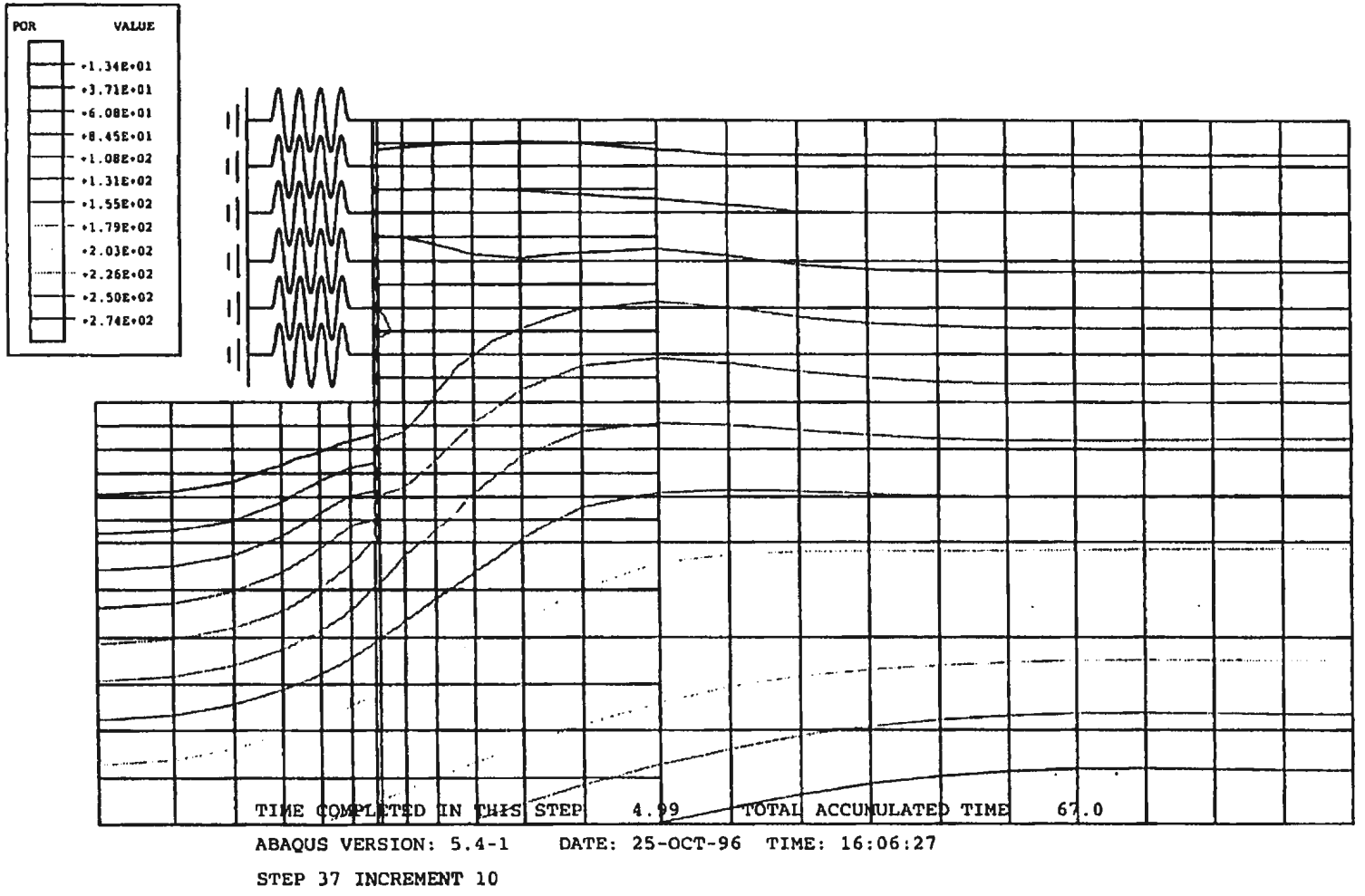

Figure 8.16: Contour plot of the pore pressure

8.2.4 Development of the stresses and pore pressures during excavation

In order to analyze the stress variation, three elements are selected. The positions of the three selected elements are shown in Fig. 8.2. Element A (number 86) is located under the dredge line and close to the sheet piles; element B (number 272) is located close to the back of the sheet piles and close to the surface; element C (number 277) and D (number 281) are located on the same vertical line as element B and element D is located on the same horizontal line as element A. Element C is about the middle between B and D.

The comparison of the variation of the pore pressures in the four elements is shown in Fig. 8.17. The stress paths of the four elements are shown in Fig. 8.18, the stresses of each element is the value of the stresses at the centroid of the elements.

Element A

For element A, the variation of the Mohr's circle is shown in Fig. 8.19. In this figure and the following figures, the numbers represent the step numbers of the excavation. Note the total steps of the excavation are more than the number of the steps listed in Table 8.7 since some steps in Table 8.7 need more steps to accomplish the actual programs. The actual state of some steps such as the excavated depth and the applied struts are shown in Fig. 8.1 (a) and (b). In total 37 steps are used in the analysis.

As the excavation proceeds, the Mohr's circles of the total stress and effective stress are moving left. This is because of the reduction of the vertical stress and the pore pressure. For the effective stress, the Mohr's circle intersects with the strength line for normal consolidation and the element does not indicate failure. This is because the element is overconsolidated. The overconsolidation ratio cannot be calculated as the ratio of previous vertical stress to the existing vertical stress, because the directions of principal stresses are changing.

Fig. 8.20 shows the theoretical division of the overconsolidation and normal consolidation. Since the original soil is normally consolidated, the strength line is a straight line passing the origin (line a in Fig. 8.20). The initial stress state of the soil is shown in the Mohr's circle A, where the minimum principal stress is $k_0\gamma z$ and the maximum principal stress is γz. If the soil is in a state of loading, the Mohr's circle would move to the right till it touches the strength line a. However if the soil is in a state of unloading, the Mohr's circle moves to the left. Touching the strength line a does not mean the failure of the element because the soil is in a state of overconsolidation. The strength line is not the line a but the line b, and these two lines intersect at point C, and the horizontal value at C is $k_0\gamma z$, which is the lateral stress of the soil before excavation.

In fact, generally speaking, the whole process of excavation puts the soil in the state of unloading. Therefore the elements exhibit the property of overconsolidation. This explains why the Mohr's circles pass the original strength lines for the elements. Since the reduction of the vertical stress of element A is greater than other three elements, the Mohr's circles for the effective stresses (Fig. 8.19) cut

the original strength line more than for the other three elements B, C and D (Fig. 8.24, 8.30 and 8.34).

Fig. 8.21 shows the variation of the vertical, lateral and shear stresses and pore pressures at each step. After step 21, the lateral stress becomes larger than the vertical stress, and this difference keeps growing till the end of the excavation. Meanwhile the shear stress is negative and reaches its maximum value at step 21. The pore pressure keeps reducing during the excavation.

The stress path for element A is drawn in Fig. 8.22, where the x axis is the mean normal stress and the y direction is the maximum shear stress. The rotation of the principal stress directions is shown, with the longer side of the element representing the direction of the major principal stress and shorter side the direction of minor principal stress. At first, the mean normal stress changes little with the shear stress reducing. After step 15, the mean stresses are reducing and the shear stress is increasing. The major principal stress direction is vertical direction in the beginning. From there it rotates clockwise, finally pointing in the horizontal direction.

The possible failure of the soil elements does not come from increments of the major principal stress, but from the reduction of the minor principal stress.

The stress path is also presented in Fig. 8.18 with the axes of p and q, where p is the mean stress of the three directions and q is the difference of the major principal stress and the minor principal stress. In this figure, the stress path can be divided into two parts: first, the mean principal stress does not change while the

difference of the shear stresses is reducing. This is reasonable because for element A, which is under the bottom of excavation, the vertical stress is reducing because of excavation while the lateral stress is increasing because the soil on the back of the sheet piles pushes the sheet piles. This is shown in Fig. 8.23. The deformation is elastic at this time because the stress path is inside the yield locus of Cam-clay model. Secondly, the mean principal stress is reducing and the difference of principal stresses is increasing. This is because that lateral stress applied by the pushing of the sheet piles is larger than the vertical stress which keeps reducing because of excavation. At the last moment, the locus of the Cam-clay model expands and plastic deformation results.

Fig. 8.23 shows the developing of normal stresses and strains, $\sigma_x - \epsilon_x$, and $\sigma_y - \epsilon_y$ and shear stress and strain, $\sigma_{xy} - \epsilon_{xy}$ during excavation. In this figure, the sign for compressive stresses and contracting strains is taken to be positive. The strains in the x and y directions are of different signs which implies that one direction is in contraction and the other is in extension.

Element B

Element B is on the back of the sheet piles and close to the surface. The variation of Mohr's circles for element B during the excavation is shown in Fig. 8.24. The Mohr's circles for the total stress and the effective stress do not move along the x axis very much because there is little change in the stresses and the pore pressures. In the effective stress state, it seems that the mean stress of the element varies little. Only the differences of the principal stresses increase, in other words, the

shear stress increases.

In Fig. 8.18, the stress path starts from the K_0 line and goes up to the critical state line (CSL) showing the property of overconsolidation. Mostly the line is almost vertical. It is also shown that the mean stress does not change very much, but the shear stress is reducing, which means the element remains in a state of elastic deformation. This conclusion is also supported from Fig. 8.7, which indicates no principal plastic strains for this element.

The strength line is drawn with $\phi = 24°$. The Mohr's circles passes the original strength line. Part of the overconsolidation may result from the manner of inputting the data for analysis. ABAQUS does not calculate the stresses and strains at the center of an element but at the four integration points. The integration points are required for the mathematical integration to obtain the stiffness matrix. The values of the initial stresses for the four points are of two lower integration points. The stresses at these points are larger than at the centroid and therefore the soil seems lightly overconsolidated. It was necessary to use the value of the stresses at these points since the Cam-clay model requires that the initial stresses should be inside the yielding locus. This would not be the case if the stresses of the centroid are used as the initial representative stresses of the element.

The variation of the directions of the principal stresses and the stress paths are shown in Fig. 8.25. The direction of the major principal stresses starts from the vertical direction and rotates clockwise a little at first and by step 15, it returns to the vertical. It then rotates anti-clockwise and finally turns to the horizontal

direction. It seems that step 15 is a critical step for the case in which the stresses and strains change a lot. The stress path can also be observed in Fig. 8.18. The increasing of the mean stress is resulted from the increasing of the lateral stress because of arching effect.

The variations of the vertical, lateral and shear stresses as well as the pore pressures are shown in Fig. 8.26. Before step 21, the vertical, lateral stresses and pore pressure do not change very much. After step 21, the vertical stress is reduced, the lateral stress and the pore pressure are increased. It should be noticed that, at the end of the excavation, the lateral stress increases to become larger than the vertical stress. The reason is given by the following explanation.

As a result of the deep excavation, the pressure of the soil on the back of the sheet piles makes the sheet piles deflect toward the lower part of the excavated area. Because of the stiffness of the sheet piles and the action of the struts, the sheet piles deforms as a continuous beam. The large movement of the lower part toward the excavated area makes the sheet piles deflect backward at the upper part. This deflection in turn pushes the soil backward and tends to mobilize the passive earth pressure in the soil. Therefore the lateral earth pressure is larger than the vertical earth pressure.

Bjerrum et al (1972) interpret the large lateral earth pressure as the arch theory. The arch theory was first presented by Terzaghi and Peck (Terzaghi and Peck, 1967). The formation of arching can be observed in Fig. 8.27 where the stresses of the three neighbouring elements at the final step are drawn. The elements are behind

the sheet pile and the positions of these three elements are shown in Fig. 8.2. It is shown that the vertical stresses of the elements are smaller than their horizontal stresses. This satisfies the condition of arching presented by Terzaghi and Peck (1967).

Arching can be clearly observed in Fig. 8.28 which shows the vector plot of the major principal stresses for the soil elements behind the sheet pile. Arching happens in the upper part of the soil just behind the excavation. It tends to form a center at the position of the lowest layer of struts. This also explains why the stresses at that part are very low. The formation of arching is the result of the complicated process of unloading of the soil and the support of the bracing system.

The stress - strain relation for element B during excavation are shown in Fig. 8.29. It also provide a proof for the elastic state of the element.

Element C

Element C is on the back of sheet piles and below element B. The Mohr's circles for element C during excavation are shown in Fig. 8.30. The Mohr's circles for the total stress move almost evenly left during the excavation and the variation of the values of the major and minor principal stresses is slight. The circles are almost all the same size. The same characteristics can also be found for the Mohr's circles for effective stresses. As shown in Fig. 8.32 the stress state for the element does not change very much during excavation. The variation of the directions for the principal stresses is shown in Fig. 8.31, where the stress path is also shown. The

direction of the major principal stress rotates clockwise until step 15 and rotates anti-clockwise after step 21 to a final position 111° to the horizontal direction. The back and forth variation of the direction of the major principal stresses of elements B and C implies a complicated distribution of stresses in the soil during excavation.

The relatively stable stress state for element C can also be observed from Fig. 8.18 where the stress path of p and q are drawn. The stress path takes an S shape but the trace is very small. The stresses vary around the K_0 line. It shows that there is some plastic strain at first and then it is in a state of elastic deformation.

The stress state of element C is also shown in Fig. 8.32. It can be seen that the effective vertical, lateral and shear stresses and pore pressure remain unchanged, and there is little change in the shear stresses. The lateral stress has the value of K_0 of the vertical stress and the pore pressure keeps almost the same value as the effective vertical stress. The stress strain curves are shown in Fig. 8.33.

Element D

Element D is at the same elevation of element A but on the back of the sheet piles. The Mohr's circles for element D are shown in Fig. 8.34. The variation of the Mohr's circles has the same characteristics as element C except that the circles keep increasing a little during excavation.

The stress path and the variation of the directions of the principal stresses are shown in Fig. 8.35. The direction of the principal stresses rotates clockwise a little and changes somewhat during the excavation. In Fig. 8.36, the variations of the

vertical and lateral stresses and pore pressure are shown. It is also shown in Fig. 8.18 that there is the smallest change of the stress state for element D, with the mean stress reducing and little change in the shear stress. This is very different from element A.

Fig. 8.37 shows the relation of stresses and strains during excavation. Comparing the relation of the shear stress and shear strain during excavation, it may be seen that element A is subjected to the largest shear stress and strain, and element D, which is on the opposite side of the sheet piles, is subjected to the smallest shear stress and strain.

In summary, the element A is in a state of overconsolidation, the element B is in a state of arching, element C does not change its mean stress very much, and finally element D does not change its shear stress and reduces its mean stress a little.

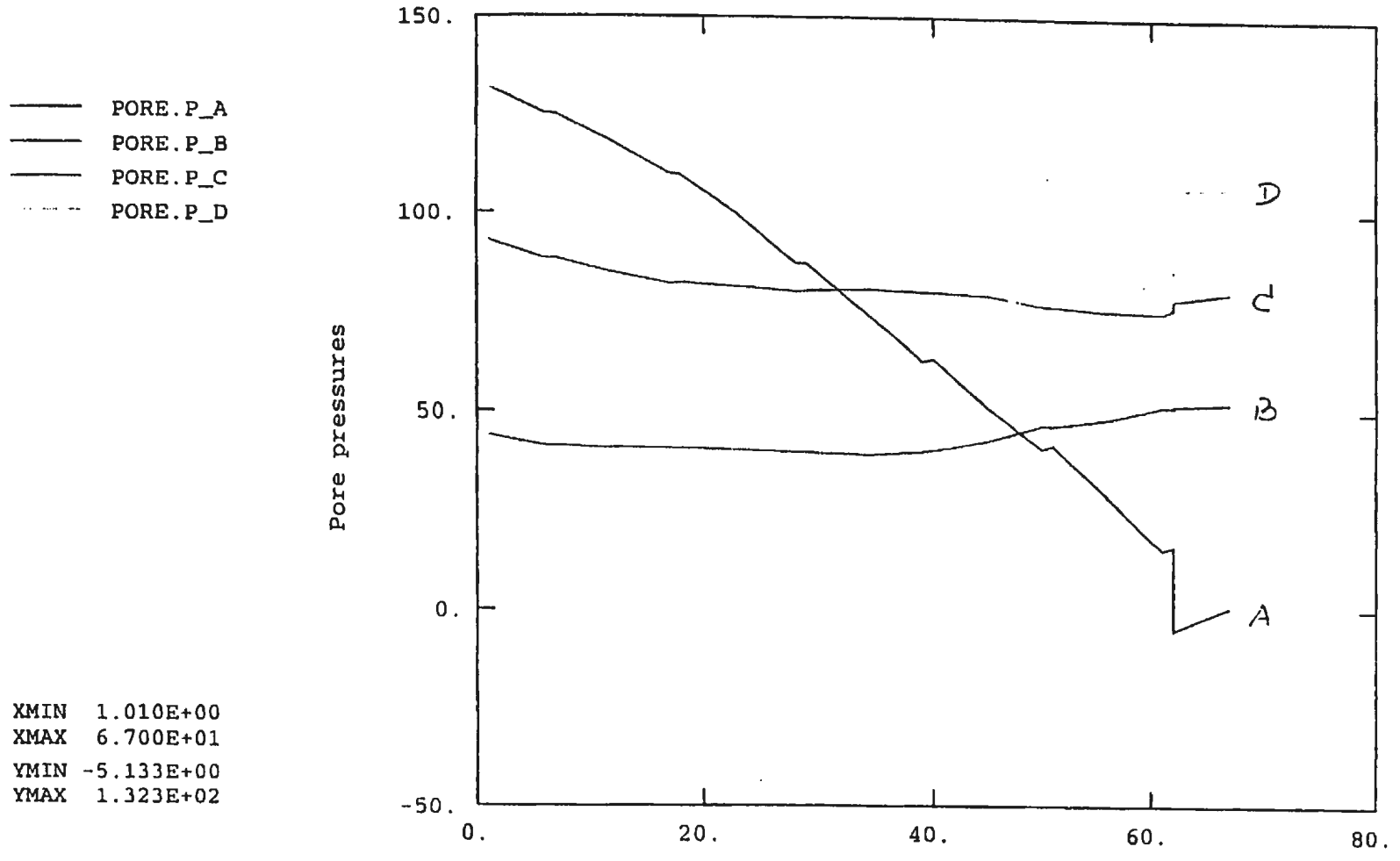

Figure 8.17: Variation of pore pressures of elements A, B, C and D

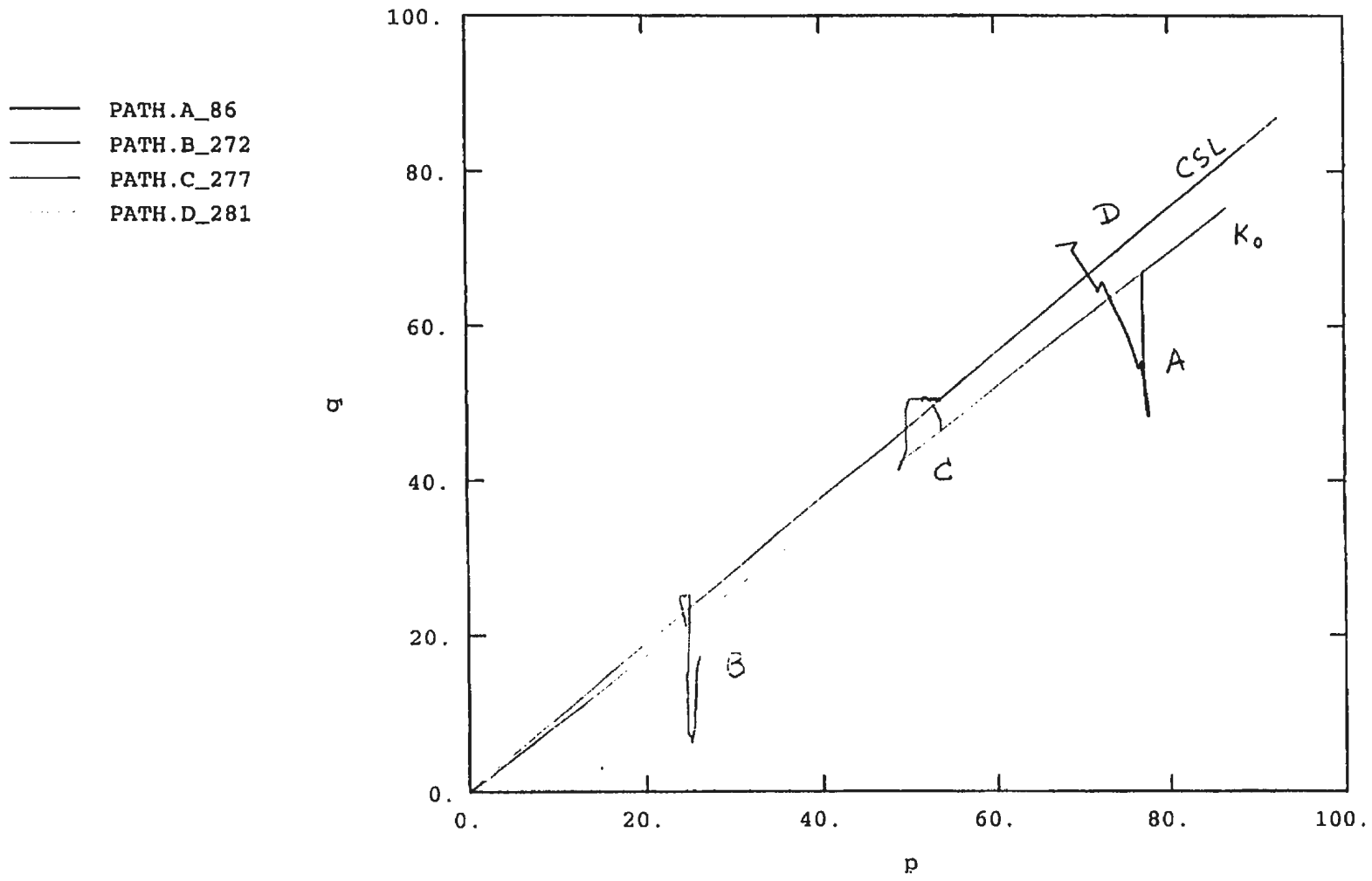

Figure 8.18: Stress paths of elements A, B, C and D

Figure 8.19: Stress variation in element A

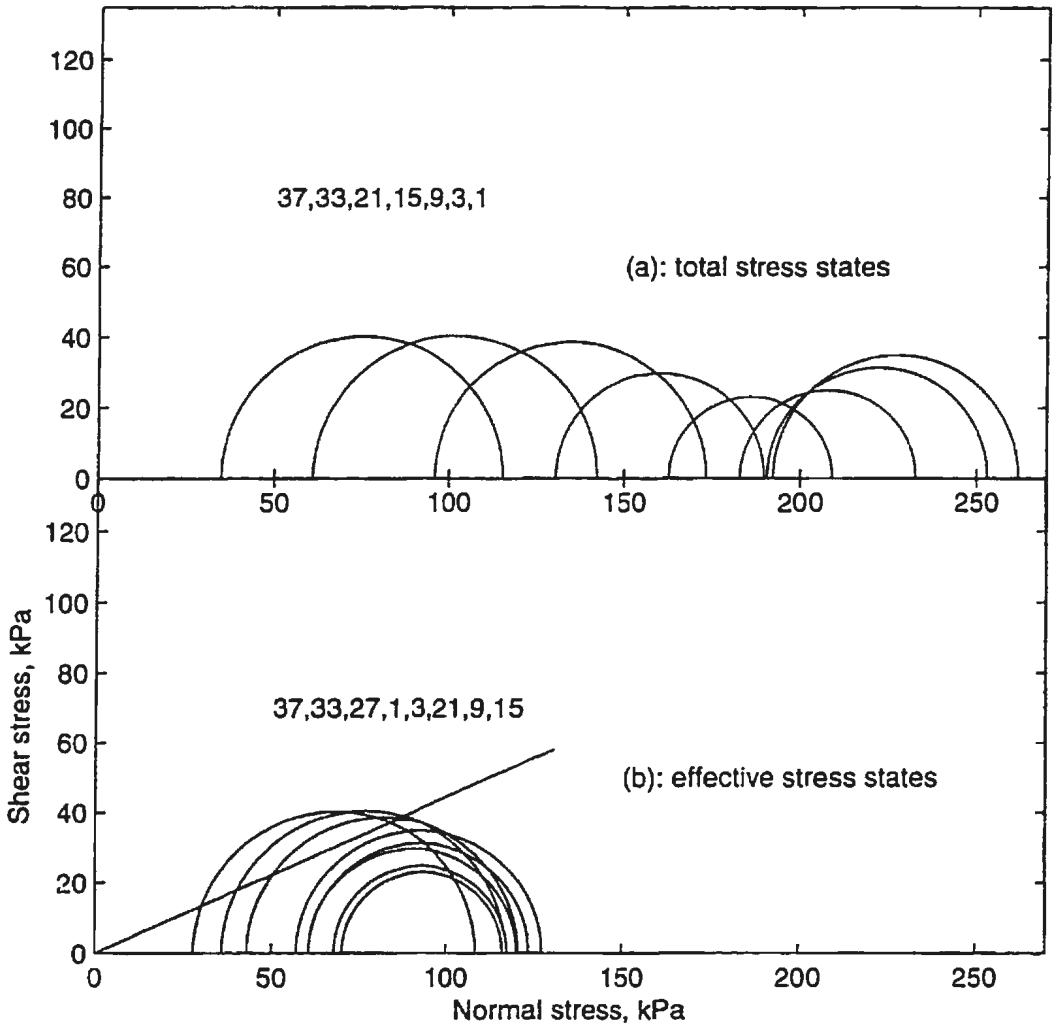

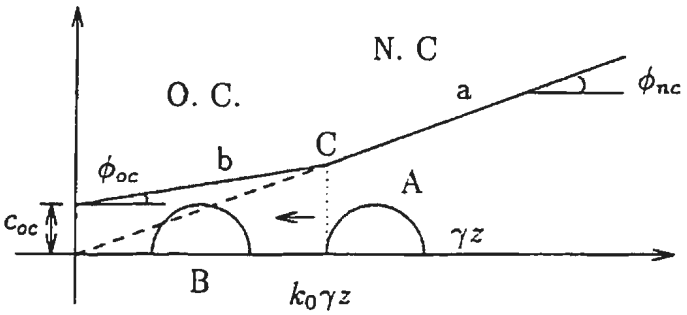

Figure 8.20: Division of normal and over consolidation

Figure 8.21: Variation of the stress state in element A during excavation

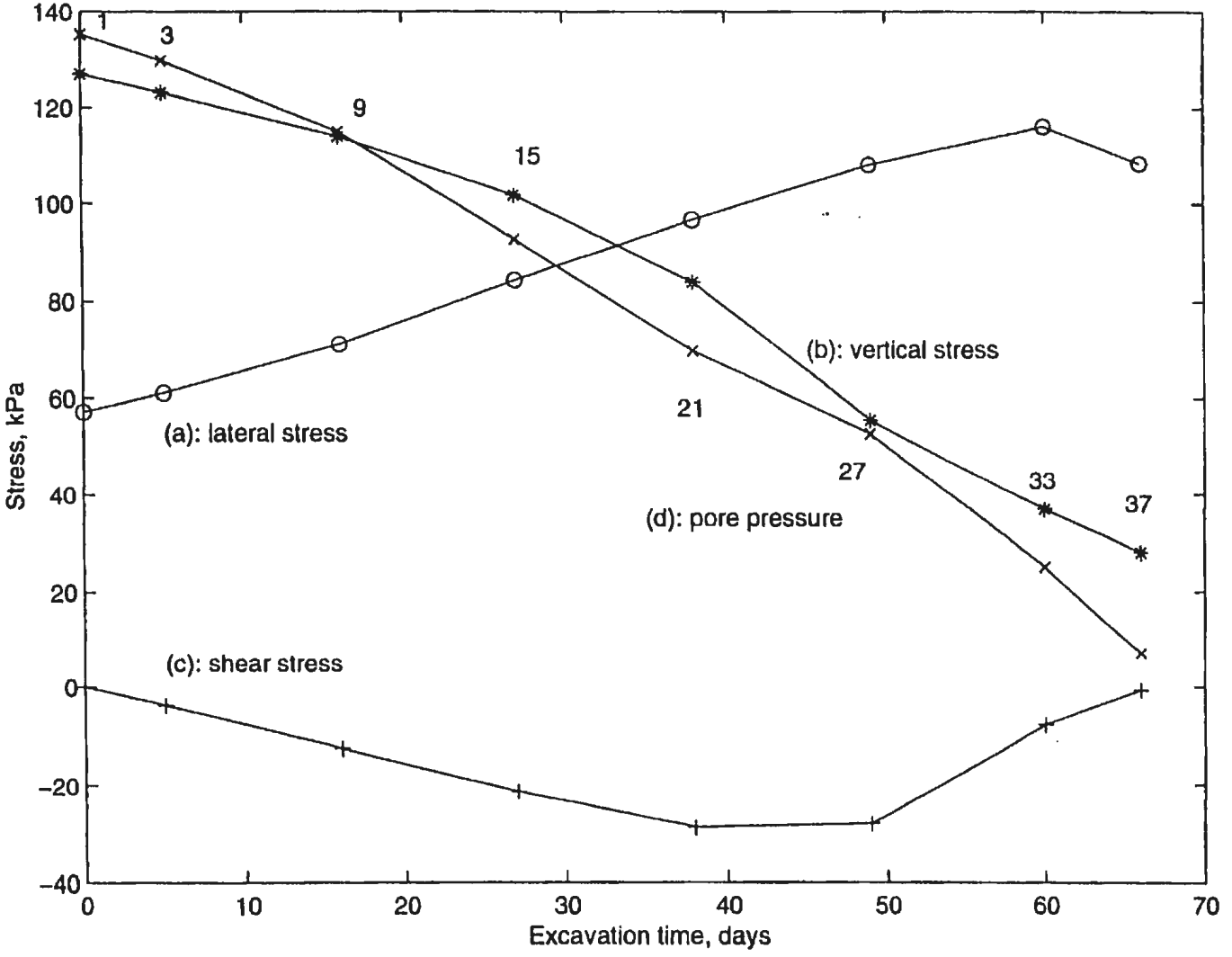

Figure 8.22: Stress path and rotation of principal stress directions in element A

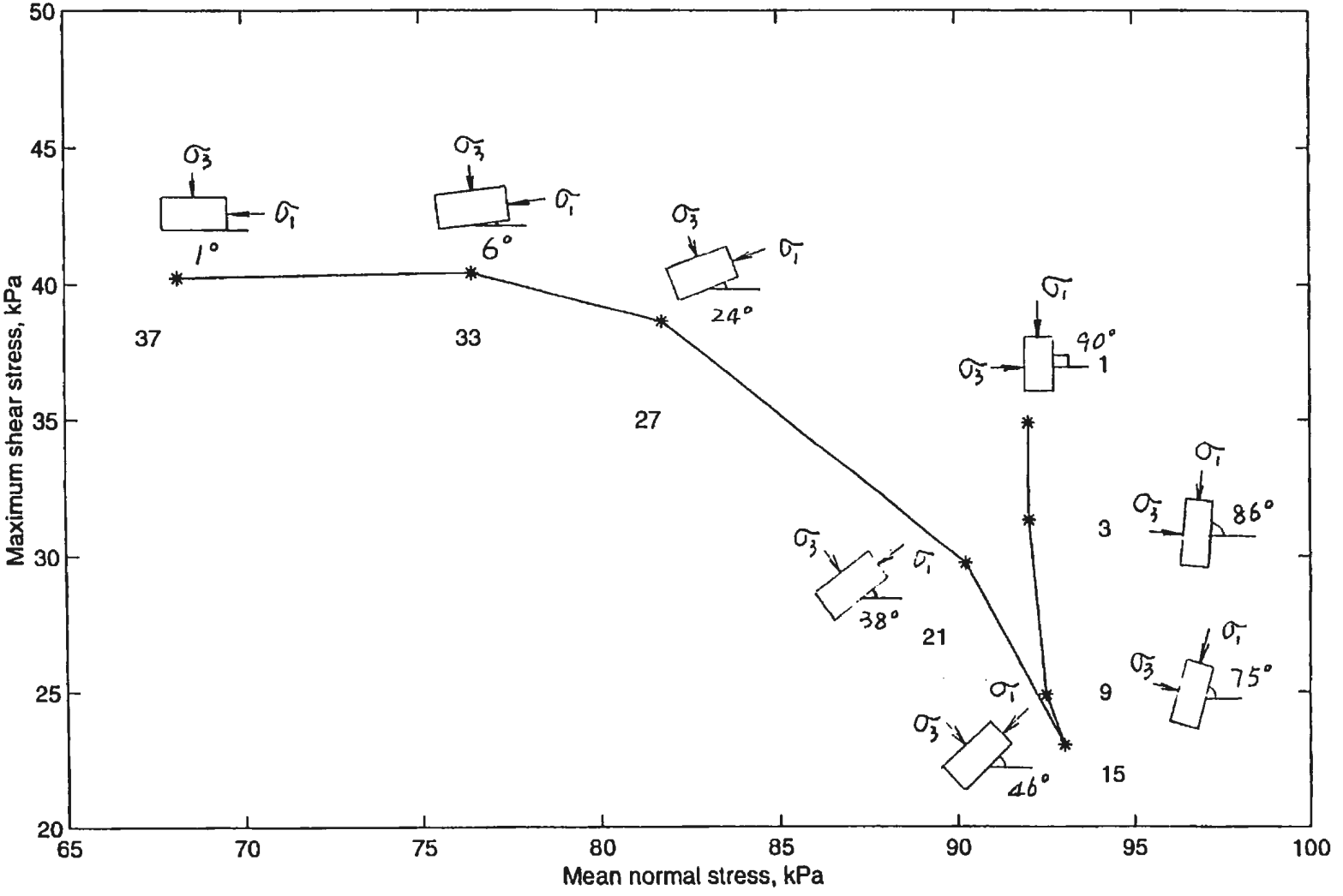

Figure 8.23: Relation of stress and strain in element A

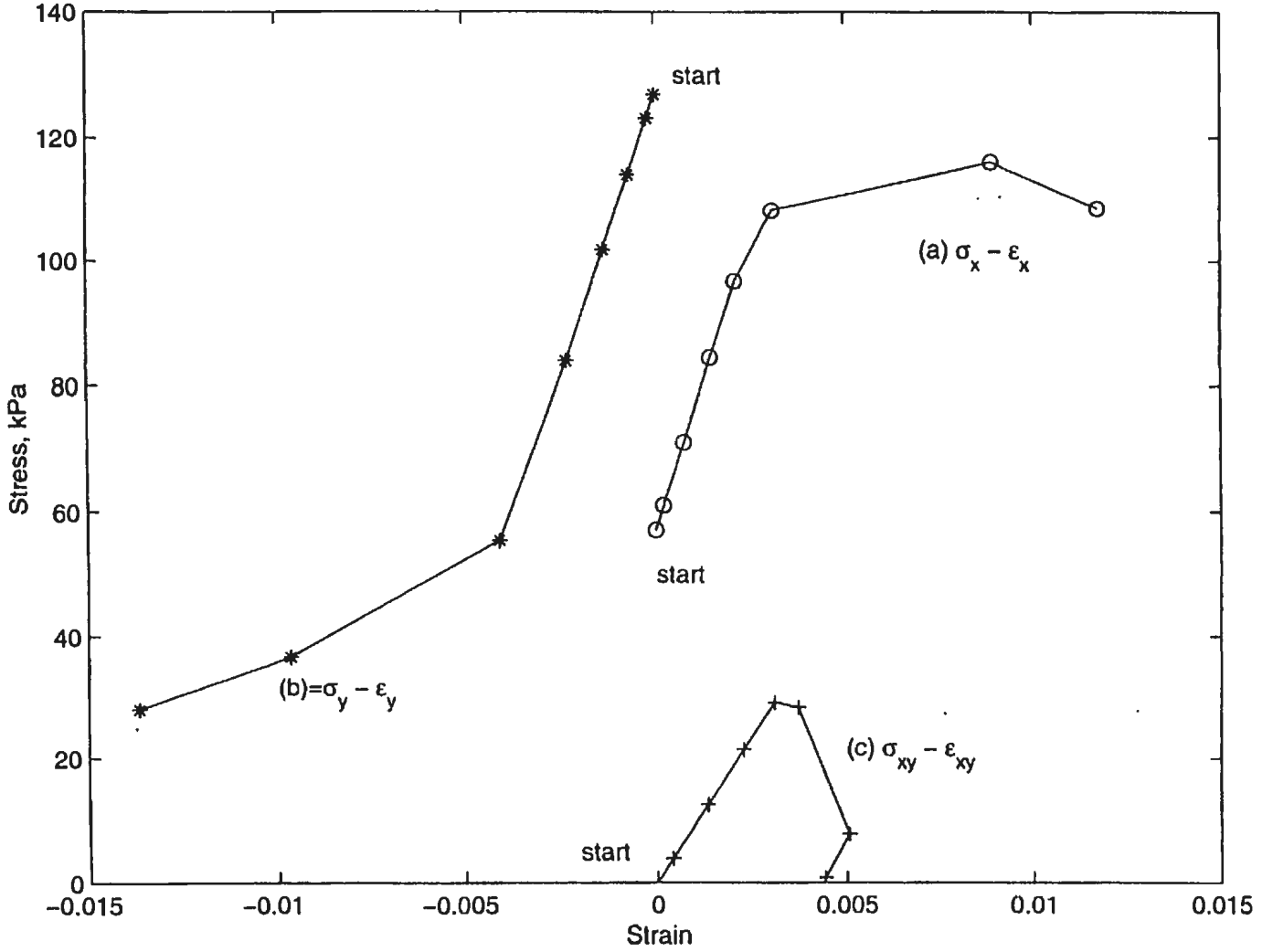

Figure 8.24: Stress variation in element B

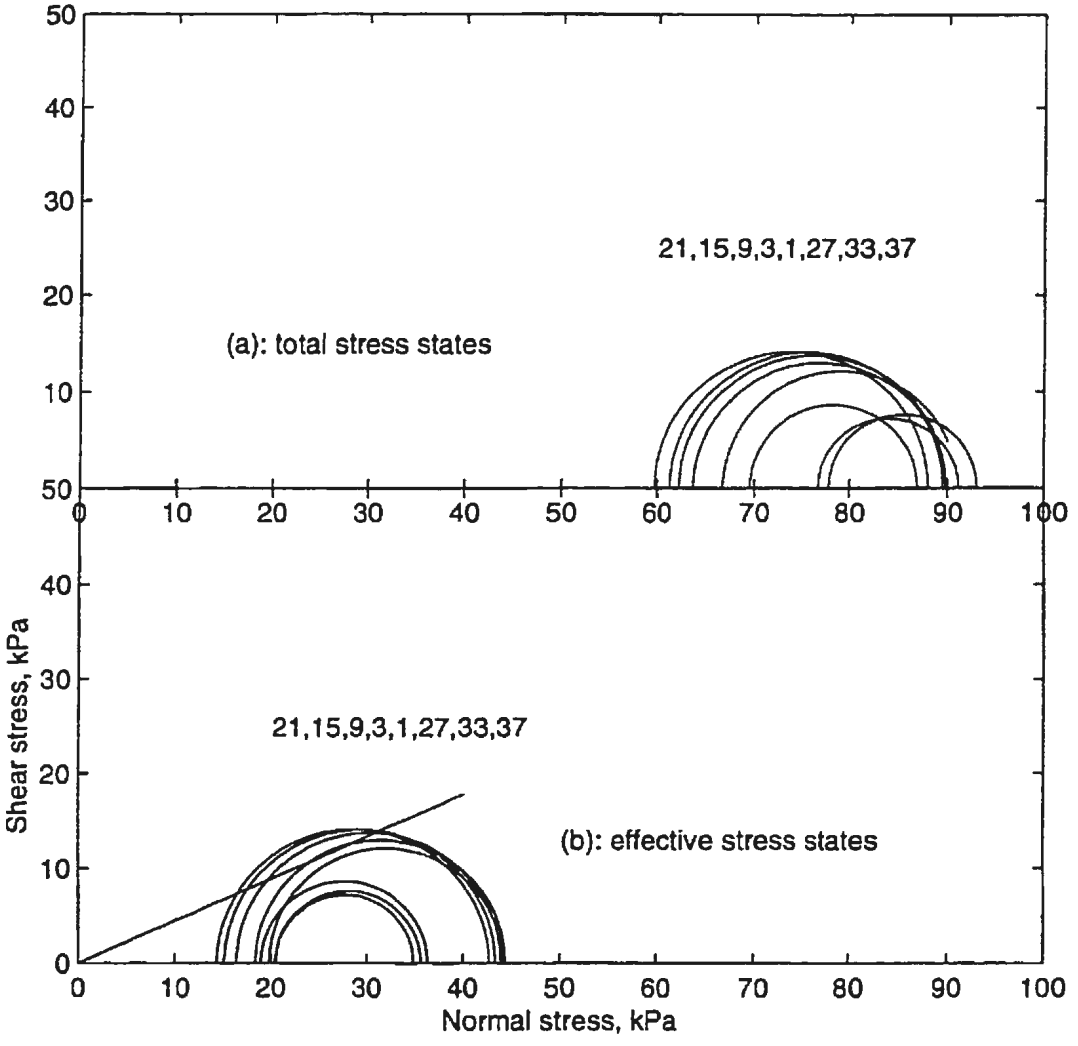

Figure 8.25: Stress path and rotation of principal stress directions in element B

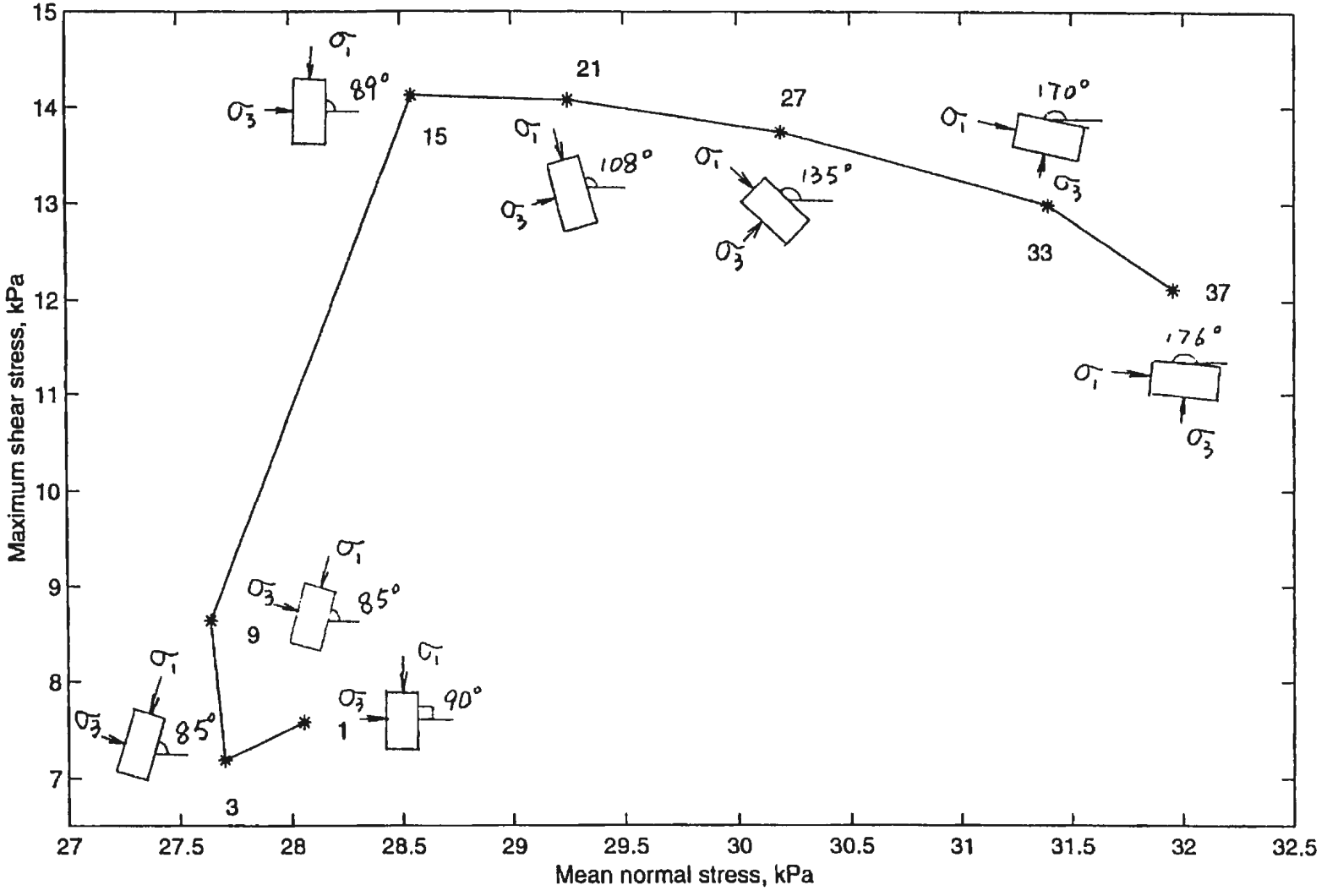

Figure 8.26: Variation of the stress state in element B during excavation

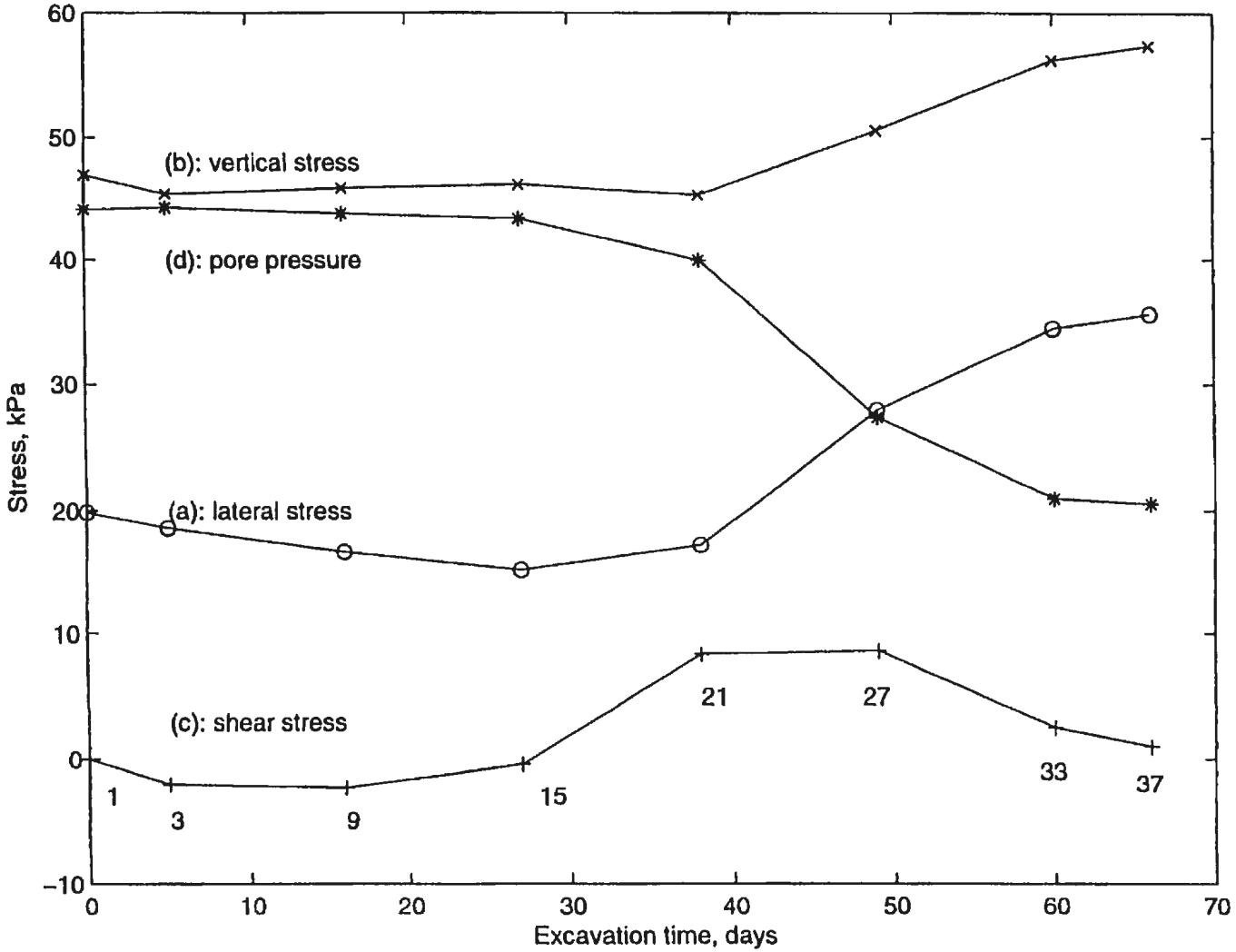

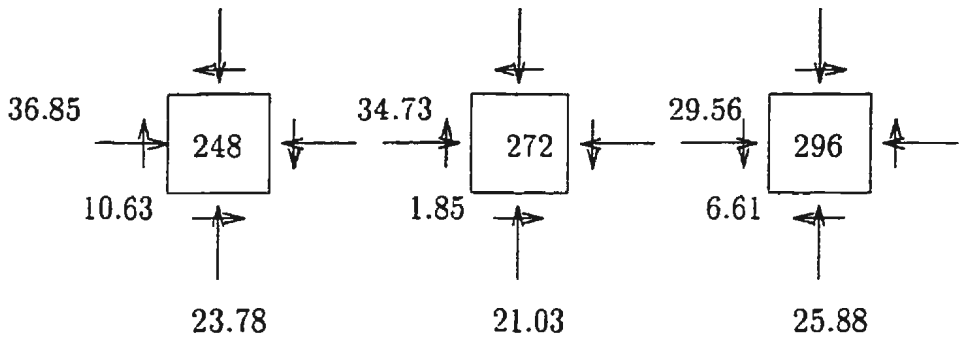

Figure 8.27: Arching

Figure 8.28: Vector plot of the major principal stresses

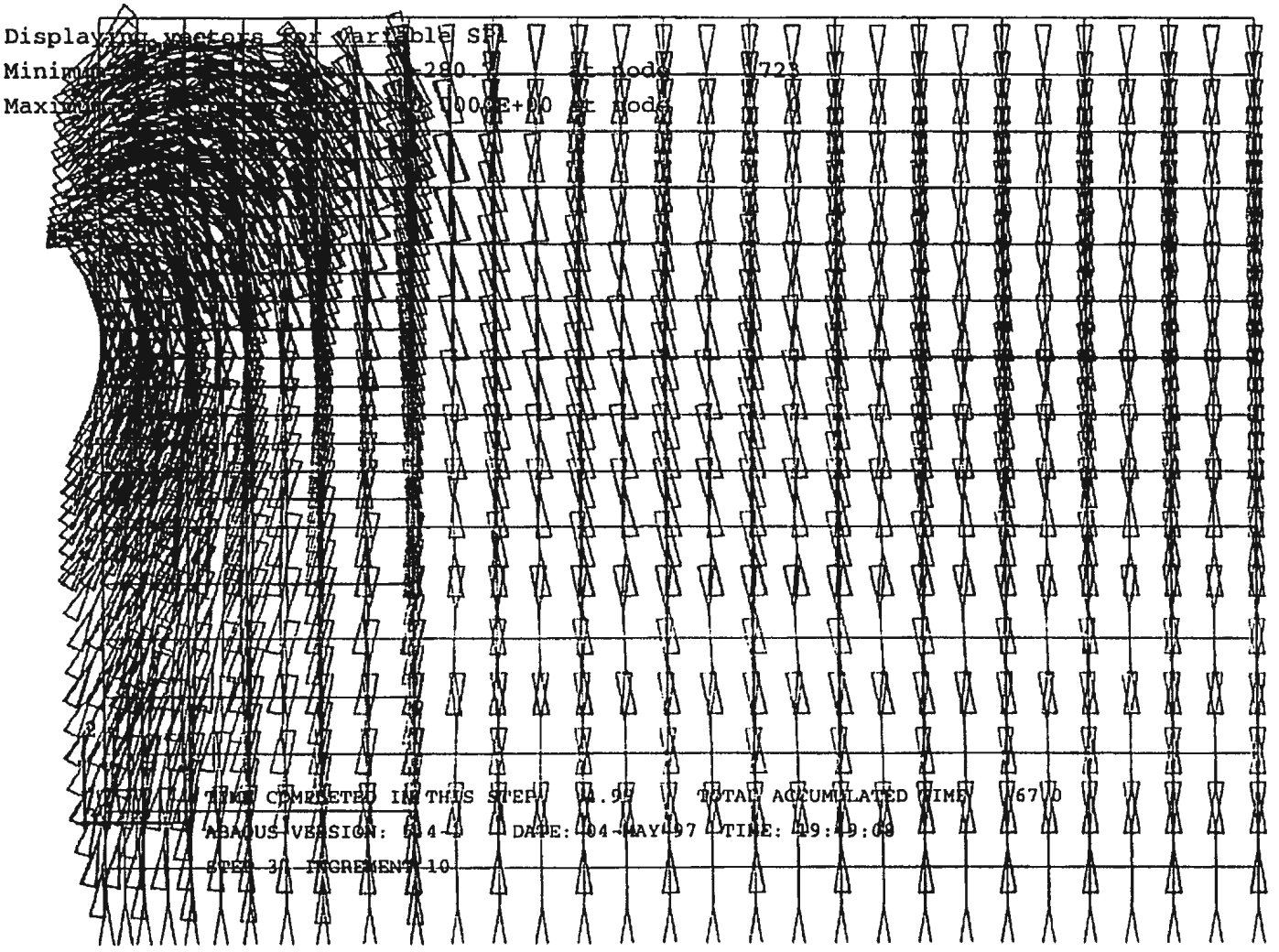

Figure 8.29: Relation of stress and strain in element B

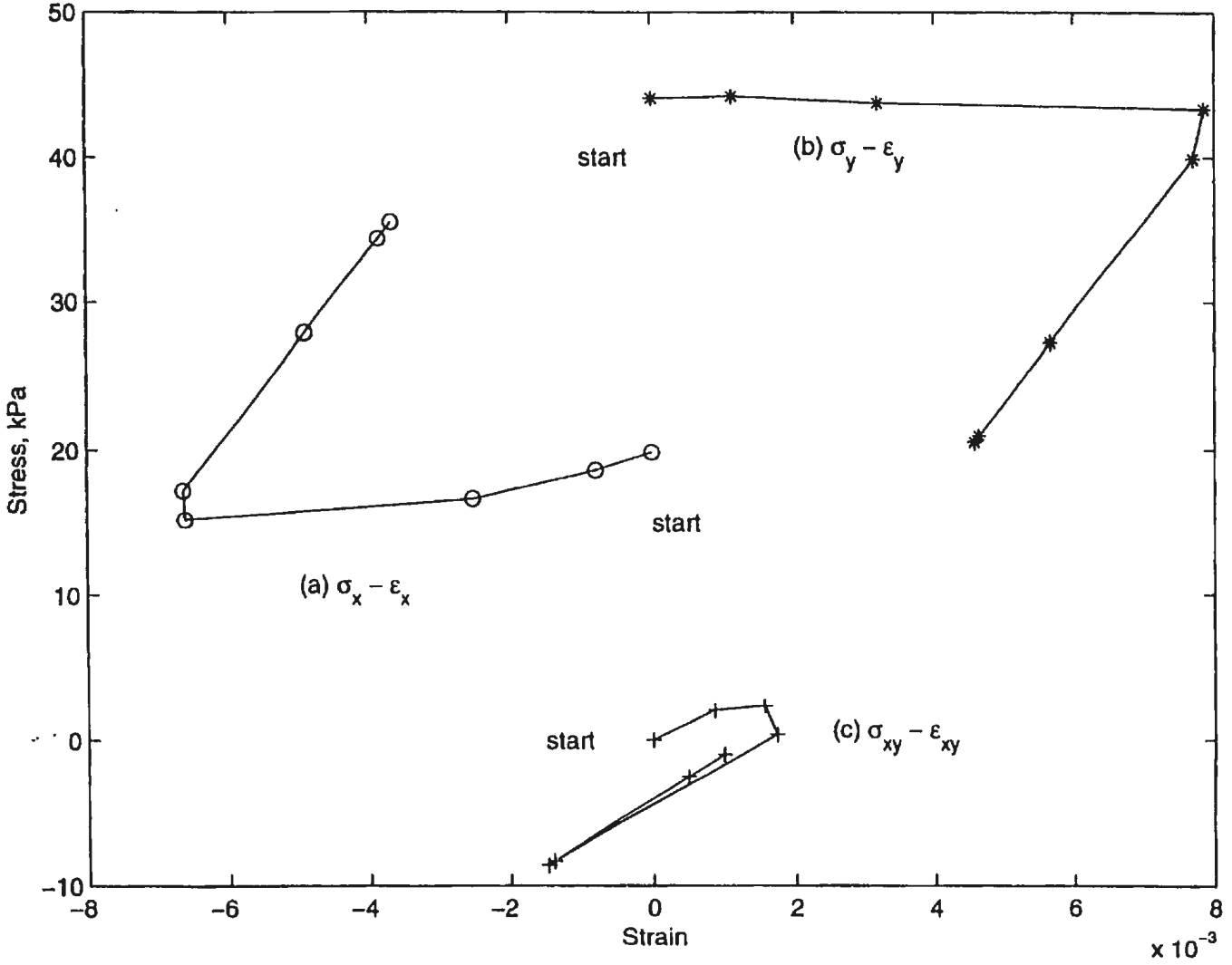

Figure 8.30: Stress variation in element C

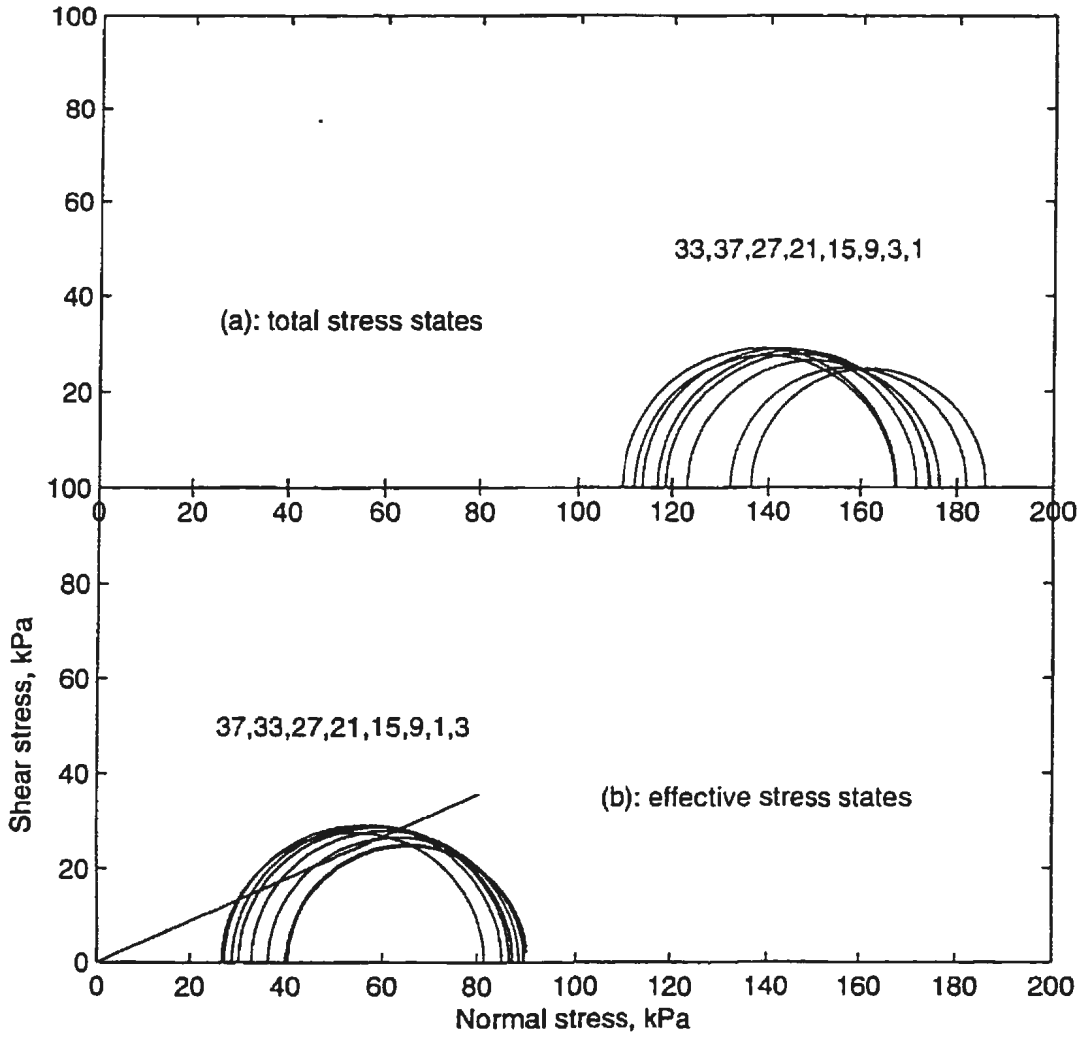

Figure 8.31: Stress path and rotation of principal stress directions in element C

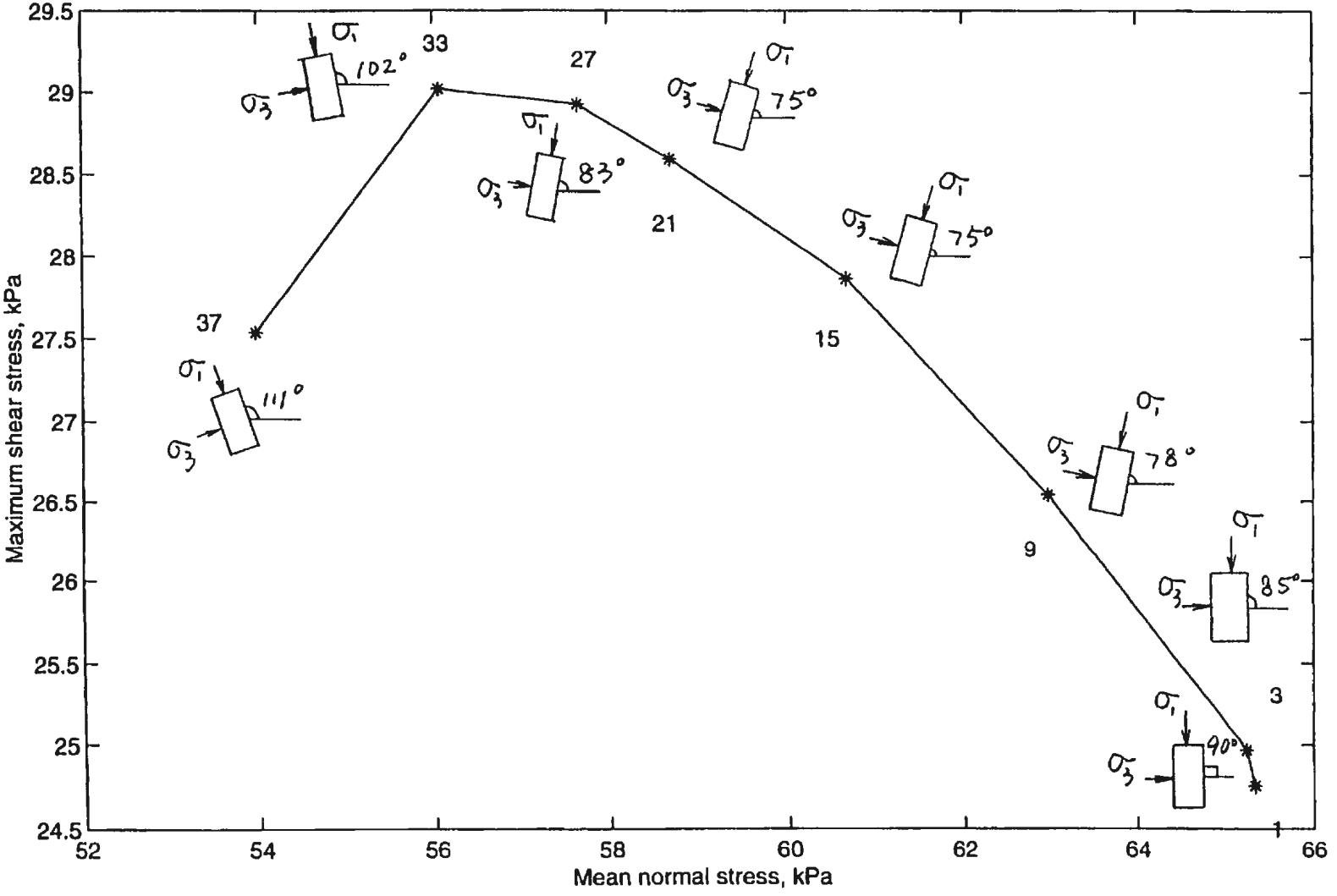

Figure 8.32: Variation of the stress state in element C during excavation

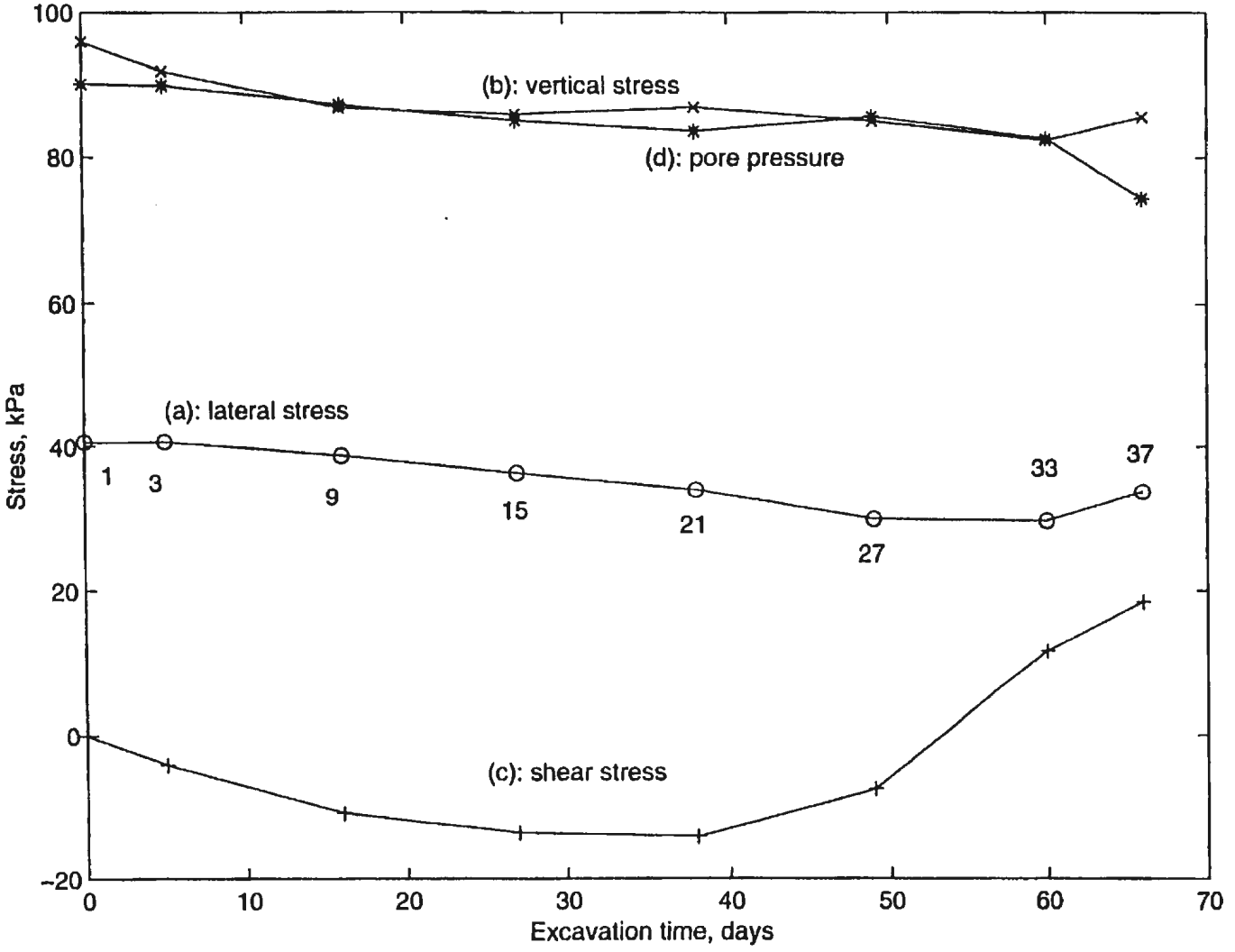

Figure 8.33: Relation of stress and strain in element C

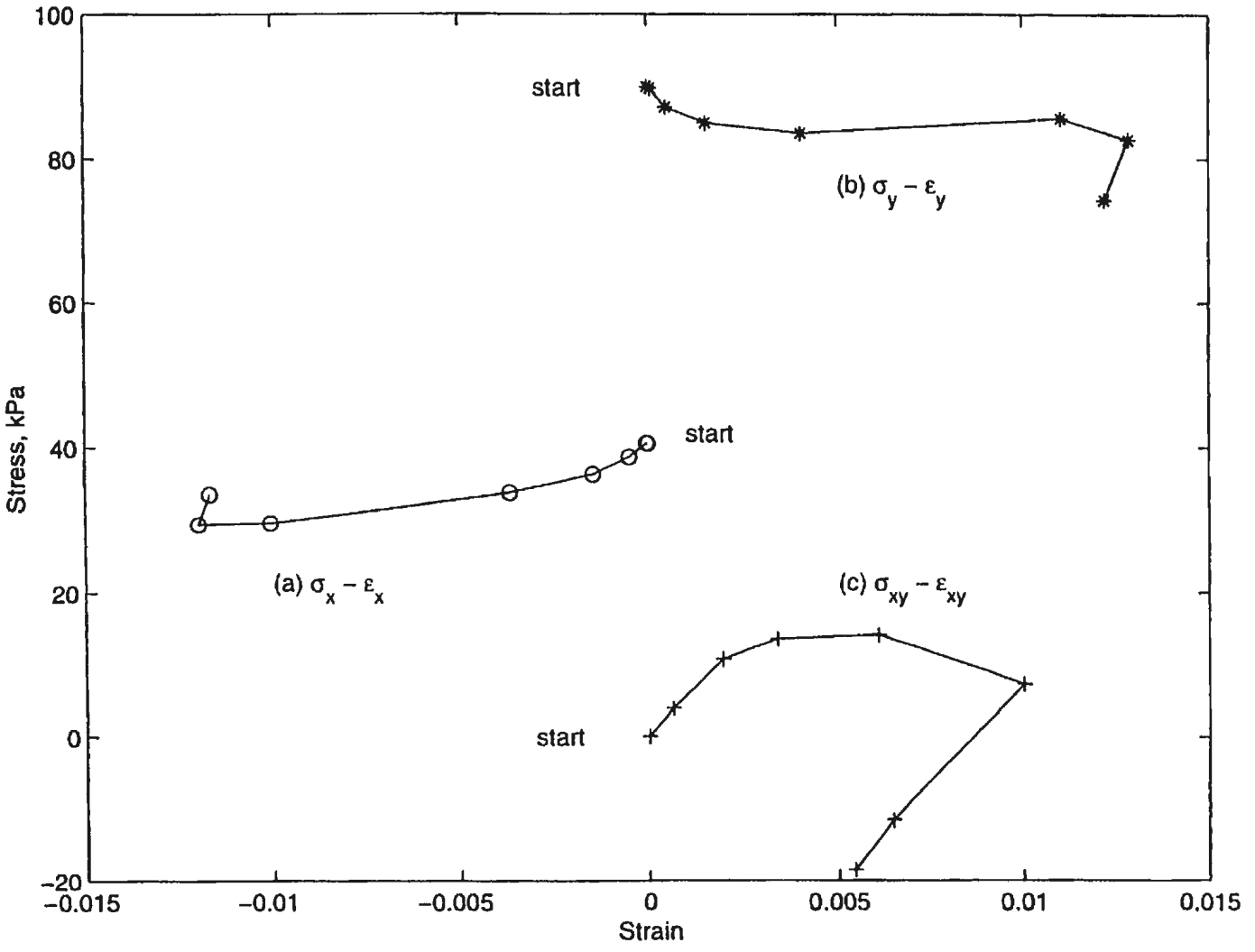

Figure 8.34 Stress variation in element D

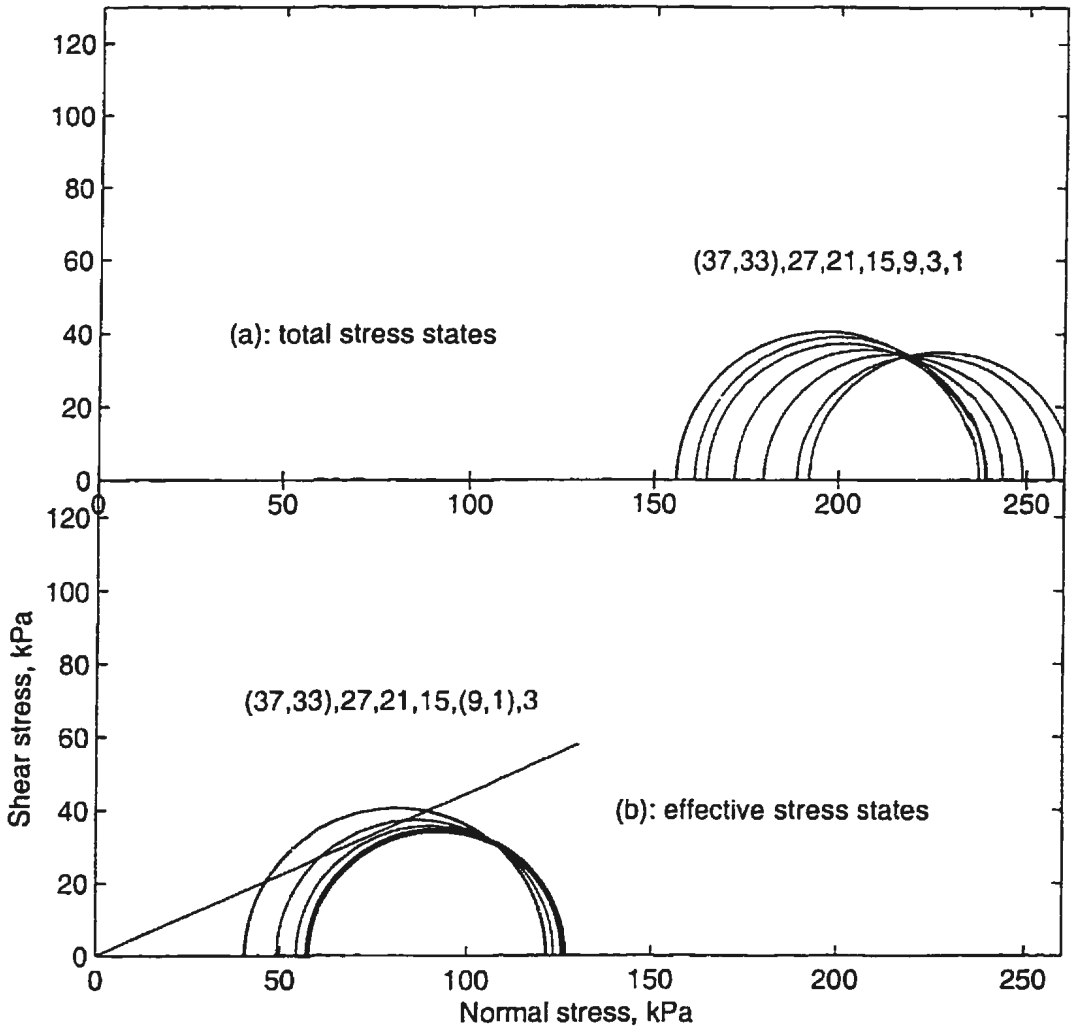

Figure 8.35: Stress path and rotation of principal stress directions in element D

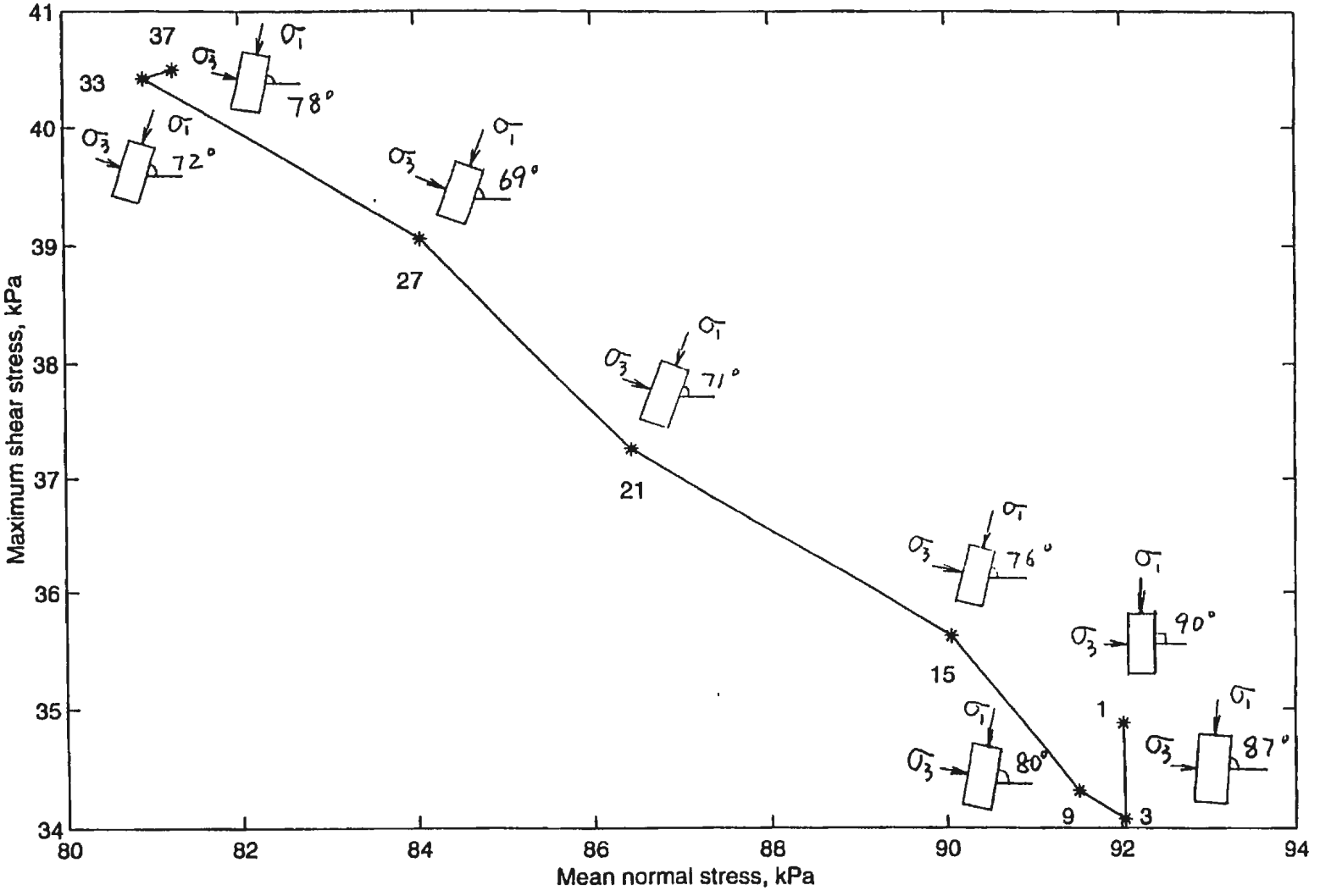

Figure 8.36: Variation of the stress state in element D during excavation

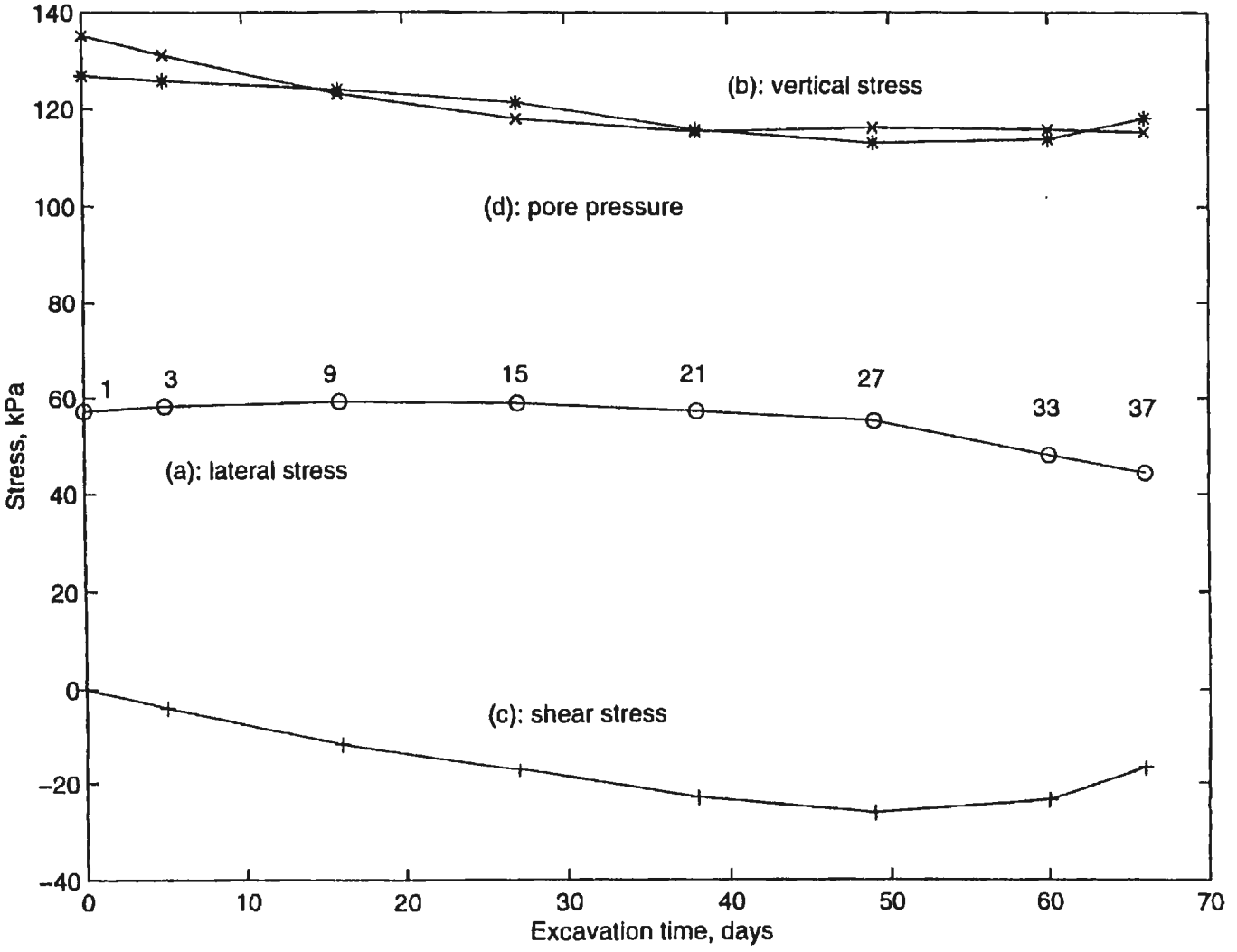

Figure 8.37: Relation of stress and strain in element D

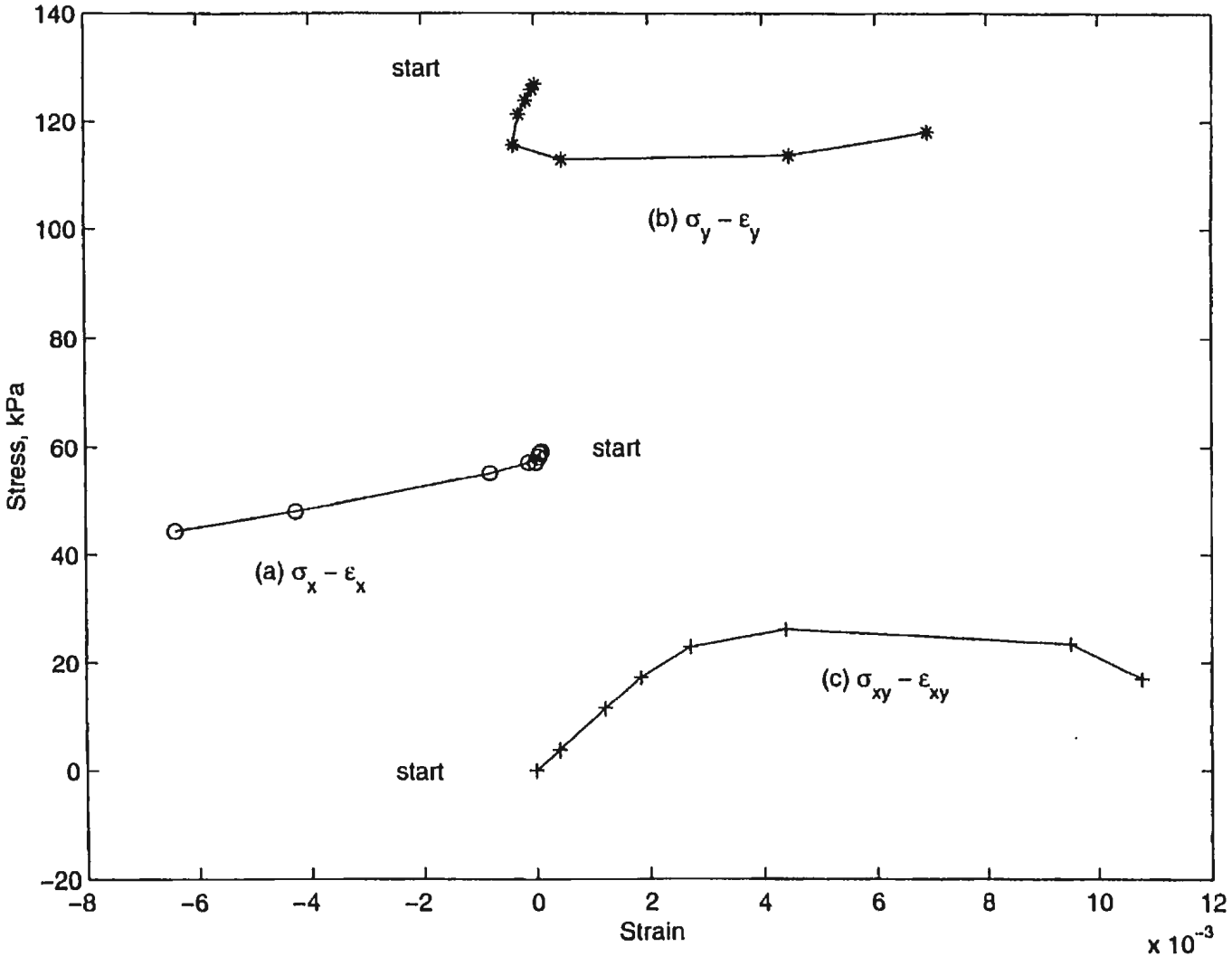

8.2.5 Earth pressure on the sheet piles during excavation

The balance of the earth pressure on the back of the sheet piles and the forces in the struts at the final step are shown in Fig. 8.38. During the process of excavation, the pressures in front and on the back of the sheet piles are changing. The variation of the pressures on the back and in front of the sheet piles are shown in Fig. 8.39. The comparison of the earth pressures and the result of the methods suggested by Peck and Tschebotarioff are shown in Fig. 8.40.

Fig. 8.39 (a) shows the earth pressure on the back of the sheet piles. The K_0 line shows the lateral static earth pressure before excavation. K_a line shows the active earth pressure according to Rankine theory. It is shown that the lateral earth pressure on the sheet piles during excavation is not on the line of active earth pressure but there is a great difference. The actual earth pressure on the sheet pile has an S shape. The upper part of the line is greater than the static earth pressure, the middle part is smaller than the active earth pressure and the lower part increases to become larger than the static pressure.

The S shape is a consequence of the deformable nature of the sheet piles. The large earth pressure at the bottom pushes the sheet pile into the excavated area, which is controlled by the struts. With a different earth pressure on the back of the sheet pile and the action of the struts, the deflection of the sheet piles toward the excavated area is not uniform. From beam theory, the deflection varies. At the upper part, the sheet piles tends to deflect backward and the lower part tends to deflect forward. Therefore the back pressure on the upper part tends to develop

passive earth pressure and the lower part tends to develop active earth pressure. However because of the plasticity of the soil, the passive earth pressure cannot be fully developed. As a result, the pressure on the upper part is larger than the static earth pressure but much less than the passive earth pressure. It is interesting that, at the middle part of the sheet pile, the back earth pressure is much less than the active earth pressure. This is because of the function of the arch. This function also results in the reduction of the vertical earth pressure on the upper part of the soil on the back of the sheet piles.

Fig. 8.39(b) shows the earth pressure in front of the sheet piles. This earth pressure is supposed to be a passive earth pressure because of the large displacement of soil towards the excavated area. It should be noticed from the figure that the actual earth pressure at the final step is larger than the passive earth pressure according to the Rankine theory which is represented by K_p line. The cause of this error is not known. There is no way to investigate this problem as the code of ABAQUS is not available.

The design of the braced support system is made according to the total earth pressure on the sheet piles. These pressures are shown in Fig. 8.40, in which the envelopes suggested by Peck and Tschebotarioff are also drawn. This figure also shows that if the struts are applied after the corresponding layer of soil is removed, there is only one extremum of earth pressure on the back of the sheet piles. This is different from the simulation to the centrifuge model in chapter 6 where the struts were in position before excavation and there were two extremums of earth pressure on the back of the sheet plate.

It is shown in the figure that the maximum pressure on the back side of the sheet piles is smaller than the value suggested by Peck. The distribution of the total earth pressure on the back of the sheet piles is similar to the profile given by Tschebotarioff, but the actual values are different. The envelope suggested by Tschebotarioff underestimates the maximum earth pressure and vertex is above his suggestion. However, it should be noticed that the envelopes are based on the assumption that the sheet piles are regarded as the simple beams supported by the struts.

8.2.6 Lateral displacement of the sheet piles

The lateral displacement or deflection of the sheet piles is another important factor in evaluating the stability of the bracing system. A large deflection means the buckling of the sheet pile and the failure of the bracing system.

The deflections of the sheet piles during the excavation are shown in Fig. 8.41. As the excavation proceeds, the deflection of the sheet piles becomes larger and larger and the location of the maximum deflection moves lower and lower. The final maximum deflection is 0.1072 m or 10.72 cm at the depth of 10 m which is at the position of the lowest layer of struts.

8.2.7 Bottom heaving during excavation

Bottom heaving during the excavation is shown in Fig. 8.42. The lines in the figure represent the upward displacement of the bottom at different steps during

the excavation. It is clear that the profile of the last step includes the values of the previous steps. The curves have a maximum close to the sheet piles and are flat in other areas of the bottom. The maximum value is restricted to some degree by the node at the corner of the excavations. This restriction is the result of not using contact elements.

8.2.8 Surface settlement of the ground during excavation

The surface settlement is shown in Fig. 8.43. During the excavation, the ground surface behind the sheet pile exhibits settling at all times. At the first, the settling is nearly homogeneous, and at later stages, maximum and minimum values are developed. For the excavation at the last step, the maximum settlement is about 7 meters behind the sheet piles with a value of 7.5 cm. The minimum value is about 15 meters behind the sheet piles and has a value of 3 cm. Even with the restriction of displacement at the node behind the top of the sheet piles, the profiles provide a reasonable view of the settlement. The profile of the settlement at the last step provides an envelope which includes the settlements in the previous steps.

8.2.9 Summary

Peck (1969) pointed out that, the volume of the settlement of the surface of soil surrounding the excavation is approximately equal to the volume of the deflection of the vertical walls toward the excavated space. Although agreement with this prediction does not in itself validate the numerical model, it is nevertheless an

interesting comparison to make. In order to check this prediction, the volume of settlement per meter along the length side of the excavation in different steps is shown in Fig. 8.44 as well as the corresponding volume of deflection. It seems that at the same step, the volume resulting from settlement is larger than the volume from deflection. This does not include the possible larger settlement behind the top of the sheet piles. This settlement is restricted by not using the contact element.

However, the figure shows that the difference between the volumes is a small portion of the volumes. Therefore the two volumes are comparable to each other. This conclusion implies that an effective way to reduce the settlement of the ground surface is to use a stronger bracing system to reduce the lateral displacement of the sheet piles.

Figure 8.38: Earth pressures on the sheet piles at final step of excavation

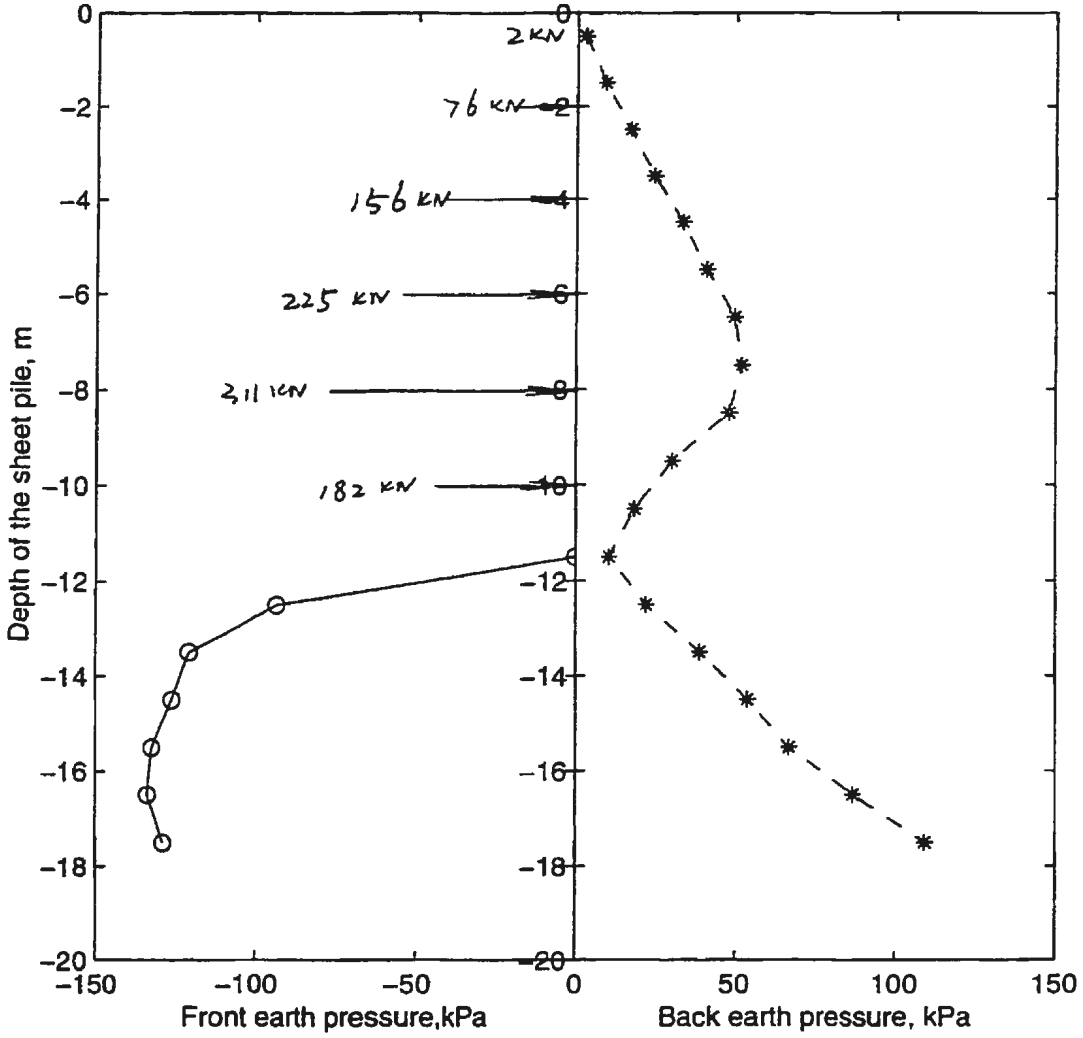

Figure 8.39(b)

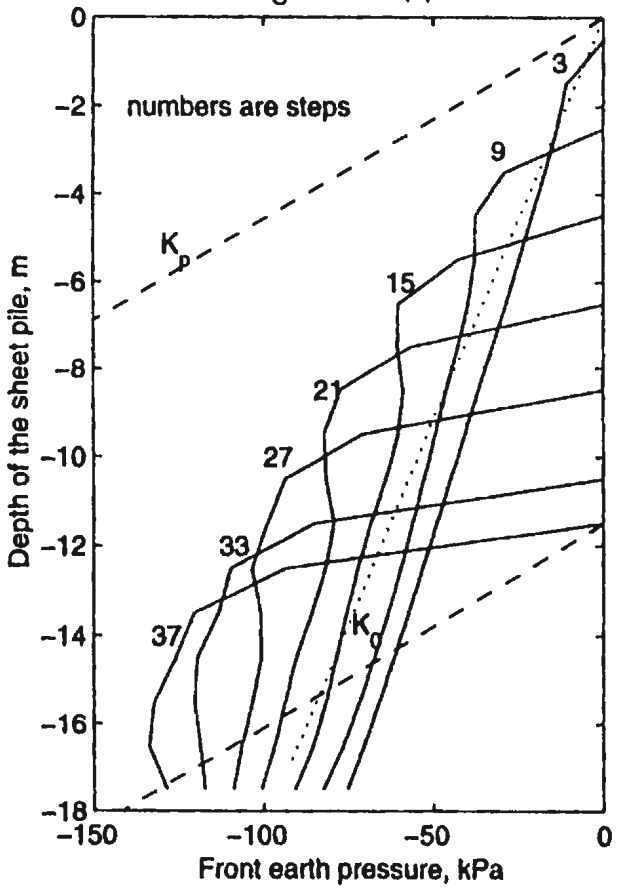

Figure 8.39(a)

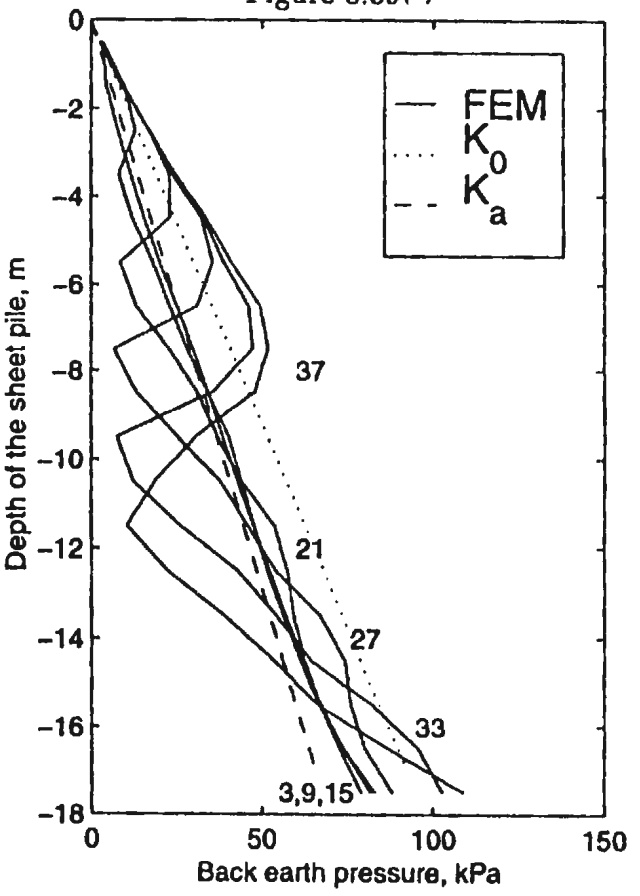

Figure 8.40: Earth pressure on the back of a sheet pile

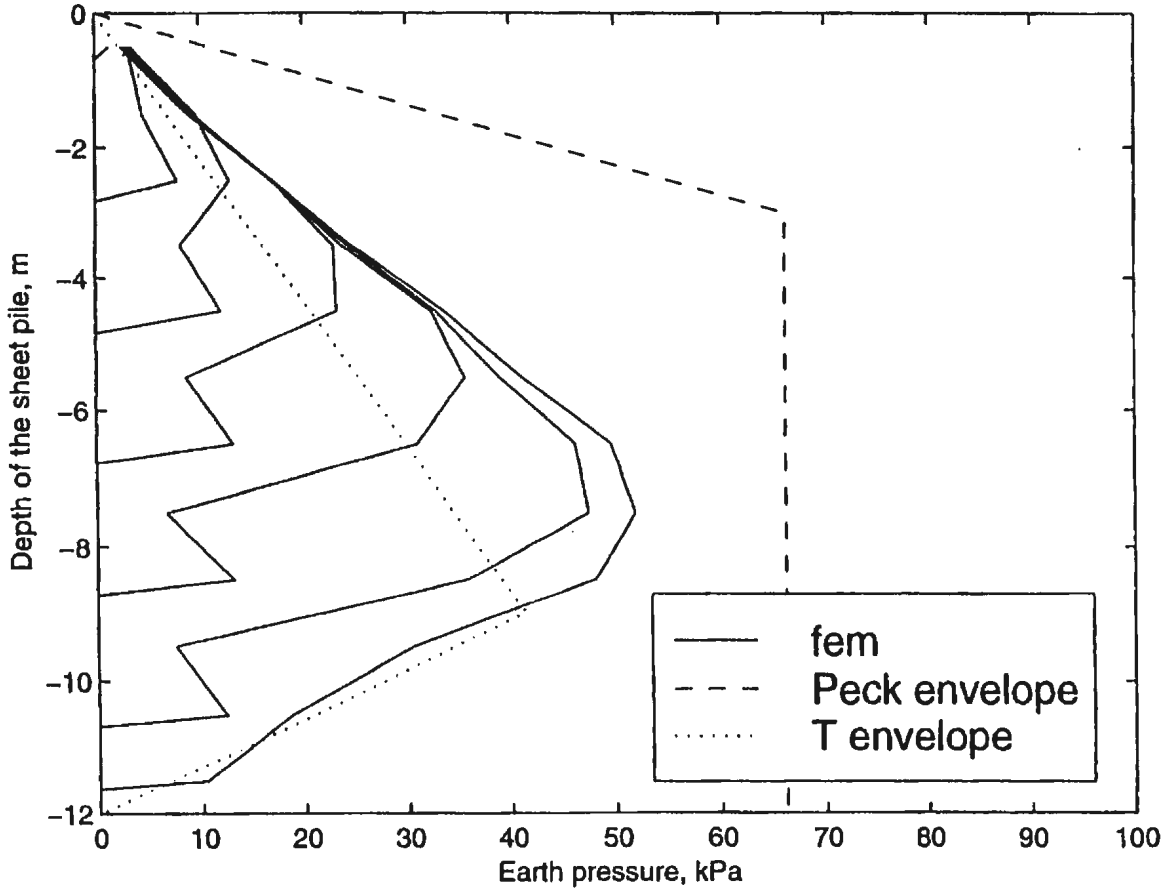

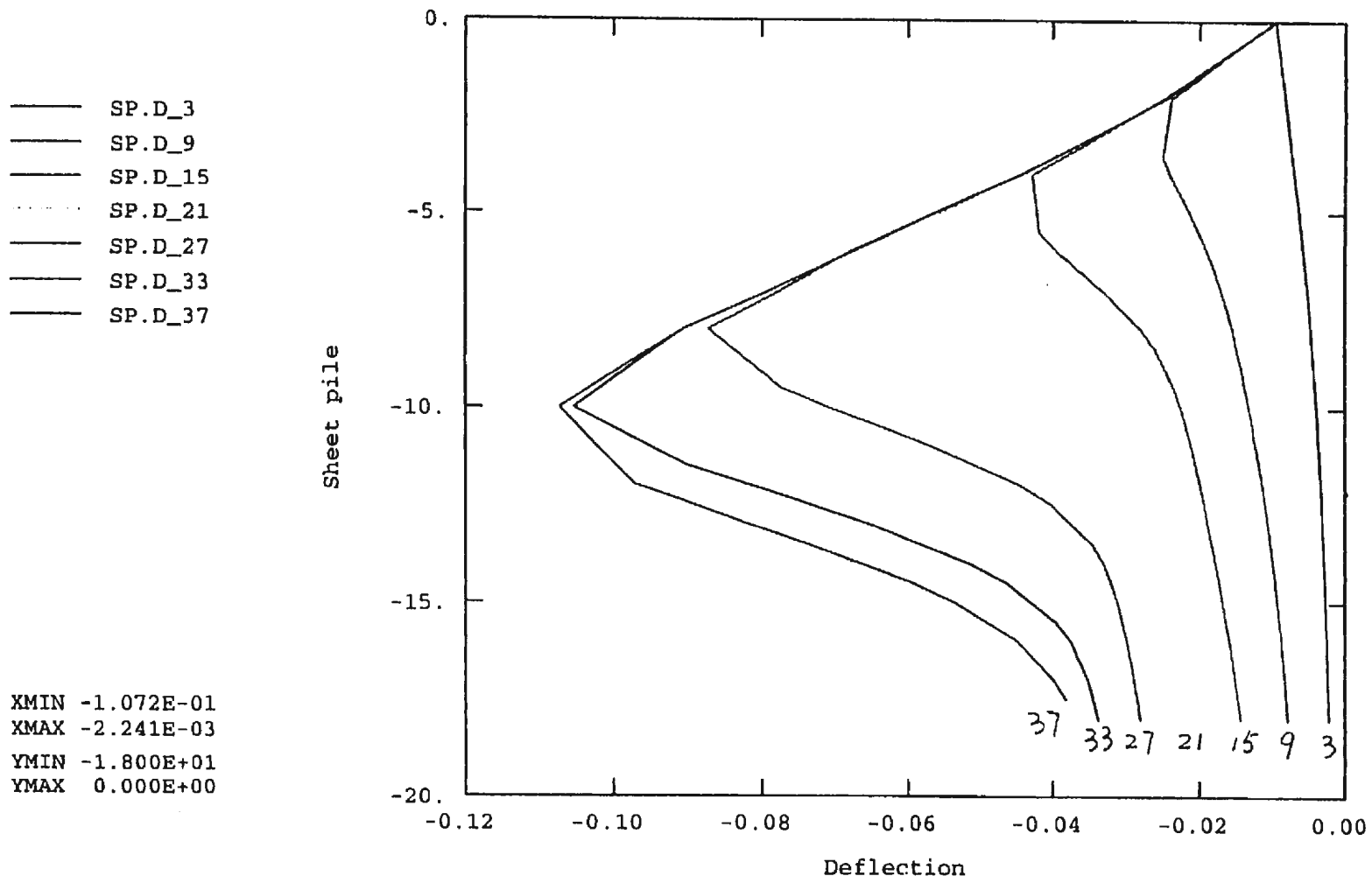

Figure 8.41: Sheet pile deflections during excavation

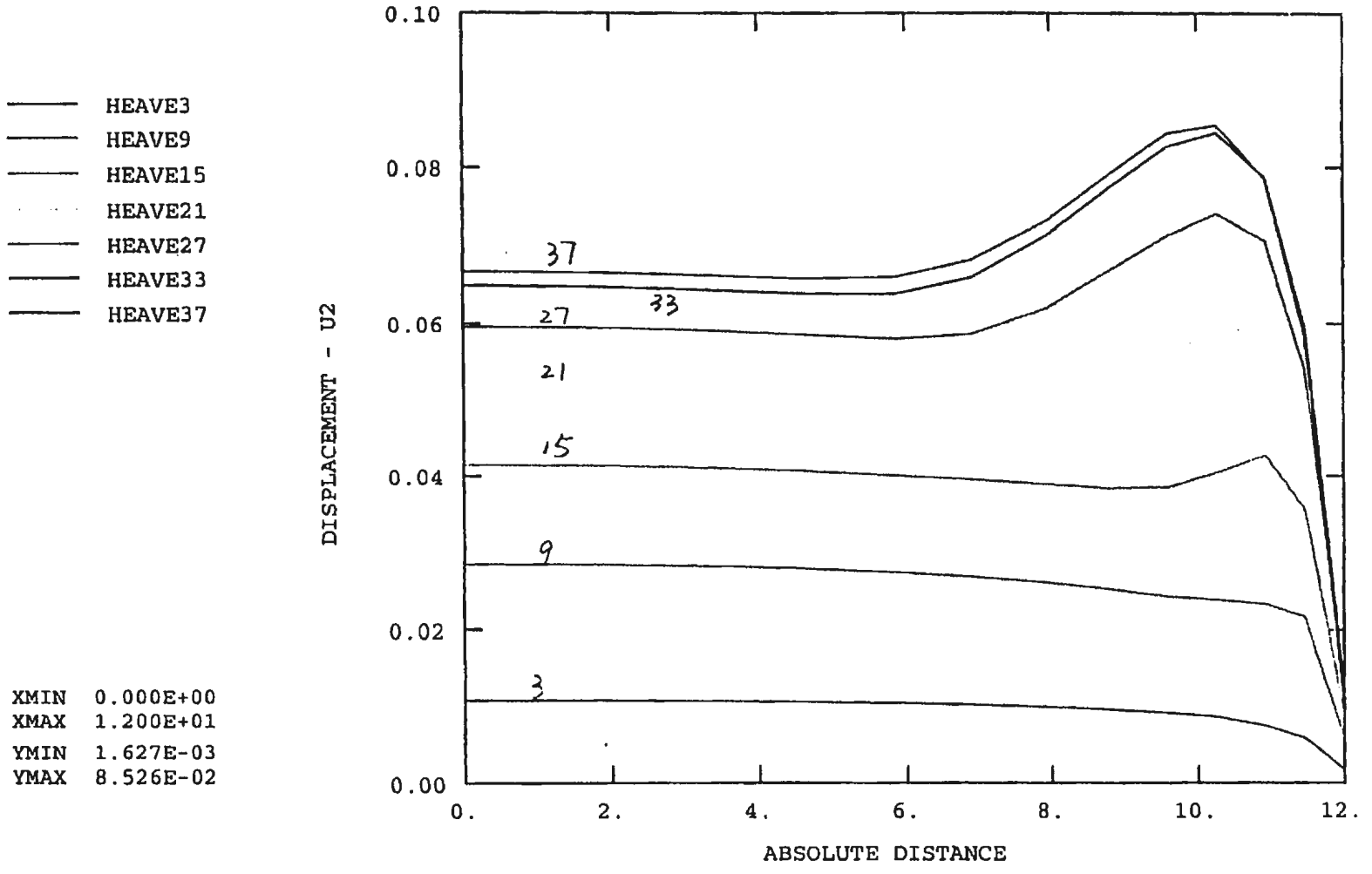

Figure 8.42: Bottom heaving during excavation

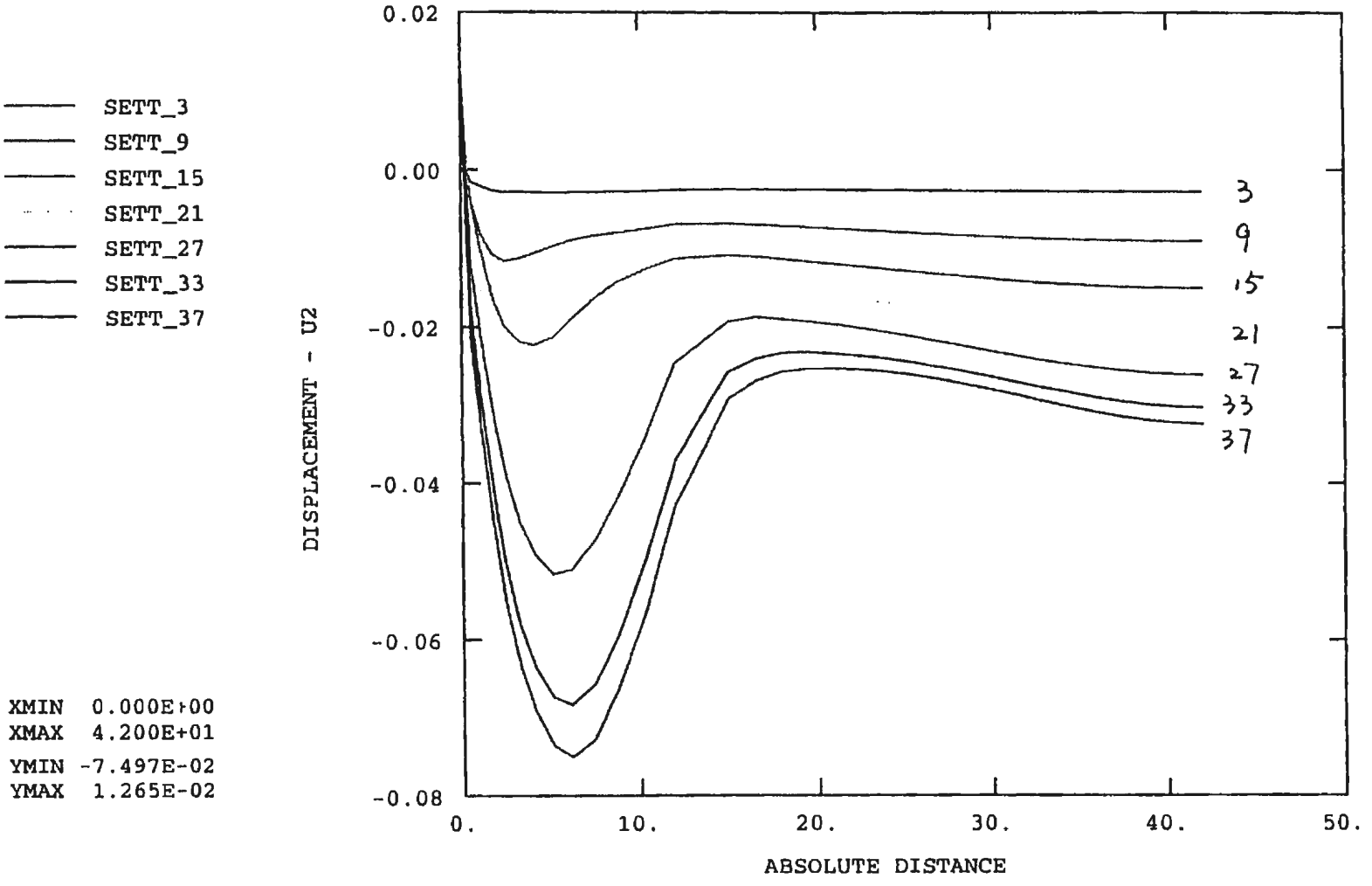

Figure 8.43: Surface settlement during excavation

Figure 8.44: Comparison of the areas of settlement and deflection

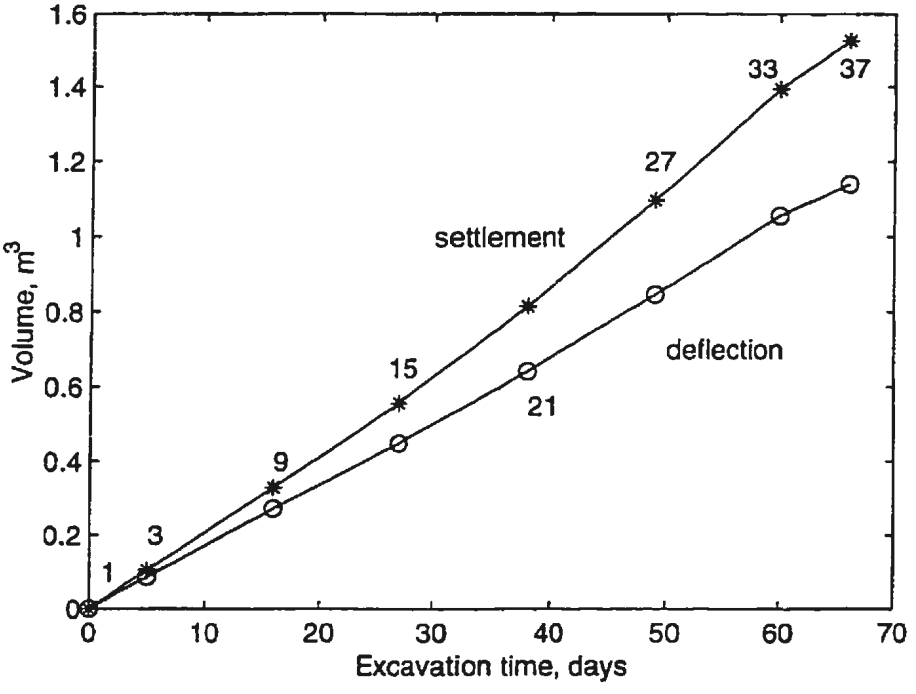

8.3 Earth Pressure on the Sheet Piles and the Forces in the Struts during Excavation

The earth pressure on the sheet piles is of most concern for the stability of the bracing system, since a large earth pressure may result in the buckling of the sheet piles and struts as well as a large lateral displacement of the sheet piles.

Fig. 8.45 shows the earth pressures in front and on the back of the sheet piles with the variation of the Cam-clay parameters of the soil. The soil parameters varied are M, λ and κ for values as shown in Fig. 8.45. Fig. 8.46 shows the variation of the bracing system for different values of the sheet thickness, the stiffness of the struts (kN/m/m) and the distance between the strut layers.

For the soil parameters, it is shown that a large difference in the earth pressures results from the variation of the parameter M in Cam-clay model. The variation of the parameters λ and κ do not result in a significant difference in the distribution of the earth pressures. This is reasonable because the increase of the parameter M implies an increase in the value in the angle of internal friction ϕ, and an increase of value ϕ means an increase in the strength of the soil. When the strength of soil is increased, the soil would apply smaller earth pressure on the sheet pile. This could be observed in the first figure in Fig. 8.45 (M=0.941, marked +). On the other hand, the figure also shows an increase of the earth pressure on the sheet piles from the soil at the bottom of the excavation.

The finite element analysis also shows that if the parameter M is reduced to

0.607 or the angle of internal friction ϕ is reduced to 16°, the last layer of the soil which is one meter thick cannot be excavated because of large bottom heaving.

It is interesting that the earth pressures on the sheet piles change little when increasing the stiffness of the sheet piles, or increasing the stiffness of the struts, and even when applying more layers of struts. The variation of the stiffness of the sheet piles and the struts does not affect the distribution of the forces in the struts. This is shown in Fig. 8.48. The effective factor is the variation of the vertical distance between the layers of the struts, in other words, the number of the layers, which changes the forces in the struts. This is obvious, since the distribution of the earth pressures does not change. The more layers of struts would result in less force in each strut.

However it should be noticed that the phenomenon that the earth pressure does not vary with the variation of the stiffness of the sheet piles and the struts is based on the assumption that the stresses in the sheet piles and the struts do not reach the value of buckling during the excavation. This was done by inputting only the parameters of elasticity in the programs for the sheet piles and struts. Even if the earth pressure does not change, the stresses in the sheet piles and the struts are different between the cases.

As to the variation of the parameters of the soil, Fig. 8.47 shows that only the parameter M affects the distribution of the forces in the struts very much. It can also be noticed from Fig. 8.47 that at the final step of an excavation, the first layer is in tension. This is because of the large bending of the sheet piles toward

the excavated area resulting in the displacement of the first layer toward the back of the sheet piles. As a result, the struts are in the state of tension. This cannot happen in actual practice because the struts are not fixed onto the sheet piles.

Figure 8.45: Variation of earth pressures with clay parameters

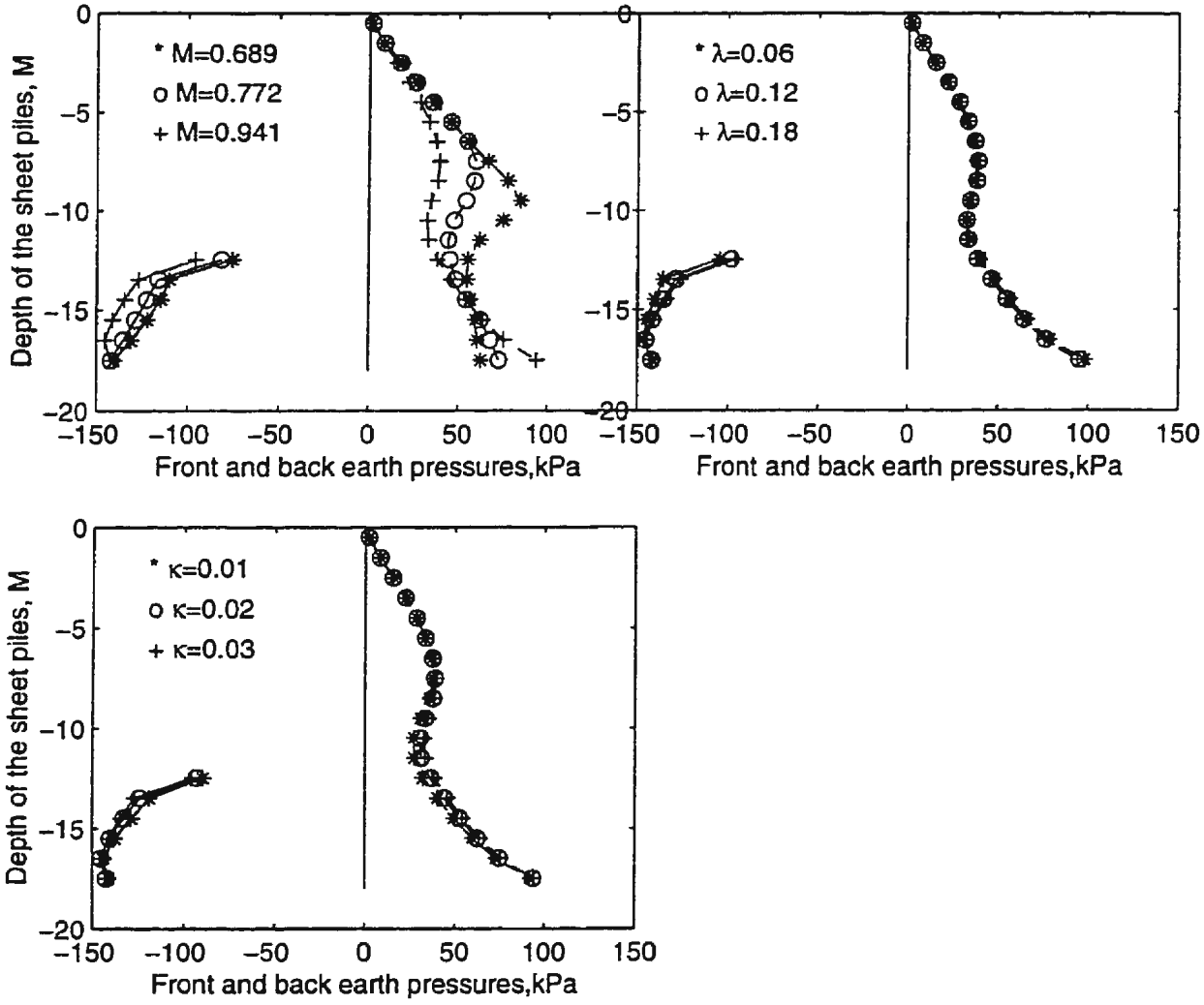

Figure 8.46: Variation of earth pressures with bracing parameters

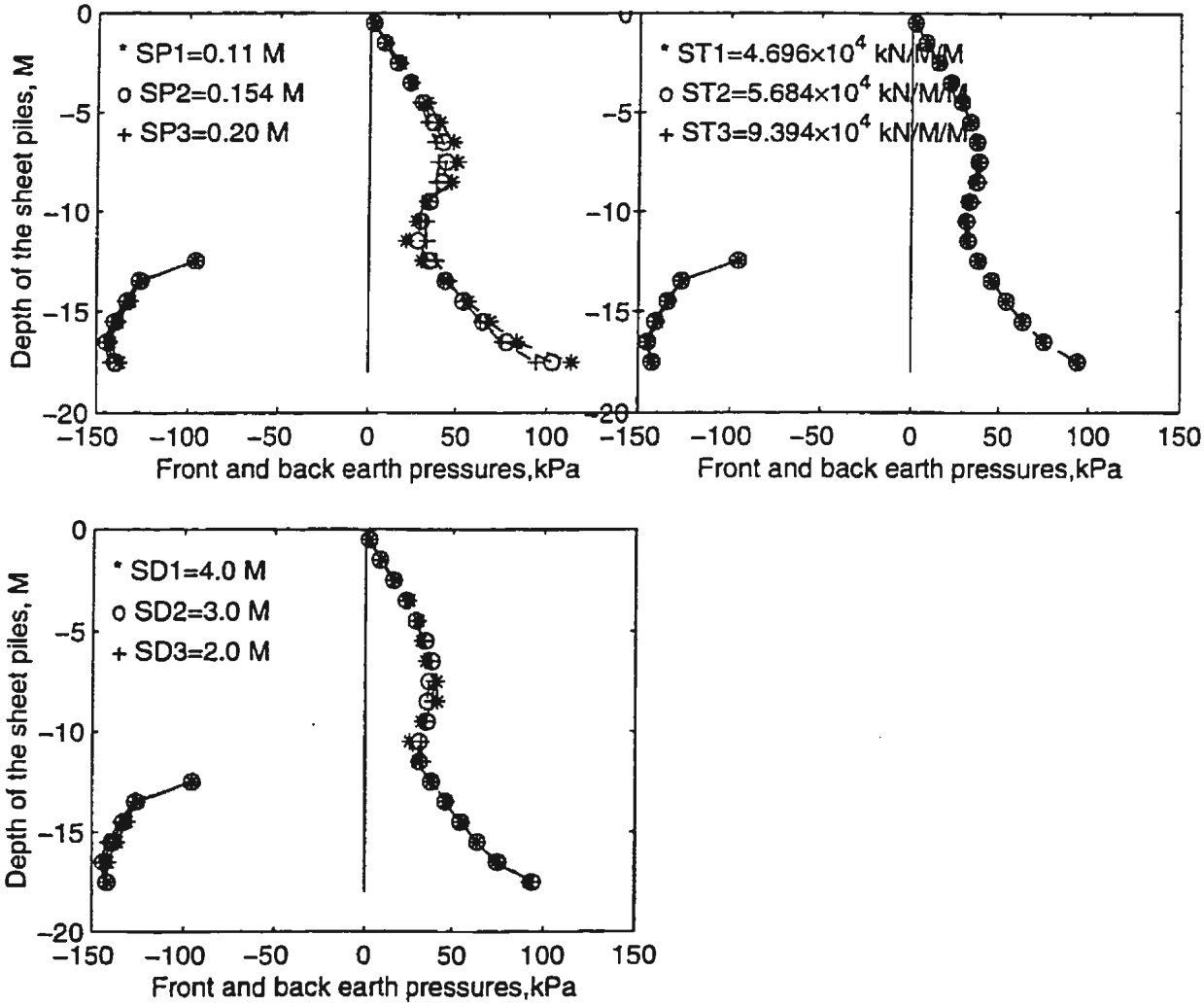

Figure 8.47: Variation of strut forces with clay parameters

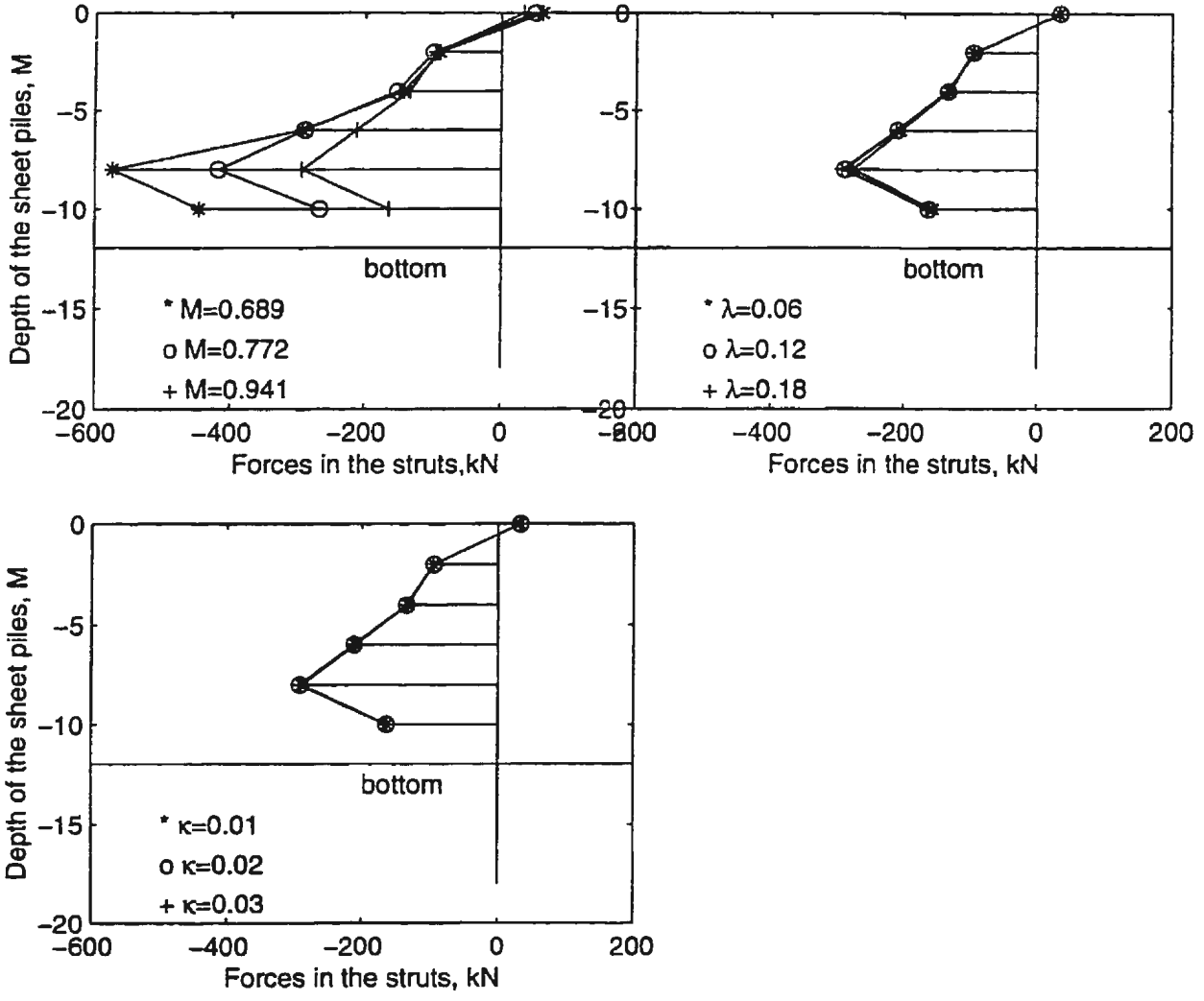

Figure 8.48: Variation of strut forces with bracing parameters

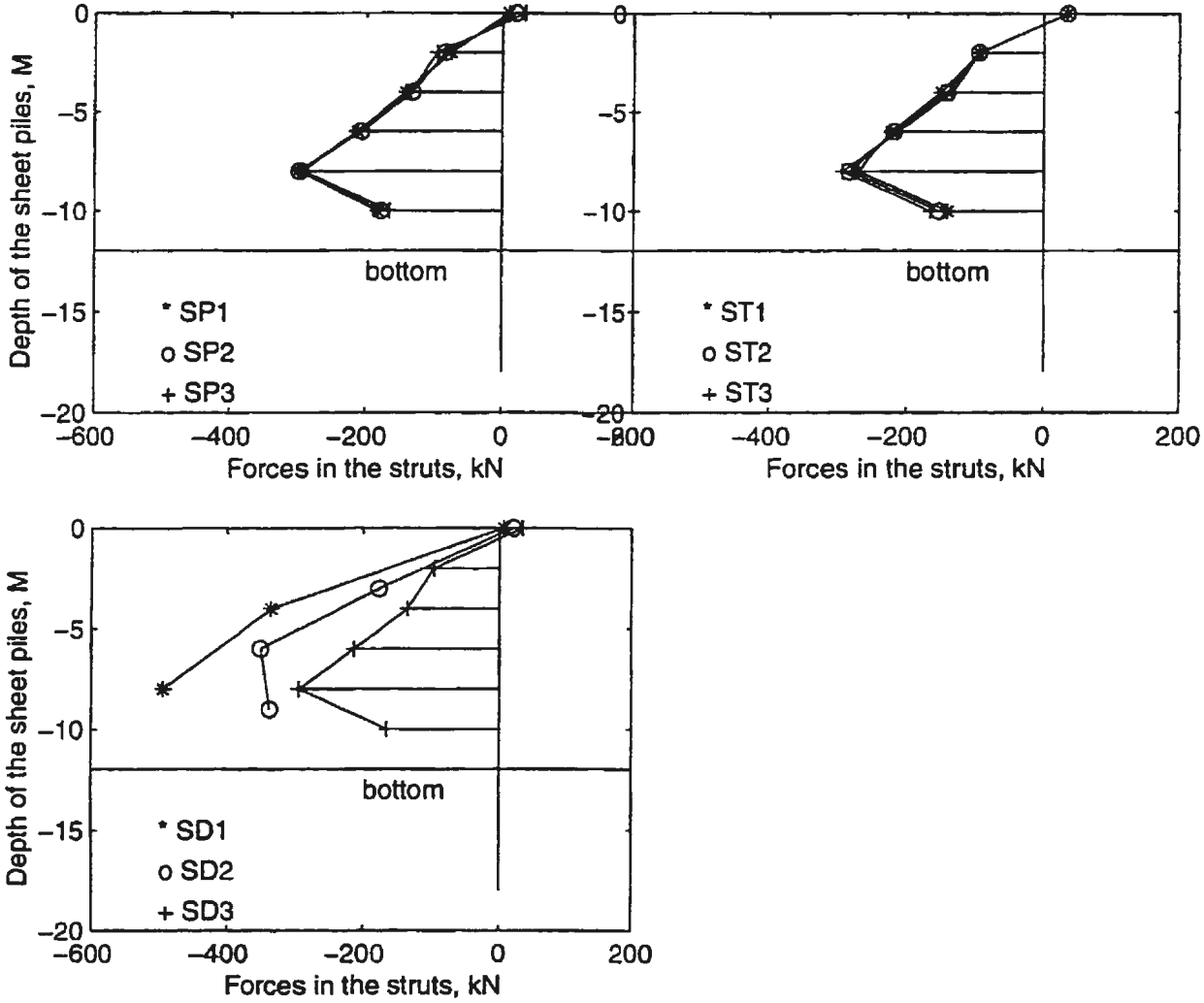

8.4 Lateral Displacement of the Sheet Piles

The development of the lateral displacement may result in problems for further excavation. Fig. 8.49 shows the variation of the final lateral displacement of the sheet piles with soil parameters. It is shown that the parameter of M has a great effect on the lateral displacement. With a small value of M, the maximum value of displacement happens at the toe of the sheet piles. When the M=0.689, where $\phi = 18°$, the displacement is several times that of the case when M=0.941 or $\phi = 24°$. However for a higher value of M, the position of the maximum lateral displacement is not at the toe but around the lower third part. The profile of the lateral displacement of the case when M=0.607 implies that the soil is close to failure. With a lower value of M, such as M=0.607 and $\phi = 16°$, the analysis diverges after the excavation reaches the depth of 11 m. The figures also show that the lateral displacement is not sensitive to the variation of the parameter λ and κ, and the maximum value happens close to the lower third points.

Fig. 8.50 shows the variation of the lateral displacement with the variations in the bracing system. With the variation of the stiffness of the sheet piles and the struts, there are some changes in the distribution of the lateral displacement. While the variation of the stiffness of the sheet piles results in the larger variations of the lateral displacements, the reduction in the number of layers of struts does not result in a large variation. With the same stiffness three layers of struts only results in about 30% larger lateral displacements compared with applying six layers of struts where the vertical distances between the layers of struts is reduced in half.

Peck pointed out that the stiffness of the sheet piles does not affect the lateral displacement very much (Terzaghi and Peck, 1967, p266). The most important factor which affects the lateral displacement of the sheet piles is the property of the soil. In the Cam-clay model, three parameters of the soil are used; M, λ and κ. From these figures we see that the parameter M affects the lateral displacement of the sheet piles the most.

The deformation pattern may be affected by the position of the first layer of struts. There is tension in the first layer struts, and the support points of the struts of the first layer displaces towards to the back of the soil. This is because the springs, which represent the struts, are fixed to the sheet piles. A higher position for the first layer helps to reduce the lateral displacement at the top area of excavation. However, if the position is lower or the stiffness is less, then the deflection pattern of the sheet piles is different, where the largest displacement happens at the top of the excavation.

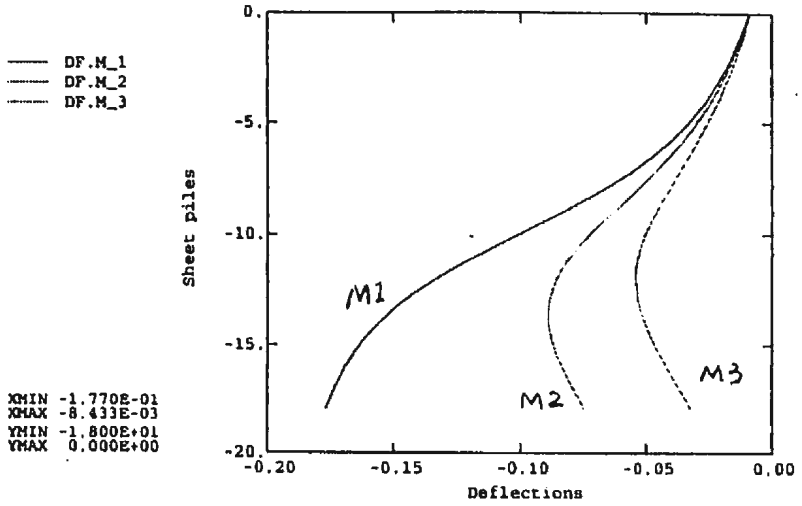

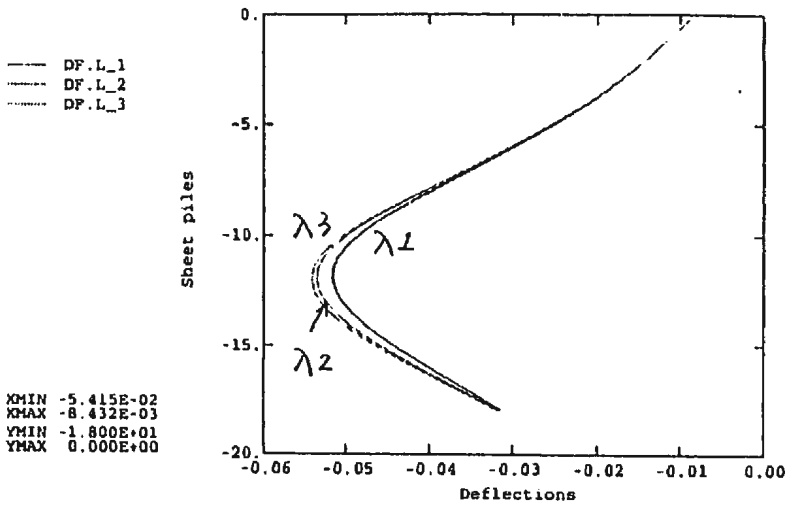

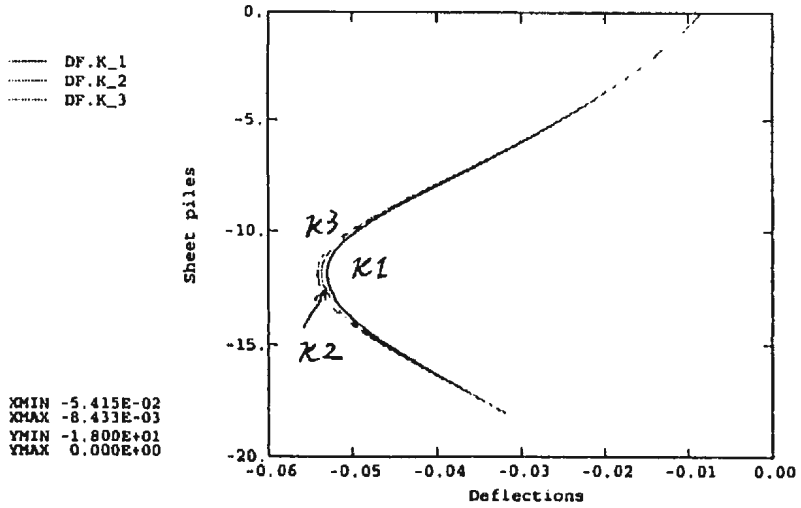

Figure 8.49 Variation of sheet pile deflection with clay parameters

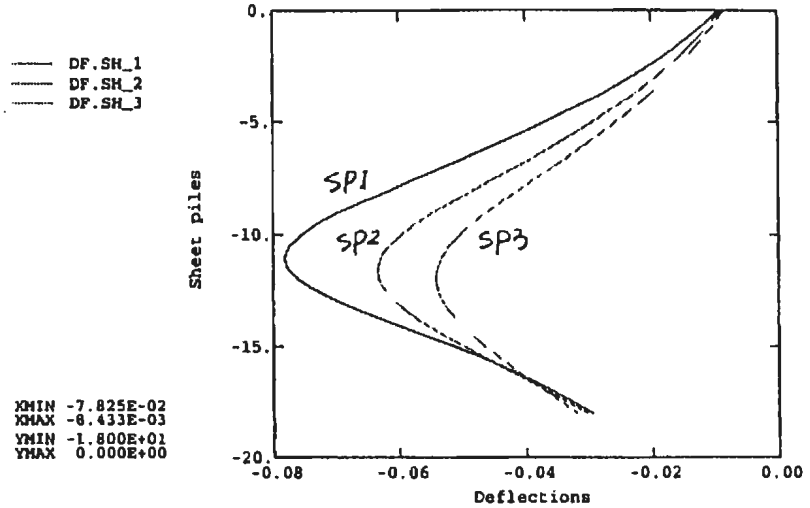

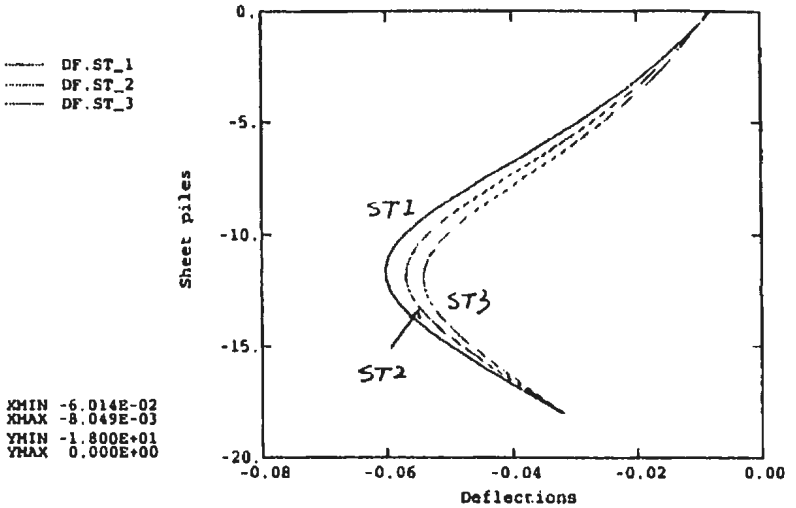

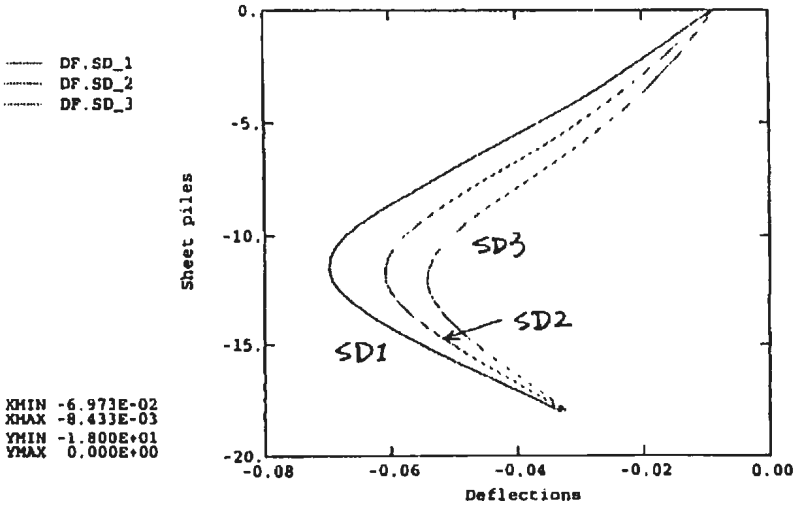

Figure 8.50 Variation of sheet pile deflection with bracing parameters

8.5 Bottom Heaving during Excavations

Bottom heaving is defined as the upward displacement of the bottom of the excavation. Large bottom heaving may cause three problems: failure of the foundation; disturbance of soil strength; vertical movement of the vertical supports – failure of the bracing.

Bottom heaving is composed of two parts: elastic rebounding of the bottom and plastic deformation. Elastic rebounding can be reduced by some special construction methods. One way is to only excavate the trenches for the footing walls in the last layer instead of excavating the whole layer. After the footings have been constructed, the soil between the footings is excavated alternatively for constructing the slab. In such a way, the rebounding of the foundation can be reduced to a satisfactory value. Plastic deformation may be avoided theoretically if the soil at the bottom is strong enough or if the excavation is not too deep. However in most cases, plastic heaving should be considered seriously.

Fig. 8.51 shows the variation of the bottom heaving with the soil parameters while Fig. 8.52 shows the variation with the stiffness of the bracing. The figures shows that only parameter, M, greatly affects the bottom heaving. In other words, the safety of the bottom of the excavation is determined by strength of the soil. It cannot be improved by increasing the stiffness of the bracing system.

With a reduction of the soil strength, the pattern of bottom heaving changes greatly. With large internal friction angle, the deformation seems to be elastic and

the bottom heaving is small. The bottom heaves uniformly. However when the internal angle changes from 21° to 18° the heaving is doubled. This implies that the bottom undergoes a large plastic deformation. The soil close to the sheet piles heaves more than the other parts. Extra analysis shows that the bottom fails when the internal friction reduces to 16°.

With Peck's theory, the stability of the bottom heaving is related to the undrained strength of the clay. As shown in Fig. 8.53, for normally consolidated clay,

$$\sin\phi = \frac{(\sigma_1' - \sigma_3')/2}{(\sigma_1' + \sigma_3')/2} \tag{8.1}$$

$$s_u = \frac{\sin\phi}{1+\sin\phi}\sigma_1', \tag{8.2}$$

or

$$s_u = \frac{\sin\phi}{1+\sin\phi}\gamma' H. \tag{8.3}$$

As defined by Peck, the stability number is

$$N_b = \frac{\gamma' H}{c_u}, \tag{8.4}$$

and therefore $N_b = (1+\sin\phi)/\sin\phi$. This equation is shown in Fig. 8.54. The critical value of N_b is 5.14 (section 2.2.4), which means $\phi = 14°$. In this case,

base failure would take place. However, in this analysis, it is shown that even with $\phi = 16°$, that base failure also happens.

From above analysis, it seems that the stability of the bottom depends on the undrained strength and not the excavation depth. However, Peck also pointed out that for soft clay, there is a critical depth of excavation. Beyond this depth, failure would happen (Peck 1969, p259). Therefore it can be concluded that the judgement made from only one parameter may not reflect the real stability of the bottom. However, it is admitted that the strength of the soil plays a major role in the stability of the bottom of an excavation.

In the bottom of an excavation, the position of the largest value of bottom heaving depends not only on the excavation depth, strength of the soil, but also on the width of the excavation. If the width of the excavation is less than the extent of the heaving resulting from the soil load on one side of the excavation, the largest heaving should be in the middle of the bottom of the excavation because of the superposition of the deformation (Tanaka 1994a). However in this analysis, the largest heaving happens close to the sheet piles. This is because the width of the excavation is larger than the possible failure extent, which is shown in the theoretical analysis in section 2.2.4.

Bottom heaving is not necessarily symmetrical in the sections of the excavation. With soil non-symmetrically distributed, heaving may be larger on one side than the other. Other conditions may also result in this situation, such as the drainage condition and even the workmanship.

It seems that bottom failure may happen in two ways: one is that the soil tends to flow around the tip of the sheet piles and push the soil upward to result in a large bottom heaving; the second is that a large pressure on the lower part of the back of the sheet piles causes the sheet piles to push the bottom soil. This allows the soil to develop passive strength and may result in failure if the strength of the soil is not enough. This explains why bottom heaving cannot be reduced by increasing the length of the sheet piles in some cases.

With a given soil, the bottom heaving may be lessened by increasing the strength of the soil. This includes the DM method (Tanaka 1994b) or some construction method such as the trench method.

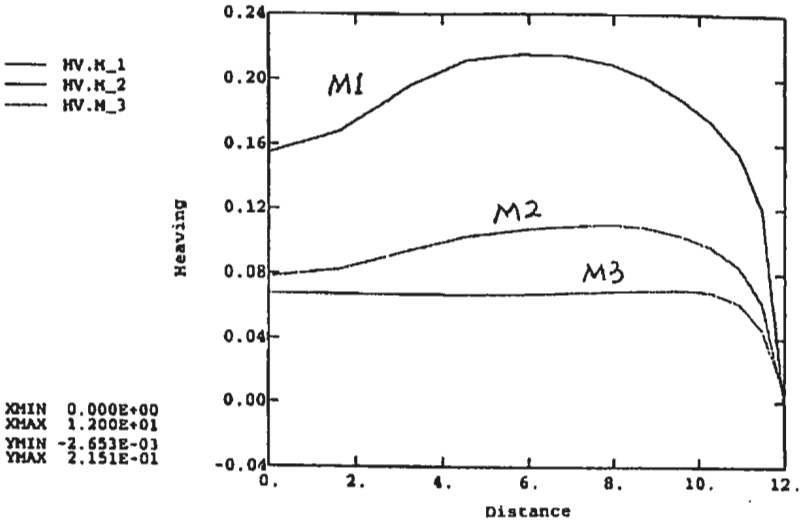

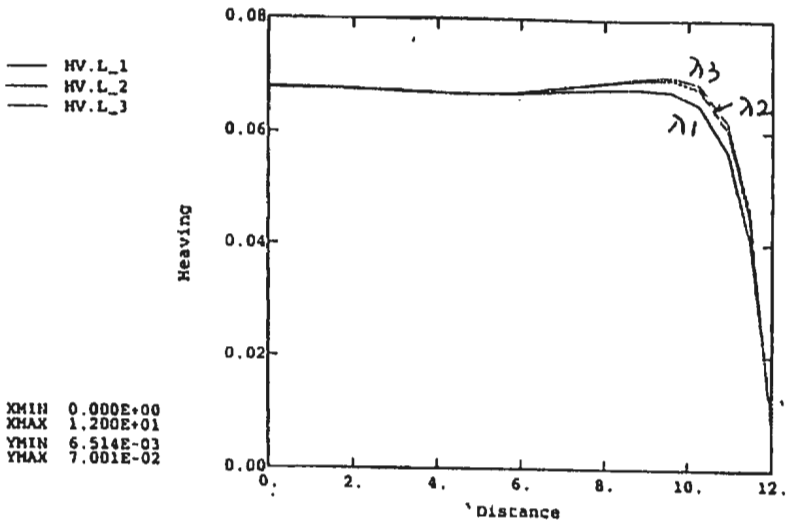

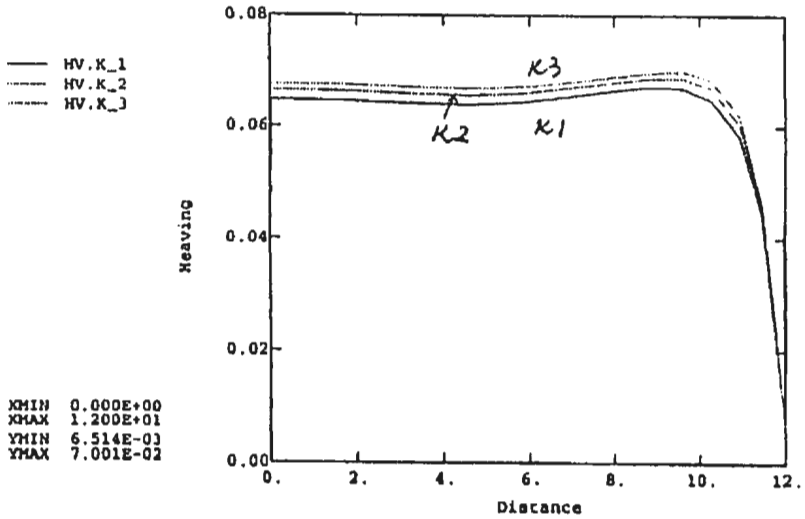

Figure 8.51 Variation of bottom heaving with clay parameters

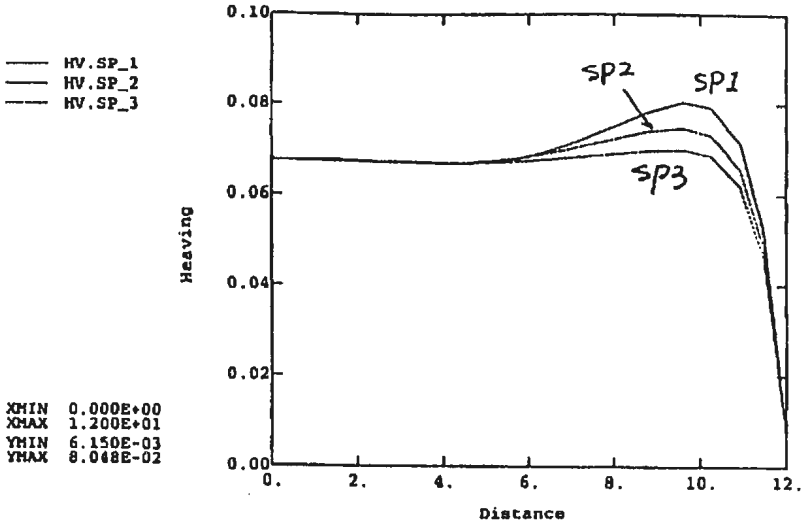

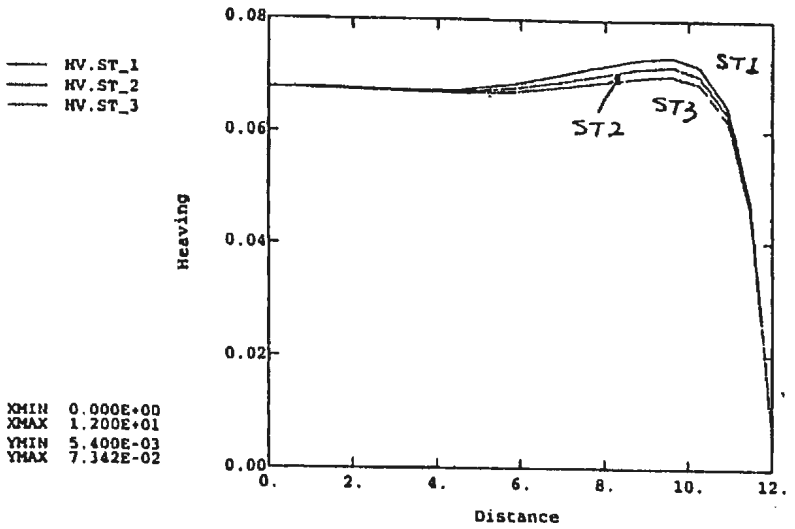

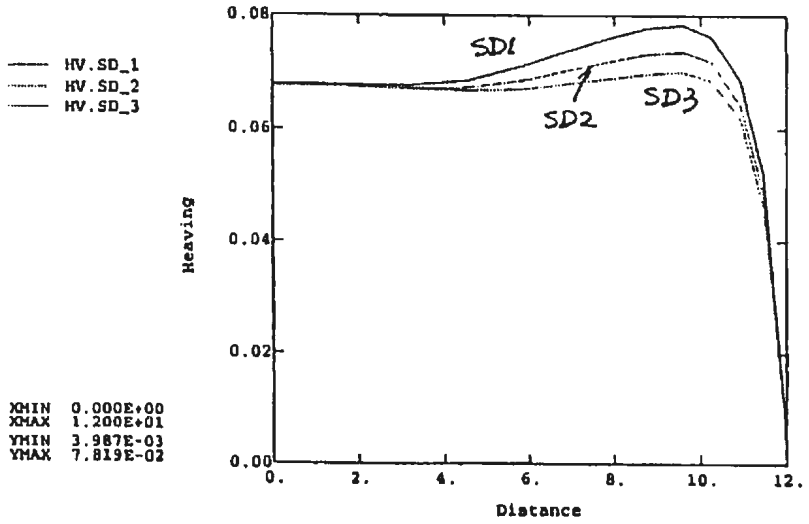

Figure 8.52 Variation of bottom heaving with bracing parameters

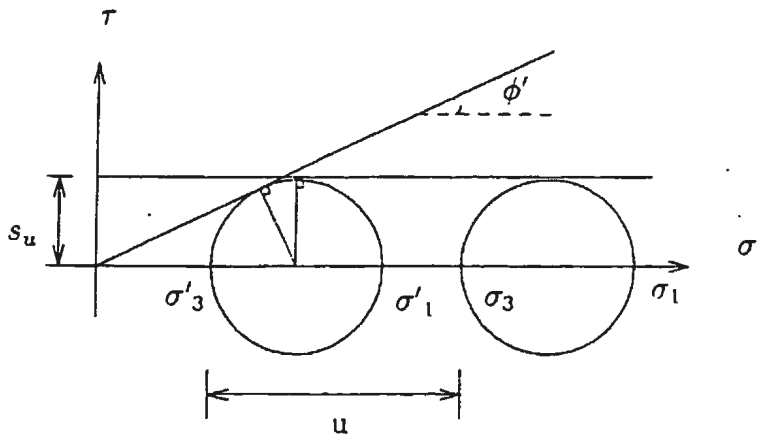

Figure 8.53: Strength of clay

Figure 8.54: Variation of N_b with ϕ

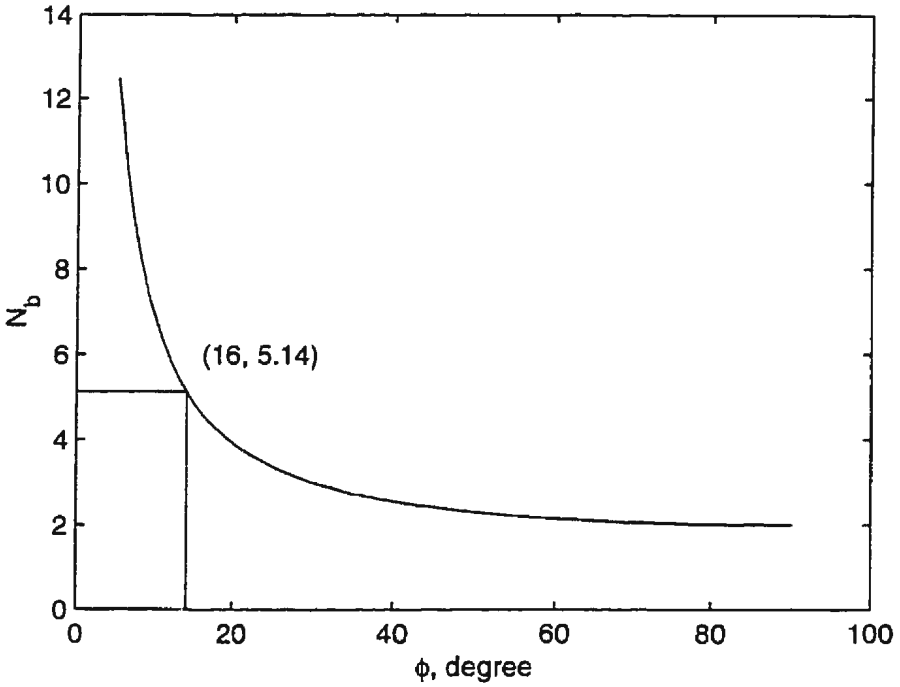

8.6 Surface Settlement of the Ground during Excavation

Surface settlement is defined as the settlement of the ground surface around the excavation. The greatest concern over surface settlement is that this settlement may result in damage to adjacent buildings, utilities and streets. Excavations may cause uneven deformation in the footings of the buildings (if there are any) near the site of excavation, and in turn extra stresses may result in the footing and the body of the building such as the beams, columns and walls.

The magnitude and the pattern of distribution of a settlement are important for engineers to know. This is needed to assess the possible damage to the surrounding installations and to estimate the need for underpinnings to nearby structures. According to different values and patterns of settlement, or different degrees of damage, engineers will use different methods. If the settlement is within a limit, the damage may not happen and no action or protection of the building will be taken. On the other hand, if the settlement is too large, protection should be taken such as underpinning. For some soils, underpinning may not work out. Peck (1969) gave an example where negative friction was produced on the surfaces of the piles of the underpinning, and an uneven settlement still occurred.

O'Rourke, et al (1976) did detailed research on the damage to buildings because of excavation. He pointed out that not only settlement but also the horizontal displacement of the ground surface determine the degree of damage to buildings. Therefore they defined two corresponding parameters: angular and lateral distor-

tion. Angular distortion is defined as the differential settlement between two points along a line perpendicular to the edge of excavation divided by the distance separating them. Lateral distortion is defined as the differential lateral displacement between two points divided by the distance separating them. From their studies, they proposed two criteria: 1) an angular distortion of 1/1000 is recommended as the threshold value for architectural damage to brick-bearing wall structures adjacent to an excavation; 2) an angular distortion of 1/750 is recommended as a conservative lower bound for architectural damage to frame structures adjacent to an excavation.

Fig. 8.55 shows the variation of the surface settlement with soil parameters. The variation of the parameter M results in much more variation in the settlement while other parameters have little effect. The maximum settlement is close to the back of the sheet piles.

However the variation of the bracing system causes a variation in the settlement (Fig. 8.56). Reduction in the stiffness of the sheet piles results in a larger settlement than in the stiffness of the struts. Varying the number of the layers of struts also causes a large settlement. The large settlements are also close to the back of the sheet piles. An increase in the number of layers of the struts may block the construction of the structures and it is more reasonable to increase the stiffness of the sheet piles.

Terzaghi and Peck (1967, p575) suggested that the inevitable large displacement including bottom heaving and the surface settlement might be reduced by adopting

a procedure that does not involve removing the weight of the excavated soil from the entire area at one time, such as the trench method. In some instances the completed base slabs have been temporarily backfilled until the weight of the superstructure has become large enough to compensate for the unloading.

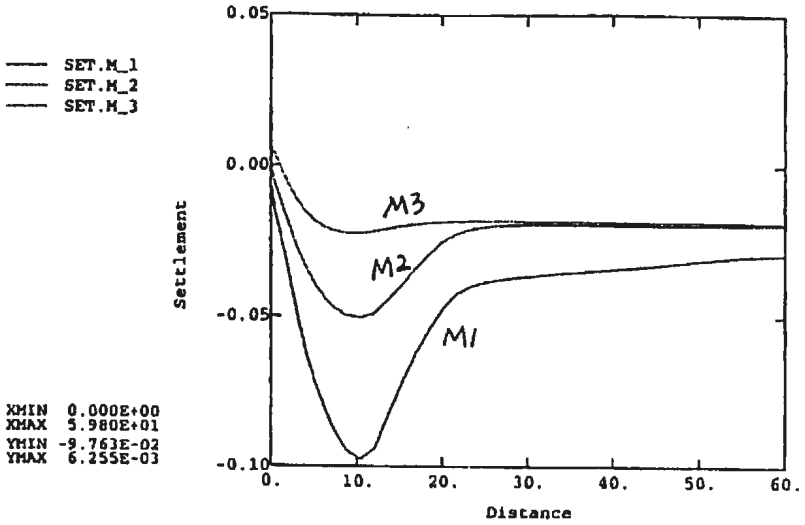

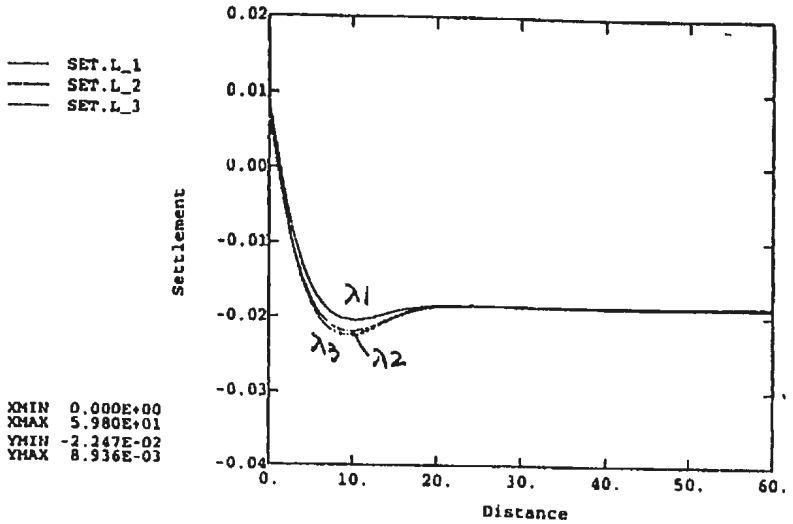

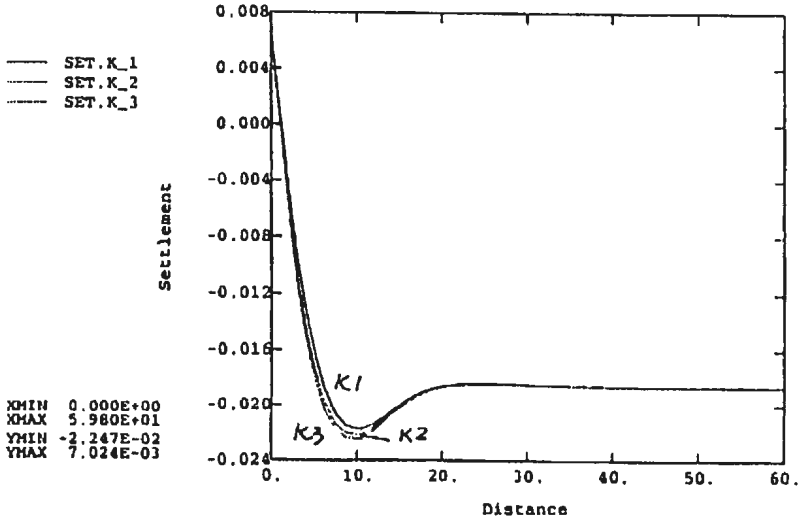

Figure 8.55 Variation of surface settlement with clay parameters

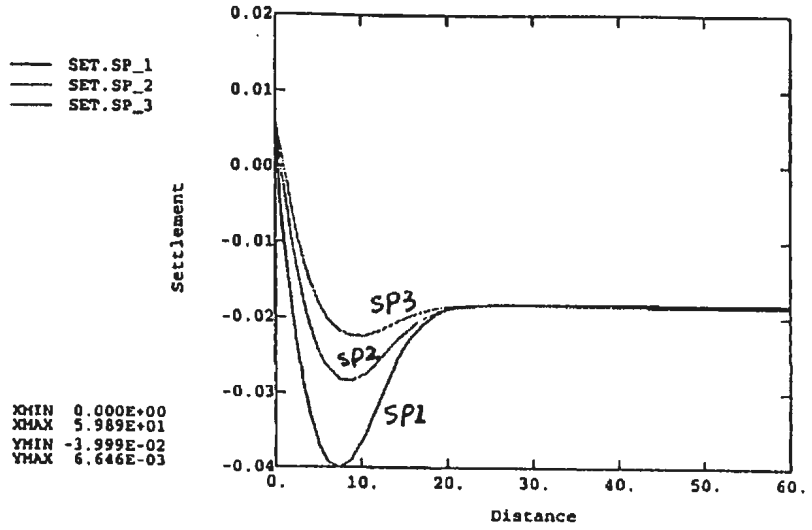

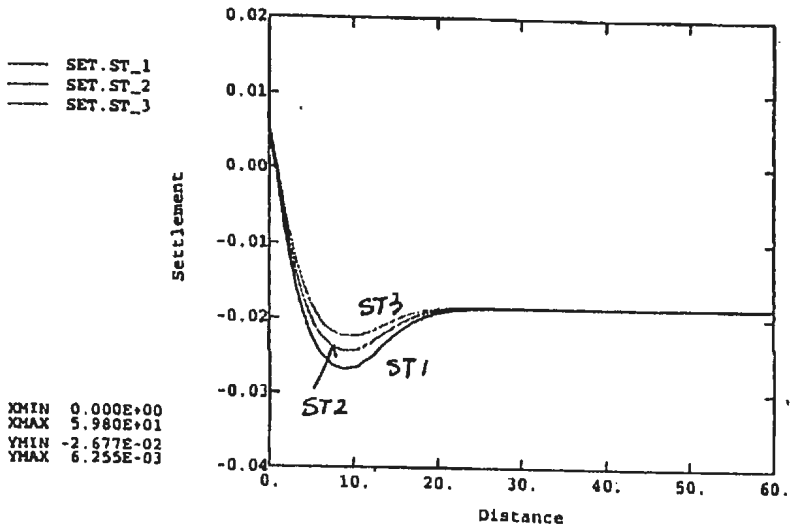

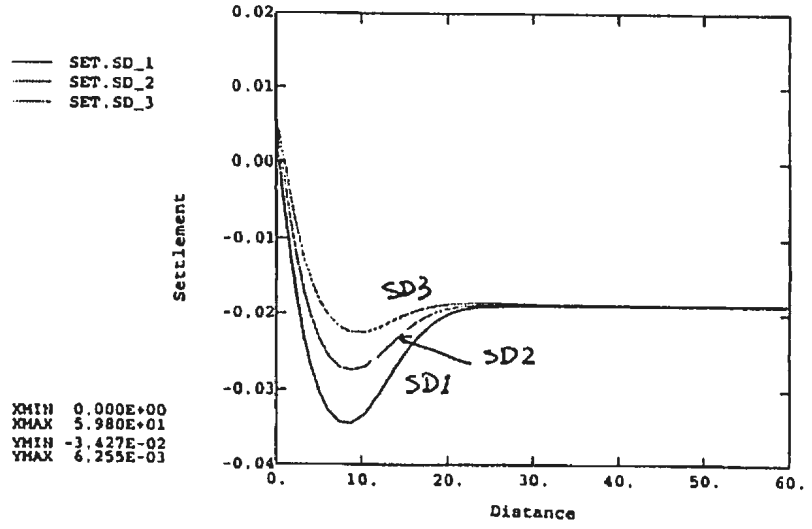

Figure 8.56 Variation of surface settlement with bracing parameters

Chapter 9

SUMMARY AND FUTURE STUDIES

This research studied braced excavations in clay using centrifuge tests and finite element analyses.

Centrifuge tests of 72 g were carried out in a strongbox under plane strain conditions. The soil was consolidated clay with a strength around 40 kPa. The sheet piles were simulated by a flat piece of aluminum plate. The earth pressures on the plate were calculated from the stresses in the plate and the loads in the struts. The stresses in the plate were measured with strain gauges forming electric bridges. Four full bridges were used along the vertical direction of the plate. There were four active gauges in each bridge: two were in the front side of the sheet plate and two were on the back.

The struts were simulated by small square section aluminum beams. There were three layers of struts and three struts in each layer. All struts were strain gauged

and the axial loads were measured. There were only two active gauges for each electric bridge. A full bridge was formed by applying two dummy gauges.

The soil in front of the sheet plate was simulated by a plastic bag containing a heavy liquid, which was a solution of the powder sodium polytungstate ($3Na_2WO_4.9WO_3.H_2O$). To lower the cost of the heavy liquid, a woodblock was used to reduce its volume. The woodblock in the excavation area was also used to hold the struts, wales and their support beams. The heavy liquid was drained gradually during the tests to simulate the excavation procedure.

Two standpipes were used: one was used at one end of the strongbox to control the level of the water table in the clay with a water supply system; the other was used to measure the water table in the soil in front of the sheet plate. Pore pressure transducers (PPTs) were used to measure the pore pressures inside the soil around the sheet plate. Four LDTs were used to measure the surface settlement of the soil on the back of the sheet plate.

Designing the centrifuge tests requires consideration of many details in order to obtain good results. These include:

- the height of the surface of the clay before testing;
- the numbers and positions of the full bridges of strain gauges on the sheet plate to obtain the stresses in the plate as well as the earth pressures on the plate;
- the possible seepage of water into the gauges disrupting them by short circuits;

- protecting the gauges and the wires;
- the possible seepage of water behind the sheet pile to the excavation area through crevices between the sheet plate and the side walls of the strongbox;
- the possible settlement of the plate into the soil under the high centrifuge forces;
- the number of struts;
- the measurement of the loads in the struts;
- the support of the wales and the struts;
- the possible blocking of the deformation of the sheet plate by the support beams;
- the full contact between the clay, plate, wales, struts, end beams and the wall of the strongbox;
- the simulation of the clay in front of the plate, which would be excavated;
- the density and volume of the heavy liquid and the bag holding the heavy liquid;
- the possible leaking of the bag;
- the procedure for collecting the heavy liquid;
- the design of the guide pipe, its stability and the possibility that it retards the consolidation of the clay;

- the connection between the bag and the drainage tube;
- the control of the rate of draining of the heavy liquid;
- the consideration of the water table in the clay in front of the plate;
- the control of the water table;
- the control of the water table in the clay behind the plate;
- the process of consolidation in the centrifuge.

The tests were carried out by increasing the acceleration to 72 g in stages. In the third test, the clay was consolidated for 260 minutes at which time, it was found that consolidation was completed. The heavy liquid was drained to simulate the process of excavation. It took 15 minutes to totally drain the heavy liquid. The model was consolidated continually for another 45 minutes and the test finished at 330 minutes.

Tests were carried out to measure Young's modulus for the sheet plate and the struts. Samples of the soil were collected after the centrifuge tests. Triaxial and oedometer tests were carried out. Some shear vane tests were also carried out. It was found that Young's modulus was 69.56 GP_a for the plate and 62.35 GP_a for the struts. It was also found that the index of compression for the clay was $C_c = 0.1213$, and the index of swelling was $C_s = 0.0167$. As a result, $\lambda = 0.2783$ and $\kappa = 0.0384$. Triaxial tests showed that for the tested clay c_{cu}=4.25 kPa and $\phi = 30°$.

The results show that the sign of the stresses in the plate change frequently

during testing. This implies a variation in the direction of bending of the sheet plate during the test. The loads in the struts were highest in the bottom layer and lowest in the top layer.

For the third test, the settlements of the first two points are within the line of Zone I (sand and soft to hard clay), which is for the soil with higher strength defined by Peck in his summary (1969). This matches the clay of this test, because after pre-consolidation and before the test, its shear strength was 41 kPa. The data of two points dropped into the top parts of Zone II and III. This shows that settlement occurred in a larger area than the definition of Peck's zones.

The earth pressures before draining the heavy liquid had their maximum value in the middle part of the sheet plate supported by the last layer of struts. Normally the pressures increased with depth. However, the earth pressures at the bottom part of the sheet plate were less than the pressures in the middle part. This is because the earth pressures were reduced by the lateral displacement of the sheet plate.

Along the vertical direction, the sheet plate can be divided into five parts. The distribution of earth pressures on the top part changed direction frequently and is not significant. The pressure at the second part was stable during draining. Actually this value was the largest earth pressure on the back of the plate at the final stage of draining the heavy liquid. In practice this value may be used to represent the actual maximum earth pressure on the sheet piles. The pressure in the middle part kept reducing during draining. The final value of the pressure was negative,

which is an error but close to zero. The pressure in the fourth part changed its direction after the heavy liquid began to drain and reached its maximum value at the final step. This pressure kept increasing with the draining of the heavy liquid, and tended to mobilize the passive earth pressure. The pressure in the bottom part of the plate had a similar distribution as the fourth part, and this value was quite stable during the whole process of draining.

By comparing the predictions of established methods and the results of the centrifuge test, it seemed that Peck's method for stiff clay might provide a good prediction. Tschebotarioff's prediction for medium clay might give the similar results but the distribution pattern did not agree. Peck's prediction for medium clay gave too large a value and Tschebotarioff's prediction for stiff clay did not give a safe value for practical design.

A finite element analysis was carried out to simulate the excavation procedures. The Cam-clay model was used for the soil. Block elements were used for the sheet plate and spring elements were used for the struts. The parameters found from the tests were used in the numerical simulation.

In comparing the results of finite element analysis and the predictions from Peck's and Tschebotarioff's methods, it was found that for K_0=1, the predictions of Tschebotarioff's method for medium clay and Peck's method for the stiff clay gave close values. While Tschebotarioff's method for stiff clay and Peck's method for medium clay gave larger predictions.

The finite element analysis and the centrifuge tests matched each other with

respect to the distribution of earth pressures at the upper part. The loads in the top layer struts were close to the measured values in the test. The loads in the bottom layer matched the measured values in the test in most steps. However, in the final steps the values from the analysis were higher than the test results. There were large differences between the measured and predicted values for the middle layer of struts. The settlement curve for K_0=0.5 was almost the same as the settlement curve of K_0=1 in the finite element analysis.

From the finite element analysis, the pore pressure curves for K_0=1 and 0.5 were the same. It was shown that the pore pressures in the test lay in the middle between the curves of the analyses. The "Reduced" curves, except that for A23, which was the point on the back of the plate and about the middle elevation of the excavation, were much closer to the test results.

Parametric studies for practical excavations showed that the variation of M resulted in the largest difference on the earth pressures. The variation of λ and κ did not result in a significant difference in the distribution of the earth pressures.

It is interesting that there was almost no change in the earth pressures on the sheet piles when the stiffness of the sheet piles or the struts increased. Even applying more layers of struts did not have a significant effect. The variation of the stiffness of the sheet piles and the struts did not affect the distribution of the forces in the struts. However varying the number of layers of struts changed the forces in the struts. This is obvious since the distribution of the earth pressures did not change and the more layers of struts would result in the less forces in each strut.

The parameter, M, greatly affected the lateral displacement. The lateral displacement was not sensitive to the variation of the parameters λ and κ. It was also found that M was the only parameter to greatly affect the surface settlement and the bottom heaving. The maximum settlement was found to be close to the back of the sheet piles.

Variation of the bracing system resulted in much more change in the settlement. There was a larger settlement with the variation of the stiffness of the sheet piles and there was some variation with the changes of the stiffness of the struts. The variation of the number of layers of struts also resulted in a large settlement which was also close to the back of the sheet piles.

Braced excavation is a complicated physical process in terms of the structure itself, the procedure of construction, the stress distribution, the variation of stresses, and the many factors affecting its stability. Contributions have largely been devoted to site investigations and numerical analyses. This study presented a new method in approaching this problem by combining the advantages of geotechnical centrifuge tests and a finite element analysis. This research shows that this combination of techniques complement each other. Progress can be made in extending this method with more centrifuge tests and finite element analyses by considering different cases. Future studies are recommended as the following:

Although it would be difficult, it would be of great value to apply the struts after the corresponding layers of soil are excavated for centrifuge tests. Preloading the struts is also worth studying. The study may provide a good guide for practical

concerns on the possible settlement of the surrounding ground surface, in other words, give a better estimation on the possible damage to nearby buildings. The suggested studies may be of even greater value if the soil is used in front of the sheet piles instead of heavy liquid. The difficulty is how to remove the soil.

The finite element analyses could be improved by using a better model for the contact between the soil and the sheet piles. The effect of preloading on ground settlement may also be useful to consider. A high degree of overconsolidation could be considered with more effective constitutive relations. It would also be of interest to examine this problem for unsaturated and anisotropic soils.

REFERENCE

Bezuijen, A. and van der Schrier, J. (1994) The Influence of a bored tunnel on pile foundations, centrifuge 94, 681-686.

Bjerrum, L., Clausen, C. J. and Duncan J. M. (1972) Earth Pressures on Flexible Structures-A State-of-the-are Report, Proc. 5th European Conference on Soil Mechanics and Foundation Engineering, 2, Madrid, Spain.

Bjerrum, L. and Eide, O. (1956) Stability of strutted excavations in clay, Geotechnique, 6, No. 1, 32-47.

Bolton, M. D. and Lau, C. K. (1988) Scale effects arising from particle size, Centrifuge 88, edited by Corte, J.-F., A.A. Balkema, Rotterdam/Brookfield.

Bolton, M. D. and Powrie, W. (1987) The Collapse of Diaphragm Walls Retaining Clay, Geotechnique 37, No. 3.

Bolton, M. D. and Powrie, W. (1988) Behaviour of diaphragm walls in clay prior to collapse, Geotechnique, 38 (2), 167-189.

Bolton, M. D., Powrie, W. and Stewart, D. I. (1988) The design of Deep In-situ Walls, Centrifuge 88, edited by Corte, J.-F., A. A. Balkema, Rotterdam, Brookfield, 405-414.

Boone, S. J. (1996) Ground-movement-related building damage, Journal of Geotechnical Engineering, ASCE, Vol. 122, No. 11, 886-896.

Borja, R. I. (1990) Analysis of Incremental Excavation Based on Critical State Theory, Journal of Geotechnical Engineering, ASCE, 116, 964-986.

Cernica, J. N. (1982) Geotechnical Engineering, Holt, Rinehart and Winston, 106.

Clough, G. W. and Reed, M. W. (1984) Measured behavior of braced wall in very soft clay, Journal of Geotechnical Engineering, ASCE, Vol. 110, No. 1, 1-19.

Clough, G. W. and Schmidt, B. (1981) Design and performance of excavations and tunnels in soft clay, Soft Clay Engineering, edited by Brand, E. W. and Brenner, R. P., Elsevier Scientific Publishing Company, 1981.

Craig, W. H. (1989) Edouard Phillips (1821-89) and the Idea of Centrifuge Modelling, Geotechnique, Vol. 39, No. 4, pp. 679-700.

Craig, W. H. and Yildirim, S. (1976) Modelling excavations and excavation processes, Proc. 6th Eur. Conf. Soil Mech. Found. Eng., Vol. 1, 33-36.

Day, R. A. and Potts, D. M. (1993) Modelling sheet pile retaining walls, Com-

puters and Geotechnics, 15, 125-143.

Dickin, E. A. (1988) Stress-displacement of buried plates and pipes, Centrifuge 88, edited by Corte, J.-F., Balkeman, Rotterdam, 205-214.

Feng, G., and Hu, Y. (1988) Centrifuge Model Test of a Highway Embankment on Soft Clay, in Centrifuge 88, edt. by Corte, 153-162.

Ferguson, K. A. and Ko, H. Y. (1981) Centrifuge Model of the Cone Penetrometer, Cone Penetrometer Testing and Experiences, edt. by Norris, G. M. and Holtz, R. D., 108-127.

Fernandes, M. A., Scardoso, A. J. S., Trigo, J. F. C. and Marques, J. M. M. C., (1994) Finite element modelling of supported excavations, in Soil-Structure interaction: Numerical analysis and modelling, edited by Bull, J. W., E & FN Spon, 337.

Finno, R. J., Harahap, I. S. (1991) Finite element analyses for HDR-4 excavation, Journal of Geotechnical Engineering, Vol. 117, No. 10, 1590-1609.

Finno, R. J., Harahap, I. S. and Sabatini, P. J. (1991) Analysis of Braced Excavations with Coupled Finite Element Formulations, Computers and Geotechnics, 12, 91-114.

Finno, R. J., Atmatzidis, D. K. and Perkins, S. B. (1989), Observed performance of a deep excavation in clay, Journal of Geotechnical Engineering, Vol. 115, No. 8, 1045-1064.

Finno, R. J. and Nerby, S. M. (1989), Saturated clay response during braced cut construction. Journal of Geotechnical Engineering, Vol. 115, No. 8, 1065-1084.

Finno, R. J., Lawrence, S. A., Allawh, N. F. and Harahap, I. S. (1991) Analysis of performance of pile groups adjacent to deep excavation, Journal of Geotechnical Engineering, ASCE, Vol. 117, No. 6, 934-955.

Flaate, K., and Peck, R. B. (1973) Braced cuts in sand and clay, Norwegian Geotechnical Institute Technical Report, No. 96, 7-29.

Fulsang, L. D. and Ovesen, N. K. (1988) The application of the theory of modelling to centrifuge studies, Centrifuges in Soil Mechanics, edited by Craig, W. H., James, R. G. and Schofield, A. N., Balkema, Rotterdam, 119-138.

Harahap, I. S. (1990) Numerical Evaluation of the Performance of the HDR-4 Excavation, thesis submitted to Northwestern University in partial fulfilment of the degree of Doctor of Philosophy.

Hashash, Y. M. A. (1992) Analysis of deep excavations in clay, Ph. D. thesis, Dept. of Civ. Engrg., Massachusetts Inst. of Technol. (MIT), Cambridge, Mass.

Hashash, Y.M.A. and Whittle, A. J. (1996) Ground Movement Prediction for Deep Excavations in Soft Clay, Journal of Geotechnical Engineering, June 1996, 474-486.

Hushmand, B., Scott, R. F. and Crouse, C. B. (1988) Centrifuge Liquefaction Tests in a Laminar Box, Geotechnique, Vol. 38, No. 2, 253-262.

Kimura, T., Kusakabe, O., and Saitoh, K. (1984) Undrained Deformation of Clay of Which Strength Increases Linearly with Depth, application of Centrifuge Modelling to Geotechnical Design, edt. by Craig, W. H., 315-335.

Kimura, T., Takemura, J., Hiro-oka, A., Okamura, M. and Park, J. (1994) Excavation in soft clay using an in-flight excavator, Centrifuge 94, edited by Liung, Lee and Tan, Balkema, Rotterdam, 649-654.

Klenner, C. (1941) Tests on the distribution of the earth pressure over the walls of braced excavations, Die Bautechnik, 19, 316-319.

Ko, H.-Y., Azevedo, R. and Sture, S. (1982) Numerical and centrifugal modelling of excavations in sand, Deformation and Failure of Granular Materials (eds. P. A. Vermeer and H. J. Luger), 609-614. Balkema, Rotterdam.

Ko, H.-Y. (1988) Summary of the state-of-the-art in centrifuge model testing, Centrifuge in Soil Mechanics, edited by Craig, W. H., James, R. G. and Schofield, A. N., Balkema, Rotterdam.

Kusakabe, O. (1982) Stability of excavations in stiff clays, Ph. D. Thesis, Cambridge University.

Kutter, B. L., Abghari, A. and Shindae, S. B. (1988) Modelling of Circular Foundations on Relatively Thin Clay Layers, Centrifuge 88, edt. by Corte, 337-344.

Lach, P. R. (1996) Centrifuge modelling of large soil deformation due to ice

scour, a thesis submitted to the School of Graduate Studies in partial fulfilment of the requirements for the degree of Doctor of Philosophy, Faculty of Engineering and Applied Science, Memorial University of Newfoundland.

Lade, P. V., Jessberger, H. L., Makowaski, E. and Jordan, P. (1981) Modelling of deep shafts on centrifuge tests. Proc. 10th Int. Conf. Soil Mech. Found. Eng., Vol. 1, 683-691.

Lambe, T. W. (1970) Braced excavations, ASCE Specialty Conference, Cornell University, 149-328.

Lardner, T. J. and Archer, R. R. (1994) Introduction to Mechanics of Solids, Inc. of McGraw-Hill, New York, page 261.

Lee, F. H., and Schofield, A. N. (1988) Centrifuge Modelling of Sand Embankments and Islands in Earthquake, Geotechnique, Vol. 38, No. 1, 45-58.

Liang, Y.-k. (1985) Evaluation of constitutive model using the centrifuge, submitted in partial satisfaction of the requirements for the degree of Ph. D. in Engineering in the Graduate Division of the University of California, Berkeley.

Lin, L. (1995) Strength Characteristics of a Modelling Silty Clay, Thesis of Master's Degree, Memorial University of Newfoundland.

Liu, w., Lee, K. M. and Zhang, S. D. (1994) Modelling of a large underground excavation in China, Centrifuge 94, edited by Leung, Lee, and Tan, 675-680.

Mana, A. I. (1978) Finite Element Analyses of Deep Excavation Behavior in Soft Clay, Technical Report No. CE-227, Stanford University.

Murphy, D. J., Clough, G. W. and Woolworth, R. S. (1975) Temporary Excavations in Varved Clay, Journal of Geotechnical Engineering Division, ASCE, 101, 279-295.

Ng, C. W. W. (1992) An evaluation of soil-structure interaction associated with a multi-propped excavation, Ph. D. thesis submitted to the University of Bristol, Faculty of Engineering.

Nomoto, T., Mto, K., Imamura, S., Veno, K. and Kusakabe, O. (1994) A miniature shield tunnelling machine for a centrifuge, Centrifuge 94, 694-704.

Norwegian Geotechnical Institute (1962) Measurements at a Strutted Excavation, Oslo Subway, Vaterland 1. Technical Report 6, Norwegian Geotechnical Institute, Oslo, Norway.

O'Rourke, T. D., Cording, E. J. and Boscardin (1976) The Ground Movements Related to Braced Excavation and Their Influence on Adjacent Buildings, Prepared for U. S. Department of Transportation, Office of the Secretary and Federal Railway Administration.

Ou, C. Y., Chiou, D. C. and Wu, T. S. (1996) Three-dimensional finite element analysis of deep excavation, Journal of Geotechnical Engineering, ASCE, 122 (5), 337-345.

Ou, C. Y. and Lai, C. H. (1994) Finite element analysis of deep excavation in layered sandy and clayey soil deposits, Canadian Geotechnical Journal, 31, 204-214.

Ou, C. Y., Wu, T. S. and Hsieh, H. S. (1996) Analysis of deep excavation with column type of ground improvement in soft clay, Journal of Geotechnical Engineering, Vol. 122, No. 9, 709-716.

Ovesen, N. K. (1979) The scaling law relationship - Panel discussion, Proc. 7th Eur. Conf. Soil Mech. Found. Eng., Brighton, No. 4, 319-323.

Palmer, J. H. and Kenney, T. C. (1972) Analytical Study of a Braced Excavation in Weak Clay, Canadian Geotechnical Journal, 9, 145-164.

Peck, R. B. (1942) Earth-pressure measurements in open cuts, Chicago Subway. American Society of Civil Engineers. Proceedings, Vol. 68, 142, No. 6, p.900-928.

Peck, R. B. (1943) Earth-pressure measurements in open cuts, Chicago, (Ill.) Subway. Transactions of the American Society of Civil Engineers, 108, (1943): 1008-1036.

Peck, R. B. (1969) Deep Excavations and Tunnelling in Soft Ground, State of the Art Volume, Seventh International Conference on Soil Mechanics and Foundation Engineering, Mexico.

Pepe, M. and Renzi, R. (1994) Modelling the stress history of Pisa clay, Centrifuge 94, edited by Leung, C. F., Lee, F. H. and Tan, T. S. (Singapore), Balkema, rotterdam.

Phillips, R. (1982) Trench excavations in clay, M. Phil. Thesis, Cambridge University.

Phillips, R. (1986) Ground deformation in the vicinity of a trench heading, Ph. D. thesis, Cambridge University.

Phillips, R. (1995) Centrifuge modelling: practical consideration, Geotechnical centrifuge technique, edited by Taylor, R. N., Blackie Academic and Professional.

Pokrovskii, G. I. and Fiodorov, I. S. (1936) Studies of soil pressures and deformations by means of a centrifuge, Proc. 1st Int. Conf. Soil Mech. Found. Eng., Vol. 1, 70.

Pokrovskii, G. I. and Fiodorov, I. S. (1953) Centrifugal modelling in structure designing, Gosstroy Publisher, Moscow.

Pokrovskii, G. I. and Fiodorov, I. S. (1975) Centrifugal model testing in the construction industry, Vols. I, II. English translation by Building Research Establishment Library Translation Service.

Pokrovsky, G. I. and Fiodorov, J. S. (1968) Centrifuge modeling in the construction industry, Moscow: Stroiiedat, In draft translation, Building Research Establishment Library, vol. 1.

Poulos, H. G. and Chen, L. T. (1997) Pile response due to excavation-induced lateral soil movement, Journal of Geotechnical Engineering, ASCE, Vol. 123, No. 2, 94-99.

Powrie, W. (1986) The behaviour of diaphragm walls in clay, a dissertation submitted for the degree of doctor philosophy at Cambridge University, St. Catharine's College, Cambridge, England.

Powrie, W. and Kantarzi, C. (1993) Installation effects of diaphragm walls in clay, Retaining structures (ed. C. R. I. Clayton), Thomas Telford, London, 37-45.

Powrie, W., Richards, D. J. and Kantartzi, C. (1994) Modelling diaphragm wall installation and excavation processes, Centrifuge 94, edited by Leung, Lee and Tan, Balkema, Rotterdam, 655-661.

Rowe, P. W. (1952) Anchored sheet-pile walls. Institution of Civil Engineers, London. Proceedings, Vol. 1, pt. 1, p.27-70.

Rowe, P. W. (1975) Displacement and Failure Modes of Model Offshore Gravity platforms Founded on Clay, in Conference of Offshore Europe, 1975, Spearhead Publications, Aberdeen.

Schcherbina, V. I. (1988) Earth Pressure Studies on Retaining Walls by Centrifuge Modelling, Centrifuge 88, edt. by Corte, 421-428.

Schlosser, F., Magnan, J. P. and Holtz, R. D. (1985) Geotechnical engineered construction, XI ICSMFE, 2499-2539.

Schofield, A. N. (1980) Cambridge Geotechnical Centrifuge Operation, Geotechnique, Vol. 30, No. 3, 227-268.

Scott, R. F. and Morgan, N. R. (1977) Feasibility and desirability of constructing a very large centrifuge for geotechnical studies, prepared for national Science Foundation.

Simpson, B. (1992) Retaining structures: displacement and design, Geotechnique, Vol. 42, No. 4, 541-576.

Skempton, A. W. (1957) Discussion: the Planning and Design of New Hong Kong Airport, Proceedings, institute of Civil Engineers, London, Vol. 7, 305-307.

Skempton, A. W. and Ward, W. H. (1952-1953) Investigations concerning a deep cofferdam in the Thames estuary clay at Shellhaven. Geotechnique, Vol. 3, No. 3, 119-139.

Smith, I. M. and Ho, D. K. H. (1992) Influence of Construction Technique on the Performance of a Braced Excavation in Marine Clay, International Journal for Numerical Analytical Methods in Geomechanics, Vol. 16, 845-867.

Sprinman, S. M. (1993) Centrifuge Modelling in Clay: Marine Applications, Proc. of the 4th Canadian Conference o Marine Geotechnical Engineering, Vol. 3, 853-896.

Tanaka, H. (1993) Behavior of braced excavations stabilized by Deep Mixing method, Soils and Foundations, Vol. 33, No. 2, 105-115.

Tanaka, H. (1994a) Behavior of a Braced Excavation in Soft Clay and the Undrained Shear Strength for Passive Earth Pressure, Soils and Foundations, Vol.

34, No.1, 53-64.

Tanaka, H. (1994b) Base failure of Braced Excavation Stabilized by DM method, Proc. of 13th ICSMFE, 1745-1748.

Taylor, R. N. (1995) Centrifuges in modelling: Principles and scale effects, Geotechnical centrifuge technology, edited by Taylor, R. N., Blackie, Academic and Professional.

Terzaghi, K. (1934) Large-retaining-wall tests. I-V. Engineering News-Record, Vol. 112, Nos. 5,8, 10, 13,16 and 23.

Terzaghi, K. (1941) General wedge theory of earth pressures, Transactions of the American Society of Civil Engineers, 106, (1941): 48.

Terzaghi, K. and Peck, R. B. (1967) Soil Mechanics in Engineering Practice, John Wiley and Sons, Inc., New York.

Tschebotarioff, G. P. (1951) Soil Mechanics, Foundations, and Earth Structures, McGraw-Hill Book Company, Inc., New York, Toronto, London, 655.

Tsuchida, T., Kobayashi, M. and Mizukami, J. (1991) Effect of aging of marine clay and its duplication by high temperature consolidation, Soils and Foundations, Vol. 31, No. , 133-147.

Tsui, Y. and Clough, G. W. (1974) Plane strain approximations in finite element analyses of temporary walls, Proc. Conf. Analysis and Design in Geotechnical

Engineering, Univ. of Texas, Austin, 1, 173.

Wang, Z.-H. (1983) Consolidation and compression properties of soil, Engineering properties of soil, edited by Huang, W.-X., Irrigation and Hydropower, Beijing, 170.

Ward, W. H. (1955) Experiences with some sheet-pile cofferdams at Tilbury, Correspondence to Geotechnique, 5, No. 4, 327-330.

Whittle, A. J. and Hashash, Y. M. A. (1994) Soil modelling and prediction of deep excavation behavior, Proc. Int. Symp. on Pre-Failure Deformation Characteristics of Geo-Mat. (IS-Hokkaido '94), A. A. Balkema, Vol. 1, 589-595.

Whittle, A. J., Hashash, Y. M. A. and Whitman, R. V. (1993) Analysis of a deep excavation in Boston, J. Geotech. Engrg., ASCE, 119(1), 69-90.

Wilson, G. P. (1992) The behavior of a deep retained excavation in soft San Francisco Bay mud, Ph. D. dissertation, Arizona State University.

Wong, I. H. (1985) Stability of deep excavations in soft clay, XI ICSMFE, San Francisco, USA, 2802-2803.

Wong, K. S., Wong, I. H. and Broms, B. B. (1987) Methods of improving the stability of deep excavations in soft clay, proc. 8th Asian Regional Conf. on Soil Mech. and Found. Engrg., Kyoto, Japan, 321-324.

Woo, S. M. (1990) Use of ground improvement in deep excavation sites for

protection of building in Taiwan, Proc. 9th Asian Regional Conf. on Soil Mech. and Found. Engrg., Panellist Rep., Bangkok, Thailand, 9-14.

Woods, D. M. (1990) Soil Behaviour and Critical State Soil Mechanics, Cambridge University Press, Cambridge, 301.

Xia, H. (1996) FEM analysis for braced excavations in clay, Poster competition, Faculty of Engineering and Applied Science, Memorial University of Newfoundland.

Xie, G. (1988) Centrifuge modelling on stress analysis for structures built on a non-uniform foundation, Centrifuge 88, edited by Corte, J.-F., Balkeman, Rotterdam, 429-434.

You, Z. and Znidarcic, D. (1994) Initial stage of soft soil consolidation, Centrifuge 94, Balkeman, Rotterdam, 399-403.

Zhang, S. D. and Zhang, H. D. (1994) Stability of deep excavations in soft clay, Centrifuge 94, edited by Leung, Lee and Tan, Balkeman, Rotterdam, 643-647.